UNIVERSITI TEKNOLOGI MALAYSIA

**BORANG PENGESAHAN
LAPORAN AKHIR PENYELIDIKAN**

TAJUK PROJEK :   Development of New Technologies for Interlocking Concrete Block

Pavements (ICBP)

Saya   PROF. IR. DR. HASANAN MD. NOR

(HURUF BESAR)

Mengaku membenarkan **Laporan Akhir Penyelidikan** ini disimpan di Perpustakaan   Universiti Teknologi Malaysia dengan syarat-syarat kegunaan seperti berikut :

1.   Laporan Akhir Penyelidikan ini adalah hakmilik Universiti Teknologi Malaysia.

2.   Perpustakaan Universiti Teknologi Malaysia dibenarkan membuat salinan untuk tujuan rujukan sahaja.

3.   Perpustakaan dibenarkan membuat penjualan salinan Laporan Akhir Penyelidikan ini bagi kategori TIDAK TERHAD.

4.   * Sila tandakan (/)

☐ SULIT   (Mengandungi maklumat yang berdarjah keselamatan atau Kepentingan Malaysia seperti yang termaktub di dalam AKTA RAHSIA RASMI 1972).

☐ TERHAD   (Mengandungi maklumat TERHAD yang telah ditentukan oleh Organisasi/badan di mana penyelidikan dijalankan).

☑ TIDAK TERHAD

_____
TANDATANGAN KETUA PENYELIDIK

Prof. Ir. Dr. Hasanan Md. Nor
_____
Nama & Cop Ketua Penyelidik

Tarikh : 17 March 2008

CATATAN :   * *Jika Laporan Akhir Penyelidikan ini SULIT atau TERHAD, sila lampirkan surat daripada pihak berkuasa/organisasi berkenaan dengan menyatakan sekali sebab dan tempoh laporan ini perlu dikelaskan sebagai SULIT dan TERHAD.*

DEVELOPMENT OF NEW TECHNOLOGIES FOR INTERLOCKING CONCRETE
BLOCK PAVEMENTS (ICBP)

PROF. IR. DR. HASANAN MD. NOR
LING TUNG CHAI

A final report (vot 74267) submitted to
Research Management Centre

Faculty of Civil Engineering
Universiti Teknologi Malaysia

MARCH 2008

UNIVERSITI TEKNOLOGI MALAYSIA
Research Management Centre

PRELIMINARY IP SCREENING & TECHNOLOGY ASSESSMENT FORM
(To be completed by Project Leader submission of Final Report to RMC or whenever IP protection arrangement is required)

1. **PROJECT TITLE IDENTIFICATION** :

   Development of New Technologies for Interlocking Concrete Block Pavements (ICBP)

   _____ Vote No: 74267

2. **PROJECT LEADER** :

   Name :
   Prof. Ir. Dr. Hasanan Md. Nor

   Address   :
   Centre for Teaching and Learning, Universiti Teknologi Malaysia, 81310 Skudai, Johor.

   Tel   : 07-5537850   Fax : _____ e-mail : hasanan@utm.my

3. **DIRECT OUTPUT OF PROJECT** *(Please tick where applicable)*

Scientific Research	Applied Research	Product/Process Development
☐ Algorithm	☑ Method/Technique	☑ Product / Component
☐ Structure	☐ Demonstration / Prototype	☐ Process
☑ Data		☐ Software
☐ Other, please specify	☐ Other, please specify	☐ Other, please specify
_____	_____	_____
_____	_____	_____
_____	_____	_____

4. **INTELLECTUAL PROPERTY** *(Please tick where applicable)*

☐ Not patentable	☐ Technology protected by patents
☐ Patent search required	☐ Patent pending
☐ Patent search completed and clean	☐ Monograph available
☑ Invention remains confidential	☐ Inventor technology champion
☐ No publications pending	☐ Inventor team player
☐ No prior claims to the technology	☐ Industrial partner identified

5.   LIST OF EQUIPMENT BOUGHT USING THIS VOT

Highway Accelerated Loading Instrument

Hand Press Concrete Paving Block Making Machine

Acer Notebook, Hp Laser Printer

Cutter for Interlocking Concrete Paving Blocks

Dial Gauges

6.   STATEMENT OF ACCOUNT

a)   APPROVED FUNDING   RM : RM 253.000.00

b)   TOTAL SPENDING   RM : RM 247468.89

c)   BALANCE   RM : RM 5531.11

7.   TECHNICAL DESCRIPTION AND PERSPECTIVE

Please tick an executive summary of the new technology product, process, etc., describing how it works. Include brief analysis that compares it with competitive technology and signals the one that it may replace. Identify potential technology user group and the strategic means for exploitation.

a)   Technology Description

The Highway Accelerated Loading Instrument (HALI) is designed to deliver objective and simulate the actual traffic conditions in a cost effective and laboratory-scale that is easily conducted. The HALI also provides a practical, easy-to-use, and suitable for various type of road materials investigation. The instrument is can easily be operated by a single electrical control panel. The dial gauges are mounted at 110 mm apart on the rigid beam for data acquisition. A three-dimensional view of the deformed surface can be obtained using the collected by means of SURFER computer program .

b)   Market Potential

- Ideal for Local government / councils, State Forestry and those responsible for research and development (R&D) in roads materials.

- The recommendation of utilizing CBP for sloping road section and data of the study are beneficial to consultant and road designer.

   c)   Commercialisation Strategies

 - <u>Present research finding in national and international conference</u>

 - <u>Publish article in national and international journal</u>

 - <u>Organize workshop for local government/ councils and those related research scientist</u>

 - <u>Linkage and transfer knowledge to industrials and contractor</u>

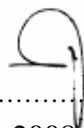**8.**   **RESEARCH PERFORMANCE EVALUATION**

   a)   FACULTY RESEARCH COORDINATOR

	Excellent	Very Good	Good	Satisfactory	Fair	Weak
Research Status	( )	( )	( )	( )	( )	( )
Spending	( )	( )	( )	( )	( )	( )
Overall Status	( )	( )	( )	( )	( )	( )

Comment/Recommendations :

_____
_____
_____
_____
_____
_____

…………………………………………   Name : ………………………………………

Signature and stamp of   Date   : 25 March 2008
JKPP Chairman

b)   RMC EVALUATION

Research Status	( )	( )	( )	( )	( )	( )
Spending	( )	( )	( )	( )	( )	( )
Overall Status	( )	( )	( )	( )	( )	( )
	Excellent	Very Good	Good	Satisfactory	Fair	Weak

Comments :-

_____

_____

_____

_____

_____

_____

Recommendations :

☐   Needs further research

☐   Patent application recommended

☐   Market without patent

☐   No tangible product. Report to be filed as reference

…………………………………..   Name : ………………………………………
Signature and Stamp of Dean /   Date : ………………………………………
Deputy Dean
Research Management Centre

Benefits Report Guidelines

A. Purpose

The purpose of the Benefits Report is to allow the IRPA Panels and their supporting experts to assess the benefits derived from IRPA-funded research projects.

B. Information Required

The Project Leader is required to provide information on the results of the research project, specifically in the following areas:

- Direct outputs of the project;

- Organisational outcomes of the project; and

- Sectoral/national impacts of the project.

C. Responsibility

The Benefits Report should be completed by the Project Leader of the IRPA-funded project.

D. Timing

The Benefits Report is to be completed within three months of notification by the IRPA Secretariat. Only IRPA-funded projects identified by MPKSN are subject to this review. Generally, the Secretariat will notify Project Leaders of selected projects within 18 months of project completion.

E. Submissin Procedure

One copy of this report is to be mailed to :

> IRPA Secretariat
> Ministry of Science, Technology and the Environment
> 14th, Floor, Wisma Sime Darby
> Jalan Raja Laut
> 55662 Kuala Lumpur

Benefit Report

1.   Description of the Project

A.   Project identification
1.   Project number : 03-02-06-0129-EA0001
2.   Project title : Development of New Technologies for Interlocking Concrete Block Pavements (ICBP)
3.   **Project leader :** Prof. Ir. Dr. Hasanan Md. Nor

B.   Type of research

Indicate the type of research of the project (Please see definitions in the Guidelines for completing the Application Form)

☐ Scientific research (fundamental research)

[√] Technology development (applied research)

☐ Product/process development (design and engineering)

☐ Social/policy research

C.   Objectives of the project

1.   Socio-economic objectives

Which socio-economic objectives are adressed by the project? (Please indentify the sector, SEO Category and SEO Group under which the project falls. Refer to the Malaysian R&D Classification System brochure for the SEO Group code)

Sector :   Manufacturing and Construction

SEO Category :   Construction (S2070000)

SEO Group and Code :   Construction Process (S2070300)

2.   Fields of research

Which are the two main FOR Categories, FOR Groups, and FOR Areas of your project? (Please refer to the Malaysia R&D Classification System brochure for the FOR Group Code)

a.   Primary field of research

FOR Category :   Engineering Science (F 1070000)

FOR Group and Code :   Civil Engineering (F1070400)

FOR Area :   Infrastructural Engineering (F1070407)

b.   Secondary field of research

FOR Category :   Applied Science and Technologies (F1060000)

FOR Group and Code :   Other Applied Science and Technologies not elsewhere classified (F1069900)

FOR Area :   Road and Highway

D.   Project duration

What was the duration of the project ?

_____42_____ Months

E.   Project manpower

How many man-months did the project involve?

_____59.0_____Man-months

F.   Project costs

What were the total project expenses of the project?

RM_247468.89_____

G.   Project funding

Which were the funding sources for the project?

Funding sources	Total Allocation (RM)
_IRPA_____	_____RM 253,000.00_____
_____	_____
_____	_____
_____	_____

ll.   Direct Outputs of the Project

A.   Technical contribution of the project

1.   **What was the achieved direct output of the project :**

For scientific (fundamental) research projects?

☐   Algorithm

☐   Structure

☑   Data

☐   Other, please specify : _____

For technology development (applied research) projects :

☑   Method/technique

☑   Demonstrator/prototype

☐   Other, please specify : _____

For product/process development (design and engineering) projects:

☑   Product/component

☐   Process

☐   Software

☐   Other, please specify : _____

2.   How would you characterise the quality of this output?

☐   Significant breakthrough

☑   Major improvement

☐   Minor improvement

B. **Contribution of the project to knowledge**

1. **How has the output of the project been documented?**

- [√] Detailed project report

- [ ] Product/process specification documents

- [ ] Other, please specify : _____

2. **Did the project create an intellectual property stock?**

- [ ] Patent obtained

- [ ] Patent pending

- [ ] Patent application will be filed

- [√] Copyright

3. **What publications are available?**

- [√] Articles (s) in scientific publications   How Many: __2_____

- [√] Papers(s) delivered at conferences/seminars   How Many: __7_____

- [ ] Book

- [ ] Other, please specify : _____

4. **How significant are citations of the results?**

- [ ] Citations in national publications   How Many: _____

- [ ] Citations in international publications   How Many: _____

- [ ] None yet

- [√] Not known

lll.   Organisational Outcomes of the Project

A.   Contribution of the project to expertise development

1.   How did the project contribute to expertise?

| √ | PhD degrees | How Many: __2__ |

| √ | MSc degrees | How Many: __1__ |

| ☐ | Research staff with new specialty | How Many: _____ |

| ☐ | Other, please specify: _____ |

2.   How significant is this expertise?

| ☐ | One of the key areas of priority for Malaysia |

| √ | An important area, but not a priority one |

B.   Economic contribution of the project?

1.   How has the economic contribution of the project materialised?

| √ | Sales of manufactured product/equipment |

| ☐ | Royalties from licensing |

| √ | Cost savings |

| √ | Time savings |

| ☐ | Other, please specify : _____ |

2.   How important is this economic contribution ?

| ☐ | High economic contribution | Value: | RM_____ |

| ☐ | Medium economic contribution | Value: | RM_____ |

| √ | Low economic contribution | Value: | RM_____ |

3. **When has this economic contribution materialised?**

☐ Already materialised

☐ Within months of project completion

☐ Within three years of project completion

☑ Expected in three years or more

☐ Unknown

C **Infrastructural contribution of the project**

1. **What infrastructural contribution has the project had?**

☑ New equipment   Value: RM _92,000.00_

☐ New/improved facility   Investment :   RM _____

☐ New information networks

☐ Other, please specify: _____

2. **How significant is this infrastructural contribution for the organisation?**

☐ Not significant/does not leverage other projects

☑ Moderately significant

☐ Very significant/significantly leverages other projects

D. **Contribution of the project to the organisation's reputation**

1. **How has the project contributed to increasing the reputation of the organisation**

☐ Recognition as a Centre of Excellence

☑ National award

☐ International award

☐ Demand for advisory services

☐ Invitations to give speeches on conferences

☐ Visits from other organisations

☑ Other, please specify: _Invitation of article to Journal of Road and Transport Research (An International Journal)_

2. **How important is the project's contribution to the organisation's reputation ?**

	Not significant
√	Moderately significant
	Very significant

1V.   National Impacts of the Project

A.   Contribution of the project to organisational linkages

1.   Which kinds of linkages did the project create?

| √ | Domestic industry linkages

| | International industry linkages

| √ | Linkages with domestic research institutions, universities

| | Linkages with international research institutions, universities

2.   What is the nature of the linkages?

| | Staff exchanges

| | Inter-organisational project team

| | Research contract with a commercial client

| | Informal consultation

| | Other, please specify: _____

B.   Social-economic contribution of the project

1.   Who are the direct customer/beneficiaries of the project output?

Customers/beneficiaries: Number:
Jabtan Keria Rava Malavsia _____   _____

Road authorities and highway research institutions.   _____

_____   _____

2.   How has/will the socio-economic contribution of the project materialised ?

| | Improvements in health

| | Improvements in safety

| | Improvements in the environment

| √ | Improvements in energy consumption/supply

| | Improvements in international relations

| | Other, please specify: _____

3. **How important is this socio-economic contribution?**

	High social contribution

	Medium social contribution

√	Low social contribution

4. **When has/will this social contribution materialised?**

	Already materialised
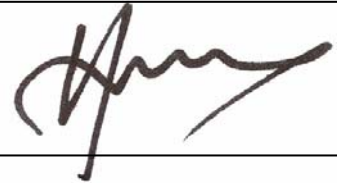
	Within three years of project completion

√	Expected in three years or more

	Unknown

Date: 25 March 2008   **Signature:**

End of Project Report Guidelines

A.   Purpose

The purpose of the End of Project is to allow the IRPA Panels and their supporting group of experts to assess the results of research projects and the technology transfer actions to be taken.

B.   Information Required

The following Information is required in the End of Project Report :

- Project summary for the Annual MPKSN Report;

- Extent of achievement of the original project objectives;

- Technology transfer and commercialisation approach;

- Benefits of the project, particularly project outputs and organisational outcomes; and

- Assessment of the project team, research approach, project schedule and project costs.

C.   Responsibility

The End of Project Report should be completed by the Project Leader of the IRPA-funded project.

D.   Timing

The End of Project Report should be submitted within three months of the completion of the research project.

E.   Submission Procedure

One copy of the End of Project is to be mailed to :

IRPA Secretariat
Ministry of Science, Technology and the Environment
14th Floor, Wisma Sime Darby
Jalan Raja Laut
55662 Kuala Lumpur

End of Project Report

A. **Project number :** 03-02-06-0129-EA0001	
Project title : Development of New Technologies for Interlocking Concrete Block Pavements (ICBP)	
Project leader: Prof. Ir. Dr. Hasanan Md. Nor	
Tel: 07-5537850	**Fax:**

B.   **Summary for the MPKSN Report** (for publication in the Annual MPKSN Report, please summarise the project objectives, significant results achieved, research approach and team structure)

Objective:
- To study the performance of CBP deformation (horizontal creep) that is affected by horizontal force with variables; laying pattern, block thickness, block shape and joint width between blocks on flat surface.
- To test and analyse various experimental of CBP in the laboratory with push-in tests for various degrees of slopes.
- To make a comparative study of experimental results in laboratory with three dimensional finite element model (3DFEM) simulations.
- To define the spacing of anchor beam on sloping road section based on degree of the slope, the effect of laying pattern, block thickness, bedding sand thickness and joint width between blocks.
- To develop laboratory-scale Highway Accelerated Loading Instrument (HALI)

Significant results achieved:
- Studies on CBP for sloping road section are limited. This study contributes to the understanding of CBP performance on slopes.
- The CBP failure caused by traction of traffic for sloping road section can be alleviated by using appropriate bedding sand thickness, block thickness, laying pattern and joint width.
- The result of the study can be used as a recommendation of utilizing CBP for sloping road section.
- Providing low cost, operational guideline and simple accelerated loading facility for road authorities and highway research institutions.

Research approach:
- Literature Review ⟶ Visit Site/Manufacture ⟶ Laboratory Scale Model ⟶ Develop HALI ⟶ Laboratory Static and Dynamic Testing ⟶ Analysis ⟶ Validation

Team structure:
- Project leader: Prof. Ir. Dr. Hasanan Md. Nor
- Key researchers: Ling Tung Chai, Rahmat Mudiyono

C.   Objectives achievement

- **Original project objectives** (Please state the specific project objectives as described in Section ll of the Application Form)

    ➢ To identify the interlocking behabiour on slope surface, corner and junction for ICBP implementation.
    ➢ To develop new technique in joint material in ICBP construction
    ➢ To produce application design of ICBP for uphill area.

- **Objectives Achieved** (Please state the extent to which the project objectives were achieved)

    ➢ All listed above were achieved

- **Objectives not achieved** (Please identify the objectives that were not achieved and give reasons)

    ➢ Nil

D.   Technology Transfer/Commercialisation Approach (Please describe the approach planned to transfer/commercialise the results of the project)

    ➢ Transfer technology will be done through seminar, conferences, workshop and etc.
    ➢ Final output of the project is to provide a comprehensive information and specification of ICBP.
    ➢ Develop the linkage with established local industries such as Sunway Paving Solution (M) Sdn. Bhd. and universities to exchange knowledge and research finding.
    ➢ International research institution linkage such as ICPI and ARRB in Australia to exchange results information and promote local findings.

E. Benefits of the Project (Please identify the actual benefits arising from the project as defined in Section lll of the Application Form. For examples of outputs, organisational outcomes and sectoral/national impacts, please refer to Section lll of the Guidelines for the Application of R&D Funding under IRPA)

- **Outputs of the project and potential beneficiaries** (Please describe as specifically as possible the outputs achieved and provide an assessment of their significance to users)

  ➢ Establishment new methods for CBP design on the slope (uphill) area.
  ➢ An alternative for a cost effective method of improving the CBP.
  ➢ Provide suitable construction materials and better construction procedure for concrete block pavement on uphill area.
  ➢ The protection technology and construction method for CBP on sloping section was proposed.
  ➢ Provide a low cost, simple and laboratory-scale accelerated loading facility for any interest road authorities and highway research institutions.

- **Organisational Outcomes** (Please describe as specifically as possible the organisational benefits arising from the project and provide an assessment of their significance)

  ➢ To solve problem faced by Interlocking Concrete Block Pavement (ICBP) industry.
  ➢ To produce MEng and PhD degree
  ➢ Recognition as a centre of excellence and provide information/knowledge to other organization.
  ➢ Publication of journals and conference papers.

- **National Impacts** (If known at this point in time, please describes specifically as possible the potential sectoral/national benefits arising from the project and provide an assessment of their significance)

  ➢ Enhance economic growth through the development of information on ICBP potentials.
  ➢ Promote the use of ICBP in pavement constructions.
  ➢ Development of linkage with established international research institution in this area.
  ➢ Reduce maintenance and repair for ICBP.

F.   Assessment of project structure

- **Project Team** (Please provide an assessment of how the project team performed and highlight any significant departures from plan in either structure or actual man-days utilised)

  ➤ The human resources consists of researchers, support staff, contract staff and PhD students were fully utilized for the completion of this project.

- **Collaborations** (Please describe the nature of collaborations with other research organisations and/or industry)
  ➤ Domestic linkage with Sunway Paving Solution (M) Sdn Bhd at senai, Johor plant.

G.   Assessment of Research Approach (Please highlight the main steps actually performed and indicate any major departure from the planned approach or any major difficulty encountered)

➤ All research approach indicated at section B was well performed.
➤ The major difficulty encountered during the research was limited funding to support contract staff and PhD students.

H.   Assessment of the Project Schedule (Please make any relevant comment regarding the actual duration of the project and highlight any significant variation from plan)

➤ The original duration proposed for this project was 36 months, but it has been extended for another 6 months due to the renovation works in Highway Laboratory at Universiti Teknologi Malaysia and delay of equipment (HALI) fabrication work.
➤ However, finally the project was complete successfully in 42 months.

I.   **Assessment of Project Costs** (Please comment on the appropriateness of the original budget and highlight any major departure from the planned budget)

- ➢ Original budget allocate for this project was RM 253,000.00.
- ➢ The major expenses of this project were used to develop HALI (RM 92,000.00) and contract staff/ PhD student's salary (RM 100,000.00 for 42 months).

J.   **Additional Project Funding Obtained** (In case of involvement of other funding sources, please indicate the source and total funding provided)
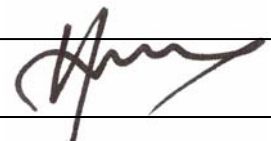
- ➢ Nil.

K.   **Other Remarks** (Please include any other comment which you feel is relevant for the evaluation of this project)

- ➢ This research has a great potential for further research to contribute towards enhancing and strengthening ICBP research and development in Malaysia.

Date : 25 March 2008   **Signature:**

ACKNOWLEDGEMENTS

ABSTRACT

In concrete block pavements, the blocks make up the wearing surface and are a major load-spreading component of the pavement. This research investigate the anchor beam spacing of concrete block pavement (CBP) on sloping road section based on the degree of slope, laying pattern, blocks shape, blocks thickness, joint width between blocks and bedding sand thickness. The results of a series of tests conducted in laboratory with horizontal force test and push-in test in several degrees of slopes. The horizontal force testing installation was constructed within the steel frame 2.00 x 2.00 metre and forced from the side until CBP failure (maximum horizontal creep). For the applied push-in test in a rigid steel box of 1.00 x 1.00 metre square in plan and 0.20 meter depth, the vertical load was increased from zero to 51 kN on the CBP sample in 0%, 4%, 8% and 12% degrees of slopes. The herringbone 45° is the best laying pattern compared to herringbone 90° and stretcher bond to restraint the horizontal force, which the blocks contribute as a whole to the friction of the pavement, the blocks being successively locked by their rotation following their horizontal creep. The uni-pave block shape has more restraint of horizontal creep than rectangular block shape, because uni-pave block shape has gear (four-dents), while rectangular block shape has no gear (dents).The difference in deflections observed between uni-pave shape and rectangular shape are small. The change in block thickness from 60 to 100 mm significantly reduces the elastic deflection of pavement. The optimum joint width between blocks is 3 mm. For joint widths less than the optimum, the jointing sand was unable to enter between blocks. The relationship between push-in force with block displacement on the varying loose thicknesses of 30, 50, and 70 mm bedding sand, shows that the deflections of pavement increase with increase in loose thickness of bedding sand. The higher the loose bedding sand thickness, the more the deflection will be. The effect of the degree of slope on concrete block pavements on sloping road section area is significant with friction between blocks and thrusting action between adjacent blocks at hinging points is more effective with thicker blocks. Thus, deflections are much less for thicker blocks with increasing degree of the slope. The spacing of anchor beam is increase with decreasing joint width, degree of slope and bedding sand thickness. To compare results between laboratory test with the simulated mechanical behaviour of concrete block pavements, a structural model based on a Three Dimensional Finite Element Model (3DFEM) for CBP was employed. The concept of HALI development, including design, fabrication, calibration and performance monitoring is presented. Before HALI can be greatly introduced highway research institutions, the equipment was tested with 1 m x 5.4 m test pavement and subjected to 10,000 cycles of load repetition. Additional tests, including shear resistance, skid resistance, and impact resistance were also conducted in order to have a better understanding of the effects of the pavement behaviour tested under HALI.

ABSTRAK

Dalam turapan blok konkrit (CBP), blok merupakan bahan binaan untuk lapis haus, iaitu lapisan penting bagi penyebaran beban. Penyelidikan ini dijalankan untuk menentukan jarak rasuk penahan pada turapan blok konkrit di bahagian jalan yang cerun berdasarkan pada darjah kecerunan, corak susunan turapan, bentuk blok, tebal blok, lebar sambungan di antara blok dan ketebalan lapisan pasir penggalas. Ujikaji yang dilakukan di makmal menggunakan uji tekan mendatar dan uji tekan masuk pada turapan yang dicerunkan beberapa darjah. Pemasangan alat ujikaji tekan mendatar menggunakan rangka keluli saiz 2.00 x 2.00 meter yang ditekan dari sisi hingga turapan blok konkrit mengalami kegagalan. Dalam ujikaji tekan masuk menggunakan rangka keluli saiz 1.00 x 1.00 meter dengan kedalaman 0.20 meter, beban tegak dikenakan ke atas sampel CBP kecerunan dari 0 hingga 51 kN, dimana sampel CBP di letakkan pada kecerunan 0%, 4%, 8% dan 12%. Keputusan menunjukkan susunan silang pangkah 45° adalah yang terbaik jika dibandingkan susunan silang pangkah 90° maupun susunan usungan untuk menahan beban mendatar. Bentuk blok uni-pave lebih kuat menahan rayapan mendatar jika dibandingkan dengan bentuk blok bersegi empat, kerana bentuk blok mempunyai gerigi (4 sisi), manakala bentuk blok bersegi empat tidak mempunyai gerigi. Pemesongan yang terjadi antara bentuk blok uni-pave dengan bentuk bersegi empat sangat kecil. Perubahan ketebalan blok dari 60 mm sampai 100 mm dapat mengurangkan pemesongan pada turapan. Semakin tebal blok semakin besar daya geserannya. Keputusan ujikaji juga menunjukkan lebar sambungan di antara blok yang optimum adalah 3 mm. Bagi lebar sambungan kurang daripada optimum, pasir pengisi tidak dapat memasuki ruang antara blok. Hubungan antara daya tekanan dengan penurunan blok pada berbagai ketebalan pasir pengisi 30, 50, dan 70 mm menunjukkan bahawa penurunan blok semakin besar dengan peningkatan ketebalan pasir pengalas dari 30 hingga 70 mm tebal. Semakin tebal pasir pengalas, semakin tinggi penurunan yang terjadi. Kesan darjah kecerunan keatas kawasan jalan cerun adalah signifikan dengan kekuatan geseran antara blok dan kekuatan mempertahan posisi blok lebih efektif dengan peningkatan tebal blok. Penurunan semakin berkurang untuk blok yang lebih tebal dan lebih besar darjah kecerunan. Jarak rasuk penahan akan bertambah dengan berkurangnya lebar sambungan antara blok, darjah kecerunan dan tebal pasir pengalas. Untuk membandingkan hasil ujikaji di makmal dengan hasil simulasi perilaku turapan blok konkrit model struktur menggunakan 3DFEM telah dibuat. Konsep pembinaan HALI termasuk rekabentuk, pembuatan, kalibrasi dan pengujian perlaksanaan juga dibentangkan. Sebelum HALI boleh diperkenalkan secara ekstensif bagi institusi penyelidikan jalan raya, alat tersebut diuji dengan mengenakan 10000 kali beban berulangan di atas turapan ujikaji bersaiz 1 m x 5.4 m. Pengujian tambahan, termasuk rintangan ricih, rintangan pengeliciran dan rintangan hentaman juga dijalankan untuk menambahkan pengetahuan kesan-kesan terhadap kelakuan turapan dibawah HALI.

TABLE OF CONTENTS

CHAPTER	TITLE	PAGE

LIST OF TABLES

LIST OF FIGURES

LIST OF SYMBOLS

D, d	-	Diameter
F	-	Force
W	-	Wheel Load
θ	-	Degree of Slope

LIST OF APPENDICES

CHAPTER 1

INTRODUCTION

1.1 Background

Concrete block pavement (CBP) was introduced in The Netherlands in the early 1950s as a replacement for baked clay brick roads (Van der Vlist 1980). The general worldwide trend towards beautification of certain city pavements and the rising cost of bitumen as a paving material, and the rapid increase in construction and maintenance cost have encouraged designers to consider alternative paving material such as concrete blocks. The strength, durability, and aesthetically pleasing paving block surfacing have made CBP ideal for many commercial, municipal, and industrial applications.

The construction of roads on steep slopes poses particularly interesting challenges for road engineers. The horizontal (inclined) forces exerted on the road surface are severely increased due to traffic accelerating (uphill), braking (downhill) or turning. These horizontal forces cause distress in most conventional pavements, resulting in opening of joints between blocks and poor riding quality. Experience has shown that CBP performs well under such severe conditions (sloping or turning). Although CBP performs well on steep slopes, there are certain considerations that must be taken into account during the design and construction of the pavement.

1.2   Problem Statement

Due to the angle of the slope, vertical traffic load will have a surface component exerted on the blocks in a downward direction. This force is aggravated by traction of accelerating vehicles uphill and braking of vehicles downhill. If unbalanced, these forces will cause horizontal creep of the blocks down the slope, resulting in opening of joints at the top of the paving blocks and weaving on the concrete block pavement.

1.3   Objectives

The objectives of the study are:

a. To study the performance of CBP deformation (horizontal creep) that is affected by horizontal force with variables; laying pattern, block thickness, block shape and joint width between blocks on flat surface.

b. To test and analyse various experimental of CBP in the laboratory with push-in tests for various degrees of slopes.

c. To make a comparative study of experimental results in laboratory with three dimensional finite element model (3DFEM) simulations.

d. To define the spacing of anchor beam on sloping road section based on degree of the slope, the effect of laying pattern, block thickness, bedding sand thickness and joint width between blocks.

e. To of developed laboratory scale accelerated loading test equipment named Highway Accelerated Loading Instrument (HALI).

1.4 Scope of The Study

The scopes of this study are:

a. Factors influencing the performance of Concrete Block Pavement (CBP) such as laying pattern, bedding sand thickness, block thickness, block shape and width of jointing sand were studied.

b. A simple laboratory-scale test was carried out to design the construction model of concrete block pavements and its performance.

c. A detail study for determining the combination of bedding sand thickness, shape and thickness of block, joint width and spacing of anchor beam for sloping road section was carried out.

d. A series of test was carried out to investigate the performance of HALI based on longitudinal and transverse rutting profiles, three-dimensional surface deformation, open joint width; skid resistance, impact resistance and shear resistance occurred on the test concrete block pavements.

1.5 Significance of Research

a. Studies on CBP for sloping road section are limited. This study contributes to the understanding of CBP performance on slopes.

b. The CBP failure caused by traction of traffic for sloping road section can be alleviated by using appropriate bedding sand thickness, block thickness, laying pattern and joint width.

c. The result of the study can be used as a recommendation of utilizing CBP for sloping road section.

d. Providing low cost, operational guideline and simple accelerated loading facility for road authorities and highway research institutions.

1.6   Thesis Organization

This thesis consists of eight chapters, and the contents of each chapter are explained as follows:

CHAPTER 1: This introductory chapter presents the background of the development of Concrete Block Pavement (CBP) used throughout world. It also explains the problem statement, objective, and scope of the study and the significance of this research.

CHAPTER 2: This chapter reviews the component of CBP, structure of CBP and construction techniques of CBP procedure is discussed step by step. The application of CBP on sloping road section is discussed with several effects i.e. degree of the slope, laying pattern, thickness of bedding sand, joint width between blocks and thickness of pavers. It also explains the detail construction of anchor beam.

CHAPTER 3: Chapter three presents the materials and testing methodology used in this research. Two materials used in this research, which are sand material for bedding and jointing sand (from Kulai in Johor) and block paving produced by Sun-Block company in Senai of Johor Bahru branch.

CHAPTER 4: Chapter four contains the interpretation of the experimental results. The effect of laying pattern, bedding sand thickness, joint width between blocks, paver's thickness, block shape and degree of the slope considered are analyzed.

CHAPTER 5: Chapter five presents the concrete block pavement (CBP) on sloping road section area with the use of the anchor beam on the CBP especially on the sloping road section, the spacing and position of the anchor beam based on the effects of joint width, bedding sand thickness, block thickness and block shape.

CHAPTER 6: This chapter presents the Three Dimensional Finite Element Model (3DFEM) of CBP construction using SOLID WORK and COSMOS Design STAR

programme package to compare with the push-in test of CBP experiment results in the laboratory.

CHAPTER 7: This chapter discuss the development process of HALI, experimental test results and its potential to the end user.

CHAPTER 8: Chapter eight presents general discussions about spacing of anchor beam on sloping road section based on degree of the slope with variables of the laying pattern effect, shape and thickness of block, bedding sand thickness and joint width between blocks. In addition, discussion of HALI development and performance was also presented.

CHAPTER 9: This chapter summarizes the main conclusions of this research and recommendations for future research.

CHAPTER 2

LITERATURE REVIEW

2.1   Introduction

Concrete block pavements (CBP) differ from other forms of pavement in that the wearing surface is made from small paving units bedded and jointed in sand rather than continuous paving. Beneath the bedding sand, the substructure is similar to that of a conventional flexible pavement. The material of concrete block pavement is rigid, but the underlying construction layer is flexible pavement as explained in an earlier literature. In the CBP, the blocks are a major load-spreading component.

The blocks are available in a variety of shapes and are installed in a number of patterns, such as stretcher bond, herringbone bond, basket weave bond, as shown in Figure 2.4. A review of existing literature revealed considerable differences in findings regarding the contribution of various block parameters to the structural capacity of pavement. This chapter discusses the experimental results of research conducted by previous researcher relating to the effect on pavement performance by changing variables such as shape and thickness of concrete block paver, thickness of bedding sand and width joint between blocks.

2.2   Structure and Component of Concrete Block Pavement

The surface of CBP comprises of concrete blocks bedded and jointed in sand. It transfers the traffic loads to the underneath layers of the pavement. The load-spreading capacity of concrete blocks layer depends on the interaction of individual blocks with jointing sand to build up resistance against applied load. The shape, size, thickness, laying patterns, etc., are important block parameters; these influence the overall performance of the pavement. Some early plate load studies (Knapton 1976; Clark 1978) suggested that load-spreading ability of the pavement was not significantly affected by block shape. Later accelerated traffic studies (Shackel 1980) and plate load studies (Shackel *et al.* 2000) established that shaped (dents) blocks exhibited smaller deformation than rectangular blocks of a similar thickness installed in the same laying pattern under the same applied load. Knapton (1996) found pavement performance was essentially independent of block thickness, whereas Clark (1978) reported a small improvement in pavement performance with an increase in block thickness. Shackel (1980), Miura *et. al.,* (1984) and Shackel *et al.* (1993) claimed that an increase in block thickness reduced elastic deflection and the stress transmitted to the sub-base.

Shackel (1980) reported that the load-associated performance of block pavements was essentially independent of the size and compressive strength of the blocks. Knapton (1976) found that laying pattern did not significantly affect the static load-spreading capacity of the pavement. From plate load studies, Miura *et al.* (1984) and Shackel *et al.* (1993) have reported that, for a given shape and thickness, blocks laid in a herringbone bond exhibited better performance than blocks laid in a stretcher bond.

The load-distributing ability of the concrete block surface course increases with increasing load (Knapton 1976; Clark 1978; Miura *et al.* 1984). This is manifested as a decrease in stress transmitted to the sub-base below the loaded area and a decrease in the rate of deformation with the increase in load. Shackel (1980),

Knapton and Barber (1979), Barber and Knapton (1980), Miura *et al*. (1984), and Jacobs and Houben (1988) found that, in their early life, block pavements stiffen progressively with an increase in the number of load repetitions. This is manifested as an increase in the load-spreading ability of blocks. However, Shackel (1980) clarified that the progressive stiffening did not influence the magnitude of resilient deflections of CBP. Jacobs and Houben (1988) and Rada *et al*. (1990) reported that the elastic deflections decrease with an increase in the number of load repetitions rather than an increase, as observed in flexible and rigid pavements. It was felt that the phenomenon of block interaction under applied load needed investigation in the light of the above discussion. Such tests could then provide insights into load-spreading ability and other structural characteristics of the block pavements.

The factors effecting performance of CBP is shown in Table 2.1 and has provided the necessary inputs for developing comprehensive structural design methods.

Table 2.1   Factors affecting the performance of CBP *(Source, Shackel 2003).*

Pavement Component	**Factors Affecting Performance under Traffic**
Concrete Block Pavers	• Paver shape • Paver thickness • Paver size • Laying pattern • Joint width
Bedding and Jointing Sands	• Sand thickness • Grading • Angularity • Moisture • Mineralogy
Base-course and Sub-base	• Material type • Grading • Plasticity • Strength and durability
Sub-grade	• Soil Type • Stiffness and strength • Moisture regime

2.2.1   Concrete Block Paver

Blocks are fully engineered products manufactured in the factory to give consistency and accuracy. The resulting interlocking characteristics of concrete block paving give it a distinct advantage over other forms of surface. Lay on a granular bedding sand and with an edge restraint, individual blocks interlock with each other to act together, distributing large point loads evenly. Concrete block paving can be used immediately after the laying procedures have been completed and require only minimal maintenance. The general worldwide were trend towards beautification of certain city pavements, the rising cost of bitumen as a paving material, and the rapid increase in construction and maintenance cost have encouraged designers to consider alternative paving material such as concrete blocks. The strength, durability, and aesthetically pleasing surface of pavers have made CBP ideal for many commercial, municipal, and industrial applications (Van der Vlist 1980).

2.2.1.1 The Effect of Block Shape

Three categories of block shapes were selected (Shackel, 1993). These were rectangular, uni-décor and uni-pave shapes as shown in Figure 2.1. These block types have the same thickness and nearly same plan area. Blocks were laid in stretcher bond for each test. The results obtained are compared in Figure 2.2.

Rectangular	Uni-décor	Uni-pave
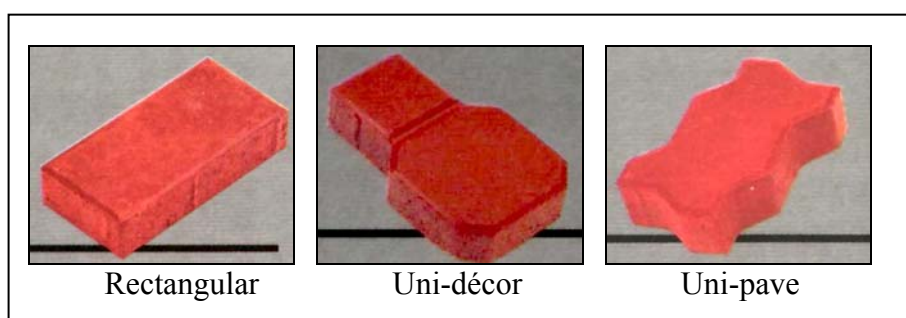
Figure 2.1   The rectangular, uni-décor and uni-pave block shapes *(Lilley, 1994)*

The shape of the load deflection path is similar for two block types. The deflections are essentially the same for rectangular shape and uni-pave shape. Smaller deflections are observed for uni-pave shape compared to rectangular shape. In general, shaped (dents) blocks exhibited smaller deformations as compared with rectangular and square blocks (Panda and Ghosh, 2002). Complex shape (uni-pave) blocks have larger vertical surface areas than rectangular or square blocks of the same plan area.
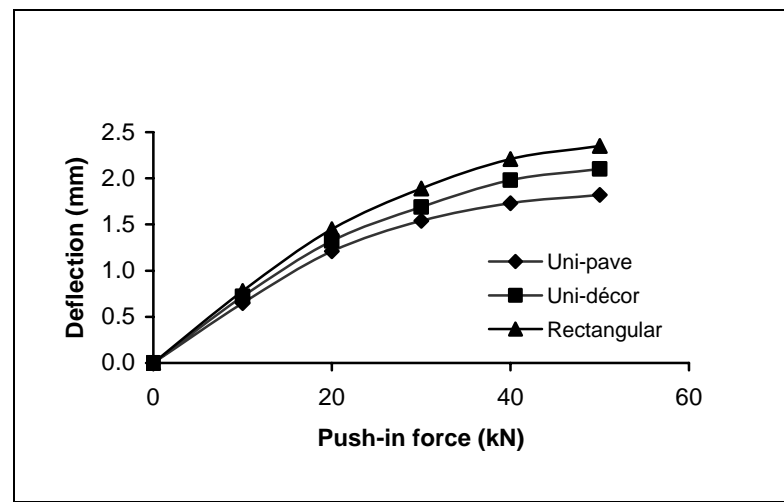
Figure 2.2 The effects of block shape on deflection (Shackel, 1993)

Consequently, shaped blocks have larger frictional areas for load transfer to adjacent blocks. It is concluded that the shape of the block influences the performance of the block pavement under load. It is postulated that the effectiveness of load transfer depends on the vertical surface area of the blocks. These results obtained are consistent with those found in earlier plate load tests by Shackel *et al*. (1993).

2.2.1.2 The Effects of Block Thickness

The rectangular shape blocks of the same plan dimension with three different thicknesses were selected for testing. The blocks thickness 60 mm, 80 mm, and 100 mm. Blocks were laid in a stretcher bond pattern for each test. The shapes of the load deflection paths are similar for all blocks thickness (Clark, 1978).
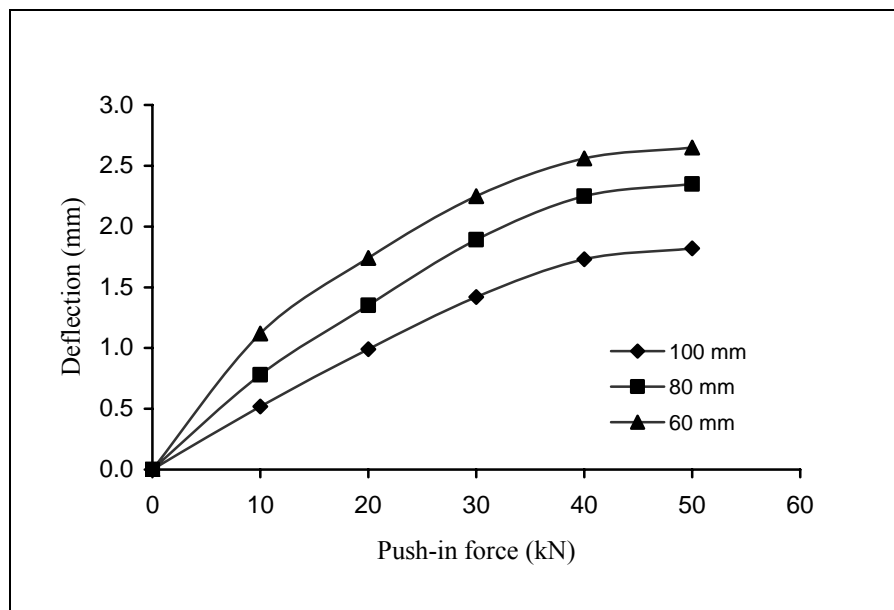
Figure 2.3   The effect of block thickness on deflection of block pavement *Sources: Clark (1978), Panda and Ghosh (2002)*

An increase in thickness from 60 to 100 mm significantly reduces the elastic deflection of pavement. The comparison is shown in Figure 2.3. Thicker blocks would provide a higher frictional area. Thus, load transfer will be high for thicker blocks.

The thrusting action between adjacent blocks at hinging points (Panda and Ghosh 2001) is more effective with thicker blocks. Thus, deflections are much less for thicker blocks. The combined effect of higher friction area and higher thrusting action for thicker blocks provides more efficient load transfer. Thus, there is a

significant change in deflection values from increasing the thickness of blocks. It is concluded that the response of the pavement is highly influenced by block thickness. The results obtained are similar to that found in earlier plate load tests by Shackel *et al*. (1993).

2.2.1.3 The Effect of Laying Pattern

Rectangular shape blocks were laid in the test pavement in three laying patterns: stretcher bond, herringbone 90^0 bond, and herringbone 45^0 bond as shown in Figure 2.4.

| Stretcher Bond | Herringbone 90° Bond | Herringbone 45° Bond |
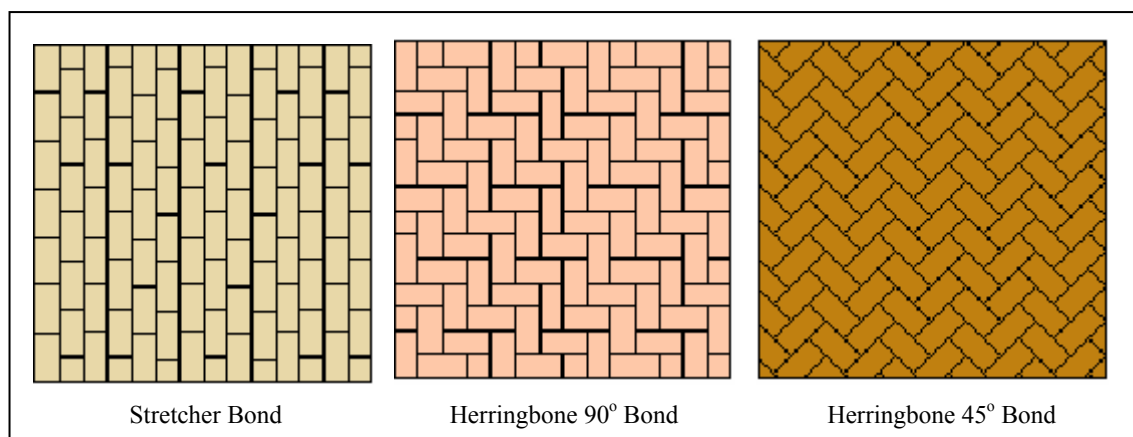
Figure 2.4   Laying patterns of CBP

The shapes of the load deflection paths are similar and the deflections are almost the same for all the laying patterns, as shown in Figure 2.5a and 2.5b. The friction areas and thickness of blocks used for all three laying patterns are the same. Thus, the same elastic deflections are observed. It is established that deflections of block pavements are independent of the laying pattern in the pavement (Panda and Gosh, 2002). The finding is inconsistent with that reported by Shackel *et al.* (1993).
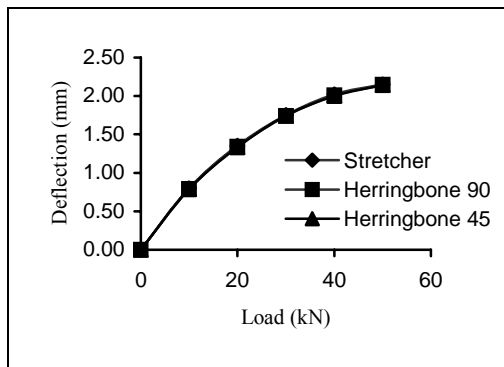
Figure 2.5a The effect of laying pattern
Source: Panda (2002)
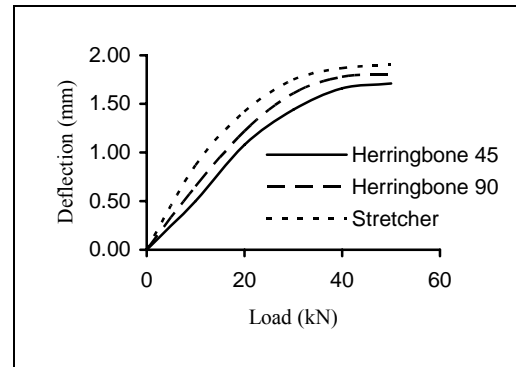
Figure 2.5b The effect of laying pattern
source: Shackel (1993)

The test pavements were conducted with load is gradually increased from 0 to 51 kN and then released slowly to 0 kN (Panda and Ghosh, 2002). The deflections were measured at each load interval, and for the remaining cycles, the deflections are measured at the 0 and 70 kN load levels (Shackel, 1993).

2.2.1.4 Optimal Choice of Block Shapes and Laying Patterns

The design guidelines direct the designer for the optimal selection of paver shapes and laying patterns was discussed. Due to the international controversy in this respect, a distinction is made between structural and functional aspects. The structural aspects for interlocking paver shapes and bi-directional laying patterns, while the functional aspects permits aesthetics considerations and self locating laying techniques. An emphasis is given to the control of optimal joint width between the blocks (Houben, 1996).

2.2.2 Bedding and Jointing Sand

The bedding sand layer in CBP is included to provide a smooth, level running surface for placing the blocks (Hudson and Sidaharja, 1992).. European practices (Eisenmenn and Leykuf 1988; Lilley and Dowson 1988; Hurmann 1997) specify a bedding sand thickness after compaction of 50 mm, whereas compacted bedding sand thickness of 20 to 30 mm is used in United States (Rada *et al.* 1990) and Australia (Shackel *et al* 1993). Simmons (1979) recommended a minimum compacted sand depth of 40 mm to accommodate free movement of blocks under initial traffic. Mavin (1980) specified a compacted bedding sand depth of 30 ± 10 mm, keeping 10 mm tolerance on sub-base.

Jointing sand is the main component of CBP, and it plays a major role in promoting load transfer between blocks ultimately in spreading the load to larger areas in lower layers. Very few studies have been carried out concerning the width of joints and the quality of jointing sand for use in CBP. There are even fewer explanations of the behaviour of sand in the joints. For optimum load spreading by friction, it is necessary to provide uniform, narrow, and fully filled joints of widths between 2 and 4 mm (Shackel *et al.* 1993; Hurman 1997). Knapton and O'Grady (1983) recommended joint widths between 0.5 and 5 mm for better pavement performance. Joint widths ranging from 2 and 8 mm are often used, depending upon the shape of blocks, laying pattern, aesthetic considerations and application areas.

In most of the pavements, the sand used for bedding course is also used in joint filling (Lilley 1980; Hurmann 1997). As reported by Shackel (1980), a finner jointing sand having a maximum particle size of 1.18 mm and less than 20 % passing the 75 μm sieve has performed well. According to Knapton and O'Grady (1983), large joints require coarser sand and tight joints require finer sand for good performance of pavement. The British Standards 1973, passing the 2.36 mm sieve as the most effective for jointing sand. Panda and Ghosh (2001) studied the dilatancy and shearing resistance of sand and recommended using coarse sand in joints of

CBP. Livneh *et al.* (1988) specified a maximum particle size of 1.2 mm and 10 % passing 75 μm for jointing sand.

Regarding the grading of bedding sand, Lilley and Dowson (1988) imposed a maximum limit on the percentage passing the 75, 150, and 300 μm sieves as 5, 15, and 50, respectively. Sharp and Simons (1980) required a sand with a maximum nominal size of 5 mm, a clay/silt content of less than 3 %, and not greater than 10 % retained on the 4.75 mm sieve. Single sized grain and/or spherical shaped grain sand are not recommended. Livneh *et al.* (1988) specified a maximum particle size of 9.52 mm with a maximum limit of 10 % passing the 75 μm sieve.

Table 2.2   Grading requirements for bedding sand and jointing sand

Sieve Size	Percent Passing For Bedding Sand	Percent Passing For Jointing Sand
3/8 in. (9.5 mm)	100	-
No. 4 (4.75 mm)	95 to 100	-
No. 8 (2.36 mm)	80 to 100	100
No.16 (1.18 mm)	50 to 85	90 – 100
No. 30 (0.600 mm)	25 to 60	60 – 90
No. 50 (0.300 mm)	10 to 30	30 – 60
No. 100 (0.150 mm)	5 to 15	15 – 30
No. 200 (0.075 mm)	0 - 10	5 – 10

(Sources: British Standard 882, 1201; Part 2: 1989, London).

2.2.2.1 The Effect of Bedding Sand Thickness

Barber and Knapton (1980) have reported that, in a block pavement subjected to truck traffic, a significant proportion of the initial deformation occurred in the bedding sand layer which had a compacted thickness of 40 mm. Similar results have been reported by Seddon (1980). These investigations tend to confirm the findings of

the earlier Australian study (1989) which demonstrated that a reduction in the loose thickness of the bedding sand from 30 mm to 50 mm was beneficial to the deformation (rutting) behaviour of block pavements. Here an almost fourfold reduction in deformation was observed.

Experience gained in more than twenty-five heavy vehicle simulator (HVS) traffic tests of prototype block pavements in South Africa has confirmed that there is no necessity to employ bedding sand thickness greater than 30 mm in the loose (initial) condition, which yields a compacted typically close to 20 mm reported by Shackel and Lim (2003).

2.2.2.2 The Effect of Sand Grading

Recently in South Africa a series of HVS accelerated trafficking tests of block pavements has been carried out with the prime objective of determining the desirable properties of the bedding and jointing sands. Here pavements utilizing block uni-pave shape laid in herringbone bond have been constructed using a loose thickness of 70 mm of sand laid over a rigid concrete base. After compacted, the sand layer thickness was reduced to between 45 and 55 mm depending on the sand and having a variety of grading, (Shackel, 1989).

It has been found that, under the action of a 40 kN single wheel load, up to 30 mm of deformation could be induced in the sand layer within 10.000 wheel passes. This clearly demonstrates the need to select the bedding sand with care. However, it has been determined that provided the grading of the sand falls within the limits recommended by Morrish (1980), a satisfactory level of performance can be achieved under traffic. Here, rutting deformations typically between 1.5 and 4 mm have been recorded after 10.000 wheels passes where the same sand has been used

for both bedding and jointing between blocks. Where, however, finer sand typically having a maximum particle size smaller than 1.0 mm has been used as jointing sand, an improvement in performance has been observed with the total deformations typically being less than 2 mm after 10.000 load repetitions. Generally, for the bedding sand, it appears that, within the limits, coarse sands tend to yield better performance than fine sands and that angular sands exhibit a marginally better performance than round sands.

Unacceptable levels of performance have been observed where the proportion of fine material smaller than 75 μm in the sand exceeds about 15 %. In sands with clay contents between 20 and 30 %, substantial deformations (up to 30 mm) have been observed especially where the sands are wet reported by Interpave (2004).

2.2.2.3 The Effect of Bedding Sand Moisture Content

Experience gained in accelerated trafficking studies in both Australia and South Africa has shown that adequate compaction of the sand bedding can be achieved at moisture contents typically lying within the range from 4 % to 8 % with a value of 6 % representing a satisfactory target value. However, Seddon (1980) has recently suggested that, for optimum compaction of the sand layer, the moisture content should be close to saturation. For sands whose grading complies with the limits set out, the effect of water content appears to have little influence under traffic. It was conducted by running HVS trafficking test whilst maintaining the sand in a soaked condition, nor has pumping been observed. However, the bedding sand contained greater than 15 % of day, the addition of water to the produce substantial increases in deformation accompanied by pumping. For this reason, the use of sands containing plastic fines should be avoided in the bedding layer, Shackel (1998). Limited experimental evidence suggests that such sands are nevertheless suitable for

jointing sands both in respect of means of their mechanical properties and as a means of inhibiting the ingress of water into the joints.

2.2.2.4 Width of Jointing Sand

The sand was used in bedding course with a 50 mm thickness for all of these experiments. Figure 2.6 shows the response of pavement deflection for design joint widths of 2 mm, 3 mm, 5 mm, 7 mm and 9 mm with same quality of sand (Hasanan, 2005). As the joint width decreases, the deflection of the pavement also decreases.
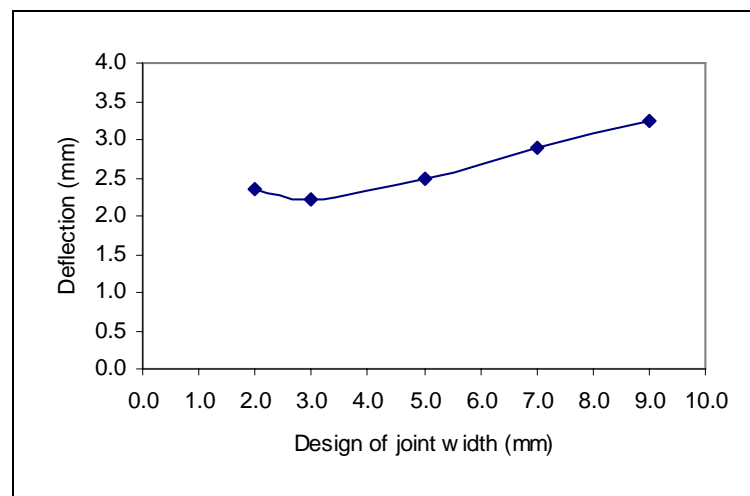
Figure 2.6 The response of pavement deflection for design joint widths

Pavement deflection decreases of up to a certain point and then increases slightly with a decrease in joint width, i.e., there is an optimal joint width. The optimum joint widths for these experiments were 3 mm, respectively.

➢   The higher the joint width, the normal stiffness of the joint will be lesser. This will lead to more rotations and translations of blocks. Thus, there will be more deflection under the same load for thicker joints.

➢   For joint widths less than the optimum, a slight increase in deflections were observed. Some of the grains coarser than the joint width were unable to enter inside. This has been observed during filling sand in joints. A large amount of sand remained outside the joint showing sand heaps on the block surface. The coarse grains of sand choked the top surface of joints and prevent movement of other fine grains into the joint.

There might be loose pockets or honeycombing inside the joint. The joint stiffness decreases and in turn reflects slightly higher deflections. The results that decrease in joint width increases the pavement performance and the concept of optimum joint width well agree with that of a series of static load tests.

2.2.2.5 Filling of Jointing Sand

Shackel (2003), the compaction might not be fully effective for a higher thickness of bedding sand during vibration. The bedding sand rises through the joints to small heights and wedges in between the blocks. Figure 2.8 shows the rise of sand through the design joints width of 3 mm, 5 mm and 7 mm with varying thickness of bedding sand. The rise of sand increases with increase in thickness of bedding sand. The wedging of these sands absorbs the major part of applied vibration energy and transfers less to the bedding sand below. As a result, the bedding sand is not fully compacted for higher thickness.
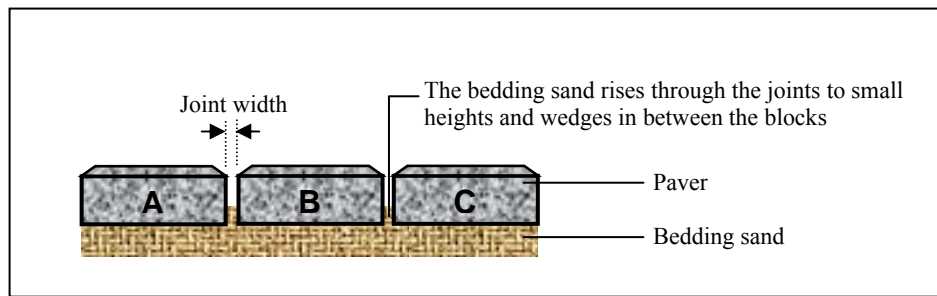
Figure 2.7 The rises of bedding sand between the blocks

Consequently, some compaction of bedding sand takes place under load and thus shows more deflection in the test pavements. The higher the bedding sand thickness, the more the deflection will be.
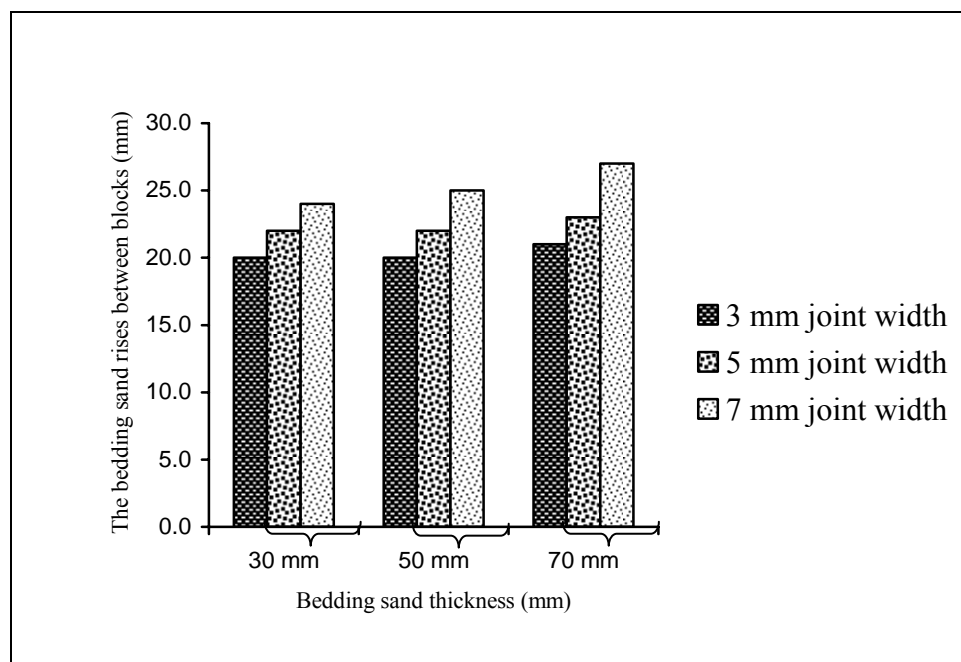
Figure 2.8 The comparison bedding sand rises in various widths joint with bedding sand thickness *(Knapton and O'Grady, 1983).*

The findings of this study are contradictory to those reported by Knapton and O'Grady (1983). Who found that an increase in bedding sand thickness produced a proportionate increase in load-carrying capacity of pavement. As the pavement response is nearly for 50 mm thickness of bedding sand can be recommended to use

in the field. But this depends on other factors, such as required level in sub-base tolerance and rise of bedding sand through the joints. Also, there should be a sufficient depth of bedding sand for deflection of pavements under load. Rise of bedding sand is essential to induce interlock.

2.2.3   Edge Restraints

The paved area must be restrained at its edges to prevent movement, either of the whole paved area or individual blocks (Huurman, 1997). Edge restraints resist lateral movement, prevent rotation of the blocks under load and restrict loss of bedding sand material at the boundaries. Edge restraints should be laid at all boundaries of the block-paved area including where block paving abuts different flexible materials, such as bituminous bound material. They should be suitable for the relevant application and sufficiently robust to resist displacement if likely to be overrun by vehicles. It may be necessary to extend sub-layers to support the edge restraint together with any base and hunching. Compaction of pavement layers near edge restraints should be delayed until any concrete bed and hunching has gained sufficient strength to prevent movement of the edge restraint.

2.2.4   Sub-base and Base Course

Sub-Base: This is the optional layer underlying the base-course. Sub-base material usually be lower grade than the base-course, Class 3 or better with a PI (Plasticity Index) not exceeding 10. The sub-base should be compacted to 95 %, the thickness of which must be consistent with the capabilities of the compaction equipment being used. This may require compacting equipment with a higher capacity than a standard

plate compactor. The sub-base may be a cement-stabilized material, British Standard (1973).

Base-Course: The base-course should be a Class 1 material with a PI not exceeding 6. It should be compacted to 98 %. Again this may require high capacity compaction equipment and the base-course may be cement stabilized material (British Standard, 1989).

2.2.5   Sub-grade

The bearing capacity of the sub-grade (or natural ground) must be determined as a basis for the overall design. The measure used is the California Bearing Ratio (CBR) which is usually determined by indirect means such as the dynamic cone penetrometer. Laboratory-soaked CBR should be used for clay sub-grades. Clay sub-grades in particular should be drained to ensure the design CBR accurately reflects that in the field. Sub-grades should be compacted prior to the placement of road-base materials (Shackel, 1993).

2.3   Compaction

The bedding sand material and blocks should be compacted using a vibrating plate compactor. Some blocks may require a rubber or neoprene faced sole plate to prevent damage to the block surfaces (Interpave, 2004).

Interlocking Concrete Pavement Institute (ICPI, 2000) reported, the block paved area should be fully compacted as soon as possible after the full blocks and cut blocks have been laid, to achieve finished pavement tolerances from the design level of ± 6 mm. Adjacent blocks should not differ in level by more than 2 mm and, when measured with a 3 m straight edge, there should be no surface irregularity (i.e. depression or high point) greater than 10 mm. No compaction should be carried out within 1.0 m of an unrestrained edge.

- Design level tolerance ± 6 mm

- Maximum block difference 2 mm

- Maximum under straight edge 10 mm

2.4   Load-Deflection Behaviour

The general load-deflection behaviour is irrespective of block shape, size, strength, thickness, and laying pattern that the load deflection profile has a similar shape. It is seen that the pavement deflection increased in a nonlinear manner with increasing load (Panda and Ghosh, 2002). An interesting observation is that the rate of deflection decreases with increasing load within the range of magnitude of load considered rather than increases, which is the case with flexible and rigid pavements. Increase in the load has caused the rotation of individual blocks to increase. This will lead to an increase in the translation of blocks and in turn an increase in the thrusting action between adjacent blocks at hinging points (Panda and Ghosh 2001). As a result, the rate of deflection of the pavement decreases. It is established that the load-distributing ability of a concrete block surface course increases with increasing load (within the range of magnitude of considered in this study). The results obtained are similar to that established in earlier plate load tests by Knapton (1976), Clark (1978), and Miura *et al*. (1984).

A type of interlock; vertical, rotational and horizontal of CBP cross section is shown in Figure 2.9, CBP is constructed of individual blocks of brick-sized units, placed in patterns with close, unmortared joints on a thin bed of sand between edge restraints overlaying a sub base. The joint spaces are then filled with sand. The blocks are available in a variety of shapes and are installed in a number of patterns, such as stretcher bond, herringbone bond, etc. The load spreading and other structural characteristics of the concrete blocks were inconsistent with different findings in respect to such factors as block shape, thickness, and laying pattern. The results of an experimental programme conducted to investigate the effects of changing parameters of bedding and jointing sand on pavement performance. A laboratory-scale model was devised to study these parameters using steel frame loading tests reported by Shackel (1988).
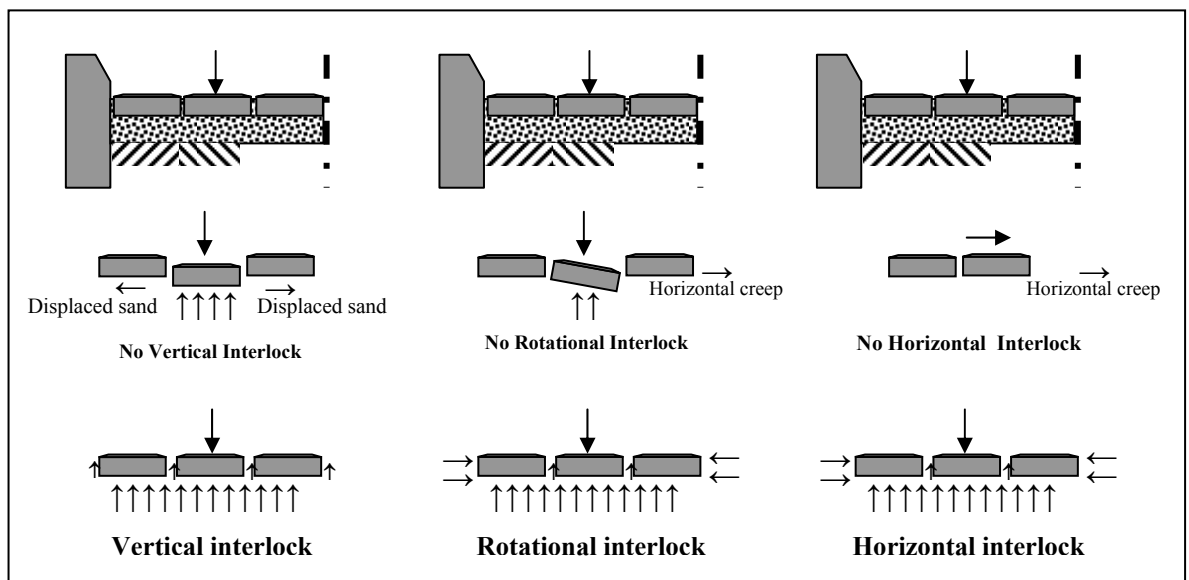
Figure 2.9 Types of CBP interlock: vertical, rotational and horizontal *(Shackel, 1988)*

2.5   Effects of Load Repetition

(Panda and Ghosh, 2002) reported that the rectangular blocks were laid in a herringbone pattern. The test pavements were subjected to 250 cycles of loading and unloading, and the resulting deflections were measured. In each cycle, load is gradually increased from 0 to 51 kN and then released slowly to 0 kN. The total time of loading and unloading operation for each cycle was within 30 seconds. For the first five cycles, the deflections were measured at each load interval, and for the remaining cycles, the deflections were measured at the 0 and 51 kN load levels. For each load repetition, the deflections during loading and recovery of deflections during unloading are determined. It may be seen that the response is nonlinear.

The deflection is not fully recovered. In other words, permanent residual deformations develop due to load repetition. During loading, additional compaction of sand under blocks occurs, and some part of the energy is lost in that way. As a result, the recovery is not full. It is the relationship of deflection during loading and its recovery with number of load repetitions. It may be observed that both deflection and recovery decrease with an increase in number of load repetitions. After about 150 load repetitions, the deflection and recovery are nearly the same; i.e., the recovery is full. In other words, the pavement acquires a fully elastic property. This is due to the fact that the additional compaction of bedding sand gradually increases with increase in load repetition. After a certain number of repetitions, the compaction of the underlying layers reaches its full extent and no energy is lost during additional loadings. As a result, the deflection and recovery become the same. Thus, it is established that block pavements stiffen progressively with an increase in the number of load repetition Panda and Ghosh (2002).

In accelerated traffic tests by Shackel (1980), the range of the number of load repetitions required to achieve fully elastic property varies from 5,000 to 20,000 depending upon the magnitude of load (24 – 70 kN). The bedding sand is compacted under the wheel load. Adjacent to the loading area, the surface of the pavement

bulges out. Thus, the bedding sand loosens. Areas under the wheel track are subjected to alternate bulging and compression as the wheel moves. For plate load tests (Shackel,1980) the load is applied at the same area and the bulging effect is nil, so it took only 150 kN load repetitions to achieve the fully elastic property.

2.6   Mechanism of Paver Interlock

Even block pavements which are judged to be well laid typically exhibit small rotations of the pavers relative to one another. These rotations develop both during construction and under traffic. (Shackel and Lim, 2003). Such small movements are almost imperceptible to the naked eye but can be measured using profilometers to map the surface of the paving. Measurement shows the rotations are usually less than 10° and are associated with surface displacements typically less than 5 mm. However, because concrete pavers are manufactured too much higher and more consistent dimensional tolerances than any other form of segmental paving they tend to be laid so that the joints between the pavers are consistently narrow and relatively uniform in width. For example, in Australia, it is customary to require paving to consistently achieve joint widths within the range 2 to 4 mm and this proves relatively easy to attain in practice provided normal tolerances are maintained during paver manufacture. With such narrow and consistent joints rotation of a paver soon results in it wedging against its neighbours as shown schematically in the cross-section, Figure 2.11 As shown in this figure, the wedging action caused by rotation of paver B around a horizontal axis leads to the development of horizontal forces within the paving.

The wedging action illustrated in Figure 2.13 explains why it is commonly observed that paver surfaces can push over inadequate edge restraints and make the reinstatement of trenches difficult or impossible unless the surrounding paving is restrained from creeping inwards (Shackel, 1990). More importantly, it also explains

why pavers act as a structural surfacing rather than merely providing a wearing course (Shackel, 1979, 1980 and 1990). It is therefore of interest to examine the factors and forces contributing to the development of horizontal creep between pavers within concrete segmental paving. These factors include the paver shape and the laying pattern (Shackel, 1993).
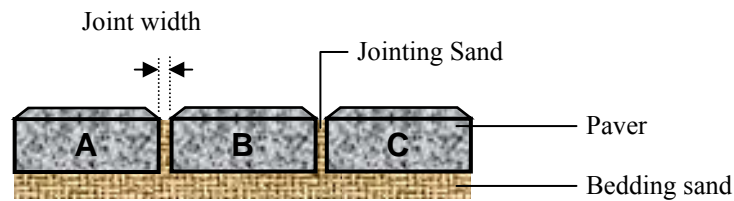
Figure 2.10   Components of concrete block pavement *(Shackel, 2003)*
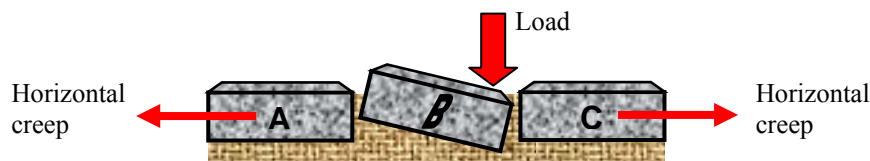
Figure 2.11   Rotation of paver B causing outward wedging of pavers A and B *(Shackel, 2003)*

The effects of paver shape can be understood by considering the effects of paver rotation upon the wedging together of the pavers. For the case of rectangular pavers this is illustrated schematically in Figure 2.11, if paver B is subject to rotation about a horizontal axis through its mid point then it is free to slide upon pavers A and C and will only push on pavers in line with the rotation such as paver D in Figure 2.12. Wedging therefore occurs only in that direction. The CBP on sloping road section, longitudinal horizontal creep is more critical than transverse. The CBP on sloping road section, the horizontal creep on longitudinal direction is more than transverse.
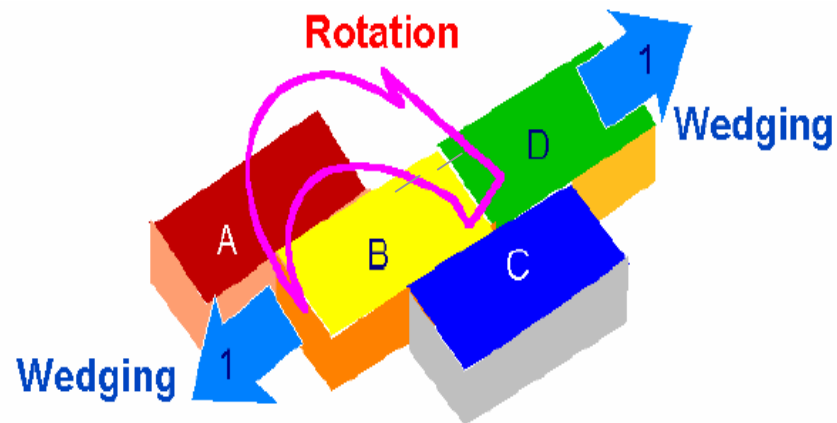
Figure 2.12 Effects of rotation on the wedging action of rectangular pavers laid on stretcher bond *(Shackel, 2003)*

By contrast, if the same rotation is applied to a shaped paver, then, as shown in Figure 2.13, paver B cannot rotate without pushing pavers A and C away. Consequently wedging now develops in the two directions shown by arrows 1 and 2 even though the applied rotation remains uni-directional. This provides a simple explanation why shaped pavers have been reported to exhibit higher module and better in-service performance than rectangular pavers (Shackel, 1979, 1980, 1990 and 1997).
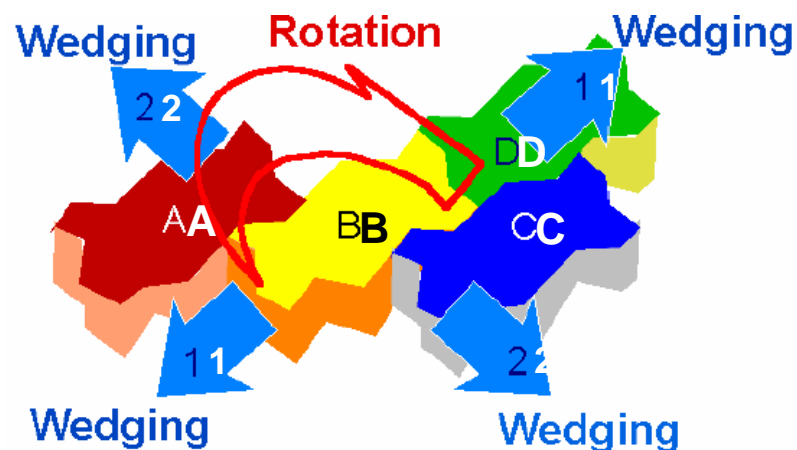
Figure 2.13 Effects of rotation on the wedging action of shaped pavers *(Shackel, 2003)*

On the basis of both tests and experience, engineers have long known that paving installed in herringbone patterns performs better than when laid in the stretcher laying pattern on interlocking neighbour of blocks, shown in Figure 2.13. Again, some explanation of this can be obtained by considering the effects of paver rotation. Figure 2.14 shows this case for rectangular pavers.
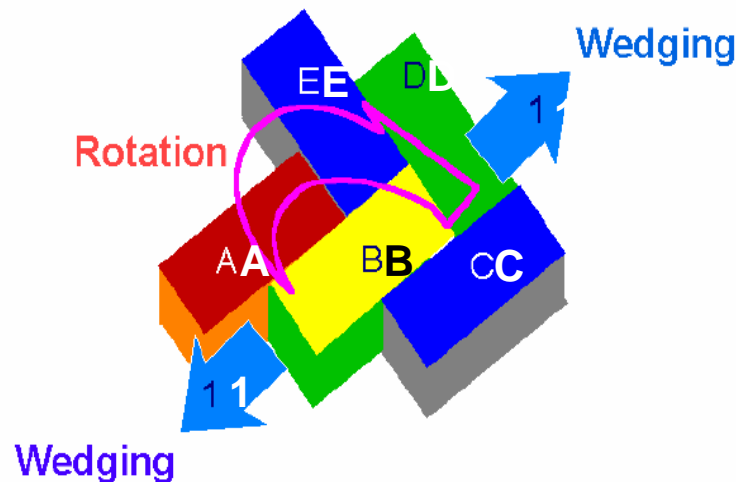
Figure 2.14   Effects of paver rotation on paving lay in herringbone 90° bond
(Shackel, 2003)

From Figure 2.14 it may be seen that whilst, as in the case of stretcher bond, rotation of paver B can still occur without horizontally displacing pavers A and C, the movement of paver B about a horizontal axis will now induce some rotation of paver D around a vertical axis. This is in addition to developing horizontal wedging as shown by the arrows 1. This will tend to increase the wedging action throughout the paved surface and provides some explanation why herringbone patterns perform better than stretcher bond.

Huurman (1997), Houben and Jacobs (1988) have claimed that, once rectangular pavers are installed in herringbone pattern, they perform in a manner similar to shaped pavers. This is, however, contradicted by the results of both traffic and laboratory load tests (Shackel, 1979, 1980, 1990). The most likely explanation for this is that, as shown in Figure 2.15, wedging in directions both along and across the axis of rotation remains the inevitable consequence of paver rotation irrespective

of the laying pattern. Here the choice of herringbone bond merely adds additional wedging movements to the paving surface because of the induced rotations of the pavers about vertical axes.
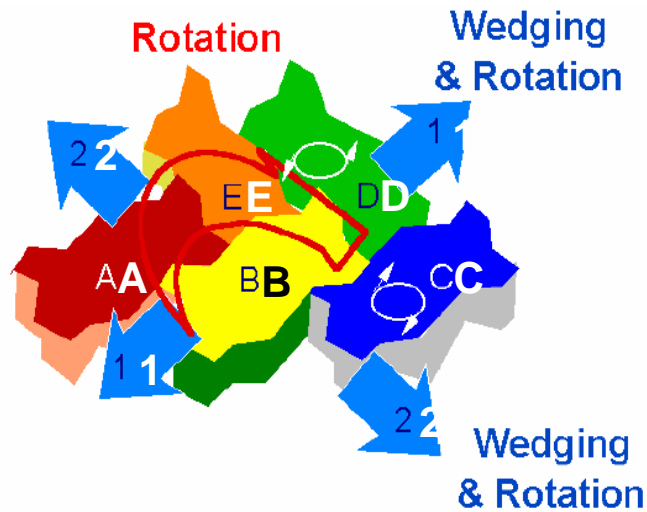
Figure 2.15 Effects of paver rotation on uni-pave shaped pavers lay in herringbone bond *(Shackel, 2003)*

The explanations of the effects of paver shape and laying pattern given above are complex, because paver rotations are seldom confined to movements about just a single axis. Moreover, no account is taken of the joint width or the nature of the joint filling material. It might be argued that because most pavers are now fitted with spacer nibs the importance of the joint width and the joint filling material is minimal. However, it is usually found that the actual joint widths measured in pavements are bigger than the spacers.

2.7   The Role of the Joints in Pavement Interlock

In describing and modelling the behaviour of segmental paving many hypotheses have been advanced to explain the role of the joints.   The movements that are likely to occur at the joints in segmental paving are shown schematically in Figure 2.16.   These comprise movements caused by rotations and linear displacements of the pavers. In practice the movements shown as (a) and (d) in Figure 2.16 are less likely to occur than the other movements because they imply net elongation of the pavement.
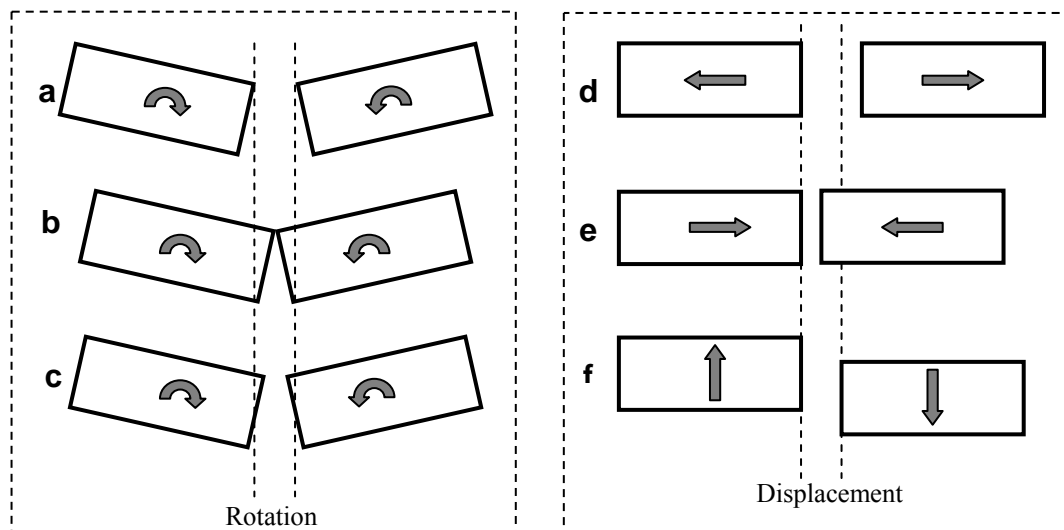
Figure 2.16   Movement of blocks at the joints, *Shackel (2003)*

This will only occur when the pavement experiences rutting or heave i.e. some departure from the as-installed profile. In normal service the movements of pavers are likely to comprise combinations of both rotations and translations. In this it can be said, for example, that movement (c) in Figure 2.16 represents the combined effects of movements (b) and (f) or (a) and (e).

To measure of rotations and lipping movement between adjacent pavers were shown in Figure 2.16 (f). However, horizontal displacements such as those illustrated as Figure 2.16 (d) and (e) can only be measured directly. Nevertheless, some

estimates of the strains in the jointing material can be obtained. Provided the stiffness of the jointing sand is known the strains can then be used to estimate the stresses in the material. Accordingly, to study the role of the jointing sand, measurements of typical jointing sand properties were combined and joint width of a range of concrete segmental pavements. The principal objective of this work was to estimate what magnitudes of force might be generated within the joints, Shackel (2003).

2.8   The Concrete Block Pavement on Sloping Road Section Area

Concrete Block Paving (CBP) differs from other forms of surfacing in that it comprises small segments and therefore is crisscrossed by a network of close spaced joints filled with sand. This means CBP is permeable and drainage of the surface and underlying layers is important. There is limited full scale testing wide world but from a study conducted by CMA (2000).

Similarly using 10 % of lime or 6 % bentonite to the jointing sand can inhibit infiltration. Generally no attempt is made to seal the joints hence attention should be directed towards reducing the consequences of water infiltration, particularly during the early life of the pavement. In practice care must be taken to select bedding sands not susceptible to water or seal the base if it comprises unbound granular materials or select base materials bound and waterproofed with cement, lime or bitumen. The management of water runoff and infiltration becomes therefore a critical aspect that will affect the performance and integrity of the CBP. Good surface and subsoil drainage is essential for satisfactory pavement performance. Drainage needs to be considered during the design, specification and construction phases of a project.

2.8.1 Basic Theory of Slope

A block at rest on an adjustable inclined plane begins to move when the angle between the plane and the horizontal reaches a certain value θ, which is known as the angle of repose. The weight W of the block can be resolved into a component F parallel to the plane and another component N perpendicular to the plane. Figure 2.17 the magnitudes of F and N are:

$F = W \sin \theta$

(2.1)

$N = W \cos \theta$

(2.2)

When the block just begins to move, the downward force along the plane F must be equal to be the maximum friction force μN of static friction, so that:

$F = \mu N$

(2.3)

$W \sin \theta = \mu W \cos \theta$

$\mu = \sin \theta / \cos \theta = \tan \theta$

Where F (direction force of the slope) and N (upright force of the slope)
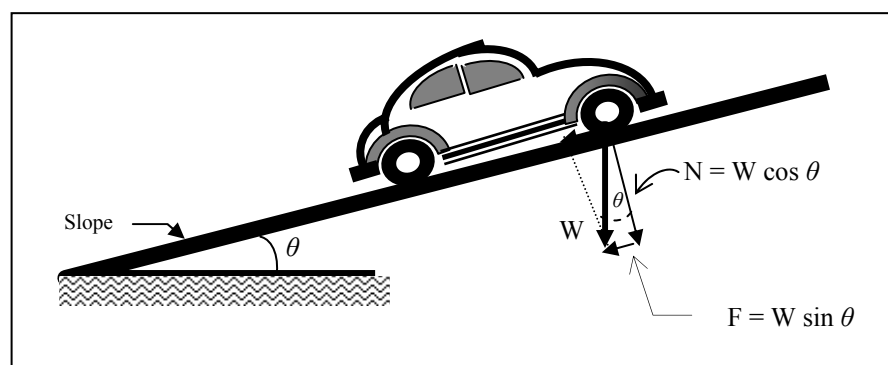
Figure 2.17   The magnitude of Force (F), Normal (N) and Load (W)

2.8.2   Construction of Steep Slopes

The construction of roads on steep slopes poses particularly interesting challenges for road engineers. The horizontal (inclined) forces exerted on the road surface are severely increased due to traffic accelerating (uphill), breaking (downhill) or turning. These horizontal forces cause distress in most conventional pavements, resulting in rutting and poor riding quality. Experience (CMA, 2000) has shown that concrete block paving (CBP) performs well under such severe conditions.

2.8.3   Anchor Beam

It is common practice to construct edge restraints (for transverse creep) and anchor beams (for longitudinal creep) along the perimeter of all paving, to contain the paving and prevent horizontal creep and subsequent opening of joints. Due to the steepness of the slope, the normally vertical traffic loading will have a surface component exerted on the blocks in a downward direction. This force is aggravated by traction of the accelerating vehicles up the hill and breaking of vehicle down the hill. If uncontained, these forces will cause horizontal creep of the blocks down the slope, resulting in opening of joints at the top of the paving. An anchor beam at the lower end of the paving is necessary to prevent this creep. Figure 2.19 shows a typical section through an anchor beams. Anchor beams should be used on roads, where the slope is greater than 10 % anchor beams should be used at the discretion of the engineer (CMA, 2000)

2.8.4 Spacing and Position of Anchor Beams

There are no fixed rules on the spacing anchor beams above the essential bottom anchor beams. Figure 2.18 can be used as a guideline of the anchor beam position.
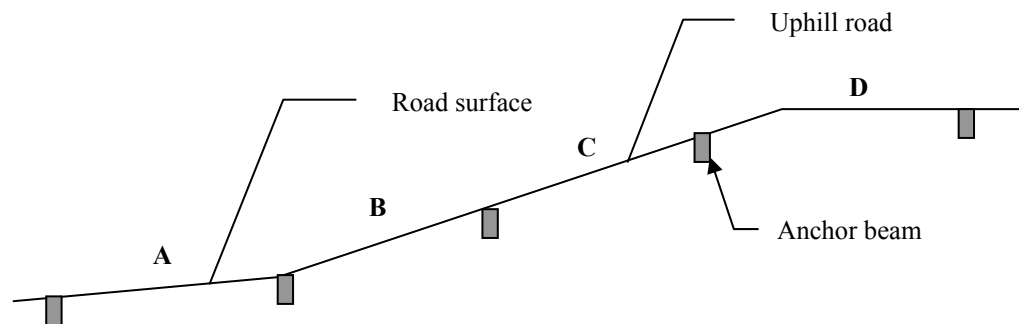
Figure 2.18 The position of anchor beams, *CMA (2000).*

It is standard practice when laying pattern of concrete block paving to start at the lower and to work upwards against the slope. This practice will ensure that if there is any movement of blocks during the laying operation, it will help to consolidate the blocks against each other, rather than to open the joints.

2.8.5 Construction of Anchor Beam

For ease of construction, it is recommended that the blocks be laid continuously up the gradient. Thereafter, two rows of blocks are uplifted in the position of the beam, the sub base excavated to the required depth and width and the beam cast, such that the top of the beam is 5 – 7 mm lower than the surrounding block work. This allows for settlement of the pavers. This method of construction

will ensure that the anchor beam interlocks, with the pavers and eliminates the need to cut small pieces of block.
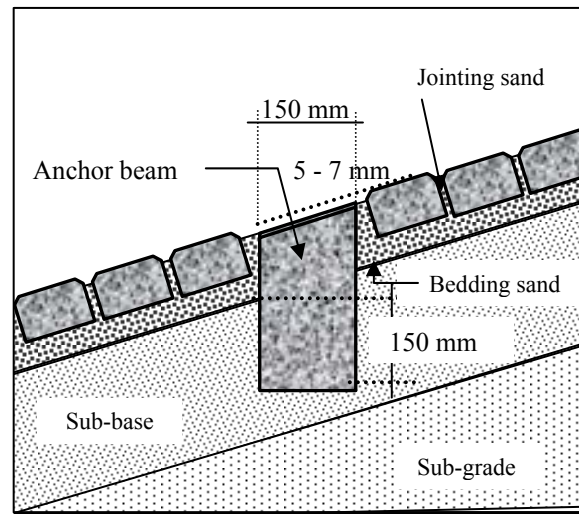
Figure 2.19   Detail construction of anchor beam *(CMA, 2000)*

2.9   Finite Element Modelling

The finite element method (FEM) is a numerical technique for solving problems with complicated geometries, loading, and material properties. It provides a solution for pavement problems, which are too complicated to solve by analytical approaches. The FE method has two general solution forms displacement (or stiffness method); and force (or flexible method). The former is the most popular form of the FE method. The basic FE process dictates that the complete structure is idealized as an assembly of individual 2D or 3D elements. The element stiffness matrices corresponding to the global degrees of freedom of the structural idealization are calculated and the total stiffness matrix is formed by the addition of element stiffness matrices.

The solution of the equilibrium equations of the assembly of elements yields nodes displacements, which are then used to calculate nodes stresses. Element displacements and stresses are then interpreted as an estimate of the actual structural behaviour (Bathe and Nishazaw, 1982). The higher the number of nodes in a structure the greater the number of equations to be solved during the FE process, hence, the longer it takes to obtain a solution. Generally, the finer the mesh, the more accurate is the FE solution for a particular problem. Therefore, a compromise is needed between mesh refinement, model size, and solution time.

2.9.1 A Review of Two-Dimensional Finite Element Modelling

The enhanced computational capabilities of computers in the recent years with the availability of the FE method resulted in an innovation in the design and analysis of rigid pavements. Cheung and Zienkiewicz (1965) developed the first algorithm for the analysis of rigid pavements. They solved the problem of isotropic and orthotropic slabs on both semi-infinite elastic continuum and Winkler foundation using the FE method. Huang and Wang (1973) followed the procedure of Cheung and Zienkiewicz to develop a FE method to calculate the response of concrete slabs with load transfer at the joints. However, the developed model was incapable of handling multilayer systems.

Tabatabaie and Barenberg (1978) developed a computer program ILLISLAB. This program is based on the classical theory of a medium-thick plate on a Winkler foundation. Aggregate interlock and keyway joints were modelled using spring elements which transfer the load between blocks with jointing sand; while bar elements were used to model dowelled joints which transfer moment as well as shear across the joint (Nasim, 1992).

Nasim developed a method to study rigid pavement damage under moving dynamic loading by combining dynamic truck tire forces with pavement response (Nasim, 1992). Computer models of trucks were used to generate truck tire forces of various trucks. The COSMOS software package programme could use for different pavement designs. Truck wheel load histories were combined with those from pavement response to calculate time histories of the response of a rigid pavement to moving dynamic truck loads and therefore predict pavement damage.

Generally, two-dimensional finite element model (2D-FEM) programs demonstrate the potential capabilities of the modelling approach and represent significant improvement over traditional design methods. Most of these programs rely on plate elements to discrete concrete blocks and foundation layers (Davids, 1998), they allow the analysis of COSMOS with or without dowel bars and incorporate aggregate interlock shear transfer at the joint with linear spring elements. However, they are capable only of performing static analysis, and have limited applications. They cannot accurately model the following 0000000: Dynamic loading, detailed local response, such as stresses at dowel bar/concrete interfaces, realistic horizontal friction force at the interface between different pavement layers and vertical friction between the concrete blocks and jointing sand.

2.9.2 A Review of Three-Dimensional Finite Element Modelling Subjected to Traffic Loads

With the increased affordability of computer time and memory, and the need for better understanding of the reasons for some modes of pavement failure, 3D-FEM approach was adopted by many researchers. Ioannides and Donelly (1988) examined the effect of sub-grade support conditions on concrete block pavement. In this study, the 3D-FEM programme was used to develop a model consisting of a single concrete block and bedding sand. The study examined the effect of mesh refinement, vertical

and lateral bedding sand extent, and boundary conditions on pavement response. Chatti (1992) developed the 3D-FEM called SOLIDWORK to examine the effect of load transfer mechanisms and vehicle speed on rigid pavement response to moving loads. The maximum tensile stress occurs at the mid point of the block along the free edge, and observed stress reversal at the transverse joint.

Many researchers opted to use general purpose 3D-FEM software packages because of the availability of interface algorithms, thermal modules, and material models that make them most suitable for analyzing pavement structures. General purpose software such as ABAQUS, DYNA3D, and NIKE3D have been in the process of development by private and public domain organizations since the 1970s, and were used in design problems ranging from bridges to underground shelters that withstand nuclear explosions. Shoukry, *et al*. (1996 and 1997) examined the dynamic response of composite and rigid pavements to FWD impact using LS-DYNA. The results indicated the reliability of LSDYNA in predicting the dynamic surface deflections measured during FWD test. These results also demonstrated that pavement layer interface properties are very important considerations when modelling pavement structures.

Purdue University and Ohio DOT examined the effect of overloaded trucks on rigid pavements, Zaghloul (1994). They used the FE code ABAQUS to develop a 3D-FEM of a multilayered pavement structure. An 80 kN (18-kip) Single Axle Load (SAL) was simulated by a tire print. The principal of superposition was used to model the SAL along the pavement. Results from this study showed that, when compared to interior loading, edge loading increased the vertical displacement and corresponding tensile stress by 45 and 40 percent, respectively. Increasing the load speed from 2.8 to 16 km/hr (1.75 to 10 mph) decreased the maximum surface deflection by 60 percent.

2.10 Type of Trafficking Test on Concrete Block Pavement

In recent years, increasing effort has been directed towards explaining the behaviour of full-scale prototype concrete block pavements under loads chosen to simulate truck wheel loads. Such tests fall into two categories. The categories are listed below:

(i)   Observation of actual concrete block pavements under real traffic.

(ii)   Accelerated trafficking tests of prototype pavements.

2.10.1 Actual Pavements Traffic Tests

The first scientific study of concrete block pavement under actual traffic appears to be that conducted by the South Australian Institute of Technology in 1976 (Dossetor and Leedham, 1976). Here, test pavements were constructed at the entrance to a CPB manufacturing plant where a record of the numbers and weights of trucks traversing the pavements could easily be obtained. Unfortunately, the experiment failed because of inadequate compaction of the base-course.

Later, a similar approach had been implemented in the United Kingdom by Barber and Knapton (1980). Here the maximum measurements have been reported to be about 4,000 kg standard axle loads. However, this amount of traffic is too low to permit any conclusions to be drawn concerning the long-term performance of the pavements. It is understood that a similar type of experiment was initiated in late 1980 by the Australian Road Research Board in Melbourne.

2.10.2 Accelerated Pavement Loading Tests

The problem of subjecting a test pavement to a realistic volume of traffic can be most conveniently solved by using accelerated trafficking tests. The first such study was conducted by the author in Australia in 1978 (Shackel and Arora 1978a; Shackel, 1979a) and made use of the full-scale road simulator at the University of New South Wales (Shackel and Arora, 1978b). Pavement may carry dynamic loads generated by a variety of vehicles whose configurations vary over a wide range. Methods for characterising these loads are now considered in detail.

2.10.2.1 Vehicles Design Loads

For convenience, the effects of wheel load and tyre pressure will be considered separately. CPB are generally smaller than the contact area of a motor tyre, and therefore, a concrete block pavement will provide only a limited load distribution. Although a wheel of a vehicle will often bear simultaneously on two or three CPB, there will still be not much load-spreading effect.

2.10.2.2 Axle and Wheel Loads

For on road vehicles such as trucks typical legally permitted maximum axle loads are give in Table 2.3. From this table, it may be seen that, in many countries, the heaviest permitted axle is an 80 kN single axle fitted with dual tyres.

42

Table 2.3   Typical maximum single axle loads

Country	Axle load (kN)
Australian	80
Austria, Denmark, Germany, Japan	98
Britain	100
European	113
France, Belgium	128

Figure 2.10 shows the distribution of axle loads actually measured on a major inter-state highway (Concrete Segmental Pavements-T54, 1997). Here the loads are shown averaged per axle rather than per axle group. From this figure, it may be seen that, in practice, there is a significant number of axles which exceed the nominal 80 kN limit. From the data in Figure 2.12, this amounts to about 16 % of the total number of axles.
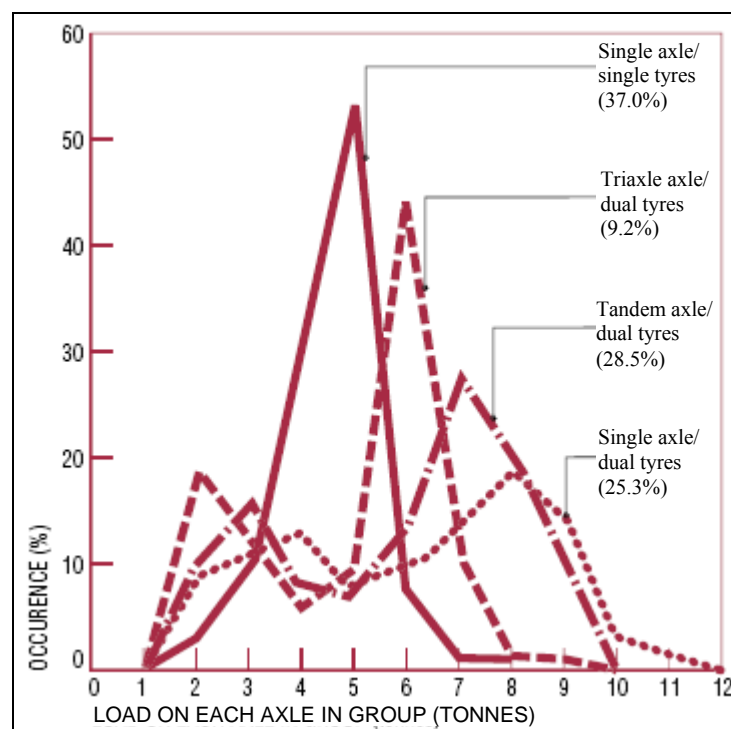
Figure 2.10 Typical distribution of truck axle loads

The loads permitted to be carried on the axles of a road depend on:

(i)   The number of tyres fitted to the axle (i.e. single or dual).

(ii)   The number of axles forming the axle group (i.e. single, tandem or triaxle).

Typical values of the permitted loads per axle type are given in Table 2.4.

Table 2.4   Standard axle loads

Axle type	Standard load (kN)
Single axle, single tyre	53
Single axle, dual tyres	80
Tandem axle, dual tyres	135
Triaxle, dual tyres	181

2.10.2.3 Tyre Pressures

Typically, for road vehicles, the tyre pressure used in thickness design calculations is about 600 kPa. However, the maximum legally permitted tyre pressure for on road vehicles is usually 700 kPa but may range up to 1.0 MPa or more for so-called "super single" axles.

Most analyses of flexible pavement systems assume a priori that the loads are applied as uniform pressures acting over circular contact areas and it is commonly supposed that the effects of dual wheels can be modelled by a single contact stress acting over an equivalent circular area. For rigid pavements, more realistic assumptions need to be made. Here it is assumed that the contact area is elliptical and that this may be simplified as to contact areas where by the dimensions are related to the thickness of slab under consideration.

2.10.2.4 Accelerated Repetitions

In highway, traffic is constrained to run in closely delineated lanes. Accordingly it is common to ignore lateral wander of vehicles and to assume that the design repetitions simply correspond to the number of axles of the vehicles using each lane.

2.10.3 Existing Accelerated Pavement Loading Test

Accelerated pavement loading devices have been widely used during the last decade to enhance pavement engineering knowledge. The main advantage of using accelerated loading devices is to evaluate the long-term pavement performance in a relatively short period of time. Many forms of accelerated pavement loading devices are used to develop and evaluate distress criteria. These devices have increased in popularity due to the high attainable benefit-to-cost ratios and their ability to test pavement responses that cannot be tested in other ways.

Over the years many accelerated pavement loading devices have been developed ranging from full-scale devices to model devices. Among the full-scale devices is the RUB-StaP in Germany, Heavy Vehicle Simulator (HVS), Newcastle University Rolling Load Facility (NUROLF) in the U.K., Accelerated Pavement Test Facility (APTF) by the Transportation group of IIT Kharagpur, Model Mobile Load Simulator (MLS) test facility in South Africa. Scaled down model loading devices have been used at the University of Nottingham in the U.K., South Africa, and Texas. Although scaled-down devices cannot predict actual pavement lives in the field accurately, they provide faster, easier and much less expensive relative comparisons among various pavement types when compared to prototype devices. Furthermore, scaled-down devices can be operated under controlled lab conditions.

2.10.3.1 Dynamic Loading Test

The laboratory setup by Vanderlaan (1994) is shown in Figure 2.11.   It consisted of a steel box measuring 1.8 m × 1.8 m × 0.3 m. This box was placed on three *I* beam which were placed directly on the concrete floor. A testing frame was built around the box to support the loading device. A simulated sub-grade was installed on the box floor in the form of a 3 mm thick sheet of hard neoprene over a 25 mm layer of foam neoprene.   Previous work by Beaty (1993) indicated that this foam base simulates a California Bearing Ratio (CBR) value equal to 6. A 250 mm thick compacted layer of ≤ 18 mm crushed rock was placed on the top of the neoprene to act as a granular base. This material originated from a local source and conformed to the New Brunswick Department of Transportation specifications for road construction. Water resistant plastic was used to cover the sub-base to avoid contaminating the sub-base with the sand and also to contain water if sand had to be saturated.   This is not a field installation; however the plastic was used as an experimental expedient.

Loading was controlled by a MAYES computer system which loaded the pavement with a sinusoidal pulse at a frequency of 5 Hz

DATA LOGGER
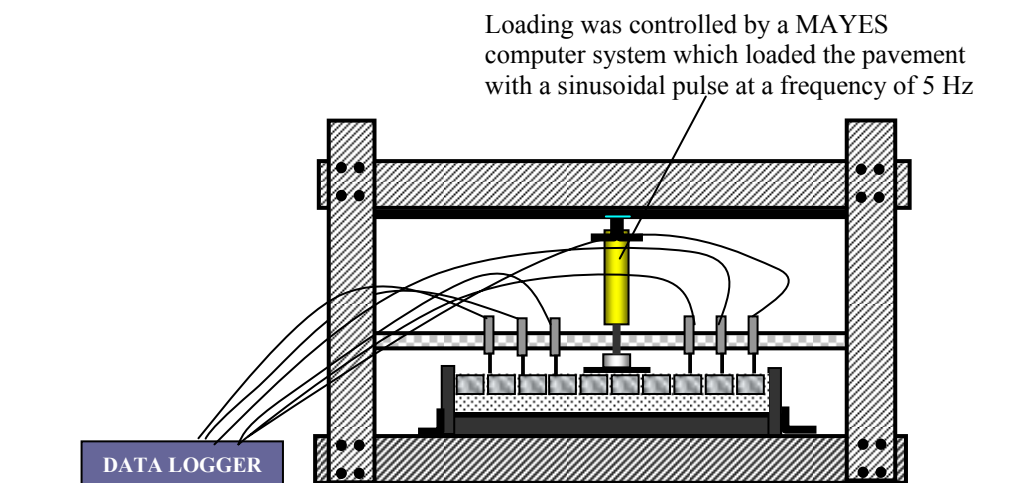
Figure 2.11 Laboratory setup showing the testing apparatus and the CPB laid in the herringbone pattern

2.10.3.2 RUB-StraP

The construction of the road testing machine (called RUB-StraP, derived from the name Ruhr-University Bochum and the German equivalent for road testing machine) is schematically illustrated in Figure 2.12. The loading tests were carried out by Koch (1999) with a single wheel.
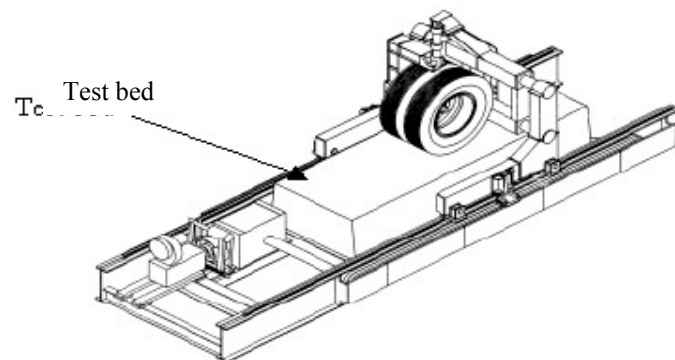
Figure 2.12 Schematic of the RUB-StraP (Koch, 1999)

Test beds were built in full size in a steel trough. The dimensions of the test bed are shown in Figure 2.13.
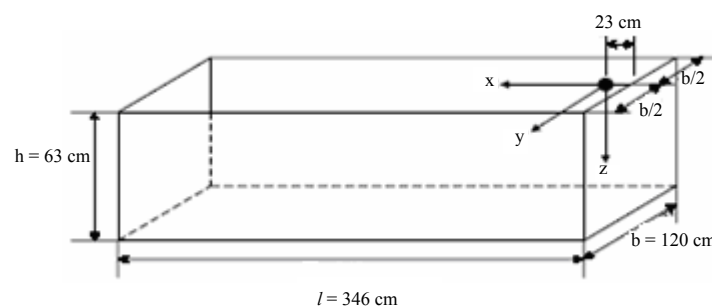
Figure 2.13 Not full scale drawing of test bed with designation of point of origin and dimensions

The test bed was loaded by a truck wheel rolling over it in one direction. The pavement construction of test beds is according to the German Directives (FGSV,

2001), traffic class III. In doing so, the thickness of sub-base results in the maximum height of test bed (63 cm).

2.10.3.3 Heavy Vehicle Simulator

The development of the HVS was reported by Steyn et. al. (1999). The HVS was developed by the National Institute for Transport and Road Research (currently the Division for Roads and Transport Technology, or Transportek) of the Council for Scientific and Industrial Research in Pretoria, South Africa in the late 1970s (Metcalf, 2004). The first prototype was a stationary conceptual model and the second generation HVS was the first mobile version. It could deliver a single rolling wheel constant load of between 20 kN and 75 kN to a pavement test section 8 m long and 1 m wide. This Heavy Vehicle Simulator is able to produce 480 repetitions per hour of load application rate at a speed of 8 km/h.

Shackel (1980d) has conducted a program of testing of block pavements commenced in 1979 using a HVS. The major aims of this testing program are intended to induce the failure in some sections of block pavement and verify the design curves published in Shackel (1979c). The test section consisted of a sub-grade CBR of 20 with optimum moisture content (modified) of 13 % and a relative compaction of 91 per cent. A natural gravel base course containing about 20 % greater than 75 mm in size was installed to a thickness of 100 mm and a relative compaction modified of 95 %. The compacted bedding sand thickness of 20 mm was laid over the gravel base course. Twenty test sections, each 15 m long and 3 m wide, were installed.

HVS testing was generally commenced at a load of 40 KN, this being the maximum permitted wheel load in most counties and loading was organized so that each section was subjected to about 105 ESAs. The tyre pressure was 600 kPa. The HVS travels at about 1 m/s in both directions and the location of the load is adjusted so that it is uniformly distributed over a width of 0.9 m.

2.10.3.4 Newcastle University Rolling Load Facility

Newcastle University Rolling Load Facility (NUROLF) is generally designed by Professor John Knapton. It was the world's first full-scale rolling load facility specifically developed for the assessment of pavers (Mills *et. al*, 2001) deformed by low speed accelerating/decelerating traffic. NUROLF allows a laboratory assessment to be made of the performance and behaviour of pavement construction materials during complete life cycle simulation tests.

The test bed with a surface area of 5 × 2 m, was designed to ensure that a full-scale life cycle assessment of the paving materials could be achieved. The examination of pavement's durability is permitted since the test section allows the evaluation of different base and surface materials. A two tonne overhead crane aids the handling of the paving materials within the NUROLF laboratory.

Generally, the NUROLF test vehicle comprises a former gully emptying vehicle that has been adapted as follows:

(i)   Engine replaced with 60 HP of 3-phase electric motor.

(ii)   Guide wheels constructed on each axle to achieve constant tracking.

(iii)   Rear axle weight increased to apply axle load of 14000 kgf.

(iv)   Power fed to motor by computer controlled inverter.

(v)   Guidance beam fitted with limit switch to achieve acceleration/ deceleration.

(vi)   Electric motor drives rear axle.

The weight on the rear axle can be altered by varying the load carried in the vehicle's water tanks and therefore the vertical and horizontal loading (up to 14000 kg and 2000 kg respectively) can be applied to the test bed. A complete cycle of the vehicle movement is 60 seconds, and running the vehicle continuously for 24 hours can simulate up to five years of traffic wear. Climate simulation controls also allow for analysis of the pavement distress under changing conditions (temperature and precipitation).

During its load cycle, NUROLF applies a vertical wheel load of 7000 kgf through its offside wheel to the centre of the test site. It commences a cycle at one end of the site and accelerates linearly over the full test site so that the load wheel has attained a speed of 2.3 m/s at the centre of the test site. It then decelerates toward the end of the test site and it applies a horizontal force of 700 kgf in the same direction to the pavement.

2.10.3.5 Accelerated Pavement Test Facility

The Accelerated Pavement Test Facility (APTF) was designed and fabricated by the Transportation group of IIT Kharagpur. The test setup consisted of a dual wheel set, which can be loaded up to 60 kN by means of mass put into the loading bin of the equipment (Teiborlang, 2005). The wheel can be made to move to and fro by a 20 kW motor over a linear track of length of 15 m. The facility has a control

system which enables the dual wheel to move to and fro continuously. The numbers of cycles of loading are recorded in a counter. In the present investigation, the loading bin was filled with steel rail sections so that the load coming on the dual tyres was about 40 kN. Load on the wheel was checked by a portable weigh bridge available in the laboratory. A tyre pressure of 586 kPa (85 psi) was maintained throughout the test.

The entire operation of APTF is controlled by a microprocessor. After the electrical switch is put on, the dual wheels start moving to and fro without any lateral wander. In the present investigation, the number of repetitions of the wheel load per hour was found to be about 240. Levels of the surface of the pavements were recorded before the start of the test and after every 1,000 repetitions of the wheel load. Permanent deformation under each wheel was measured with reference to a fixed datum.

A falling weight deflectometer (FWD) was used to determine the deflection profile of the test pavement after every 1,000 repetitions of the wheel load. The deflections were measured at 0, 300, 600 and 900 mm from the centre of the loading plate of the FWD. The modulus values of different layers were evaluated by a computer program available in the Transportation laboratory. Though the dimensions of the test sections were about 2.1 m by 2 m, the FWD data may yield a reasonable estimate of the elastic modulus of the concrete block layer.

2.10.3.6 Model Mobile Load Simulator

The Model Mobile Load Simulator (MLS) is recently developed in South Africa (Hugo and Martin, 2004). The device is a 1:10 scale accelerated pavement testing machine which is used for testing scaled down model pavement sections. The

simulator is about 1.7 meters long × 0.76 meters high × 0.45 meters wide (5.7 ft long × 2.5 ft high × 1.6 ft wide). The machine has six double bogies, linked together to form an endless chain which moves around a set of looped rails mounted in the vertical plane on a fixed frame. Each double bogie contains two axles, each with suspension springs and two sets of dual tyres. One axle in each double bogie is electrically driven. The double bogies are similar to the rear axles of a heavy truck. The solid rubber tyres have a resilience which is comparable to that of full-scale truck tires. Lateral distribution of the wheel paths is achieved by different lengths of axles.

When a bogie moves along the bottom part of the rails, it is loaded by the weight of the fixed frame while the tyres are in contact with the underlying pavement. During this phase the bogies are powered via sliding contacts and a power rail. Wheel load can be changed by varying the dead weight placed on top of the frame. Loading on the wheels can also be adjusted by raising or lowering the fixed frame on its four adjustable pods. The speed can be controlled and trafficking can be applied at a rate of up to more than 10,000 axle loads per hour.

A special compaction roller is used to prepare test pavements to an accuracy of 1.0 mm (0.05 in). The machine can be used inside an air conditioned lab or an environmental chamber so that tests can be carried out at any chosen temperature. Loading of the wheels are monitored by two displacement transducers on the two suspension springs of one of the axles. The two signals are transmitted by an infrared link from the moving bogie to a receiver on the fixed frame, from where it can be recorded on an oscilloscope or data logger. The number of applied axle loads is recorded by a mechanical counter.

CHAPTER 3

MATERIALS SPECIFICATION AND TESTING METHODOLOGY

3.1 Introduction

This research begins by studying the interactions that develop between adjacent blocks (surface course) with the bedding and jointing sands especially on sloping road section. A series of tests were conducted to investigate the effects of changing parameters of block shape, block thickness, laying pattern, bedding sand thickness and joint width between blocks. (Dutrufl and Dardare, 1984) a laboratory-scale model to study the behaviour of concrete block pavement testing to highlight i.e. horizontal force test (to find the maximum horizontal creep) and push in test on various degree of slope (to find the maximum displacement). It can be shown that these horizontal and vertical forces can be significant to define the spacing of anchor beam that was used in construction of CBP on sloping road section. The spacing of anchor beam was determined from maximum horizontal creep. The horizontal creep on sloping road section was affected by breaking or accelerating vehicle and rotation of blocks affected of vertical force (load) of vehicle.

3.2   Flow Chart of Research

```
                    ┌─────────────────────────┐
                    │     Construction of     │
                    │   laboratory scale model│
                    └─────────────────────────┘
                                 │
                                 ▼
                    ┌─────────────────────────┐
                    │    Verifying the model  │
                    └─────────────────────────┘
                                 │
                                 ▼
                    ┌─────────────────────────┐
                    │  Performance of CBP on  │
                    │          slope          │
                    └─────────────────────────┘
                        │                 │
                        ▼                 ▼
            ┌────────────────────┐  ┌────────────────────┐
            │ Horizontal force   │  │    Push-in test    │
            │       test         │  │                    │
            └────────────────────┘  └────────────────────┘
                        │                 │
                        └────────┬────────┘
                                 ▼
                    ┌─────────────────────────┐
                    │      Data analyses      │
                    └─────────────────────────┘
                                 │
                                 ▼
                    ┌─────────────────────────┐
                    │  Compare with simulation│
                    │    model – 3DFEM        │
                    └─────────────────────────┘
                                 │
                                 ▼
              ┌────────────────────────────────────┐
              │  Development and performance of     │
              │  Highway Accelerated Loading        │
              │  Instrument (HALI)                  │
              └────────────────────────────────────┘
                                 │
                                 ▼
                    ┌─────────────────────────┐
                    │ Discussions and         │
                    │ conclusions             │
                    └─────────────────────────┘
```
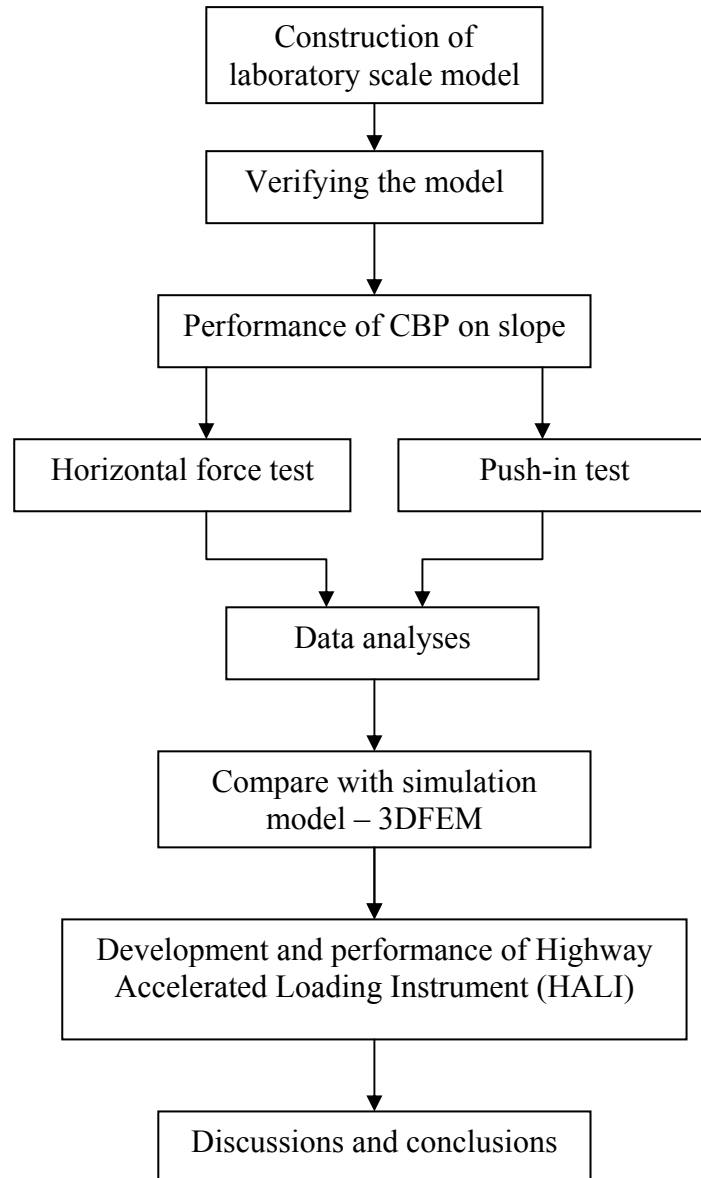
Figure 3.1   Flow chart of research

3.3   Material Properties

In this study, a series of horizontal force and push-in tests were performed to examine the interlocking concrete block pavement. Two blocks thickness (60 mm and 100 mm) were used in each experimental. Rectangular and uni-pave block shapes were used in horizontal force test.

3.3.1   Sand Material

River sand (mainly rounded quartz) from Kulai in Johor was used in this research. Sand was prepared from the coarse to fine in eight different gradations (for bedding sand) and six for jointing sand. The particle size distributions for bedding and jointing sand are described in Table 2.2. Prior to use in each experiment, the sand was oven dried at 110°C for 24 hours to maintain uniformity in test results. A maximum dry density of 17.3 kN/m^3 was obtained, corresponding to the optimum moisture content of 7.4 %.

The bedding and jointing sand material should have uniform moisture content. As a guide, after the material has been squeezed in the hand, when the hand was opened the sand bind together without showing free moisture on its surface. Where bedding sand material is stored on site it was covered to reduce moisture loss due to evaporation, or saturation from rainfall. If the sand became saturated after lying then it removed and replaced with bedding sand material having the correct moisture content. Alternatively the bedding sand can be left in place until it dries to the 12 % moisture content.

3.3.2   Paver Material

The concrete blocks were supplied by Sun-Block Sdn. Bhd. in Senai Johor Bahru Malaysia. These were made using ordinary Portland cement, siliceous fine aggregate, dolerite coarse aggregate and tap water. The portland cement conformed to the requirements of British Standard (BS). The coarse and fine aggregates complied with the requirements of BS (1983). The parameters studied in this research project include block shape and thickness. The details of block shapes studied (Lilley, 1994) and (Rohleder, 2002) are given in Figure 3.2 and Table 3.1.

| | Rectangular shape | | Uni-pave shape |
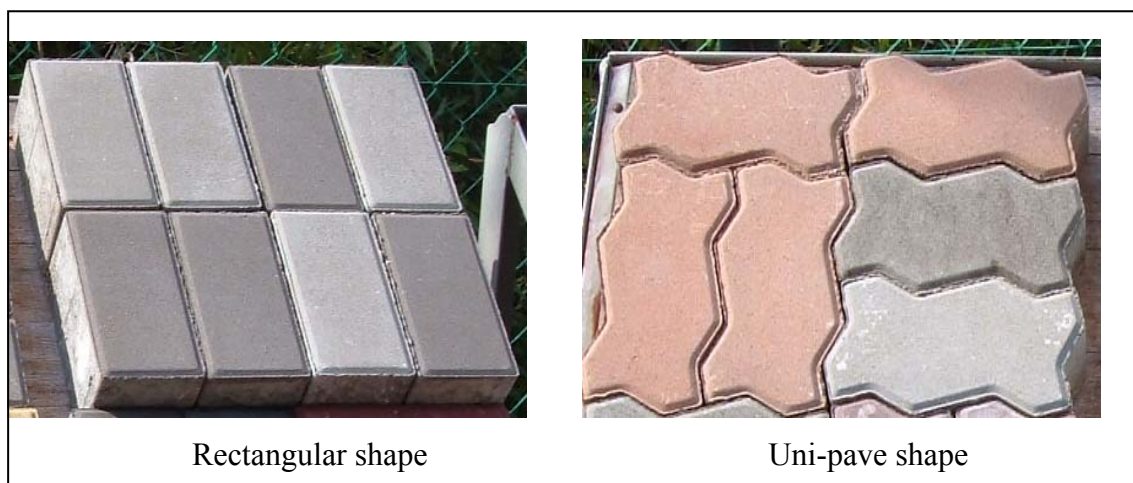
Figure 3.2   The shape of concrete block paver

Table 3.1:   Details of blocks used in this study

Block type	Block shape	Length " L " (mm)	Width " B " (mm)	Area Coverage (pieces/m^2)	Thickness (mm)	Compressive strength (kg/cm^2)
1	Rectangular	198	98	49.5	60	350
2	Rectangular	198	98	49.5	100	350
3	Uni-pave	225	112.5	39.5	60	350
4	Uni-pave	225	112.5	39.5	100	350

Sun-Block Sdn. Bhd. (2004)

3.4 The Testing Installation

The horizontal force testing installation was constructed within the steel frame 2.00 x 2.00 metre. In this study, the effects of changing of laying pattern, joint width, block shape and block thickness are investigated. The steel frame as edge restraint was placed on the concrete floor and welded to the concrete floor.
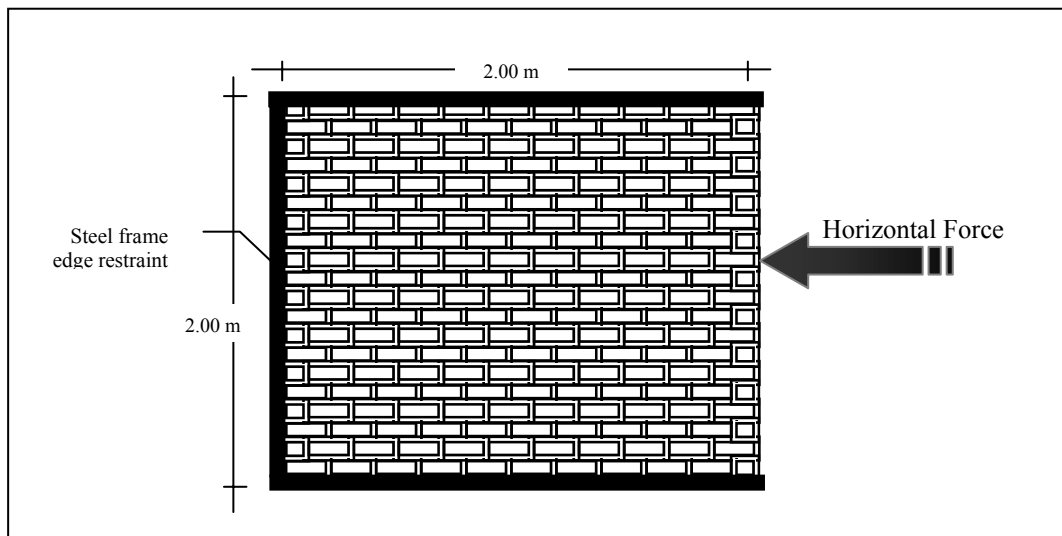
Figure 3.3   Stretcher bond laying pattern
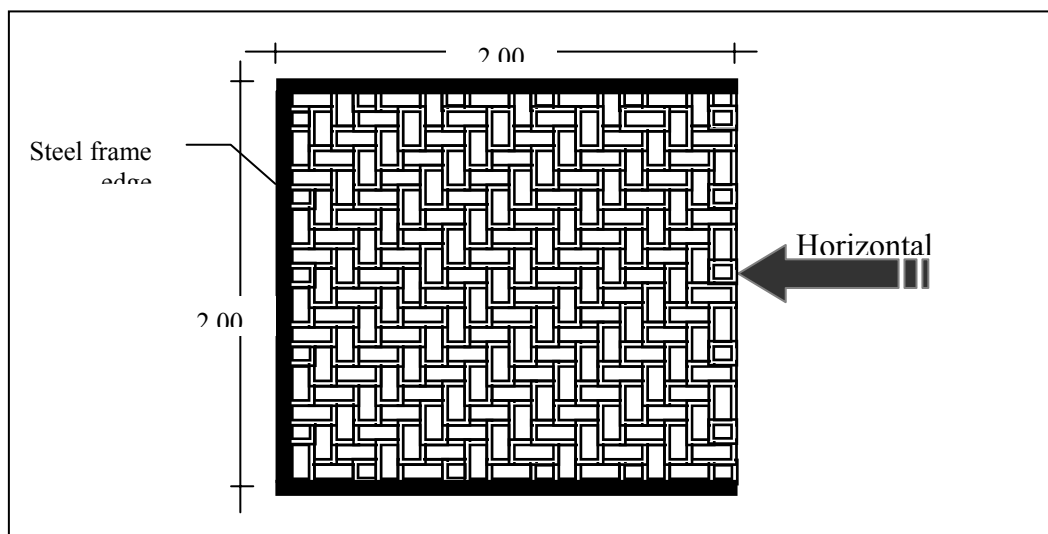
Figure 3.4   Herringbone 90° bond laying pattern
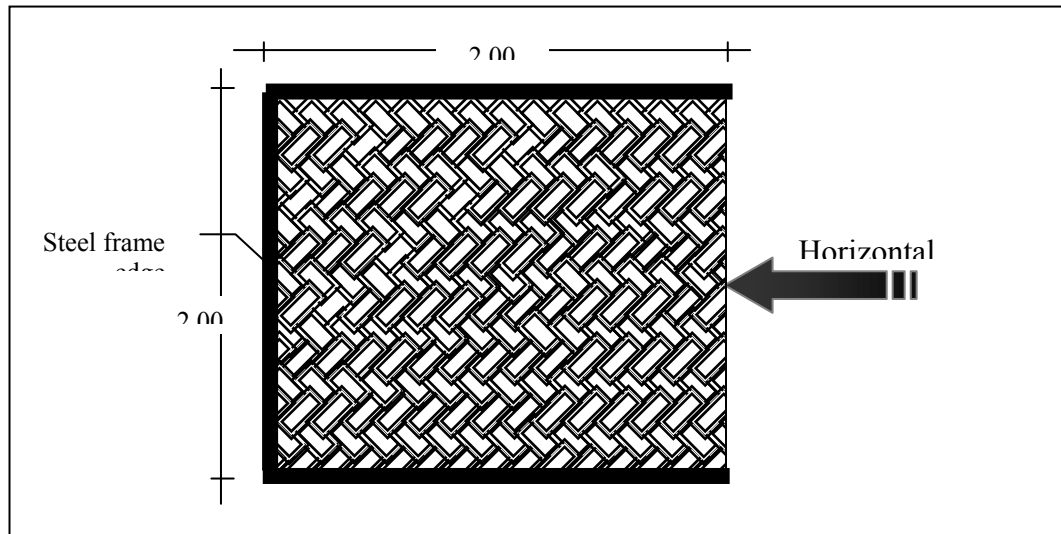
Figure 3.5 Herringbone 45° bond laying pattern
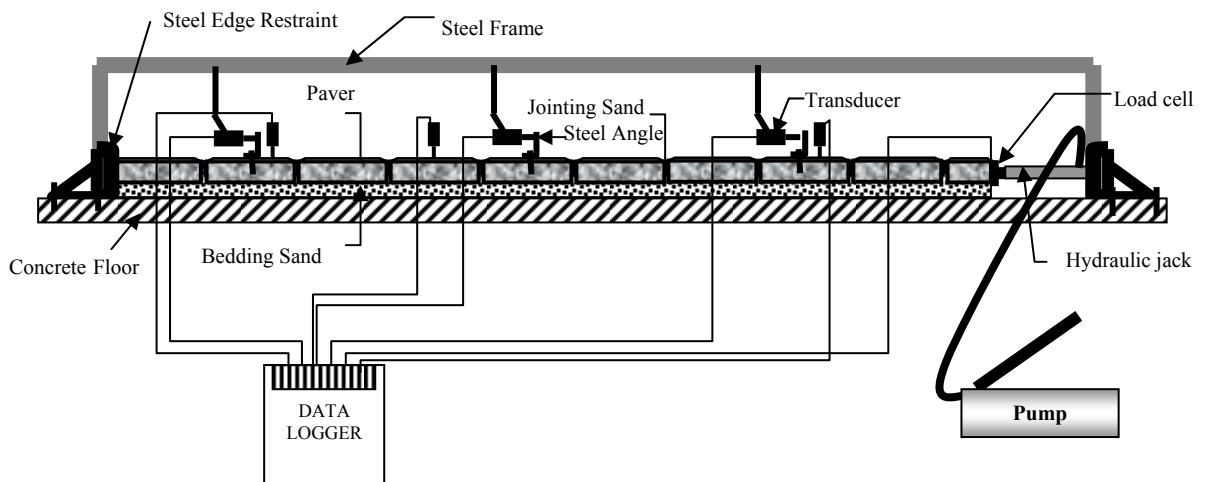
Figure 3.6 Horizontal force testing arrangement (*before testing*)
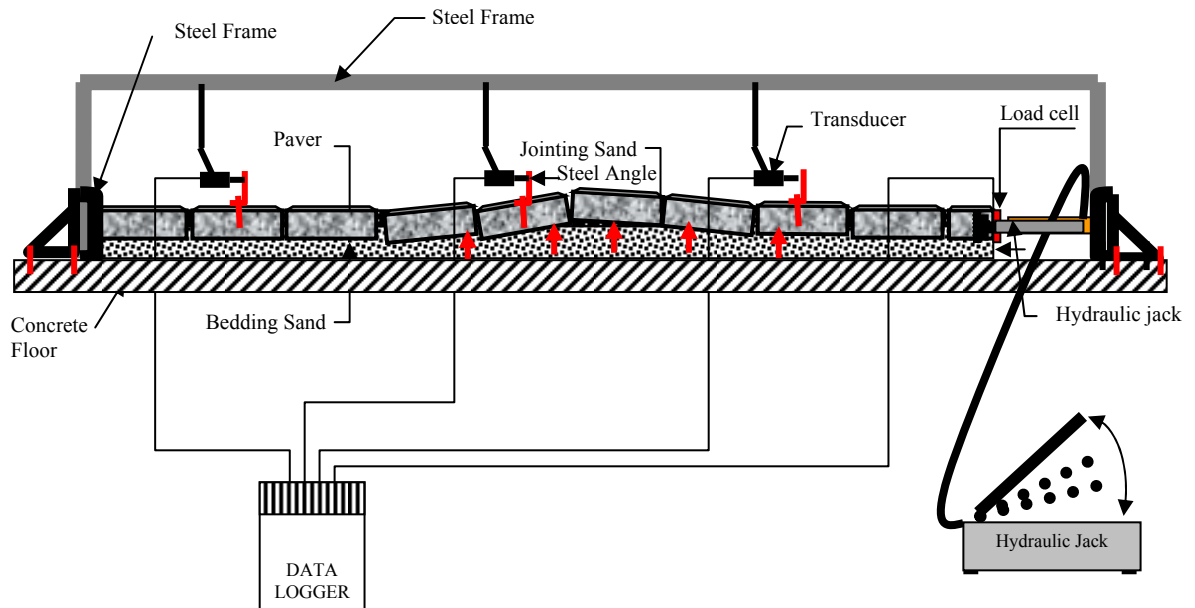
Figure 3.7 Horizontal force test condition (*after testing*)

3.5   Horizontal Force Testing Procedure

➢   Characterizing of the materials before testing (density, moisture content and sand grading).

➢   A layer of bedding sand should be spread loose and screened to a uniform thickness, it is important that the bedding sand layer remains undisturbed prior to the laying of blocks.

➢   Installation of the blocks and sealing of the jointing sand.

➢   General compaction of the block pavement with a hand-guided plate vibrator until it is firmly embedded in the bedding sand layer.

➢   Setting of measuring apparatus (zero settings),

➢   Horizontal force in successive stagestest until failure 11 kN and measurements of horizontal creep used data logger with position of transducer as shown in Figure 3.6 and Figure 3.7.

➢   Characterizing of the CBP after experiment.

Figure 3.8   Installation of concrete block pavement (CBP)
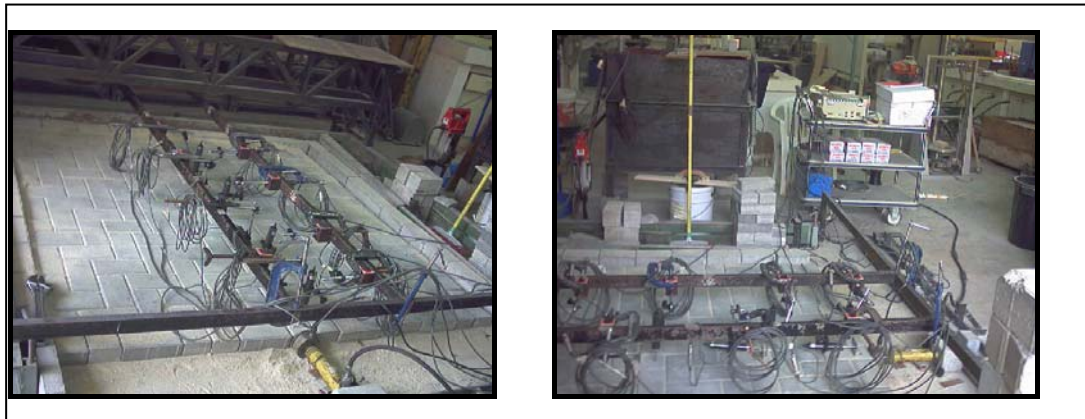
Figure 3.9   Horizontal force test installation

Figure 3.10 CBP failure after testing

3.6   Set up Parameters for Horizontal Test

The horizontal tests of concrete block pavement (CBP) that were conducted in the laboratory were divided on variations as shown in Table 3.2.

Table 3.2:   Set up for horizontal force tests

Shape and thickness of paver	Laying Pattern	Joint Width	Bedding Sand Thickness	Test No.
Rectangular 60 mm	Stretcher bond	3 mm	30 mm	1
			50 mm	2
			70 mm	3
		5 mm	50 mm	4
		7 mm	50 mm	5
	Herringbone 90°	3 mm	50 mm	6
	Herringbone 45°	3 mm	50 mm	7
Rectangular 100 mm	Stretcher bond	3 mm	30 mm	8
			50 mm	9
			70 mm	10
		5 mm	50 mm	11
		7 mm	50 mm	12
	Herringbone 90°	3 mm	50 mm	13
	Herringbone 45°	3 mm	50 mm	14
Uni-pave 60 mm	Stretcher bond	3 mm	30 mm	15
			50 mm	16
			70 mm	17
		5 mm	50 mm	18
		7 mm	50 mm	19
	Herringbone 90°	3 mm	50 mm	20
	Herringbone 45°	3 mm	50 mm	21
Uni-pave 100 mm	Stretcher bond	3 mm	30 mm	22
			50 mm	23
			70 mm	24
		5 mm	50 mm	25
		7 mm	50 mm	26
	Herringbone 90°	3 mm	50 mm	27
	Herringbone 45°	3 mm	50 mm	28

3.7　Push-in Test Arrangement

The test was conducted using steel frame tests in a laboratory-scale model assembled for this purpose (Figure 3.11). The test setup was a modified form of that used by Shackel *et al* (1993). Blocks paver were laid and compacted within a steel frame in isolation from the bedding sand, sub-base course, and other elements of CBP. Here, instead of a steel frame, the tests were conducted in a box to incorporate the bedding sand, paver and jointing sand. In consists of a rigid steel box of 1000 x 1000 mm square in plan and 200 mm depth, in which pavement test sections were conducted. The box was placed on a steel frame; loads were applied to the test CBP through a rigid steel plate using a hydraulic jacking system of 100 kN capacity clamped to the reaction frame.

1. Block pavers	6. Pipe of hydraulic jack
2. Load Cell	7. Edge restraint
3. Hydraulic Jack	8. Hydraulic pump
4. Steel Frame	9. Profile steel C channel
5. Bedding sand	T. Transducer
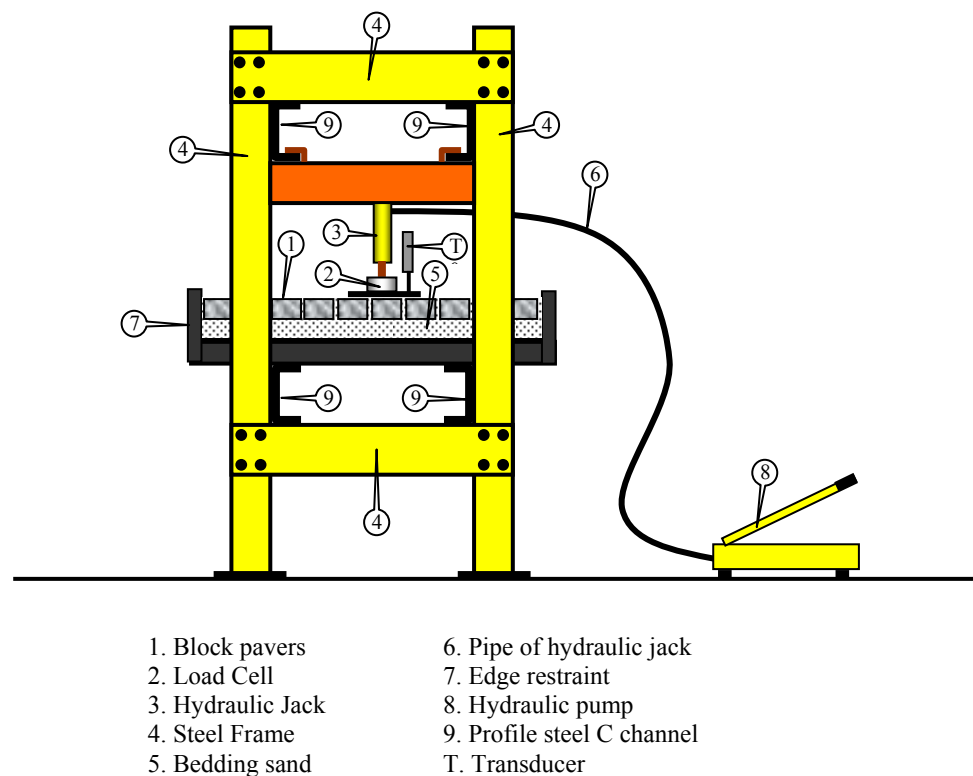
Figure 3.11　Push-in test setup

3.8   Push-in Testing Procedure

A hydraulic jack fitted to the reaction frame applied a central load to the pavement through a rigid circular plate with a diameter of 250 mm. This diameter corresponds to the tyre contact area of a single wheel, normally used in pavement analysis and design. A maximum load of 51 kN was applied to the pavement. The load of 51 kN corresponds to half the single axle legal limit presently in force. Deflections of the pavements were measured using three transducers to an accuracy of 0.01 mm corresponding to a load of 51 kN. The transducers were placed on opposite sides of the plate at a distance of 100 mm from the centre of the loading plate. The average value of three deflection readings was used for comparing experimental results. The parameters, including joint width, thickness of bedding sand, and thickness of block, were varied in the experimental program. For each variation of a parameter, the test was repeated three times to check the consistency of readings. The average of the three readings is presented in the experimental results in graphical form. The range of the standard deviations (SD) of the readings for each parameter is presented in the respective figures. For each test, measurements of joint width were made at 20 randomly selected locations. The mean and standard deviation were calculated to assess the deviation from the design joint width. Design joint width as referred to herein be the desired width established in the experiment; however, the achieved joint widths always varied.

Figure 3.12 Steel frame and sand paper   **Figure 3.13** Bedding sand

Figure 3.14 Installation of CBP

Figure 3.15 Compaction

Figure 3.16 LVDT connection

Figure 3.17 Data logger in print-out

Figure 3.18   Push in test on sloping section

Table 3.3: Push-in test set up parameters for 0 % slope

Shape and thickness of paver	Laying Pattern	Joint Width	Bedding Sand Thickness	Test No.	Slope (%)
Rectangular 60 mm	Stretcher bond	3 mm	30 mm	1	0
			50 mm	2	0
			70 mm	3	0
		5 mm	50 mm	4	0
		7 mm	50 mm	5	0
	Herringbone 90°	3 mm	50 mm	6	0
	Herringbone 45°	3 mm	50 mm	7	0
Rectangular 100 mm	Stretcher bond	3 mm	30 mm	8	0
			50 mm	9	0
			70 mm	10	0
		5 mm	50 mm	11	0
		7 mm	50 mm	12	0
	Herringbone 90°	3 mm	50 mm	13	0
	Herringbone 45°	3 mm	50 mm	14	0
Uni-pave 60 mm	Stretcher bond	3 mm	30 mm	15	0
			50 mm	16	0
			70 mm	17	0
		5 mm	50 mm	18	0
		7 mm	50 mm	19	0
	Herringbone 90°	3 mm	50 mm	20	0
	Herringbone 45°	3 mm	50 mm	21	0
Uni-pave 100 mm	Stretcher bond	3 mm	30 mm	22	0
			50 mm	23	0
			70 mm	24	0
		5 mm	50 mm	25	0
		7 mm	50 mm	26	0
	Herringbone 90°	3 mm	50 mm	27	0
	Herringbone 45°	3 mm	50 mm	28	0

Table 3.4:   Push-in test set up parameters for 4 % slope

Shape and thickness of paver	Laying Pattern	Joint Width	Bedding Sand Thickness	Test No.	Slope (%)
Rectangular 60 mm	Stretcher bond	3 mm	30 mm	1	4
			50 mm	2	4
			70 mm	3	4
		5 mm	50 mm	4	4
		7 mm	50 mm	5	4
	Herringbone 90°	3 mm	50 mm	6	4
	Herringbone 45°	3 mm	50 mm	7	4
Rectangular 100 mm	Stretcher bond	3 mm	30 mm	8	4
			50 mm	9	4
			70 mm	10	4
		5 mm	50 mm	11	4
		7 mm	50 mm	12	4
	Herringbone 90°	3 mm	50 mm	13	4
	Herringbone 45°	3 mm	50 mm	14	4
Uni-pave 60 mm	Stretcher bond	3 mm	30 mm	15	4
			50 mm	16	4
			70 mm	17	4
		5 mm	50 mm	18	4
		7 mm	50 mm	19	4
	Herringbone 90°	3 mm	50 mm	20	4
	Herringbone 45°	3 mm	50 mm	21	4
Uni-pave 100 mm	Stretcher bond	3 mm	30 mm	22	4
			50 mm	23	4
			70 mm	24	4
		5 mm	50 mm	25	4
		7 mm	50 mm	26	4
	Herringbone 90°	3 mm	50 mm	27	4
	Herringbone 45°	3 mm	50 mm	28	4

Table 3.5: Push-in test set up parameters for 8 % slope

Shape and thickness of paver	Laying Pattern	Joint Width	Bedding Sand Thickness	Test No.	Slope (%)
Rectangular 60 mm	Stretcher bond	3 mm	30 mm	1	8
			50 mm	2	8
			70 mm	3	8
		5 mm	50 mm	4	8
		7 mm	50 mm	5	8
	Herringbone 90°	3 mm	50 mm	6	8
	Herringbone 45°	3 mm	50 mm	7	8
Rectangular 100 mm	Stretcher bond	3 mm	30 mm	8	8
			50 mm	9	8
			70 mm	10	8
		5 mm	50 mm	11	8
		7 mm	50 mm	12	8
	Herringbone 90°	3 mm	50 mm	13	8
	Herringbone 45°	3 mm	50 mm	14	8
Uni-pave 60 mm	Stretcher bond	3 mm	30 mm	15	8
			50 mm	16	8
			70 mm	17	8
		5 mm	50 mm	18	8
		7 mm	50 mm	19	8
	Herringbone 90°	3 mm	50 mm	20	8
	Herringbone 45°	3 mm	50 mm	21	8
Uni-pave 100 mm	Stretcher bond	3 mm	30 mm	22	8
			50 mm	23	8
			70 mm	24	8
		5 mm	50 mm	25	8
		7 mm	50 mm	26	8
	Herringbone 90°	3 mm	50 mm	27	8
	Herringbone 45°	3 mm	50 mm	28	8

Table 3.6: Push-in test set up parameters for 12 % slope

Shape and thickness of paver	Laying Pattern	Joint Width	Bedding Sand Thickness	Test No.	Slope (%)
Rectangular 60 mm	Stretcher bond	3 mm	30 mm	1	12
			50 mm	2	12
			70 mm	3	12
		5 mm	50 mm	4	12
		7 mm	50 mm	5	12
	Herringbone 90°	3 mm	50 mm	6	12
	Herringbone 45°	3 mm	50 mm	7	12
Rectangular 100 mm	Stretcher bond	3 mm	30 mm	8	12
			50 mm	9	12
			70 mm	10	12
		5 mm	50 mm	11	12
		7 mm	50 mm	12	12
	Herringbone 90°	3 mm	50 mm	13	12
	Herringbone 45°	3 mm	50 mm	14	12
Uni-pave 60 mm	Stretcher bond	3 mm	30 mm	15	12
			50 mm	16	12
			70 mm	17	12
		5 mm	50 mm	18	12
		7 mm	50 mm	19	12
	Herringbone 90°	3 mm	50 mm	20	12
	Herringbone 45°	3 mm	50 mm	21	12
Uni-pave 100 mm	Stretcher bond	3 mm	30 mm	22	12
			50 mm	23	12
			70 mm	24	12
		5 mm	50 mm	25	12
		7 mm	50 mm	26	12
	Herringbone 90°	3 mm	50 mm	27	12
	Herringbone 45°	3 mm	50 mm	28	12

3.9   Accelerated Trafficking Test Arrangement

In this study, the joint width, thickness and quality of bedding and jointing sand were kept constant for the accelerated trafficking test. The test section of concrete block pavement is constructed within a rigid steel box of 1.7 m x 5.5 m square in plan and 0.25 m in depth. The equipments used for the preparation of the pavement model was basically a screed board to leveling the bedding course and a steel compactor for the concrete block pavement. The pavement model was prepared as follows:

➢   A simulated sub-grade consists of a 3 mm thick sheet of hard neoprene laid on the box floor.

➢   A plastic sheet was placed over the hard neoprene. It was used to cover the hard neoprene to avoid contaminating the hard neoprene with the bedding sand and also to contain water if sand had to be saturated. This was not a field installation; however the plastic was used as an experimental expedient.

➢   The dry bedding sand was spread in a uniform layer to give a depth of 50 mm. This value was selected based on the experimental results discussed in the previous study by Shackel. The screed bedding sand was laid overnight before the CPB were installed over it.

➢   Over the bedding sand, the rectangular CPB with a depth of 60 mm was laid. Where necessary, at the edges of the test frame, CPB were sawed to fix the box. The jointing width was kept at 5mm.

➢   The jointing sand was placed on the pavement and filled up in each cell.

➢   The whole pavement was compacted by a plate vibrator. The second joint filling operation is carried out to ensure that the joints were fully filled.

➢   The locations of rut depth measurement points were marked on the pavement model. Figure 3.19 shows the plan view of the locations of rut depth measurement points marked on the pavement model.

Once the test pavement is constructed, 5 conditioning cycles were undertaken to ensure that the pavement was correctly bedded, prior to commencing measurements.

3.10   Accelerated Trafficking Testing Procedures

After preparing the pavement model, the accelerated loading test was performed. The following steps were followed:

➢   The initial elevations of the 162 points marked on the pavement were measured using the dial gauge (see Figure 3.20). The measuring process was conducted from one cross section to another cross section of the pavement model.

➢   The control panel was programmed to a constant speed of 0.2 m/s. It undertakes a complete cycle in 20 seconds. The axle load of 10 kN (1 ton) was set to the wheel load during the trafficked test.

➢   The machine was run at 50, 100, 250, 500, 1000 and 2500 repetition of axle load. After each level of axle load repetition, the elevations of 162 points previously marked on the pavement surface were measured. In addition, joint width at panel A, B, C and D as shown in Figure 3.19 was measured.
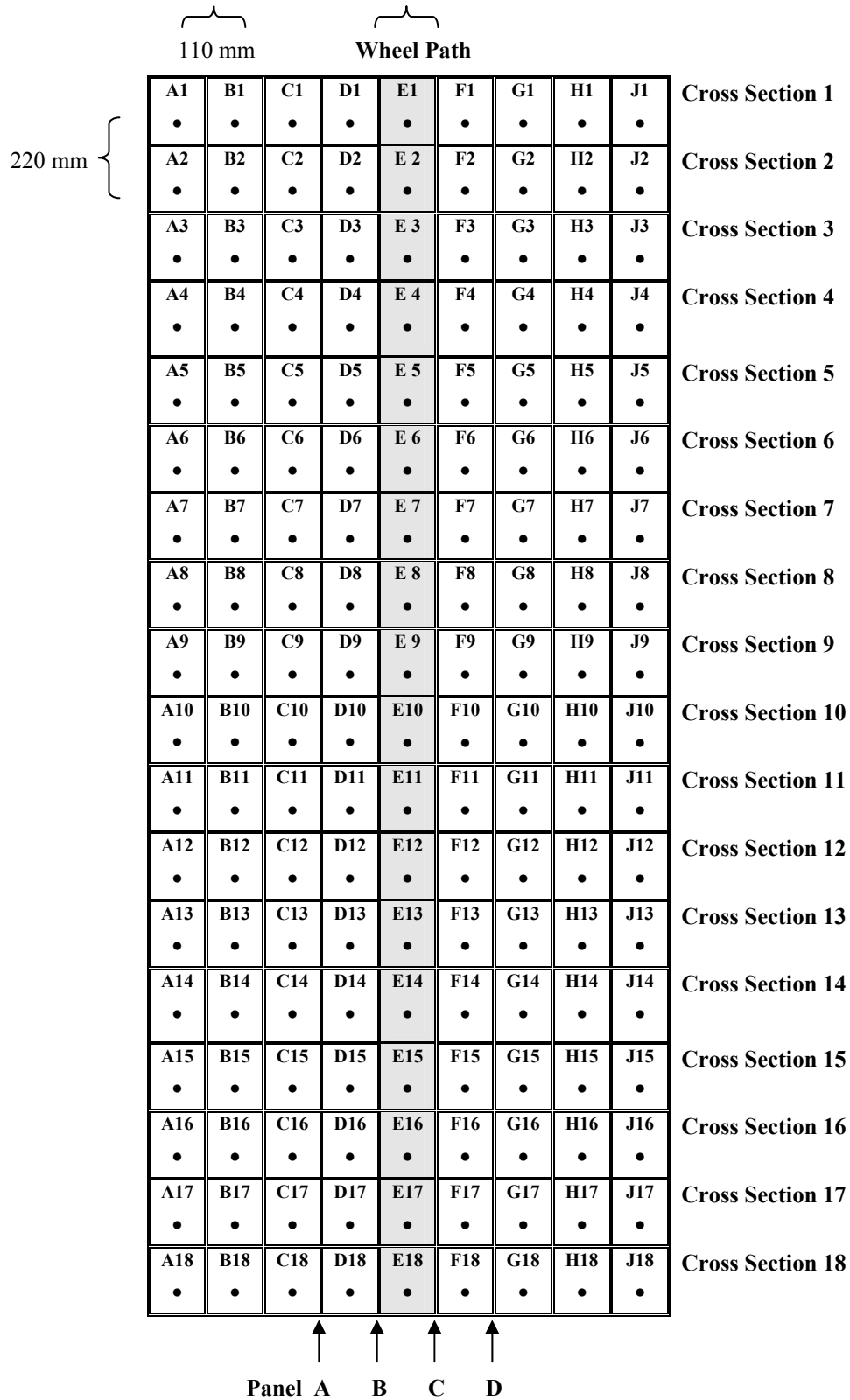
Figure 3.19 Location of rut depth permanent deformation measurement points

Figure 3.20   Measurement of pavement model deformation using the dial gauges

3.11   HALI Performance Monitoring

The purpose of this session is to investigate the deformation development of concrete block pavement subjected to accelerated trafficking test. The HALI test setup consists of a single wheel to apply the loading throughout the pavement. The tyre pressure of 600 kPa is maintained throughout the test. All the CPB were installed manually by hand on the entire pavement track. The speed of the mobile carriage was set to the value equal to 0.2 m/s. After the repetition loads, the rut depth profile of the pavement can be achieved by using the dials gauge measurement. After this test, the constant speed length and the accelerating/decelerating area was obtained for the pavement track. The entire operation of HALI was controlled by a microprocessor.

3.11.1 Rut Depth and Permanent Deformation Measurement

Rut depth and permanent deformation under the HALI testing was measured with reference to a fixed datum after 50 repetitions to the maximum repetitions of 2500 cycles. Dial gauges were positioned at the referenced points to measure the deformation of pavement after the commencement of the accelerated trafficking test. The test pavement was positioned initially to survey the surface profile at a distance of 110 mm between the dial gauges along the test pavement width (X-axis). The test pavement was also positioned at a distance of 220 mm between each cross section along the length (Y-axis). The system provides 108 height measurements at known plan positions on the surface (on a 1000 mm x 2580 mm grid test bed). Nine dial gauges were mounted at 110 mm apart on the rigid beam of test unit. This rigid beam was moved along the test pavement to take the measurement of each cross section. Once the data was recorded, the instrument was moved to the next cross section and the process was repeated. When all the cross sections had been measured, the survey data was processed using the SURFER program which uses a Kriging routine to generate a representative surface from the survey data (Mills *et al.* 2001). A three-dimensional view of the deformed surface is obtained from using the SURFER computer program. In addition, joint widths at panels beside the wheel path were measured.

3.11.2 Joint Width Measurement

The measurement of joint width is important because it partly determines the failure of the pavement. During this study, irregular joint widths were visually inspected. An area that exhibited this distress was identified. Digital vernier calipers was inserted into the joint below the chamfer at the middle of the length of the CPB and measurement was read. This measurement technique is introduced by UNILOCK (1997) for joint width identification. Location of the joint width at panel A, B, C and

D of three cross sections was measured. Each panel joint width value represents the average results of 18 cross sections.

3.12   Construction Procedures of RCPB Pavement

The construction procedure of the RCPB pavement model was the same as conducted in Section 3.9, except for the surface layer (CPB themselves). The detailed layout of the RCPB pavement is shown schematically in Figure 3.21. As shown in Figure 5.12, four types of RCPB: CCPB, 10-RCPB, 20-RCPB and 30-RCPB with equal areas were constructed under HALI (1000 mm x 645 mm, 27 blocks/section) for trafficking test.

Beneath the surface layer, the RCPB pavement comprises of a 50 mm dry bedding sand, plastic sheet and 3 mm thick sheet of hard neoprene. Regarding these layers and the type and quality of the materials, the construction methods and the construction standards are similar to those needed in the previous test at Section 5.4. A test width was set at about 1000 mm for lateral movements under accelerated trafficking test.

Prior to the testing, a control panel was programmed to a constant speed of 0.18 m/s that was the same as used in Section 3.10. When working continuously, HALI achieved 150 cycles per hour. The axle load of 1000 kg with a tyre (contact) pressure of 600 kPa was set to the wheel load to simulate the traffic load. The instrument was run up to 10000 repetitions for a complete trafficking test.
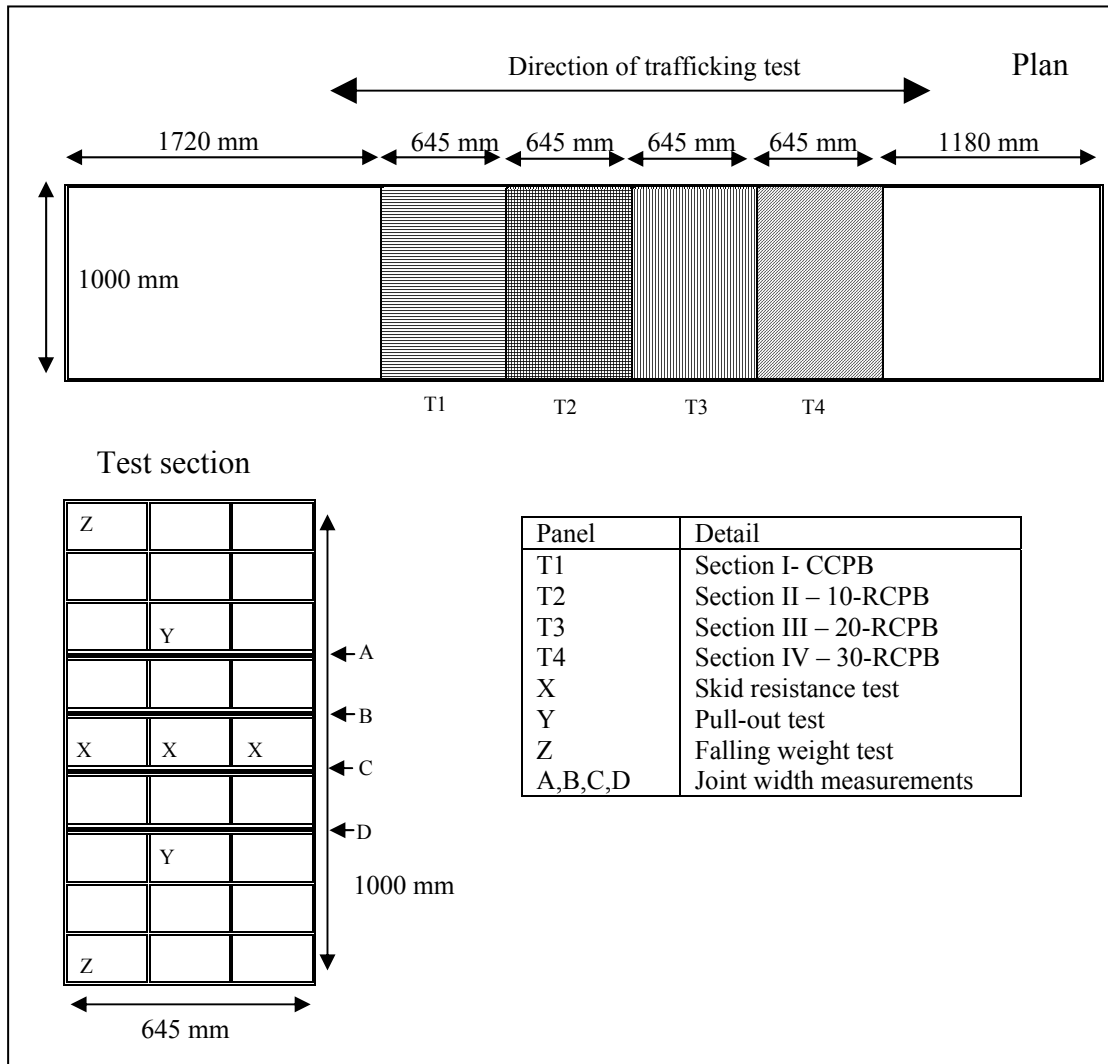
Figure 3.21   Layout detail of RCPB pavement model

3.13 Test Methods for RCPB Pavement

Rut depth measurement and three-dimensional deformation view, using dial gauges and SURFER program were the same as those used in Section 3.11.1. A similar joint width measurement method used in Section 3.11.2 was also applied in measuring the open joint width of RCPB pavement after 50, 100, 250, 500, 1000, 2500, 5000 and 10000 load repetitions.

3.13.1 Pull-Out Test

Figure 3.22 shows the pull-out test equipment which allows an individual RCPB to be extracted from the RCPB pavement. To ensure that the adjacent RCPB did not rotate during the extraction process and thereby grip the RCPB from being extracted, the test equipment applied its reaction load directly onto the adjacent RCPB.

In order to eliminate the effects of the bedding sand and the sub-layers under the RCPB, the instrument was designed to allow unrestrained upward movement under load of an individual RCPB from its matrix without affecting the surrounding RCPB. In this way, the shear resistance would apply to the joints only. It is noted that in practice a load applied to the pavement would induce stresses principally in a downwards direction but no means of measuring the effect on the joints. The extraction force measured by the instrument in lifting the RCPB was considered to be identical in magnitude to a downwards load (except for the effects of gravity). The instrument therefore provides an effective yet a simple means of identifying actual stress within the joints occurring under a variety of simulated loading conditions (Clifford 1984).

Load application and measurement were facilitated using a hydraulic jack and an electronic load cell of 100 kN capacity stacked centrally on the reaction beam. The two anchor bolts were extended in length using threaded studding and studding connectors. The upward movement was measured at each end of the RCPB at mid-point using two dial indicators accurate to 0.01 mm, impinging upon datum brackets to the surface of the RCPB.
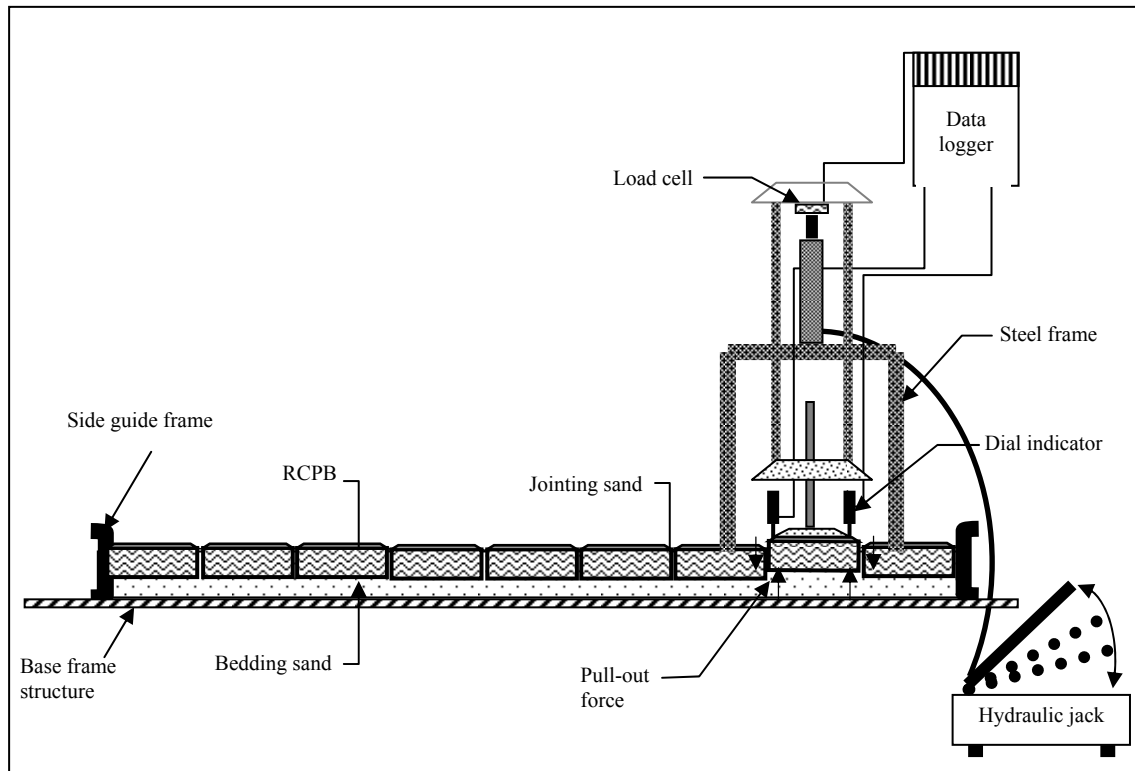
Figure3.22   Pull-out test set up

3.13.2 Skid Resistance Test

The British Pendulum device is a portable skid resistance tester for measuring the skid resistance of a wet pavement surface. The apparatus measures the frictional resistance between a rubber slider and the pavement surface. The rubber slider is mounted on the end of a pendulum arm. The RCPB (under the wheel path) of each test sections were therefore chosen to represent the pavements in use.

The visual inspection and skid resistances at four test sections were monitored prior to trafficking. Monitoring was stopped at the end of the trafficking test after 10000 load repetitions. In accordance to ASTM E-303 the average of four readings

was calculated for each of the tested RCPB. Some aggregates or rubber particle polished under traffic were recorded.

3.13.3 Falling Weight Test

To perform impact resistance test, an existing falling weight method was used. A 3.76 kg falling weight was dropped from a height of up to 50 cm, directly onto a RCPB sitting on a constructed RCPB pavement model. The loading face had a diameter of 44.6 mm for the purpose of uniformly transferring the impact load to the RCPB. Test was conducted at the end of the trafficking test, loading was dropped on a single RCPB of the pavement model which consisted of a layer of 50 mm thick loose bedding sand.

CHAPTER 4

PRESENTATION OF EXPERIMENTAL RESULTS

4.1 Introduction

Results obtained from two tests conducted in laboratories which are horizontal force and push-in tests will be discussed in this chapter. First, for the horizontal test, the discussion will be about the effect of laying pattern, block shape, block thickness and joint width between blocks. Secondly, for the push-in test, the effects of bedding sand thickness, joint width and block thickness will be discussed. The rectangular block shape was used in each push-in test.

Tests data for horizontal force and push-in tests were collected and presented in the graphical form. The maximum force of the model horizontal force and horizontal creep used rectangular and uni-pave block shapes are shown in Appendices A1 and A2. While maximum horizontal creep for each rectangular and unit-pave block shape, 60 mm and 100 mm block thickness and 3 mm, 5 mm and 7 mm joints width are shown in Appendices B1, B2, B3 and B4.

4.2   Sieve Analysis for Bedding and Jointing Sand

The sieve analysis results from the experiment are shown in Table 4.1. From the graph plot, even though the sand distribution percentage of passing sieve 0.15 mm and 0.075 mm is small, the curve of distribution sand size still fulfil the BS requirement 882 (1201) Part 2 (1989) which is still in the state grade of curve envelope. Sieve analysis has been done separately for sand which has been used for bedding sand layer and also jointing sand. Sieve analysis for bedding sand is between 0.075 mm and 9.52 mm while for the jointing sand sieve size is between 0.075 mm and 2.36 mm.

Table 4.1: The average of sand grading distribution used for bedding and jointing sand

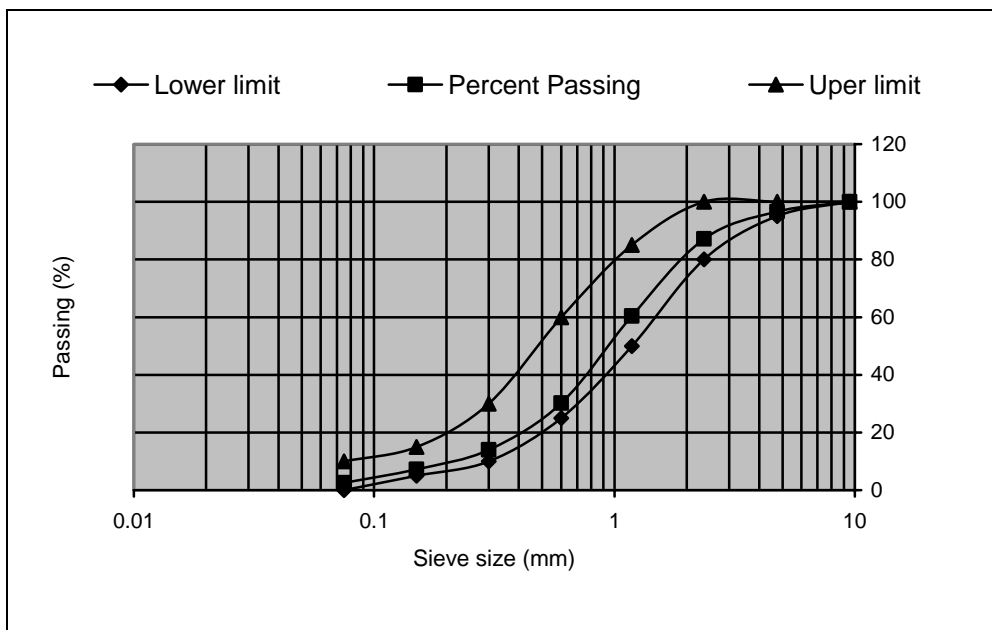| Sieve Size	Bedding Sand			Jointing Sand		
	Percent Passing (%)	Lower limit (%)	Upper Limit (%)	Percent Passing (%)	Lower limit (%)	Upper limit (%)
9.52 mm	100	100	100	-	-	-
4.75 mm	95.6	95	100	-	-	-
2.36 mm	81.1	80	100	100.0	100	100
1.18 mm	50.4	50	85	91.2	90	100
600 μm	30.2	25	60	65.2	60	90
300 μm	14.0	10	30	40.1	30	60
150 μm	6.2	5	15	20.6	15	30
75 μm	2.6	0	10	6.5	5	10

Figure 4.1   Particle size distributions for bedding sand
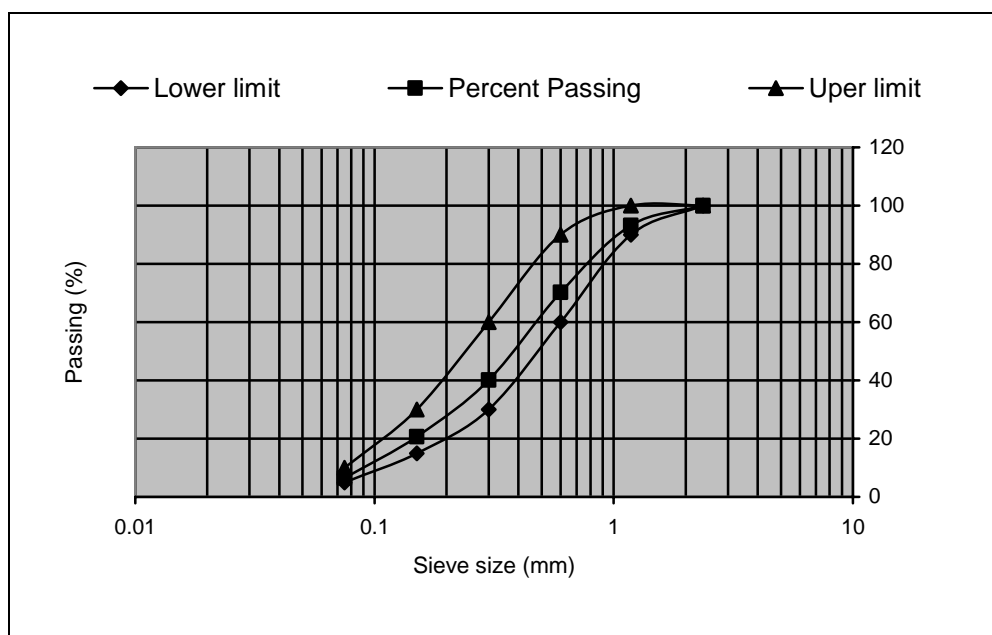
Figure 4.2   Particle size distributions for bedding sand

4.3   Moisture Content of Sand

The moisture content of sand required for bedding sand and jointing sand is between 4 to 8 %. From the experiment, the average of three samples is 7.4 %. Bedding sand and jointing sand moisture content should been counted because both influence the displacement and friction between blocks.

4.4   Horizontal Force Test Results

For the behaviour of block pavements under horizontal forces, the pavement may present various types of horizontal creeps submitted to a horizontal force, depending on the laying pattern, blocks thickness, joint width between blocks and blocks shape.

4.4.1   The Effect of Laying Pattern

The effect of the laying pattern on concrete block pavements is significant with the effect of neighbour blocks movement under horizontal forces. The herringbone 45$^{\text{o}}$ bond and herringbone 90$^{\text{o}}$ bond have more neighbour movement effect than stretcher bond laying pattern.

4.4.1.1 Rectangular Block Shape

In the case of rectangular block shape, the experimental results from the laboratory based on joint width variable indicate that from the relationship between horizontal forces with horizontal creep, stretcher laying pattern is the highest on the horizontal creep, while herringbone 45° laying pattern is the lowest. Here, the herringbone 90° laying pattern has more horizontal creep than herringbone 45° bond. There is about 1.60 mm horizontal creep differences between stretcher laying pattern with herringbone 45° and 1.20 mm to herringbone 90° laying pattern. This was caused by the effect of distribution horizontal load in each laying pattern. In this case herringbone 45° pattern is wider than herringbone 90° and stretcher bond. For more details see Figure 4.3, Figure 4.4 and Figure 4.5. Each test was applied on CBP with 60 mm block thickness and variation of joint width (3 mm, 5 mm and 7 mm).

Figure 4.3   Relationship between horizontal forces with horizontal creep on CBP: rectangular block shape, 60 mm block thickness and 3 mm joint width
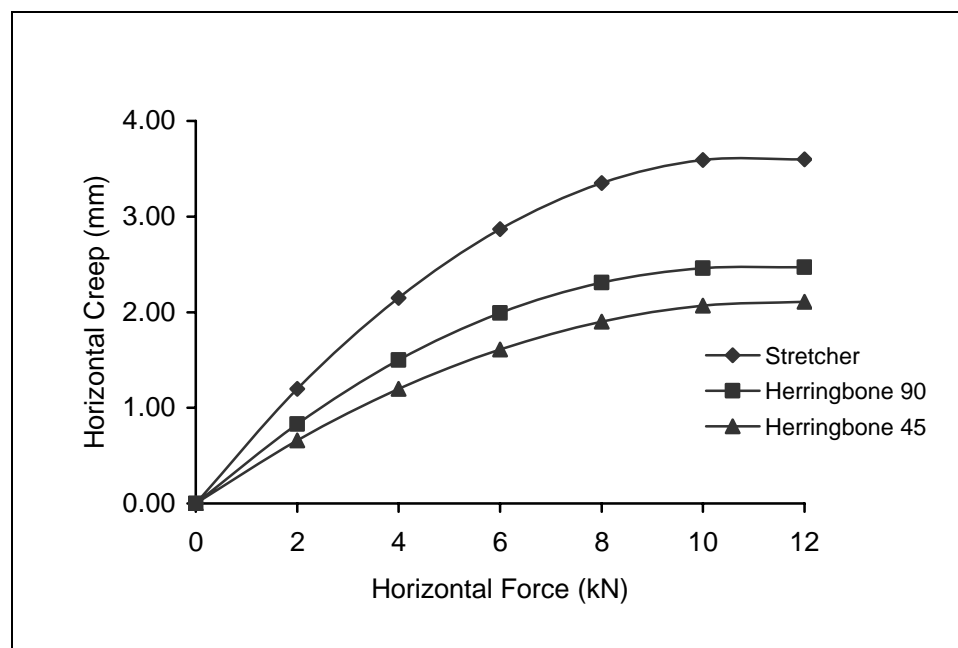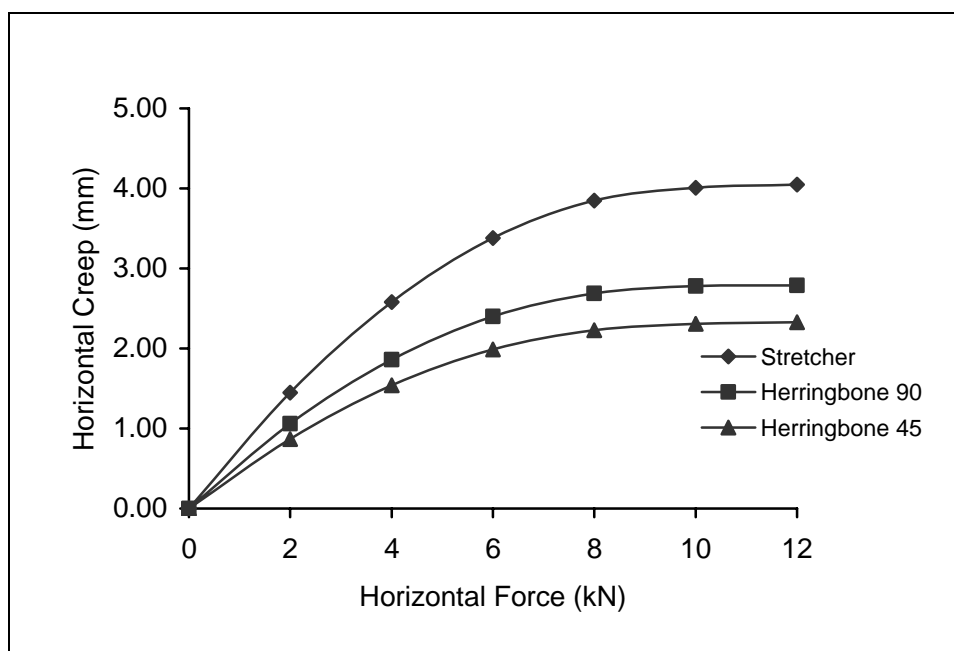
Figure 4.4   Relationship between horizontal forces with horizontal creep on CBP: rectangular block shape, 60 mm block thickness and 5 mm joint width
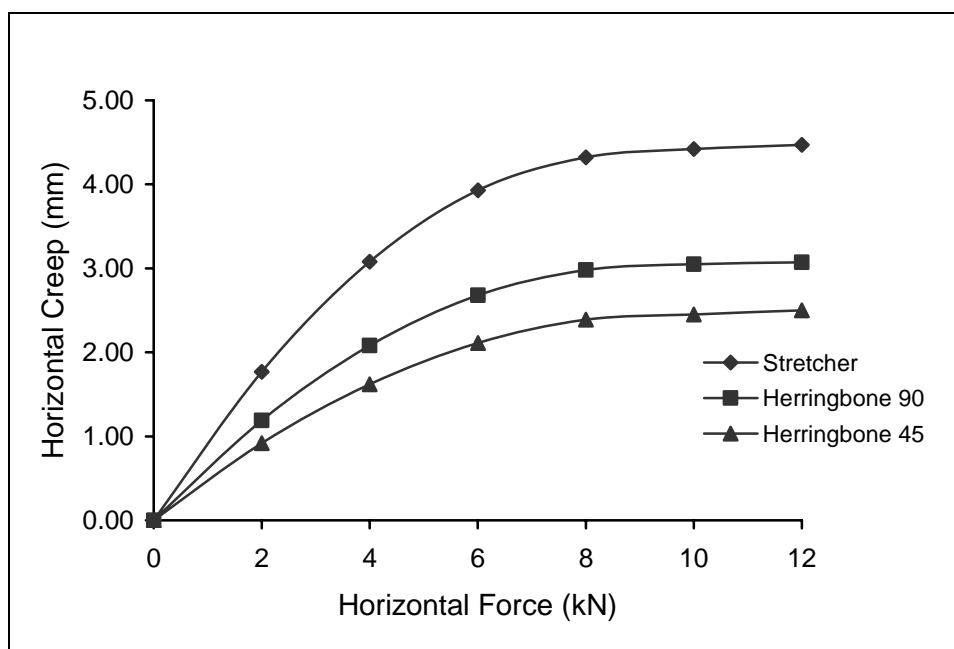

Figure 4.5   Relationship between horizontal forces with horizontal creep on CBP: rectangular block shape, 60 mm block thickness and 7 mm joint width

4.4.1.2 Uni-pave Block Shape

In the case of uni-pave block shape, the experimental results from the laboratory based on joint width variable indicate that from the relationship between horizontal forces with horizontal creep, stretcher laying pattern is the highest the horizontal creep, while herringbone 45° laying pattern is the lowest. Compared by rectangular block shape, the horizontal creep of CBP by used uni-pave block shape has more restraint movement blocks. This was caused the uni-pave block shape has gear on each sides. The difference of horizontal creep between rectangular with uni-pave block shape is about 1.50 mm. Figure 4.6 to Figure 4.8 are shown the difference of horizontal creep for CBP by various joint width (3 mm, 5 mm and 7 mm). The difference horizontal creep between stretcher bond with herringbone 90° (in Figure 4.7 and Figure 4.8) was caused by variation of joint width (in this case joint widths are 5 mm and 7 mm). The results are shown in Figure 4.6, Figure 4.7 and Figure 4.8.

Figure 4.6 Relationship between horizontal forces with horizontal creep on CBP: uni-pave block shape, 60 mm block thickness and 3 mm joint width
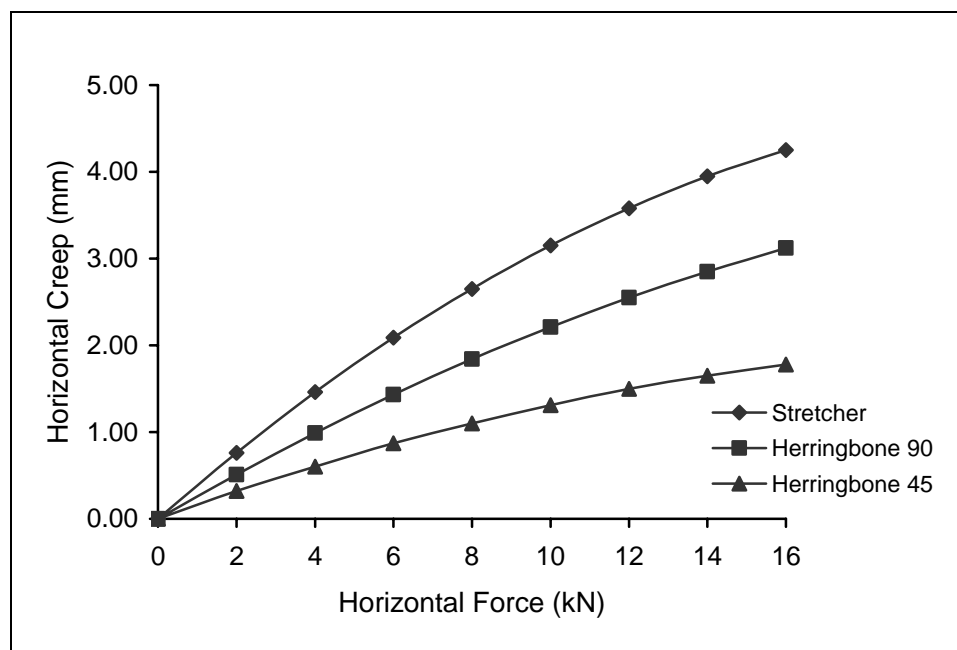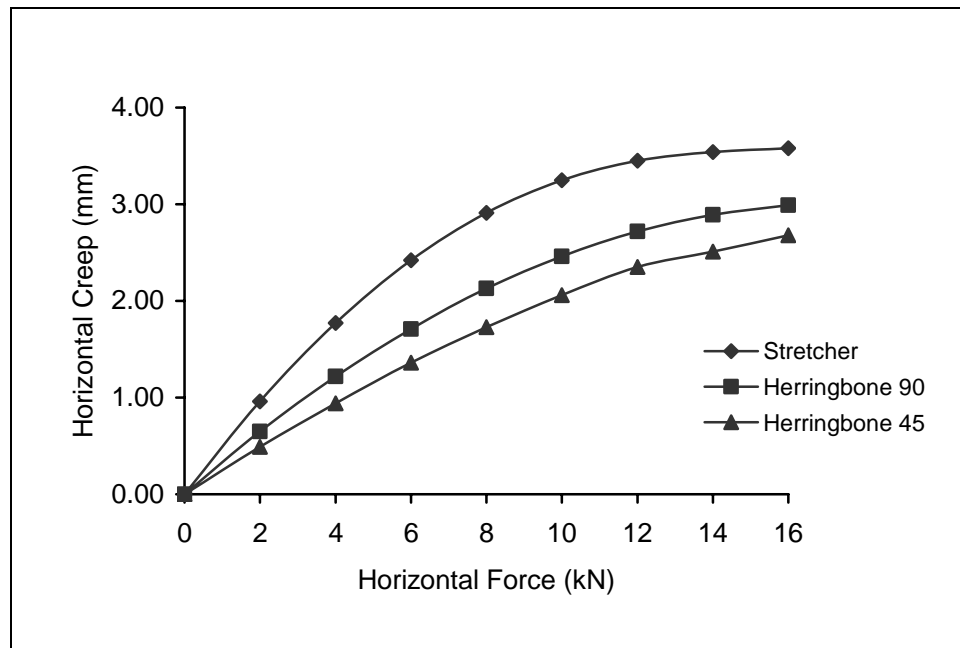
Figure 4.7   Relationship between horizontal forces with horizontal creep on CBP: uni-pave block shape, 60 mm block thickness and 5 mm joint width
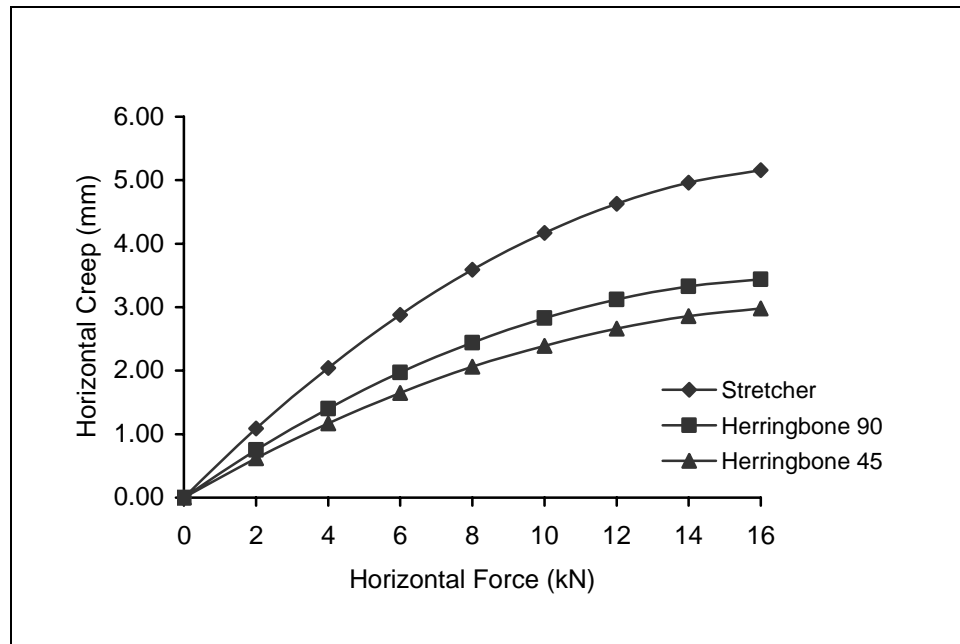

Figure 4.8   Relationship between horizontal forces with horizontal creep on CBP: uni-pave block shape, 60 mm block thickness and 7 mm joint width

4.4.2   The Effect of Block Thickness

The effect of block thickness on concrete block pavements is significant with friction between blocks and the weight of block itself. The block thickness used was 60 mm and 100 mm thick. The rectangular unit weight 60 mm thickness (2.6 kg / unit) and 100 mm thickness (4.2 kg / unit).

This study includes an examination of block thickness ranging from 60 mm to 100 mm. Three parameters were used to asses the response of the pavements. These are: the surface deformations or rutting, surface elastic or resilient deflections and vertical compressive stresses transmitted to the sub-grade.

4.4.2.1   Rectangular Block Shape

The rectangular block shape has frictional area for load transfer to adjacent blocks. The friction areas for rectangular shape between blocks depend on the thickness of the side surface of the block. It can be concluded that the shape of the block influences the performance of the block pavement under load. It is postulated that the effectiveness of load transfer depends on the vertical surface area of the blocks.

In the case of rectangular block shape, the experimental results from the laboratory based on block thickness indicate that, the relationship between horizontal forces with horizontal creep for 100 mm block thickness is better than 60 mm block to restrain the horizontal creep. The results are shown in Figure 4.9, Figure 4.10 and Figure 4.11. Each test was applied on CBP with stretcher bond laying pattern and joint thickness of 3 mm, 5 mm and 7 mm.

Figure 4.9   Relationship between horizontal forces with horizontal creep on CBP: rectangular block shape, stretcher bond laying pattern and 3 mm joint width

Figure 4.10   Relationship between horizontal forces with horizontal creep on CBP: rectangular block shape, 60 mm block thickness and 5 mm joint width

Figure 4.11 Relationship between horizontal forces with horizontal creep on CBP: rectangular block shape, 60 mm block thickness and 7 mm joint width

4.4.2.2 Uni-pave Block Shape

The uni-pave block shape has frictional area better than rectangular shape for load transfer to adjacent blocks. It can be concluded that the blocks provided geometrical interlock along all four sides. Compared to the rectangular block shape, the uni-pave block shape has better performance on interlocking between blocks and tends to restrain horizontal creep on the pavement. The influence of block thickness in uni-pave block shape is better to interlock between blocks than rectangular. It is postulated that the effectiveness of load transfer depends on the vertical surface area of the blocks. The block thickness is increase, the vertical surface area increase, so the rotation and horizontal interlock increase.

In the case of uni-pave block shape, the experimental results based on varying block thicknesses indicate that the relationship between horizontal forces with horizontal creep, found that 100 mm block thickness is better than 60 mm block thick to restrain the horizontal creep. The difference of horizontal creep between 60 mm with 100 mm block thicknesses is about 2.00 mm to 2.50 mm. The increase of block thickness will cause provide a higher frictional area. The results are as shown in Figure 4.12, Figure 4.13 and Figure 4.14. Each test was applied on CBP with stretcher bond laying pattern and variation of joint width (3 mm, 5 mm and 7 mm).
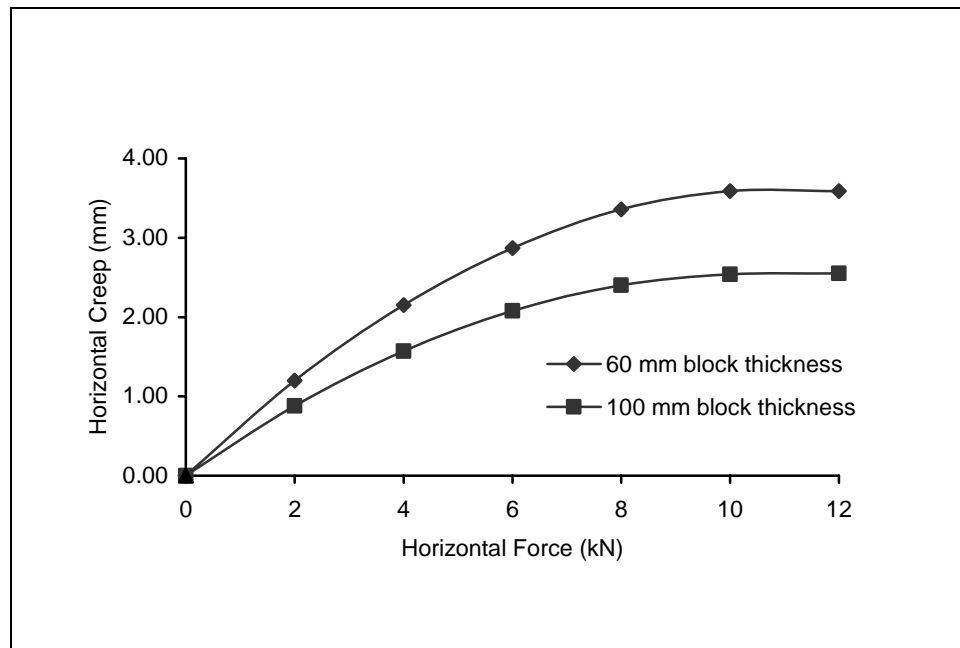

Figure 4.12 Relationship between horizontal forces with horizontal creep on CBP: uni-pave block shape, 60 mm block thickness and 3 mm joint width
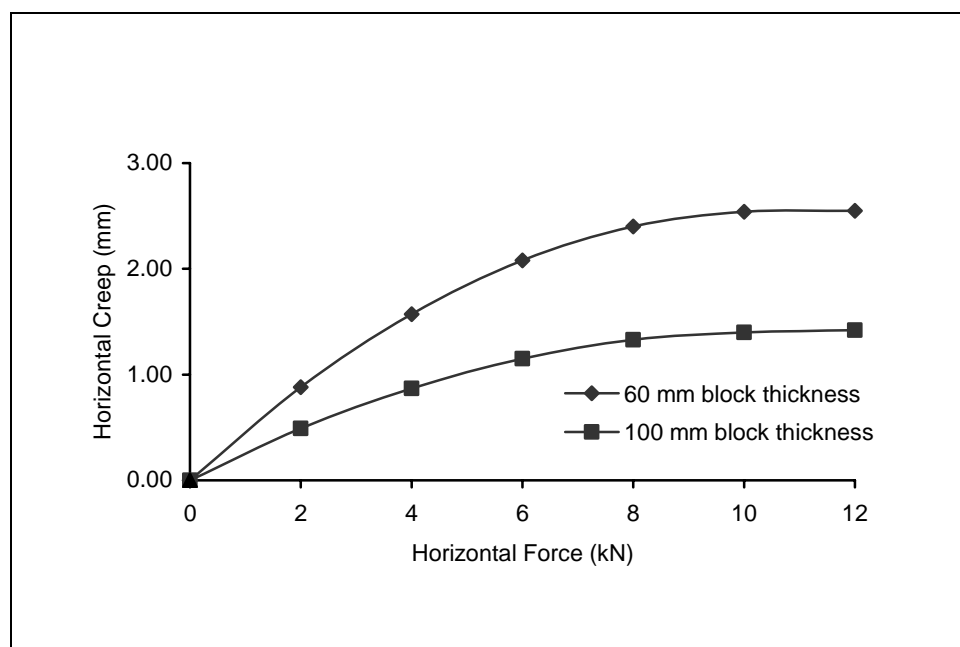
Figure 4.13   Relationship between horizontal forces with horizontal creep on CBP:
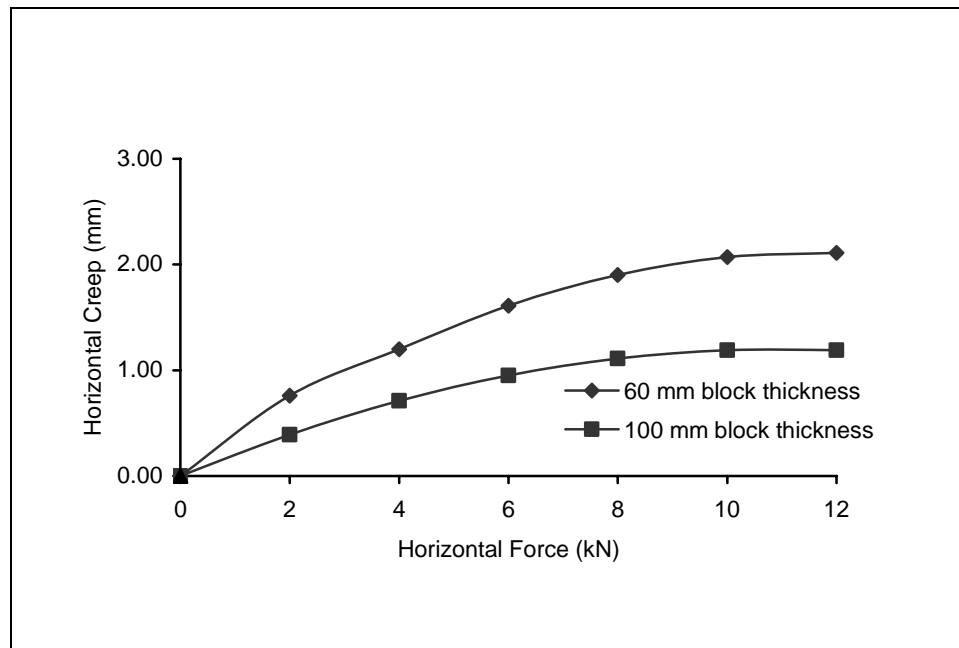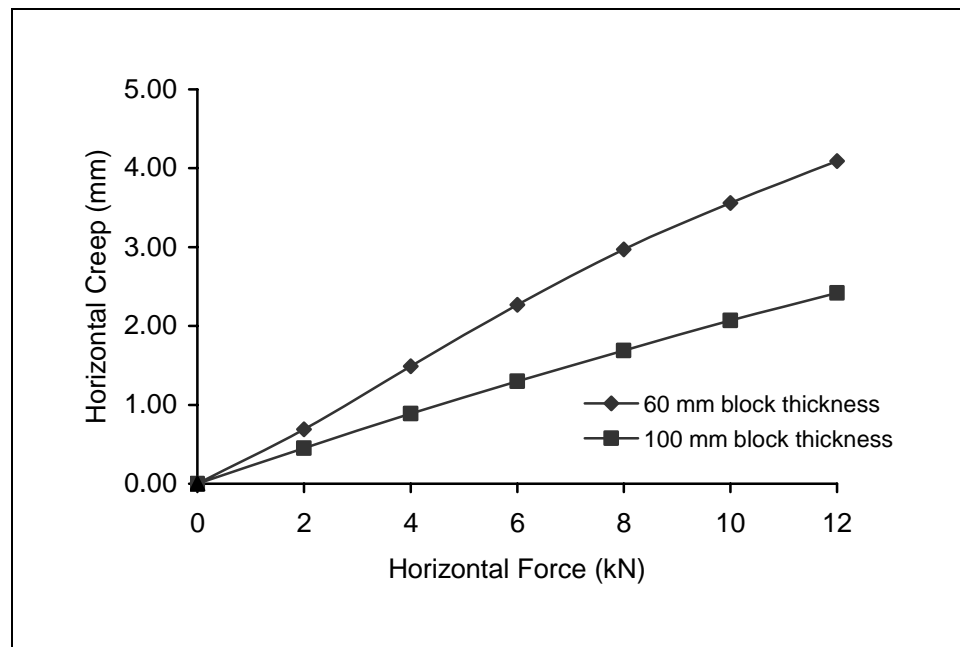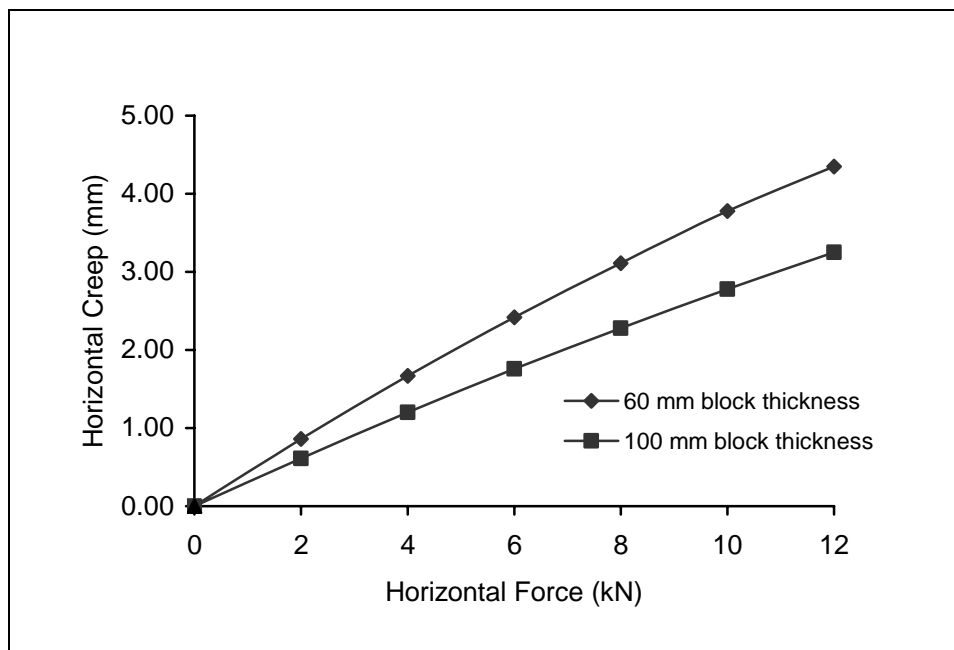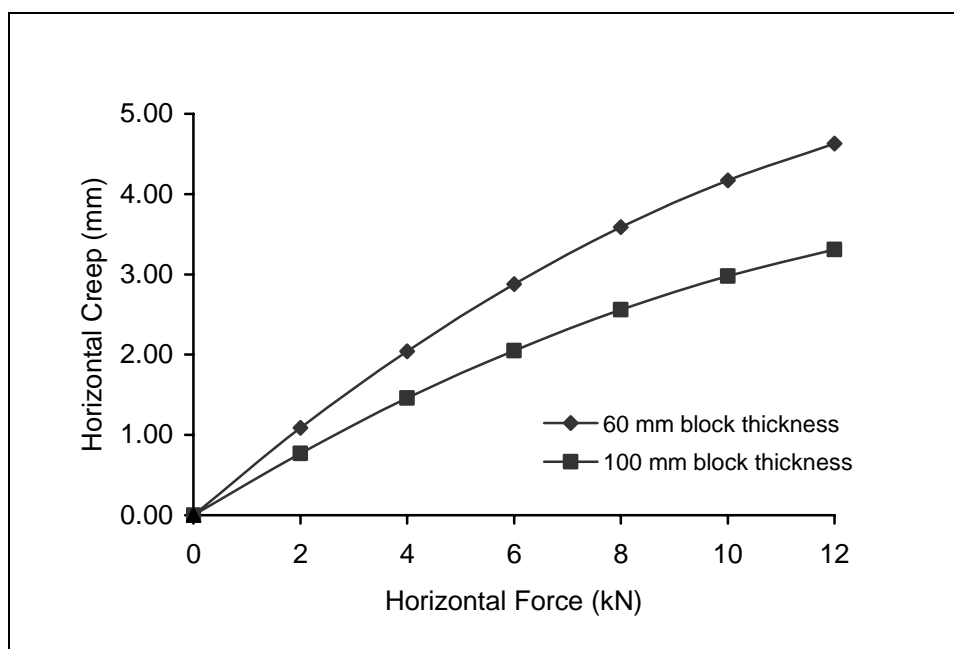uni-pave block shape, 60 mm block thickness and 5 mm joint width

Figure 4.14   Relationship between horizontal force with horizontal creep on CBP:
uni-pave block shape, 60 mm block thickness and 7 mm joint width

4.4.3 The Effect of Joint Width

Sand filled joints are an integral part of concrete block pavement. They permit the block surface course to behave flexibly by allowing some articulation of individual blocks and they provide the structural interlock necessary for stresses to be distributed among adjacent blocks. Joints need to be sufficiently wide to allow this flexible behaviour, but not so wide as to permit excessive movement of the pavers. In the experiments were used joint widths 3 mm, 5 mm and 7 mm. Those wider than 5 mm should not be accepted. Two mm wide spacer ribs cast integrally on the vertical surfaces of the pavers ensure minimum joint width and assist in rapid placement of the blocks.

4.4.3.1 Rectangular Block Shape

The rectangular block shape has frictional area for load transfer to adjacent blocks. The friction area for rectangular shape is between blocks depending on joint width between blocks. It is concluded that the shape of the block influences the performance of the block pavement under load. It is postulated that the effectiveness of load transfer depends on the filling of jointing sand and also joint width between blocks.

In the case of rectangular block shape, the experimental results from the laboratory based on varying the joint width indicate that from the relationship between horizontal forces with horizontal creep, 100 mm block thickness is better than 60 mm block thickness for restraining of the horizontal creep. The difference of horizontal creep with varying joint width 3 mm, 5 mm and 7 mm) is about 0.50 mm to 1.20 mm. The results are shown in Figure 4.15 to Figure 4.20. In this case was applied on CBP with stretcher bond laying pattern and variation of joint width.

Figure 4.15   Relationship between horizontal forces with horizontal creep on CBP: rectangular block shape, stretcher bond laying pattern and 60 mm block thickness

Figure 4.16   Relationship between horizontal forces with horizontal creep on CBP: rectangular block shape, Herringbone 90$^{\text{o}}$ laying pattern and 60 mm block thicknes

Figure 4.17 Relationship between horizontal forces with horizontal creep on CBP: rectangular block shape, Herringbone 45° laying pattern and 60 mm block thickness

Figure 4.18 Relationship between horizontal forces with horizontal creep on CBP: rectangular block shape, stretcher laying pattern and 100 mm block thickness

Figure 4.19   Relationship between horizontal forces with horizontal creep on CBP: rectangular block shape, herringbone 90° pattern and 100 mm block thickness
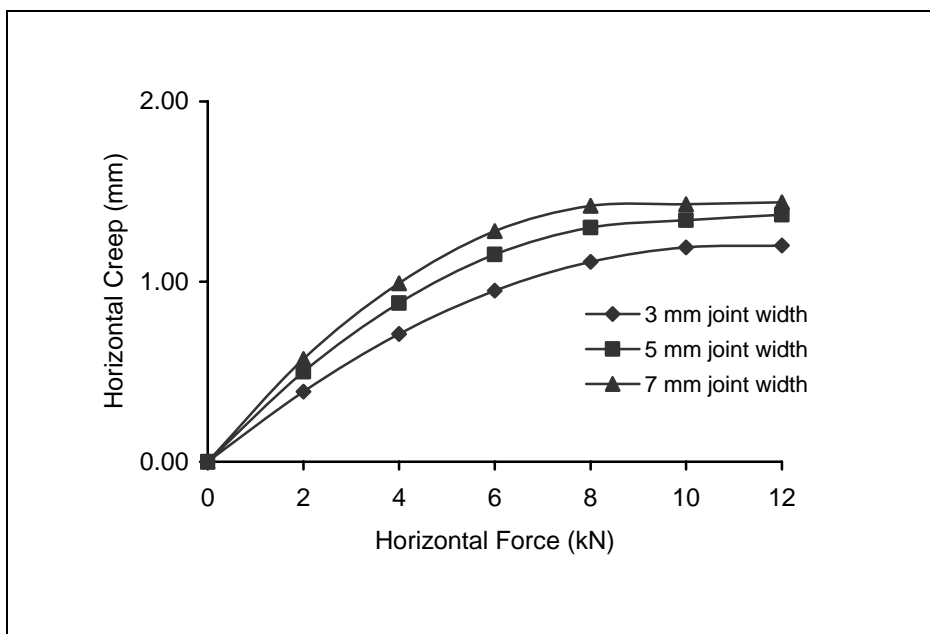
Figure 4.20   Relationship between horizontal forces with horizontal creep on CBP: rectangular block shape, herringbone 45° pattern and 100 mm block thickness

The results from Figure 4.15 to 4.20 are shown, that changing of joint width from 3 mm to 7 mm illustrated the increase of joint width, increase the horizontal creep. This case was caused by jointing sand between blocks may be there are the void and less compaction. The previous experiment was funded that the optimum joint width is 3 mm. For joint widths less than the optimum, the jointing sand was unable to enter between blocks. A large amount of sand remained outside the joint showing sand heaps on the block surface.

4.4.3.2 Uni-pave Block Shape

The uni-pave block shape has frictional area that is better than rectangular shape for load transfer to adjacent blocks. It shape has more restraint of horizontal creep than rectangular block shape, because uni-pave block shape has gear (four-dents). It is concluded that the shape of the block influences the performance of the block pavement under load. It is postulated that the effectiveness of load transfer depends on the width of jointing sand between blocks.

In case of uni-pave block shape, the experimental results from the laboratory based on joint width variable indicate that from the relationship between horizontal forces with horizontal creep, 100 mm block thickness is better than 60 mm block thickness for restraining of the horizontal creep. In Figure 4.21 was shown that the graphic relation between horizontal forces with horizontal creep is steeper if compared than rectangular block shape. It is caused the CBP sample used 3 mm width joint than pushed horizontal force until 12 kN, the construction is not failure. The results are shown in Figure 4.21 to Figure 4.26. Each test was applied on CBP with stretcher bond laying pattern and variation of joint width (3 mm, 5 mm and 7 mm).
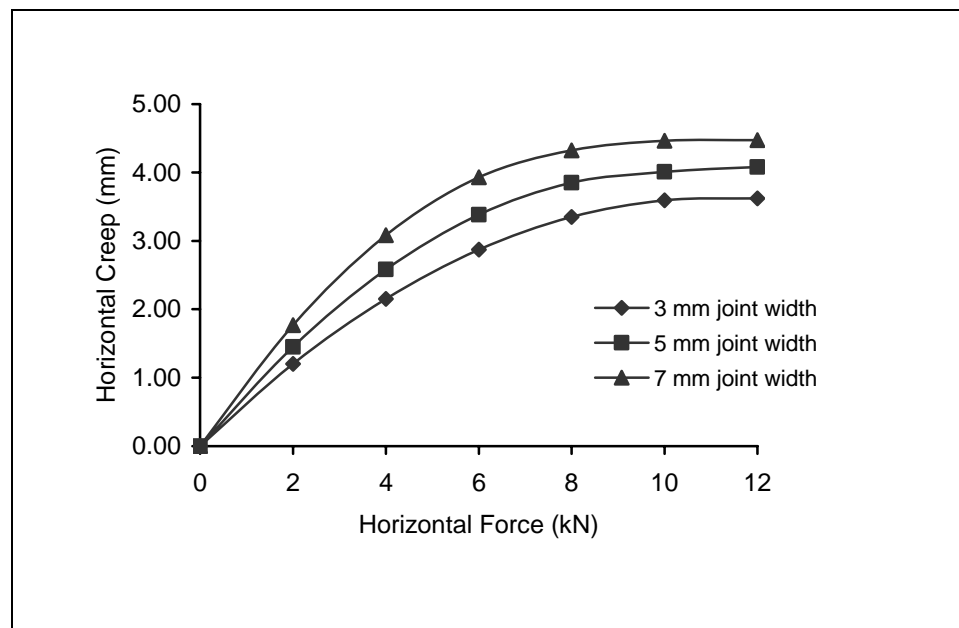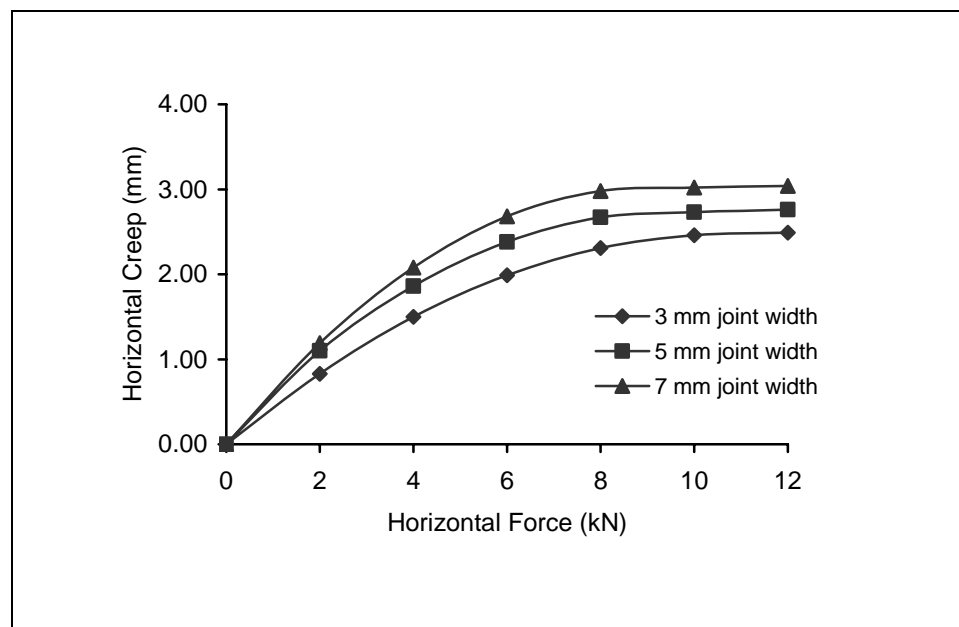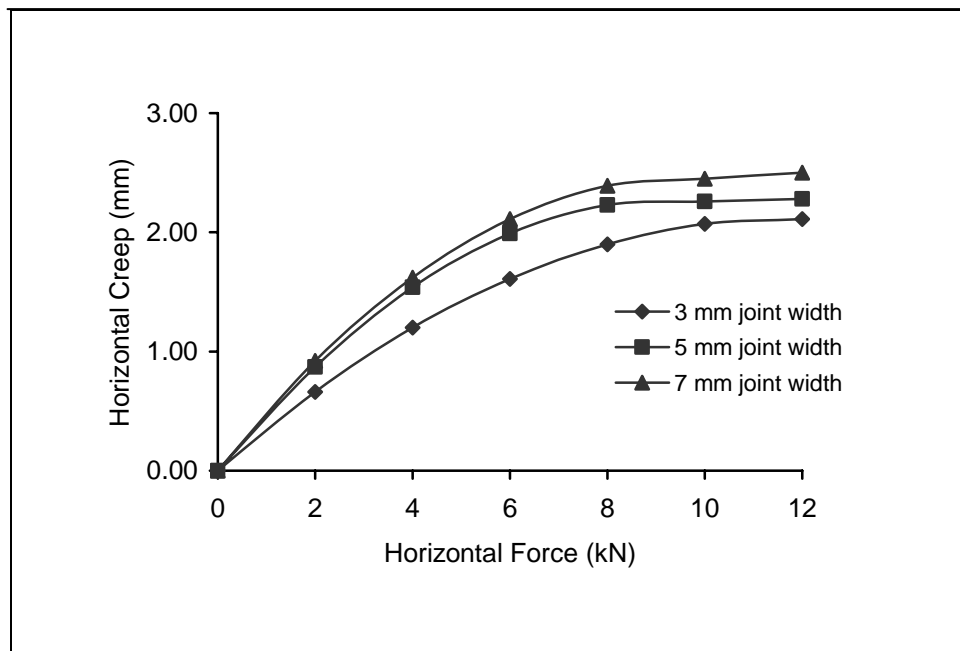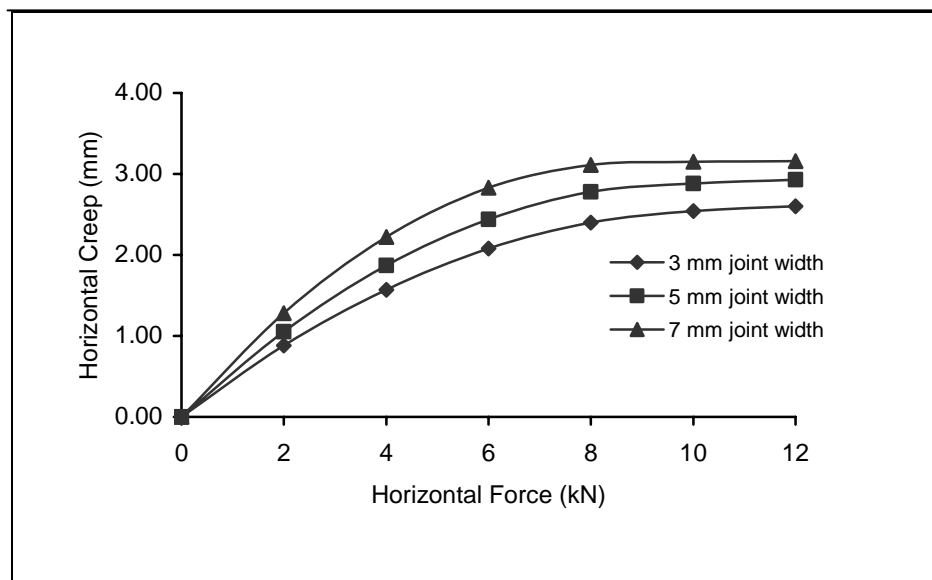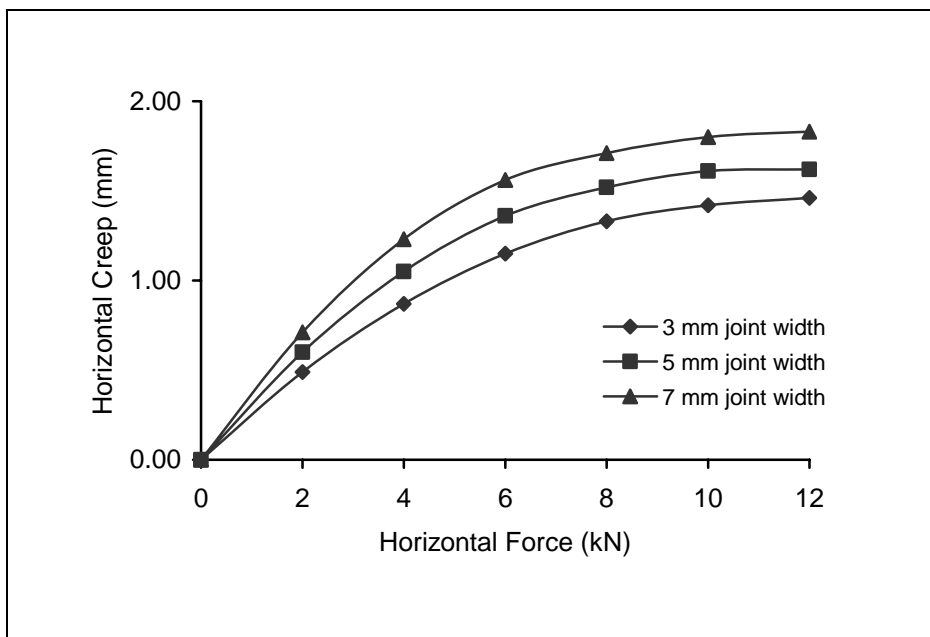
Figure 4.21 Relationship between horizontal forces with horizontal creep on CBP: uni-pave shape, 60 mm thickness, stretcher bond laying pattern

Figure 4.22 Relationship between horizontal forces with horizontal creep on CBP: uni-pave shape, 60 mm thickness, herringbone bond 90° laying pattern

In Figure 4.21 and 4.22 are shown that horizontal creep on CBP by 3 mm joint width is the lowest to movement, because each blocks was completed by nib spacer ($\pm$ 2 mm thickness).
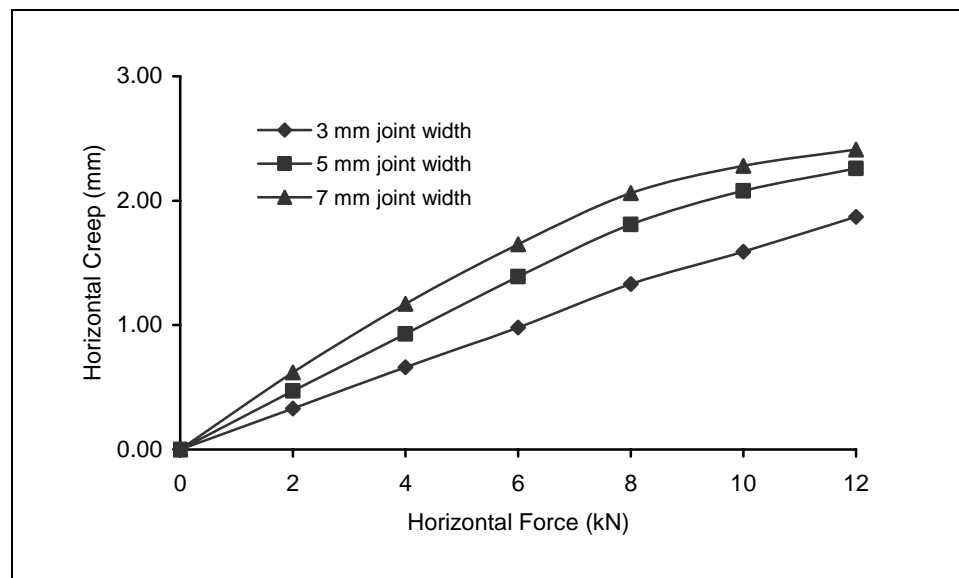
Figure 4.23   Relationship between horizontal forces with horizontal creep on CBP: uni-pave shape, 60 mm thickness, herringbone bond 45° laying pattern
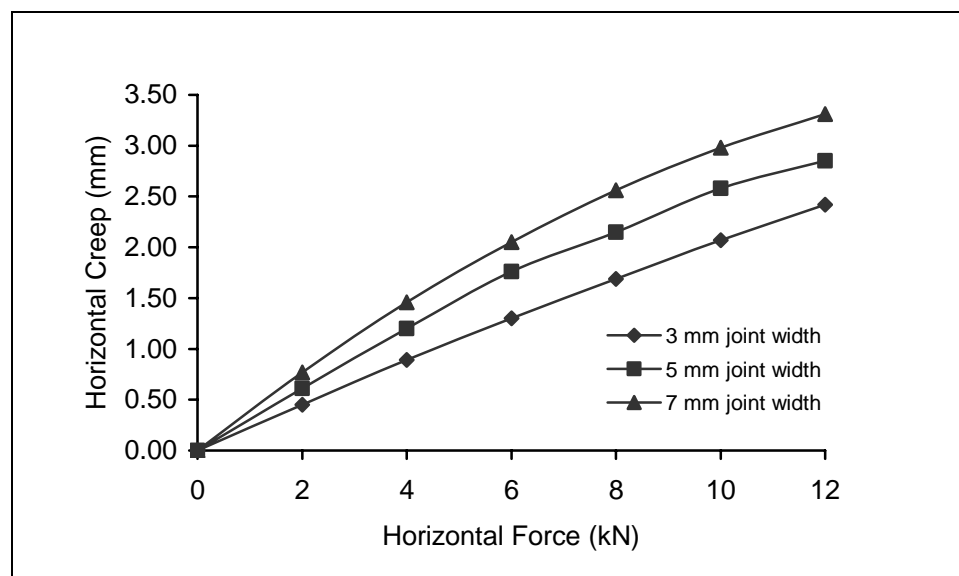
Figure 4.24   Relationship between horizontal forces with horizontal creep on CBP: uni-pave shape, 100 mm thickness, stretcher laying pattern
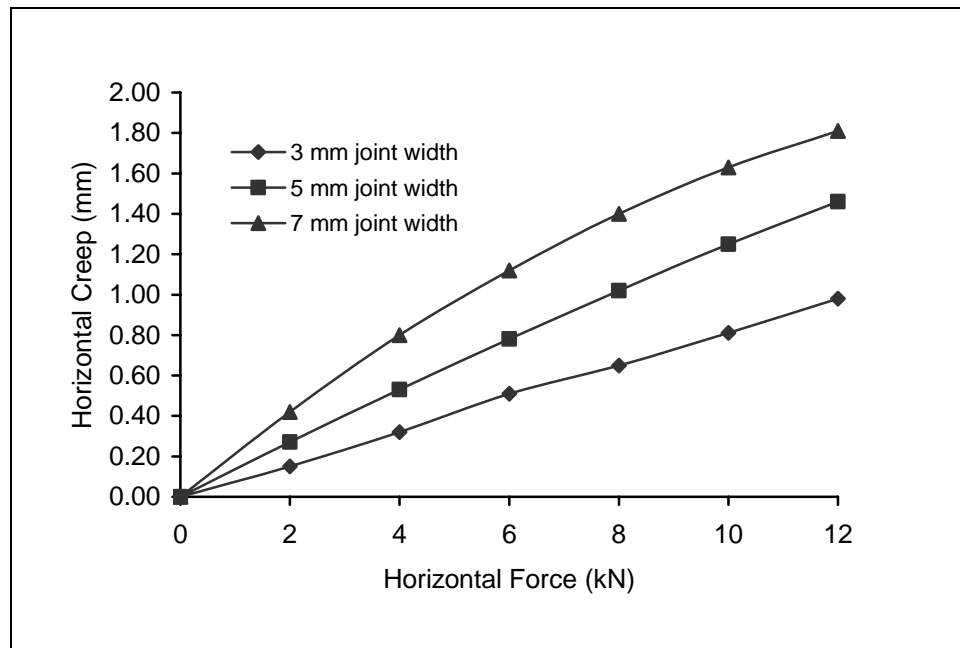
Figure 4.25   Relationship between horizontal forces with horizontal creep on CBP:
uni-pave shape, 100 mm thickness, herringbone 90° laying pattern

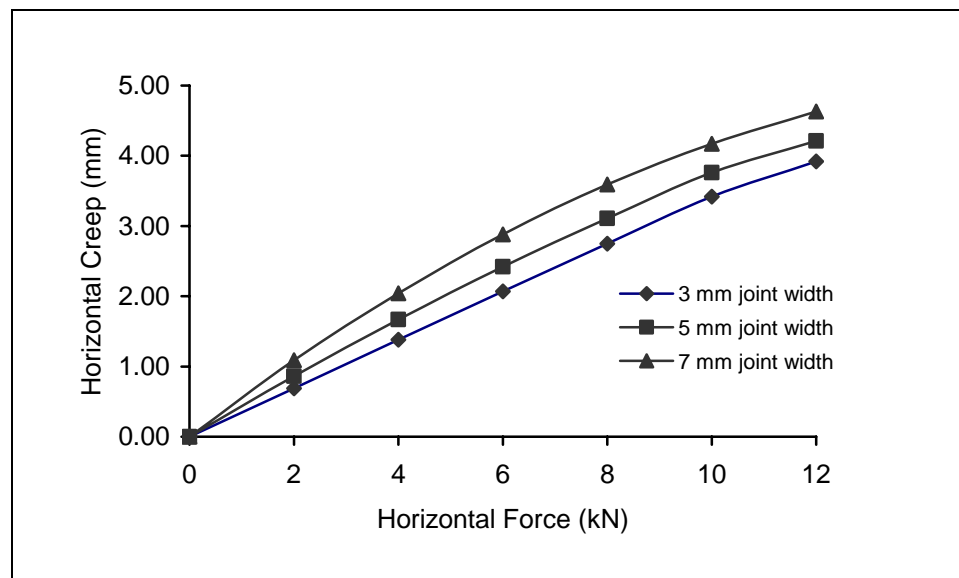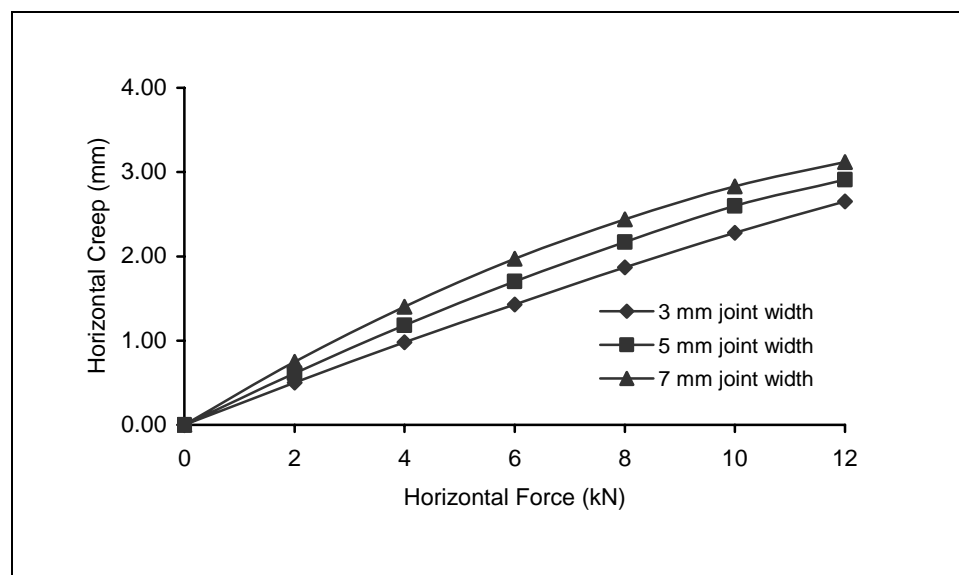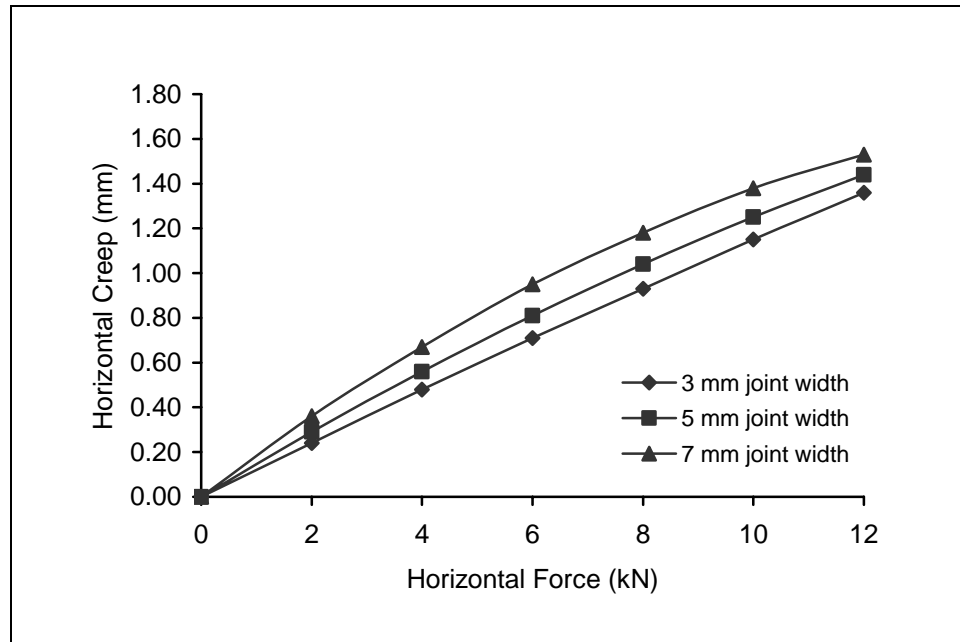**Figure 4.26**   Relationship between horizontal forces with horizontal creep on CBP:
uni-pave shape, 100 mm thickness, herringbone 45° laying patter

4.4.4   The Effect of Block Shape

The effect of block shape has a major influence on concrete block pavement performance. In the experiment, rectangular and uni-pave block shape, 60 mm blocks thickness were laid on (30 mm, 50 mm and 70 mm) of bedding sand thickness and various joint width (3 mm, 5 mm and 7 mm).

The differences in performance between the various blocks shapes have been discussed in detail elsewhere. In general it can be concluded that blocks which provide geometrical interlock along all (uni-pave) four sides tend to yield similar levels of performance regardless of shape, and that shaped (interlocking) blocks yield much better performance than rectangular (non-interlocking) blocks.

4.5   Push-in Test Results

For the behaviour of block pavements under push-in test, the pavement may present various types of mechanical behaviour submitted to a horizontal creep, depending on the bedding sand thickness, joint width between blocks, blocks thickness and degree of slope.

4.5.1   The Effect of Bedding Sand Thickness

Figure 4.27 to Figure 4.32 show the relationship between push-in force with horizontal creep on the varying loose thicknesses of 30, 50, and 70 mm bedding sand. It is seen that the deflections of pavement decrease with the increase in loose

thickness of bedding sand from 30 to 70 mm. The deflection is minimum at a loose thickness of 30 mm bedding course.

The compaction might not be fully effective for a higher thickness of bedding sand during vibration. During vibration of blocks, the bedding sand rises through the joints to small heights and wedges in between the blocks. The rise of sand increases with the increase in loose thickness of bedding sand. The wedging of these sands absorbs the major part of applied vibration energy and transfers less to the bedding sand below. As a result, the bedding sand is not fully compacted for higher thicknesses. Consequently, some compaction of bedding sand takes place under load and thus shows more deflection in the test pavements. The higher the loose bedding sand thickness, the more the deflection will be.

Figure 4.27   Relationship between push-in forces with horizontal creep on CBP: rectangular shape, 60 mm block thickness and 3 mm joint width

Figure 4.28 Relationship between push-in forces with horizontal creep on CBP: rectangular shape, 60 mm block thickness and 5 mm joint width

Figure 4.29 Relationship between push-in forces with horizontal creep on CBP: rectangular shape, 60 mm block thickness and 7 mm joint width

Figure 4.30   Relationship between push-in forces with horizontal creep on CBP: rectangular shape, 100 mm block thickness and 3 mm joint width

Figure 4.31   Relationship between push-in forces with horizontal creep on CBP: rectangular shape, 100 mm block thickness and 5 mm joint width

Figure 4.32   Relationship between push-in forces with horizontal creep on CBP: rectangular shape, 100 mm block thickness and 7 mm joint width

4.5.2   The Effect of Joint Width

Figure 4.33 to Figure 4.38 showed the response of pavement for design joint widths of 3 mm, 5 mm and 7 mm with varying block thickness and bedding sand thickness. As the joint width decreases, the deflection of the pavement also decreases. The higher of block and bedding sand thickness, the lesser the normal stiffness of the joint will be. This will lead to more rotations and translations of blocks. Thus, there will be more deflection under the same load for thicker joints. Some of the grains coarser than the joint width were unable to enter inside. This has been observed during filling sand in joints. A large amount of sand remained outside the joint showing sand heaps on the block surface. The coarse grains of sand choked the top surface of joints and prevent movement of other fine grains into the joint. There might be loose pockets or honeycombing inside the joint. The joint stiffness decreases and in turn reflects slightly higher deflections. At the optimum joint width,

there is the maximum chance that single grains of average size, close to the joint width, will be retained in the joints during joint filling.

Figure 4.33   Relationship between push-in forces with horizontal creep on CBP: rectangular shape, 60 mm block thickness and 30 mm bedding sand thickness

Figure 4.34   Relationship between push-in forces with horizontal creep on CBP: rectangular shape, 60 mm block thickness and 50 mm bedding sand thickness

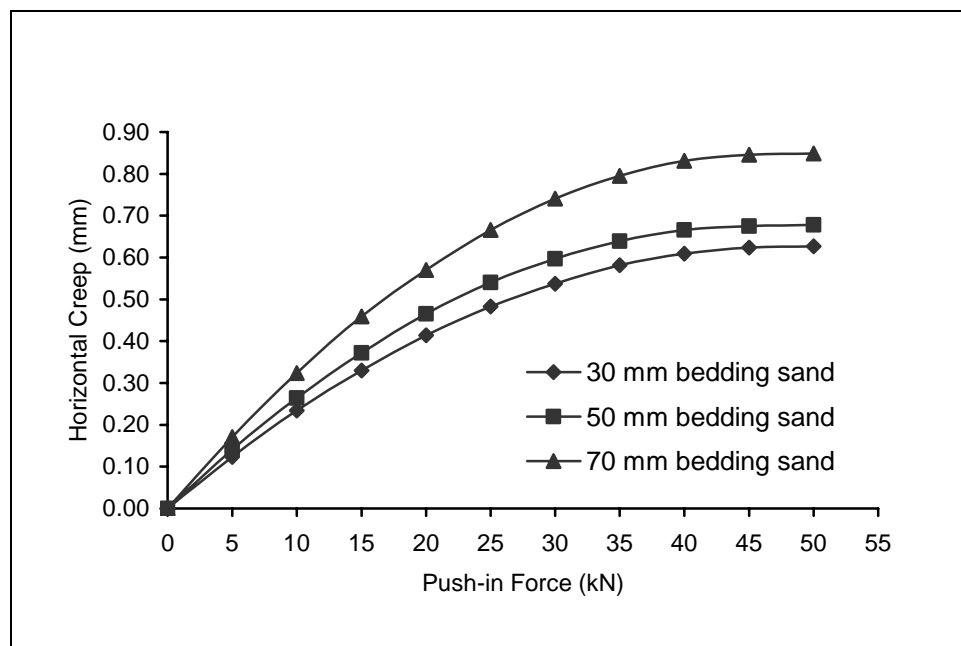**Figure 4.35**   Relationship between push-in forces with horizontal creep on CBP: rectangular shape, 60 mm block thickness and 70 mm bedding sand thickness

Figure 4.36   Relationship between push-in forces with horizontal creep on CBP: rectangular shape, 100 mm block thickness and 30 mm bedding sand thickness

Figure 4.37   Relationship between push-in forces with horizontal creep on CBP:
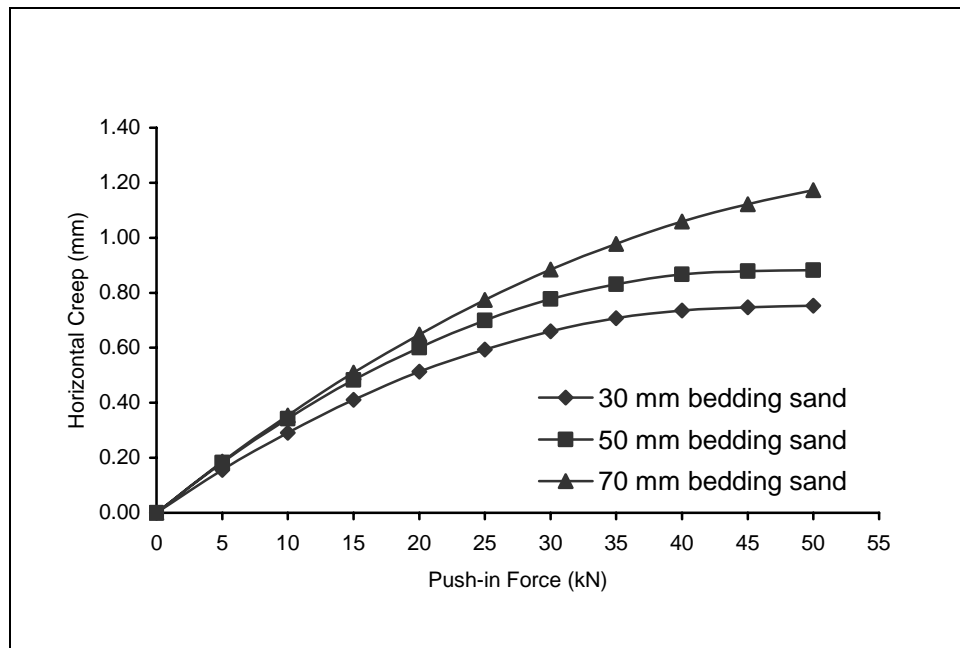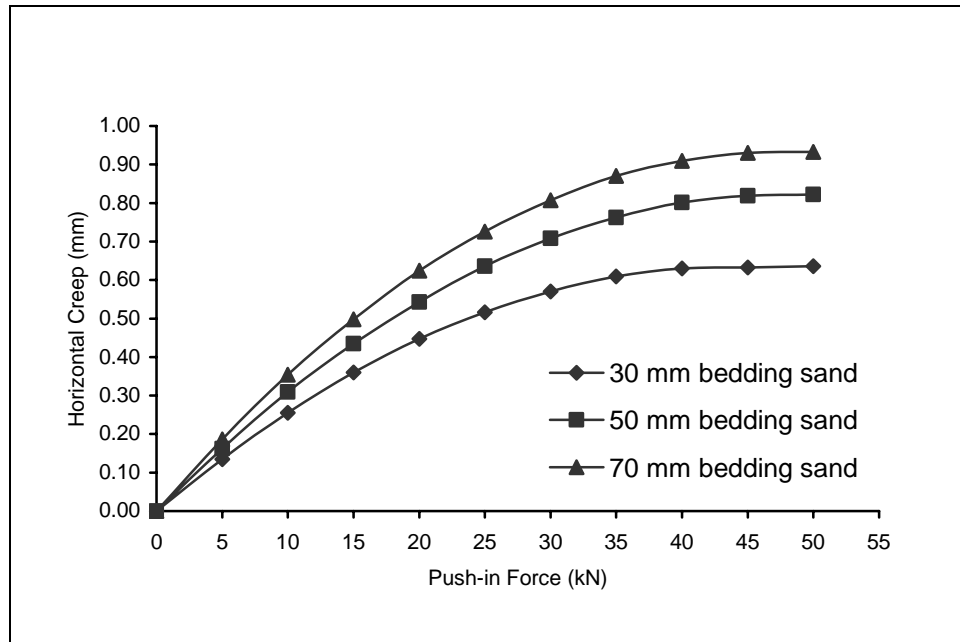rectangular shape, 100 mm block thickness and 50 mm bedding sand
thickness

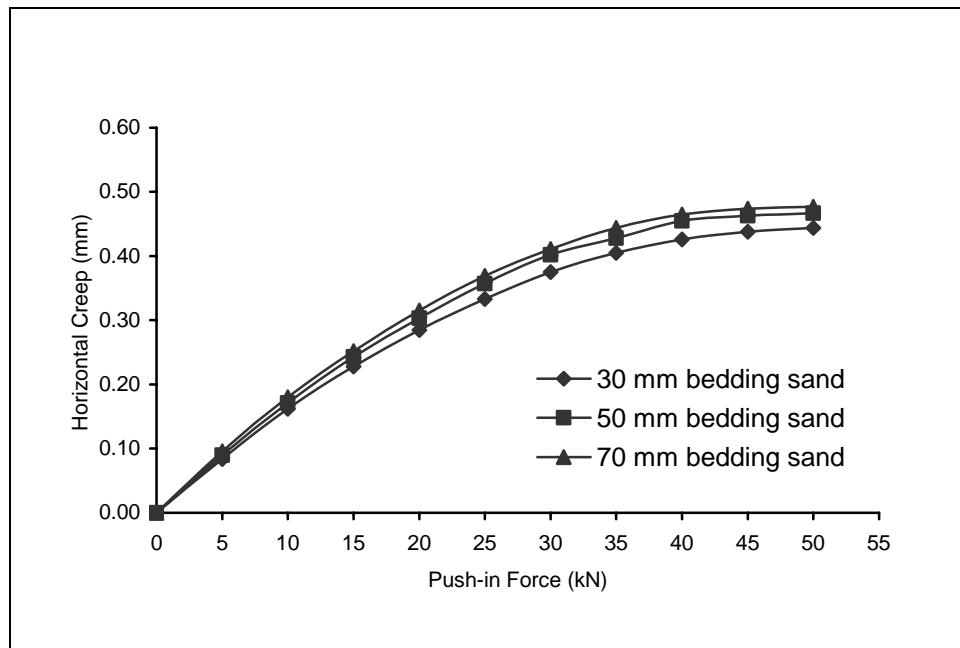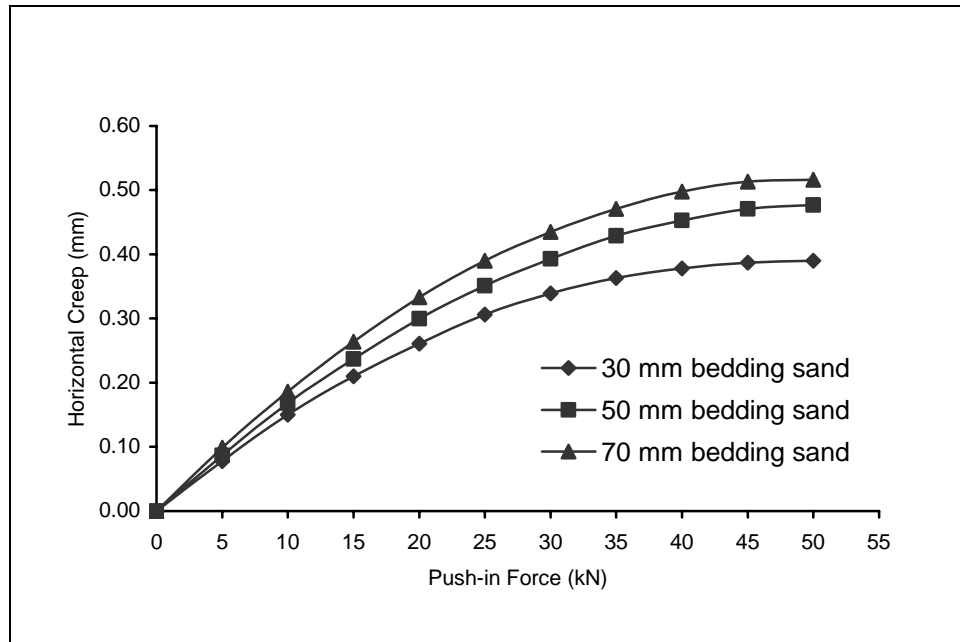**Figure 4.38**   Relationship between push-in forces with horizontal creep on CBP:
rectangular shape, 100 mm block thickness and 70 mm bedding sand
thickness

4.5.3 The Effect of Block Thickness

Rectangular blocks shape of the same plan dimension with two different thicknesses was selected for testing. The thicknesses were 60 mm and 100 mm. Blocks were laid in a stretcher bond pattern for each test. The shapes of the load deflection paths are similar for all block thicknesses. A change in thickness from 60 to 100 mm significantly reduces the elastic deflection of pavement. The comparison is shown in Figure 4.39 to Figure 4.47. Thicker blocks provide a higher frictional area. Thus, load transfer will be high for thicker blocks. For thicker blocks, the individual block translation is more with the same amount of block rotation. As a result, the back thrust from edge restraint will be more. The thrusting action between adjacent blocks at hinging points is more effective with thicker blocks. Thus, deflections are much less for thicker blocks.

The combined effect of higher friction area and higher thrusting action for thicker blocks provides more efficient load transfer. Thus, there is a significant change in deflection values from increasing the thickness of blocks. It is concluded that the response of the pavement is highly influenced by block thickness
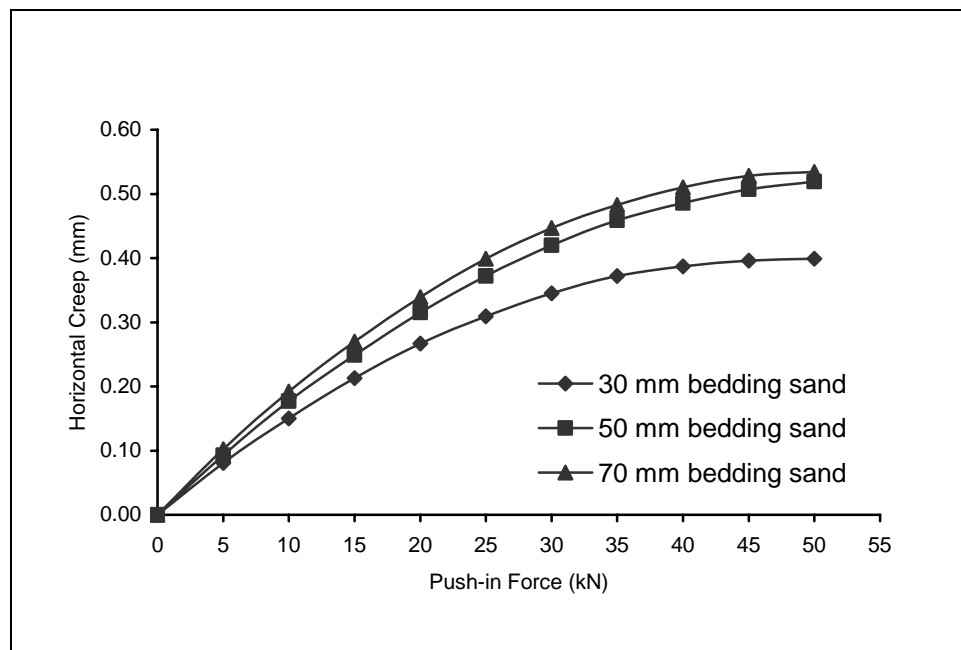
Figure 4.39 Relationship between push-in forces with horizontal creep on CBP: rectangular shape, 30 mm bedding sand thickness and 3 mm joint width

Figure 4.40 Relationship between push-in forces with horizontal creep on CBP: rectangular shape, 30 mm bedding sand thickness and 5 mm joint width

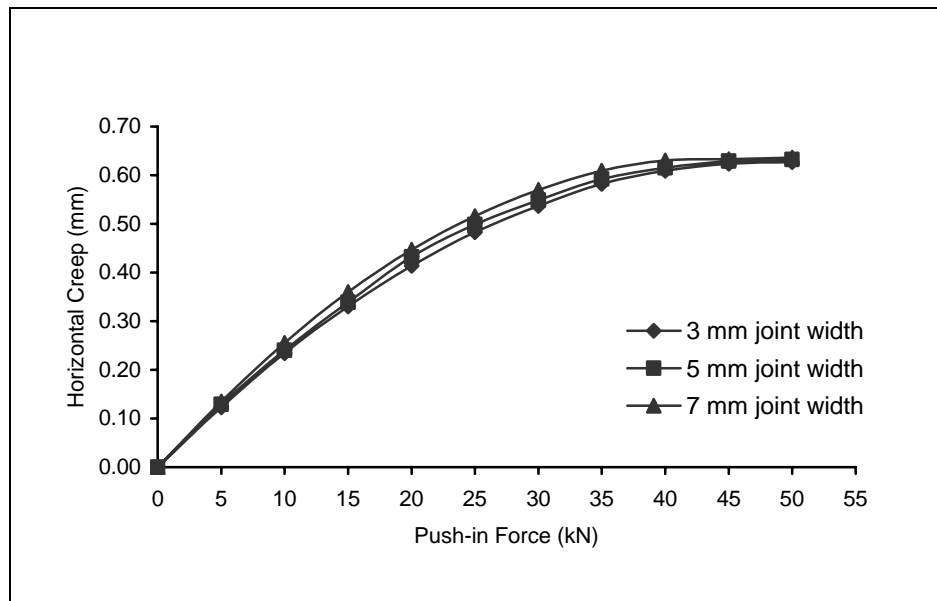**Figure 4.41**   Relationship between push-in forces with horizontal creep on CBP: rectangular shape, 30 mm bedding sand thickness and 7 mm joint width

Figure 4.42   Relationship between push-in forces with horizontal creep on CBP: rectangular shape, 50 mm bedding sand thickness and 3 mm joint width

Figure 4.43 Relationship between push-in forces with horizontal creep on CBP: rectangular shape, 50 mm bedding sand thickness and 5 mm joint width

Figure 4.44 Relationship between push-in forces with horizontal creep on CBP: rectangular shape, 50 mm bedding sand thickness and 7 mm joint width

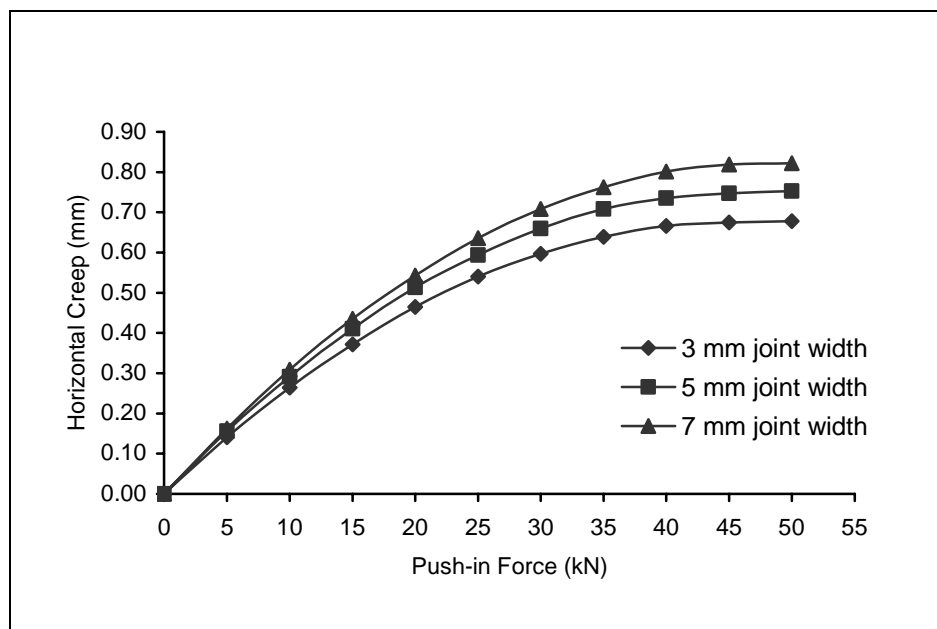**Figure 4.45** Relationship between push-in forces with horizontal creep on CBP: rectangular shape, 70 mm bedding sand thickness and 3 mm joint width

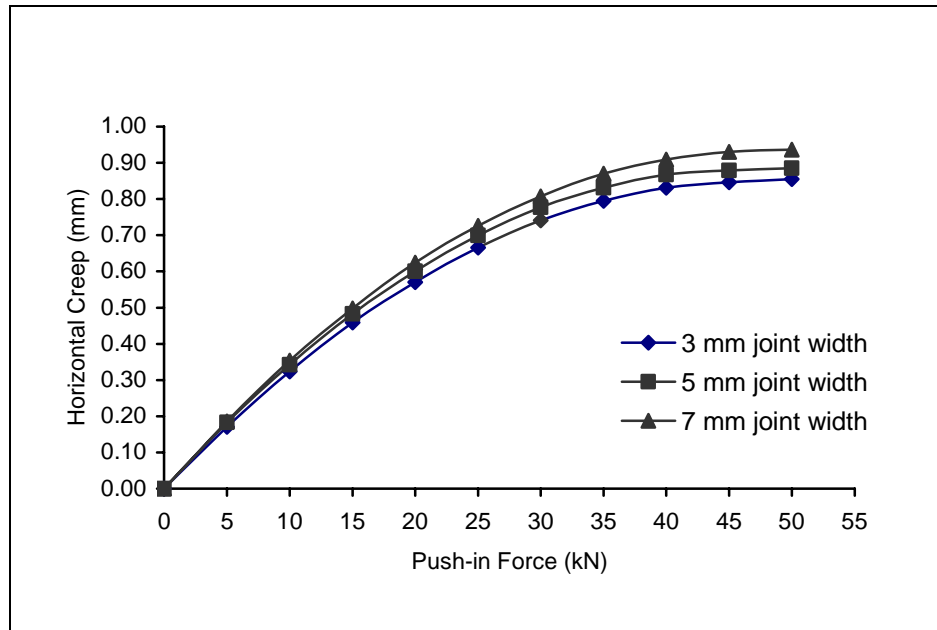**Figure 4.46** Relationship between push-in forces with horizontal creep on CBP: rectangular shape, 70 mm bedding sand thickness and 5 mm joint width

Figure 4.47   Relationship between push-in forces with horizontal creep on CBP: rectangular shape, 70 mm bedding sand thickness and 7 mm joint width

4.5.4   The Effect of Degree of Slope

The effect of degree of the slope on concrete block pavements on sloping road section area significant with friction between blocks and thrusting action between adjacent blocks at hinging points is more effective with thicker blocks. Thus, deflections are much less for thicker blocks with increasing degree of the slope. As shown in Figure 4.48 to Figure 4.65.
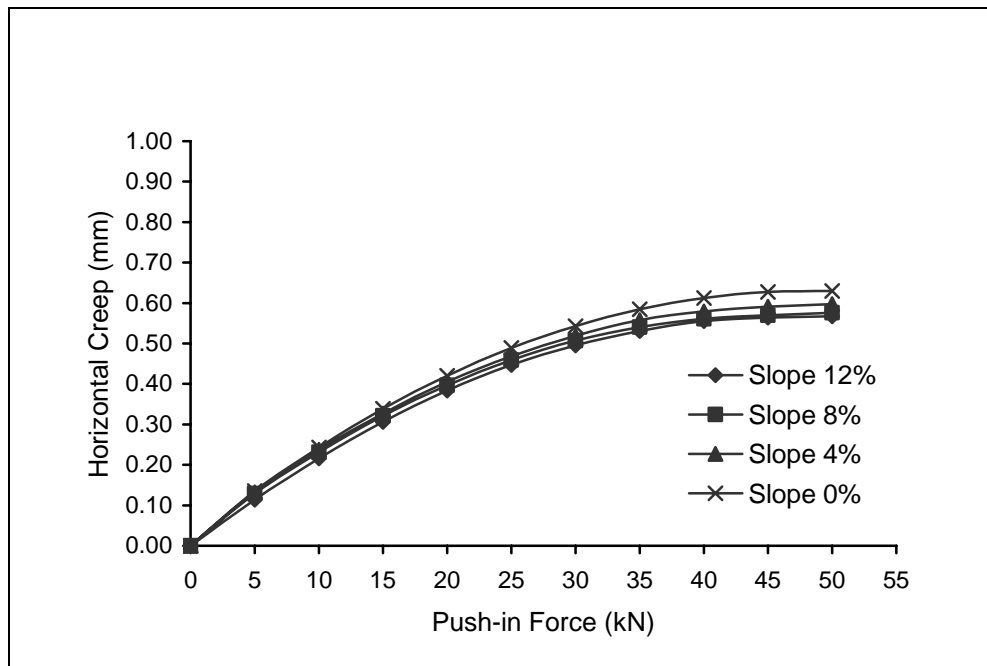
Figure 4.48 Relationship between push-in forces with horizontal creep on CBP: rectangular shape, 60 mm block thick, 30 mm bedding sand thickness and 3 mm joint width
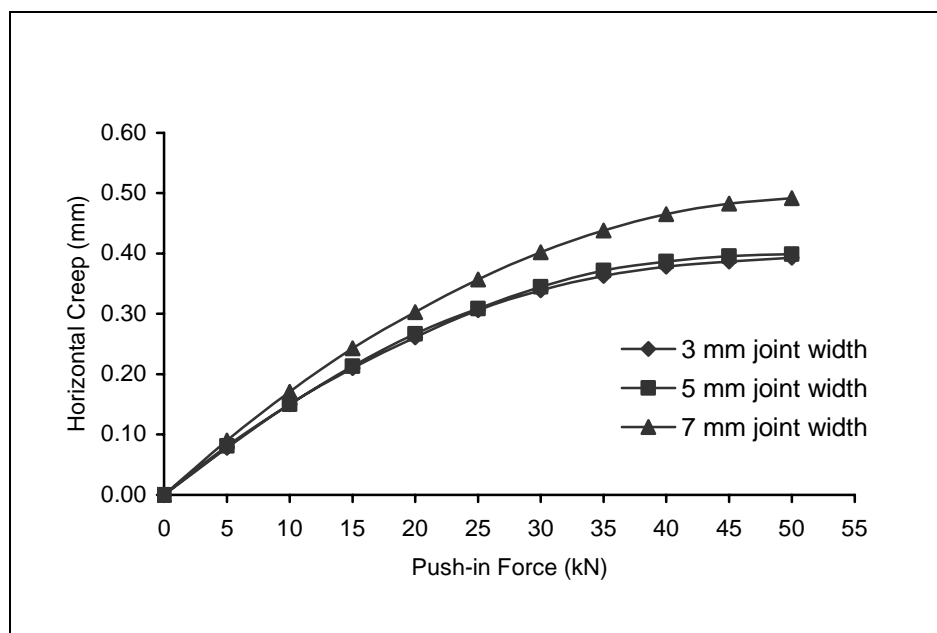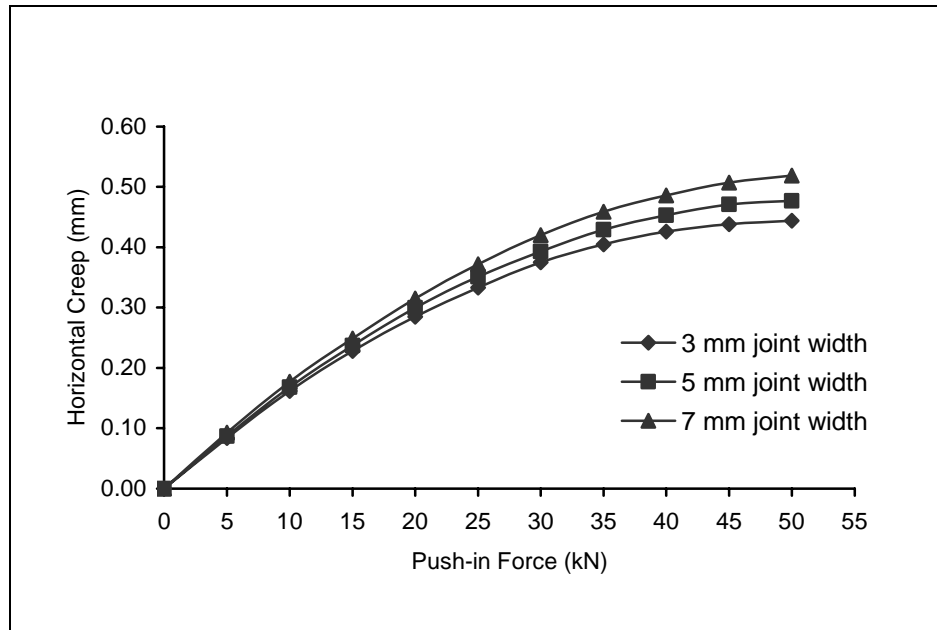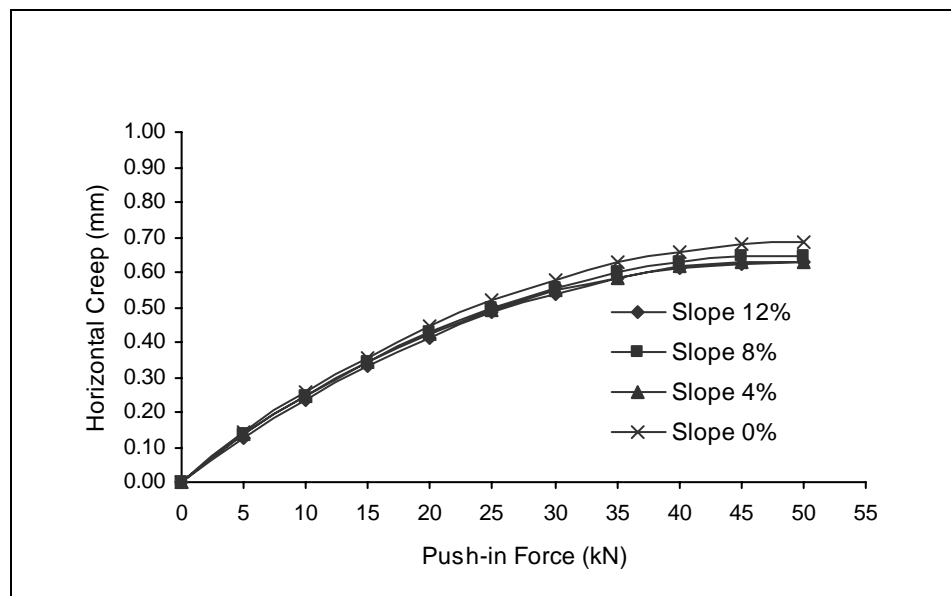

Figure 4.49 Relationship between push-in forces with horizontal creep on CBP: rectangular shape, 60 mm block thick, 50 mm bedding sand thickness and 3 mm joint width
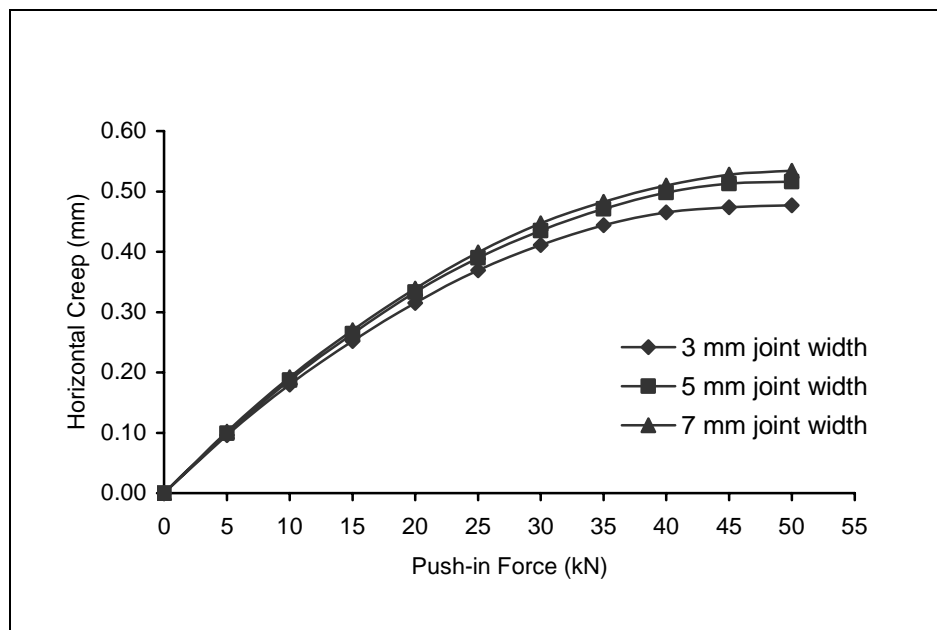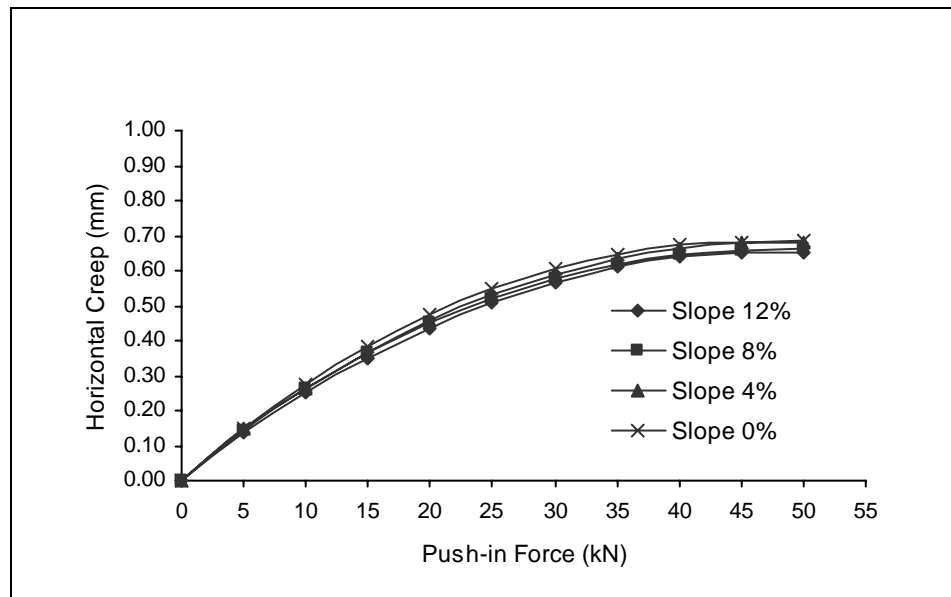
Figure 4.50 Relationship between push-in forces with horizontal creep on CBP: rectangular shape, 60 mm block thick, 70 mm bedding sand thickness and 3 mm joint width
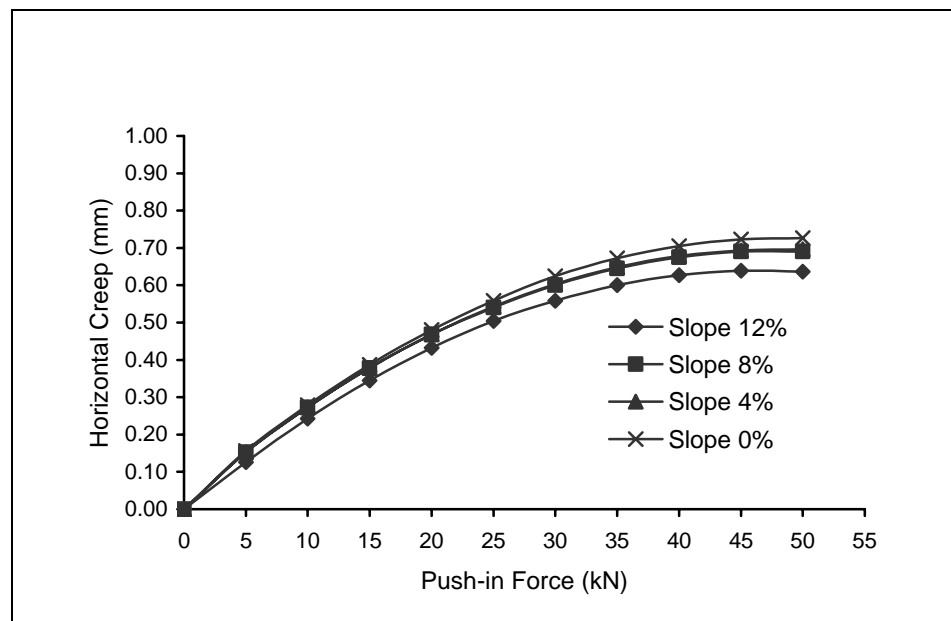
Figure 4.51 Relationship between push-in forces with horizontal creep on CBP: rectangular shape, 100 mm block thick, 30 mm bedding sand thickness and 3 mm joint width
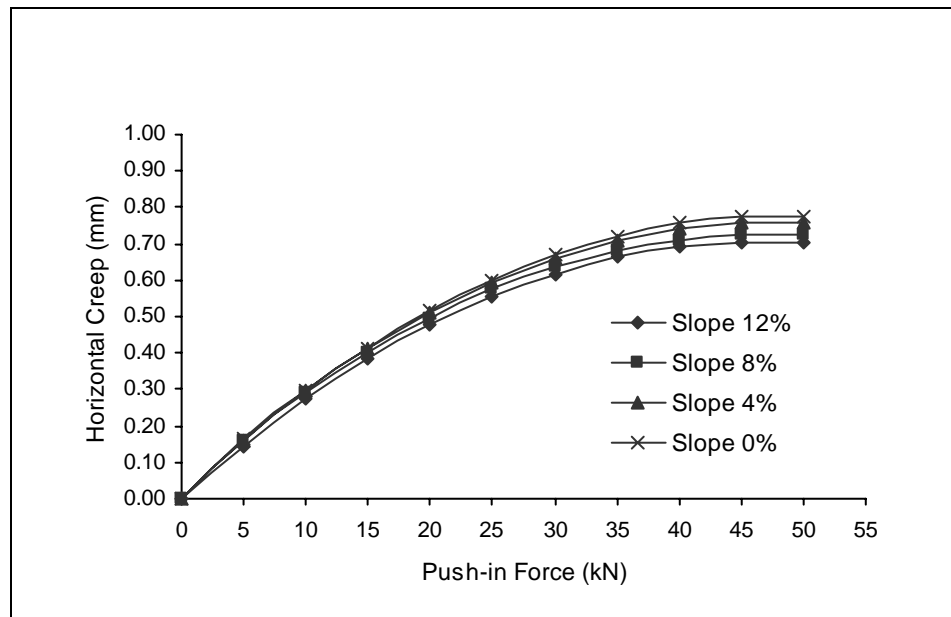
Figure 4.52 Relationship between push-in forces with horizontal creep on CBP: rectangular shape, 100 mm block thick, 50 mm bedding sand thickness and 3 mm joint width
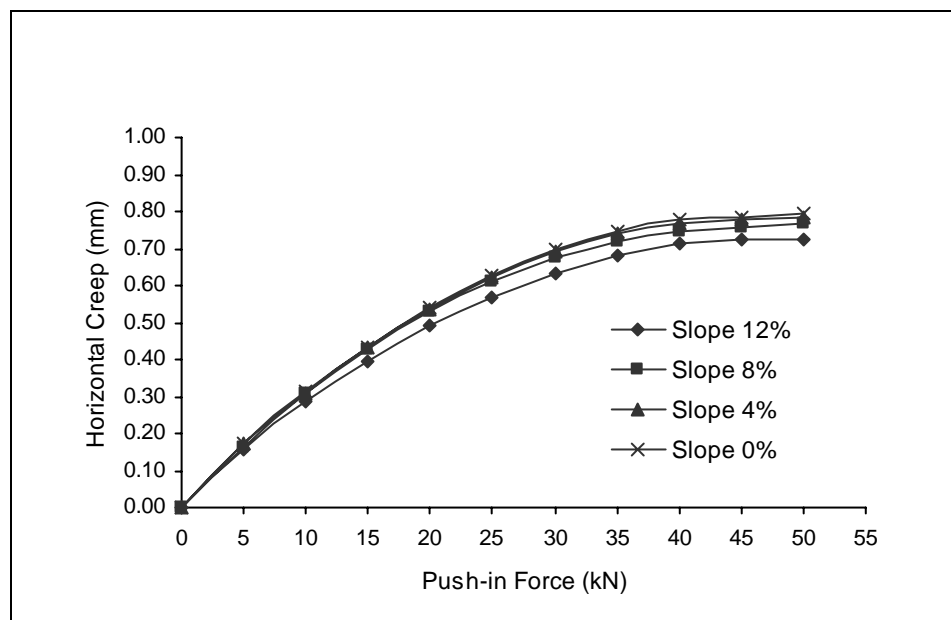
Figure 4.53 Relationship between push-in forces with horizontal creep on CBP: rectangular shape, 100 mm block thick, 70 mm bedding sand thickness and 3 mm joint width
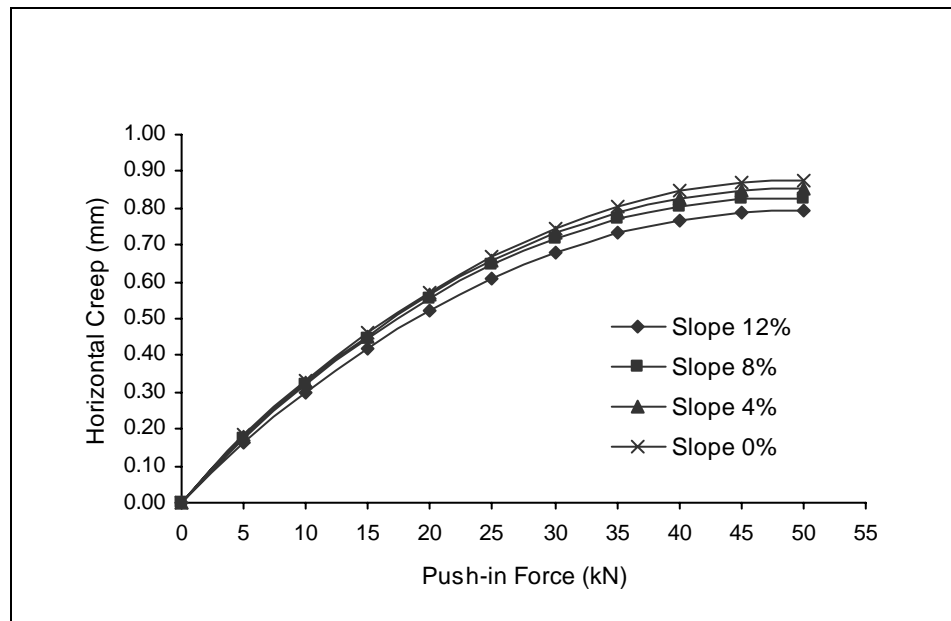
Figure 4.54 Relationship between push-in forces with horizontal creep on CBP: rectangular shape, 60 mm block thick, 30 mm bedding sand thickness and 5 mm joint width
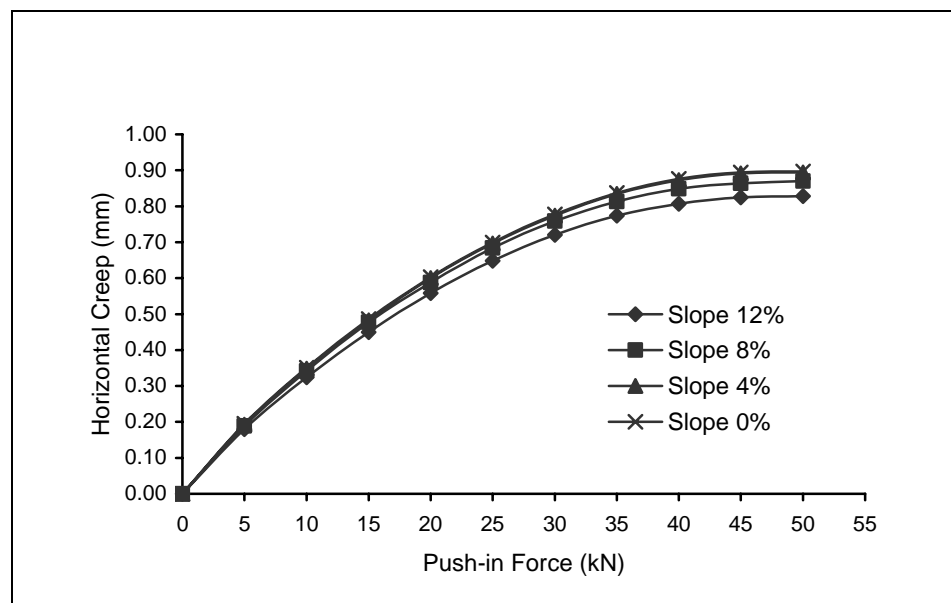
Figure 4.55 Relationship between push-in forces with horizontal creep on CBP: rectangular shape, 60 mm block thick, 50 mm bedding sand thickness and 5 mm joint width
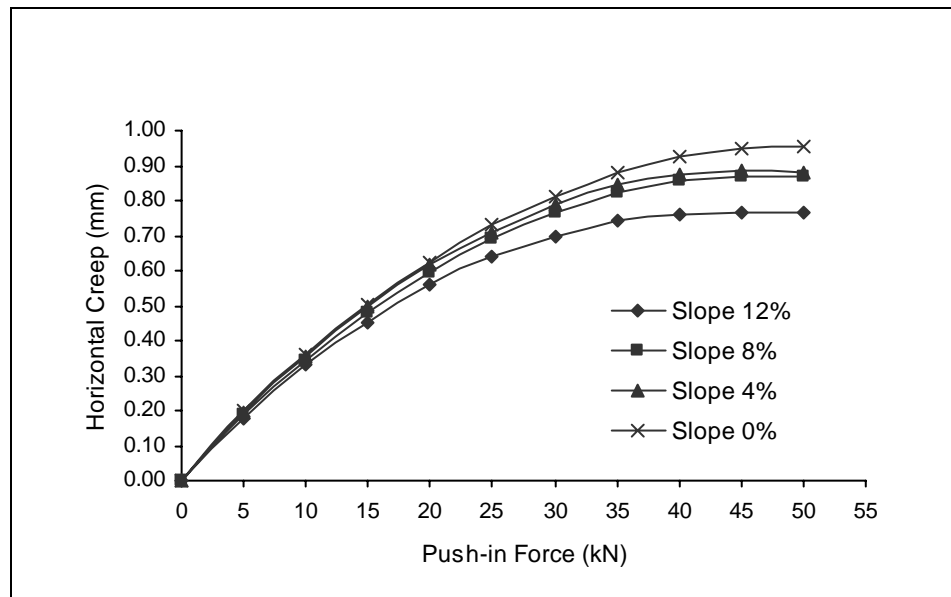
Figure 4.56 Relationship between push-in forces with horizontal creep on CBP: rectangular shape, 60 mm block thick, 70 mm bedding sand thickness and 5 mm joint width
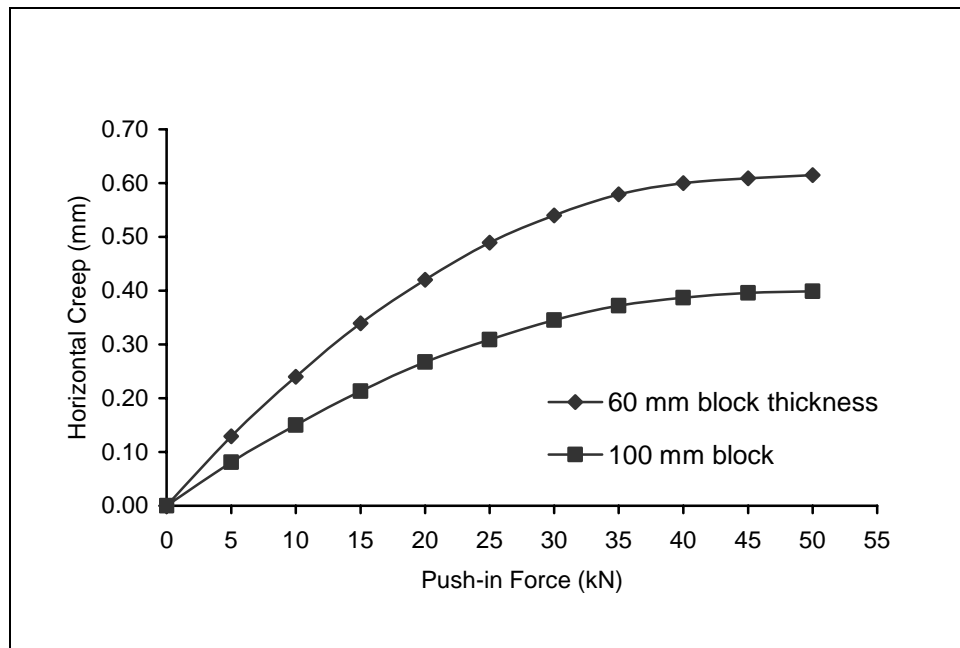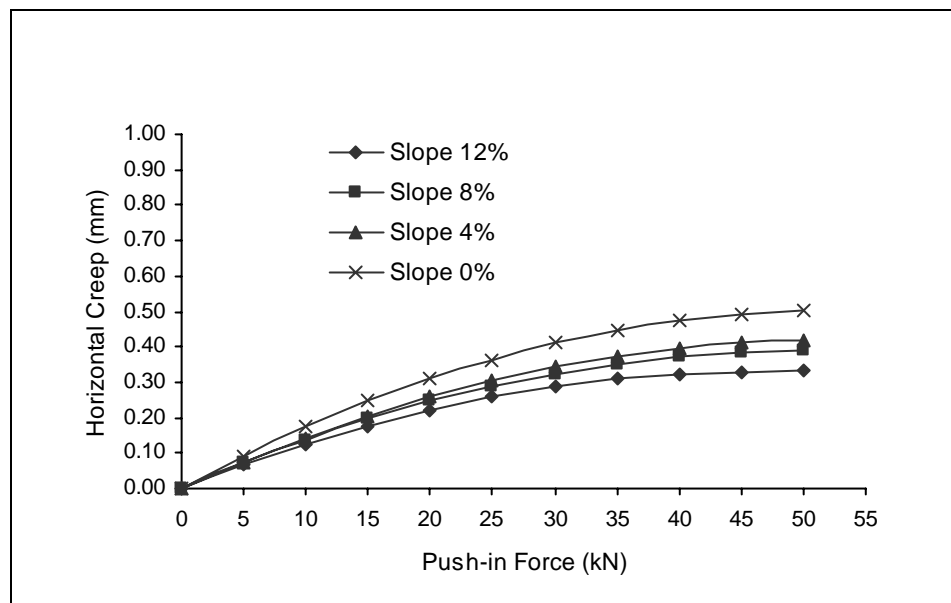

Figure 4.57 Relationship between push-in forces with horizontal creep on CBP: rectangular shape, 100 mm block thick, 30 mm bedding sand thickness and 5 mm joint width
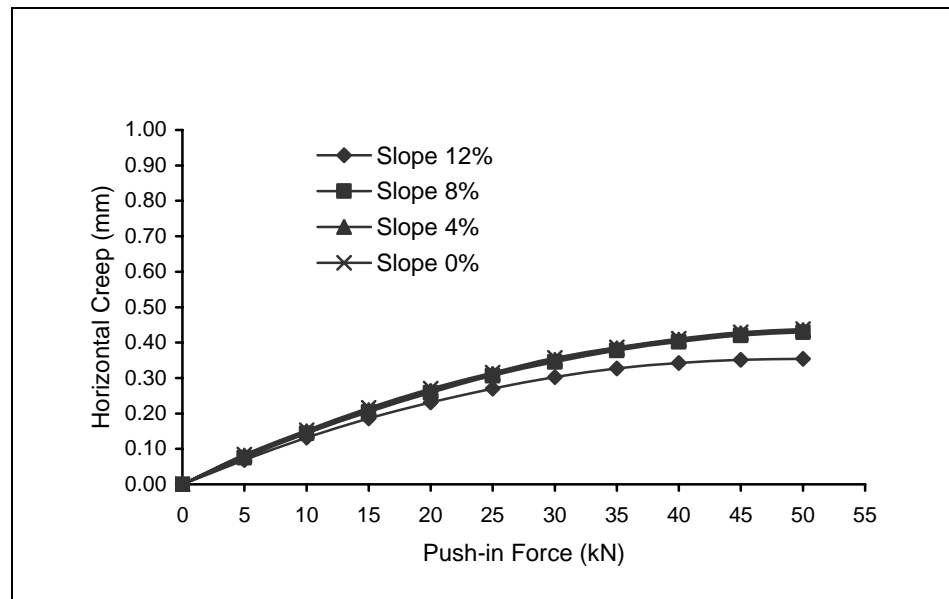
Figure 4.58 Relationship between push-in forces with horizontal creep on CBP: rectangular shape, 100 mm block thick, 50 mm bedding sand thickness and 5 mm joint width
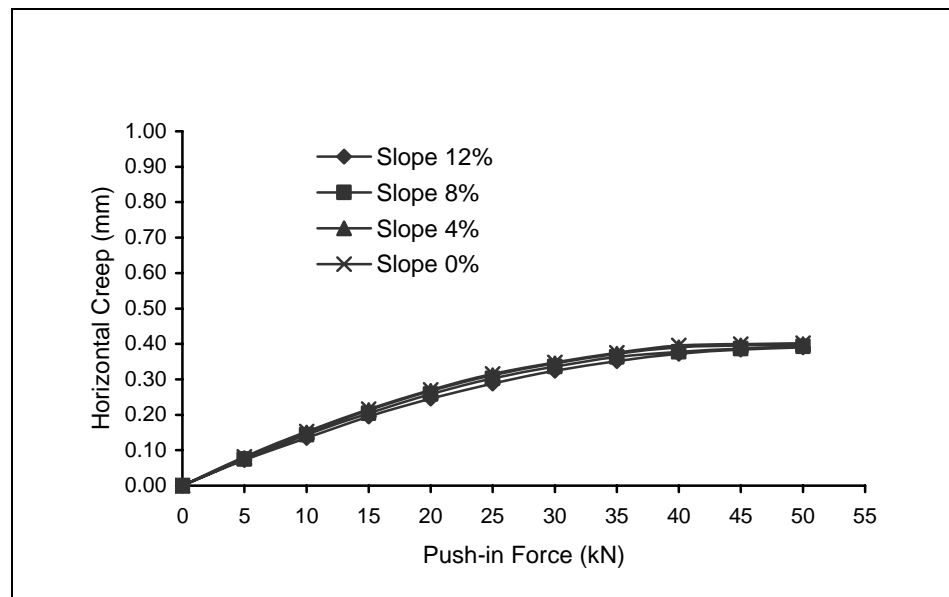
Figure 4.59 Relationship between push-in forces with horizontal creep on CBP: rectangular shape, 100 mm block thick, 70 mm bedding sand thickness and 5 mm joint width
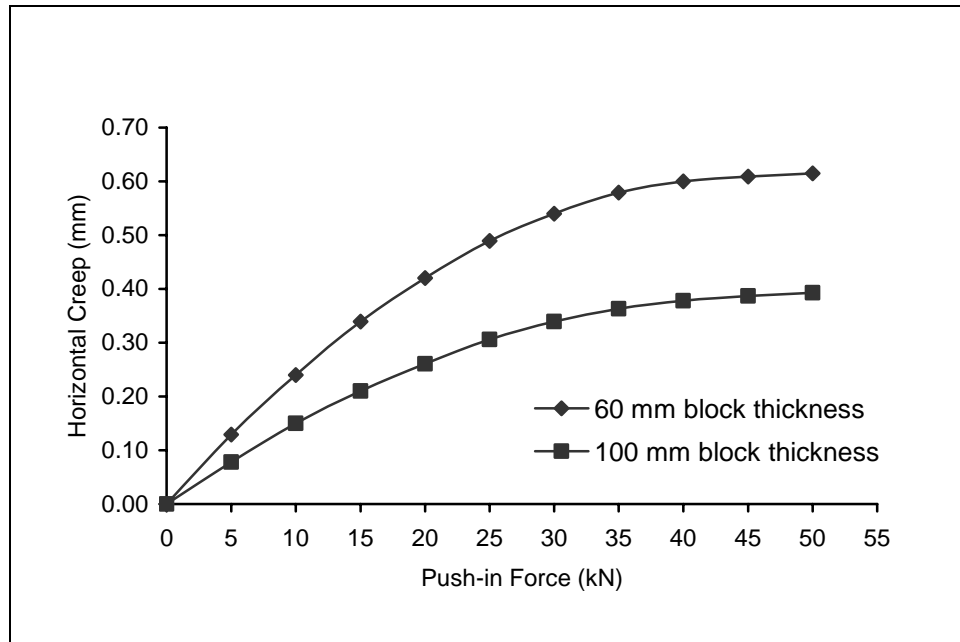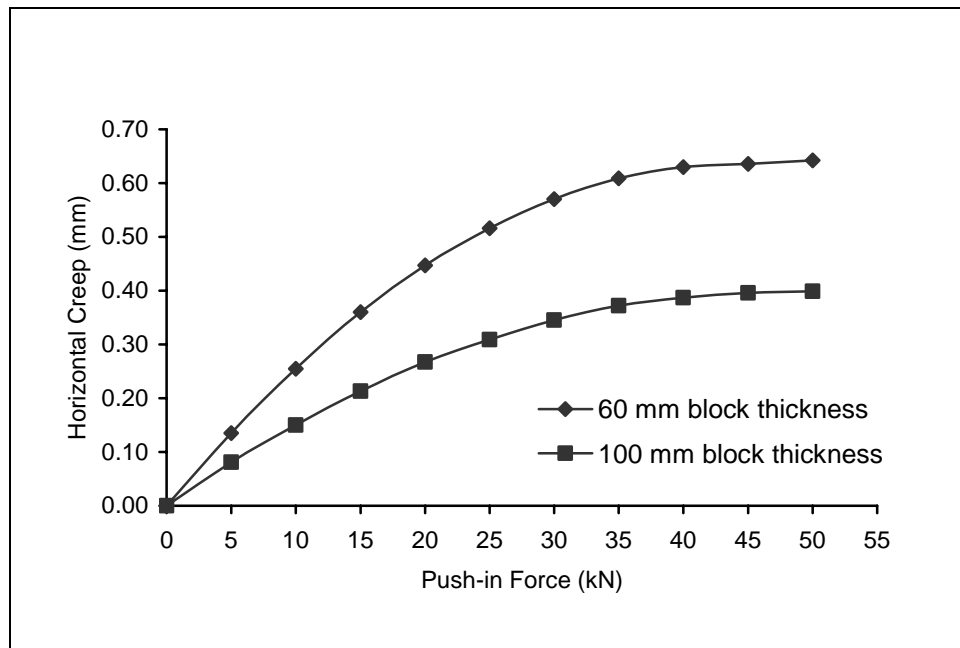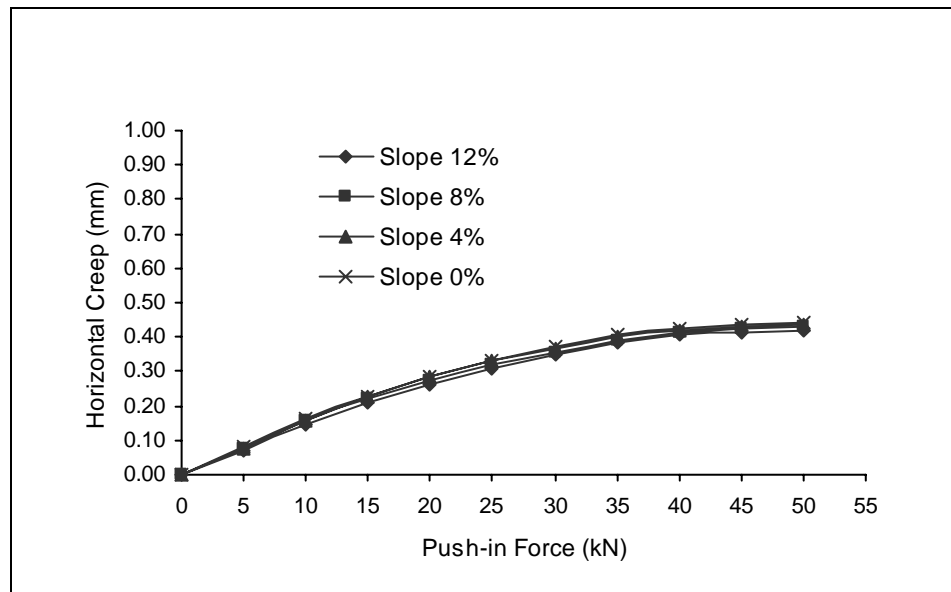
Figure 4.60 Relationship between push-in forces with horizontal creep on CBP: rectangular shape, 60 mm block thick, 30 mm bedding sand thickness and 7 mm joint width
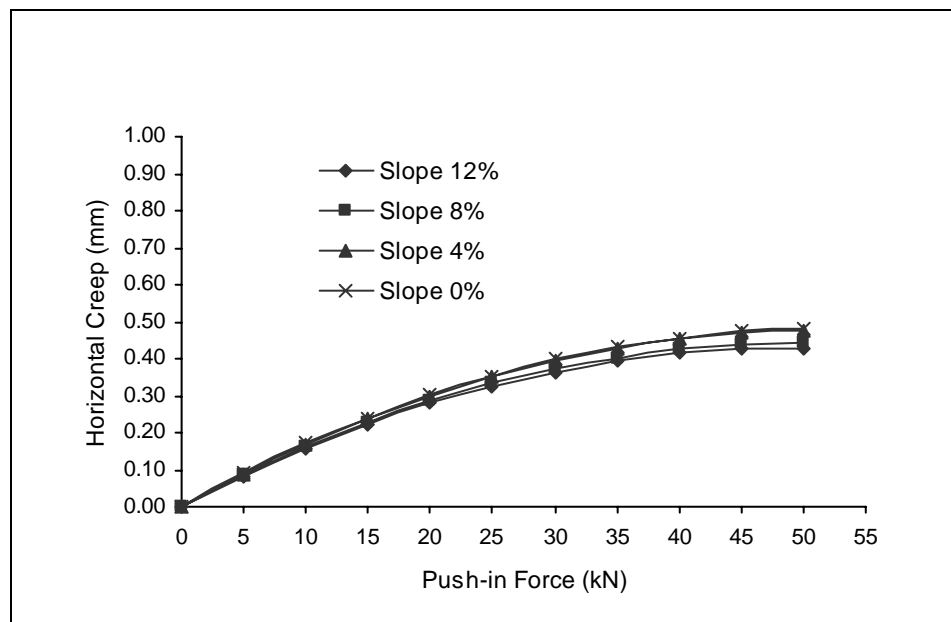
Figure 4.61 Relationship between push-in forces with horizontal creep on CBP: rectangular shape, 60 mm block thick, 50 mm bedding sand thickness and 7 mm joint width
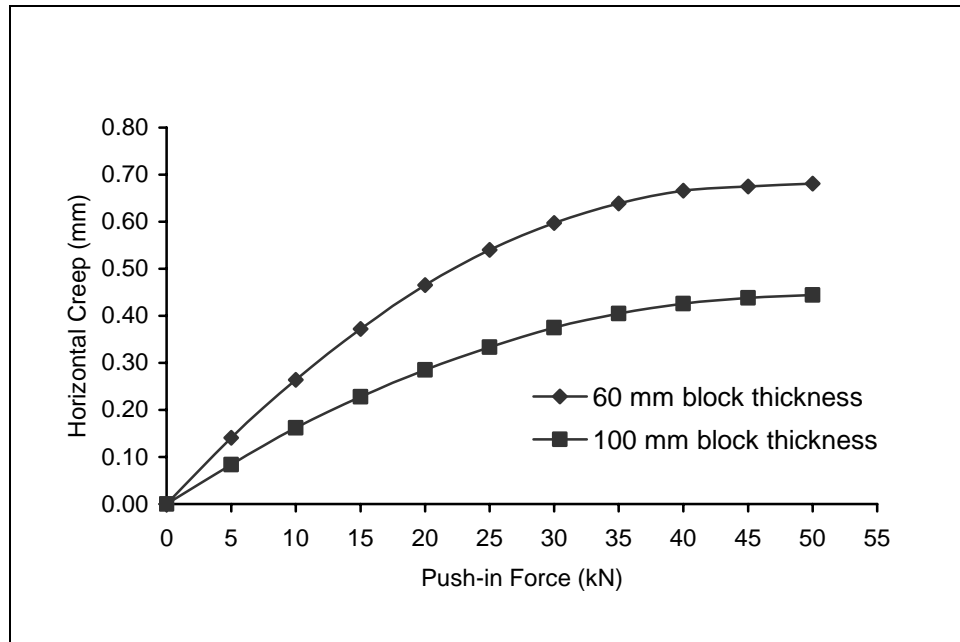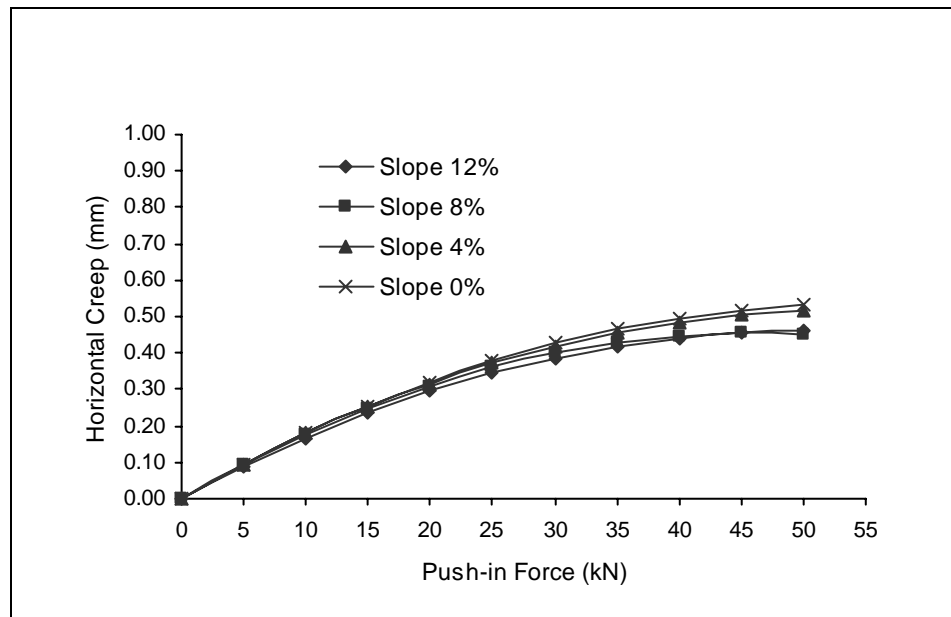
Figure 4.62 Relationship between push-in forces with horizontal creep on CBP: rectangular shape, 60 mm block thick, 70 mm bedding sand thickness and 7 mm joint width
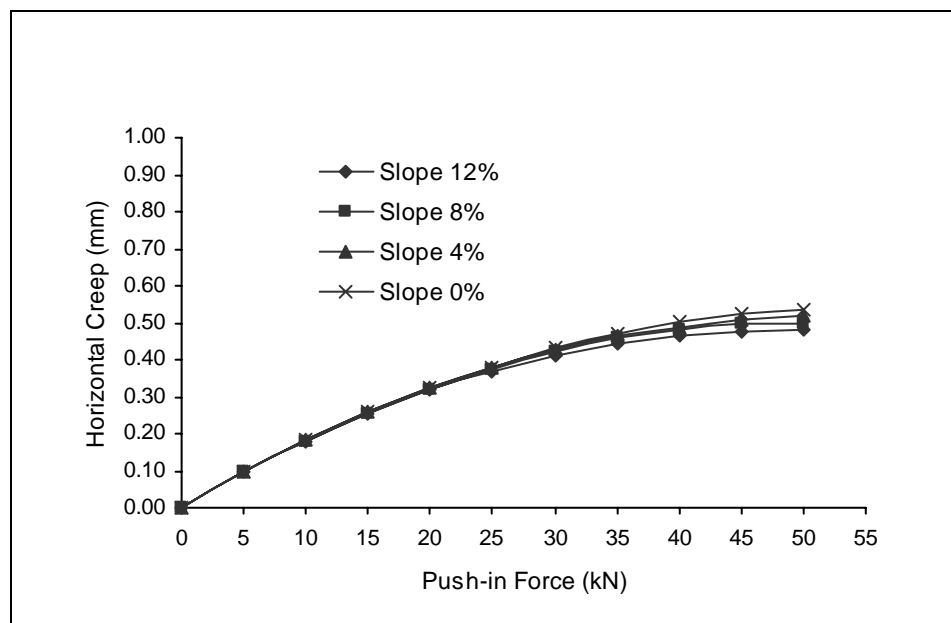
Figure 4.63 Relationship between push-in forces with horizontal creep on CBP: rectangular shape, 100 mm block thick, 30 mm bedding sand thickness and 7 mm joint width
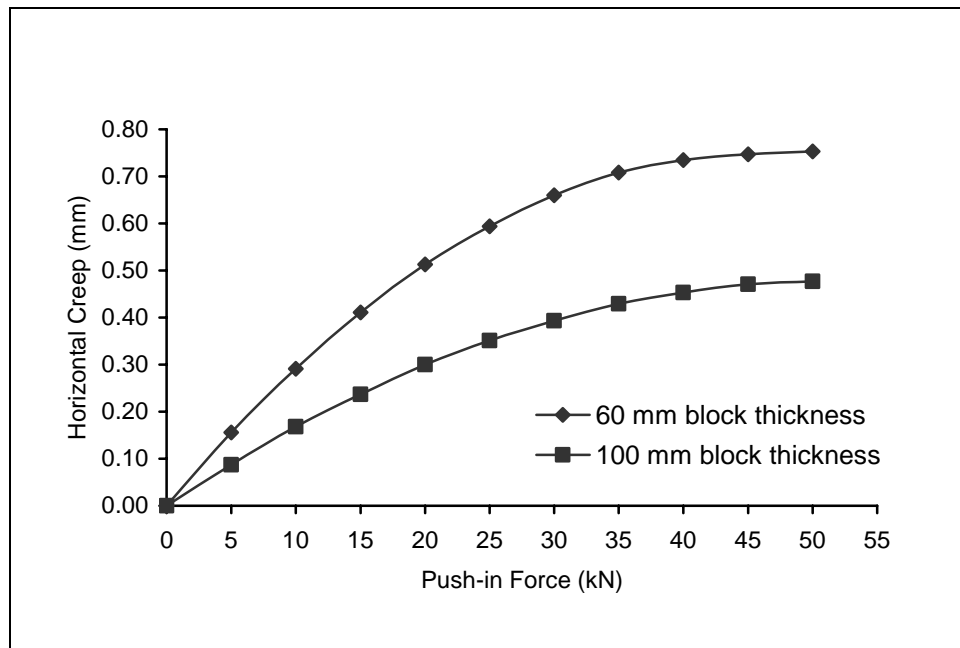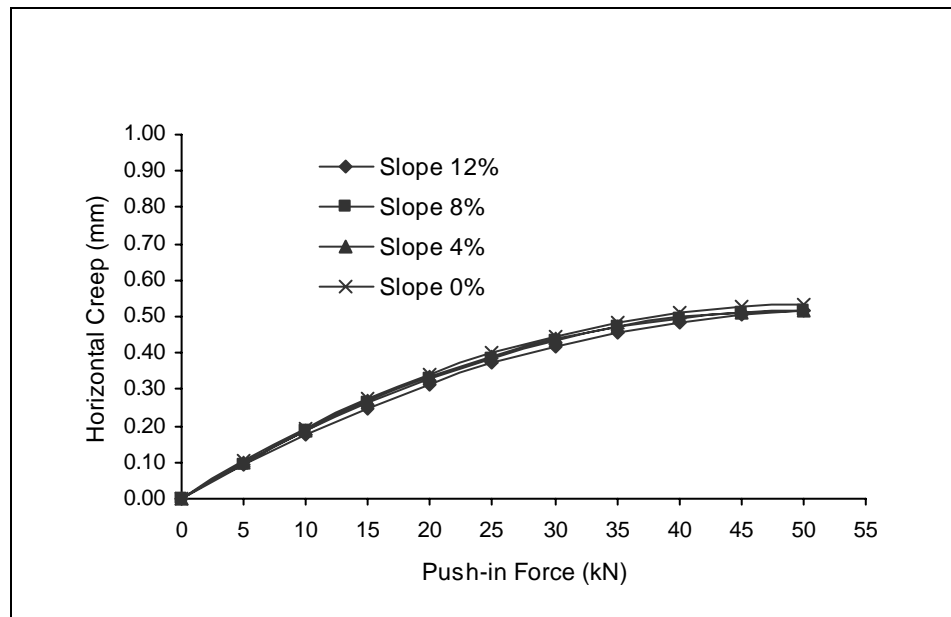
Figure 4.64 Relationship between push-in forces with horizontal creep on CBP: rectangular shape, 100 mm block thick, 50 mm bedding sand thickness and 7 mm joint width
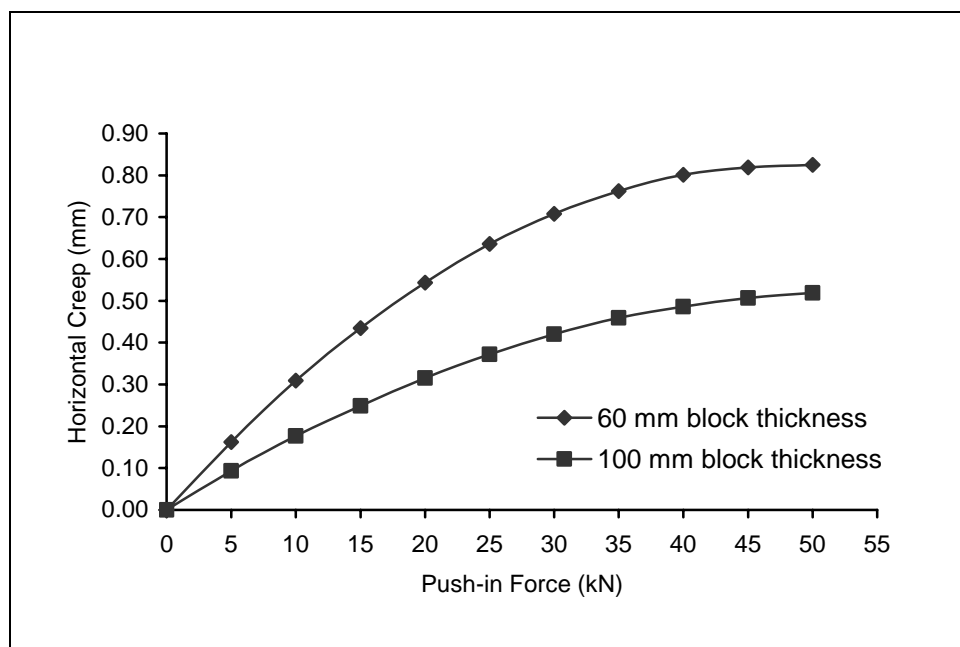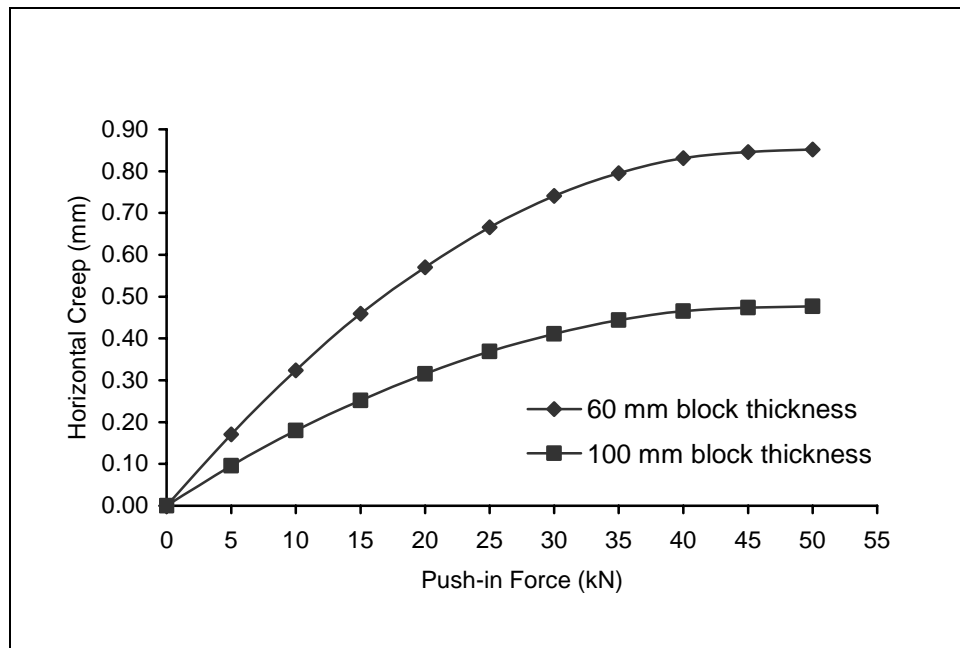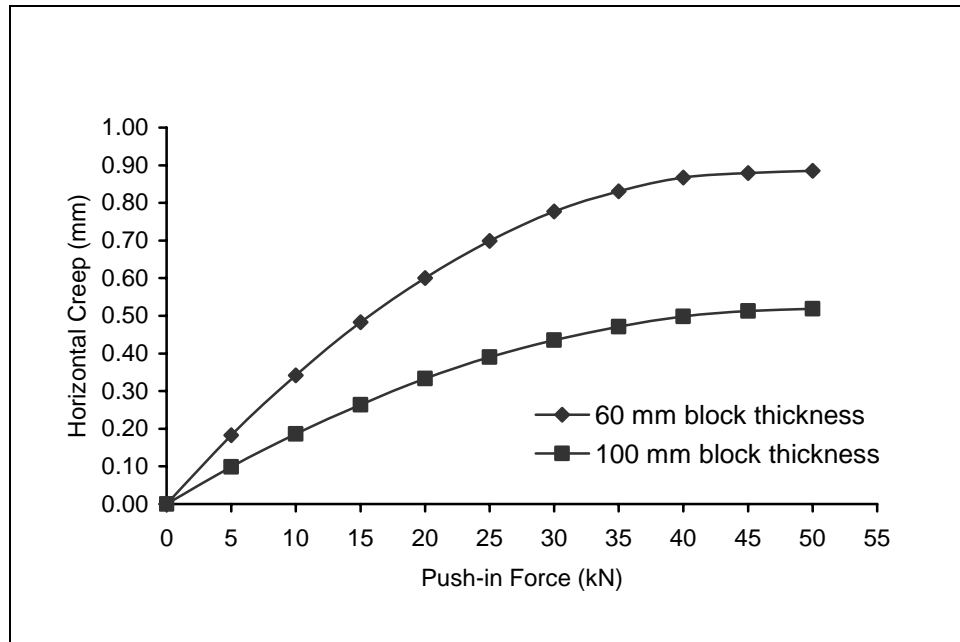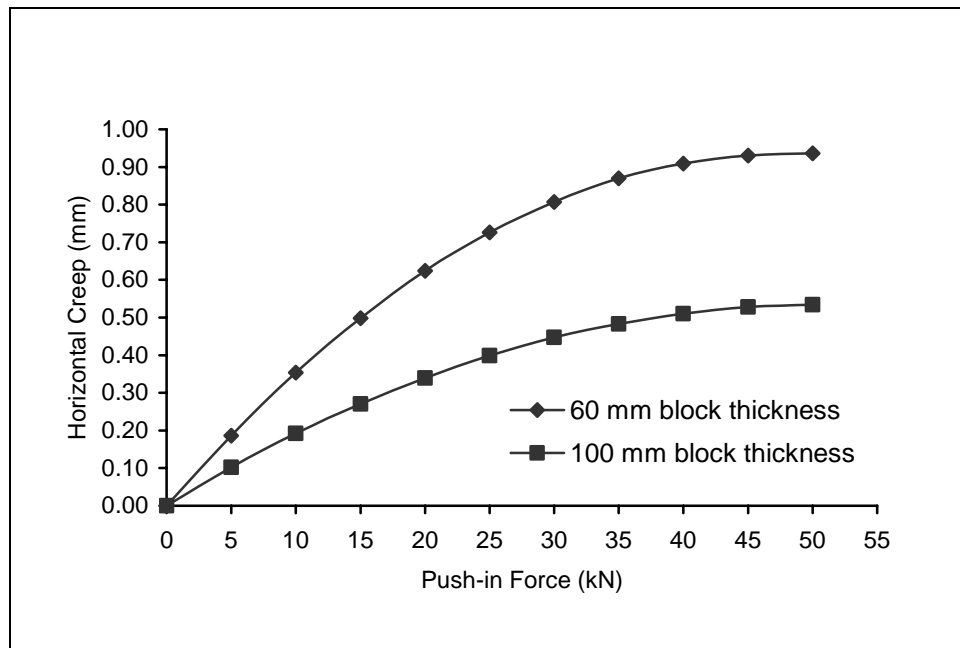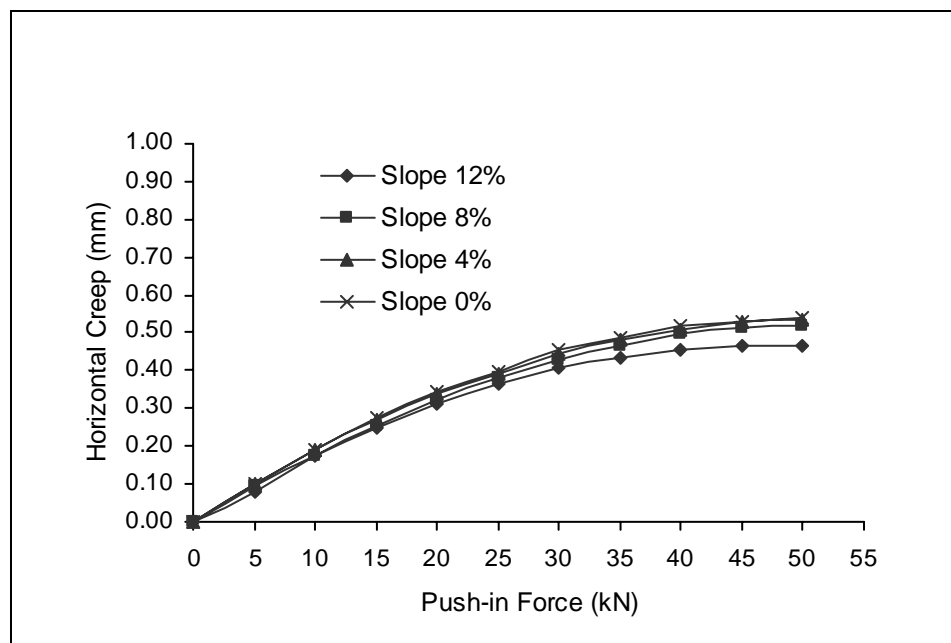

Figure 4.65 Relationship between push-in forces with horizontal creep on CBP: rectangular shape, 100 mm block thick, 70 mm bedding sand thickness and 7 mm joint width

CHAPTER 5

CONCRETE BLOCK PAVEMENT ON SLOPING ROAD SECTION AND SPACING OF ANCHOR BEAM

5.1   Introduction

The construction of roads on sloping road section poses particularly interesting challenges for road design. The horizontal (inclined) forces exerted on the road surface are severely increased due to traffic friction of accelerating (uphill), braking (downhill) or turning. These horizontal forces cause distress in most conventional pavements, resulting in rutting and poor riding quality. Concrete Block Pavement (CBP) performs well under such severe conditions, but the effects of degree of slope, bedding sand thickness, block thickness, joint width between blocks, laying pattern and block shape must be estimated. Each factor is used in the design of the anchor beam spacing for sloping road section.

The load distribution and failure modes of concrete block pavement and flexible asphalt are very similar permanent deformation from repetitive loads.

5.2 **The Concept of Load Transfer on Concrete Block Pavement**

Load transfer is the ability of a loaded block in a paving system to influence neighbouring blocks by causing them to deflect vertically. This load transfer reduces the vertical stress under the loaded block. The greater this spread of influence of vertical movement, the greater the degree of vertical interlock and hence the greater the load transfer.
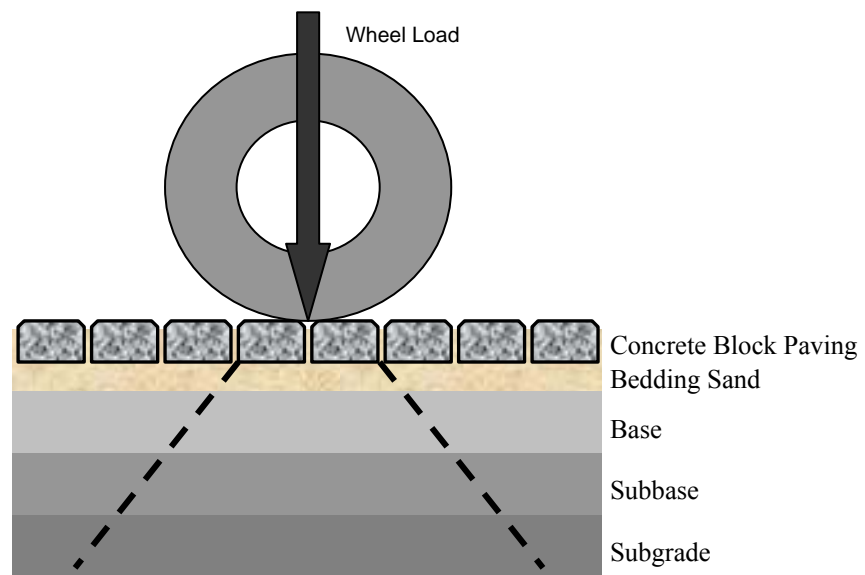
Figure 5.1   Wheel load distribution
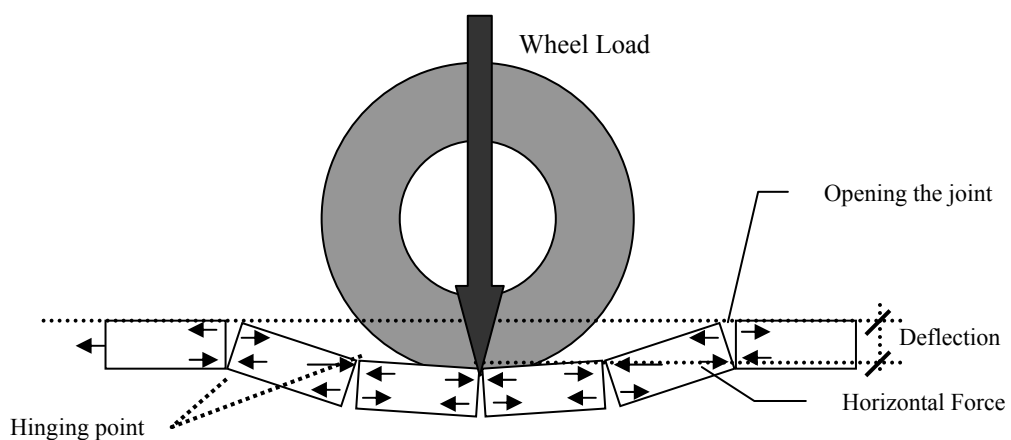
Figure 5.2   The behaviour of a concrete block pavement under load

A block at rest on an adjustable inclined plane begins to move when the angle between the plane and the horizontal reaches a certain value θ (degree of slope), which is known as the angle repose. The weight W of the block can be resolved into a component F parallel to the plane and another component N perpendicular to the plane. For detail see Figure 5.3.
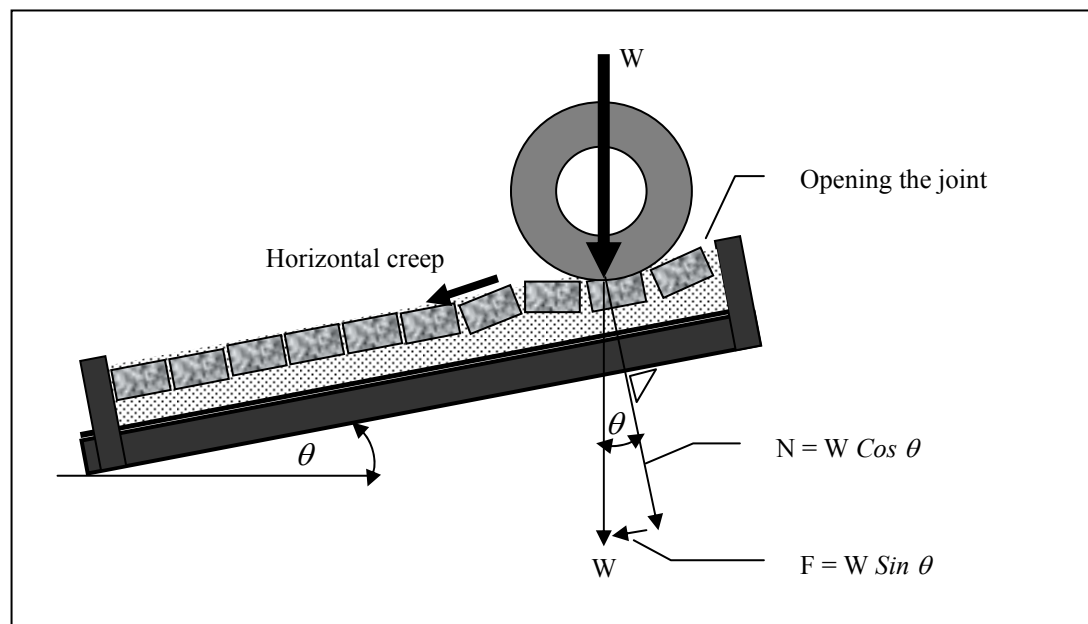
Figure 5.3 The magnitude load transfer of Force (F), Normal (N) and Wheel load (W)

5.3 CBP on Sloping Road Section Using Anchor Beam

It is common practice to construct edge restraints (kerbing and anchor beams) along the perimeter of all paving, to contain the paving and prevent horizontal creep and subsequent opening of joints. Due to the steepness of the slope, the normally vertical traffic loading will have a surface component exerted on the blocks in a downward direction. This force is aggravated by traction of accelerating vehicles up the hill and breaking of vehicles down the hill. If uncontained, these forces will cause horizontal creep (longitudinal creep) of the blocks down the slope, resulting in

opening of joints at the top of the paving. An anchor beam at the lower end of the paving is necessary to prevent this creep.
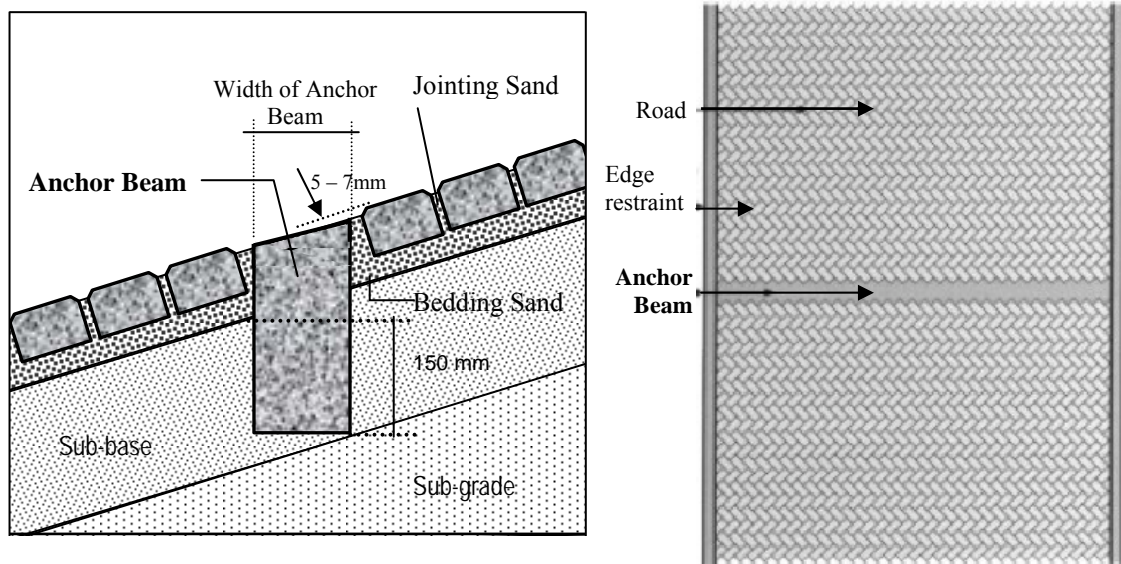
Figure 5.4   Detail construction of anchor beam.

For ease of CBP construction, the anchor beam was recommended that the blocks are laid continuously up the gradient. Thereafter, two rows of blocks are uplifted in the position of the beam, the sub-base excavated to the required depth and width and the beam cast, such that the top of the beam is 5 – 7 mm lower than the surrounding block work. This allows for settlement of the pavers. This method of construction will ensure that the anchor beam interlocks with the pavers and eliminates the need to cut small pieces of block. The schematic of spacing and position of the anchor beam for sloping road section is shown in Figure 5.5.

5.3.1 Spacing of Anchor Beam

The spacing of anchor beam should be determined by using horizontal force test and push-in test. The horizontal force test include changing variables of laying pattern, block thickness, block shape and joint width between blocks. While the push-in test include changing variables of bedding sand thickness, joint width between blocks, block thickness and degree of the slope. The different changes of each variable result in the different spacing of anchor beam.
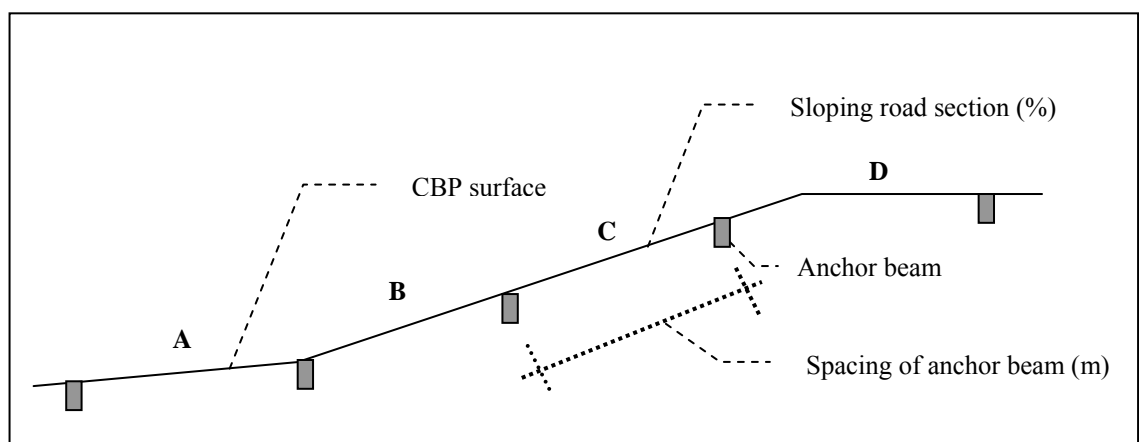
Figure 5.5   Schematic of spacing and position of anchor beam.

5.3.1.1 Horizontal Force Test

Horizontal interlock is not achieved if horizontal movement is allowed. In vehicular traffic areas, horizontal braking, cornering and accelerating forces try to move pavers along the road; this is known as creep. Sand filled joints and an interlocking bond pattern transfer these forces within a paving area to rigid edging. Loads created by turning vehicular traffic are distributed more evenly in all directions by a herringbone pattern than by running bond pattern, which has acceptable horizontal interlock in only one direction (Figure 5.6). Sand set brick

pavers initially develop greater horizontal interlock than bituminous set brick pavers as the joint sand is better compacted.
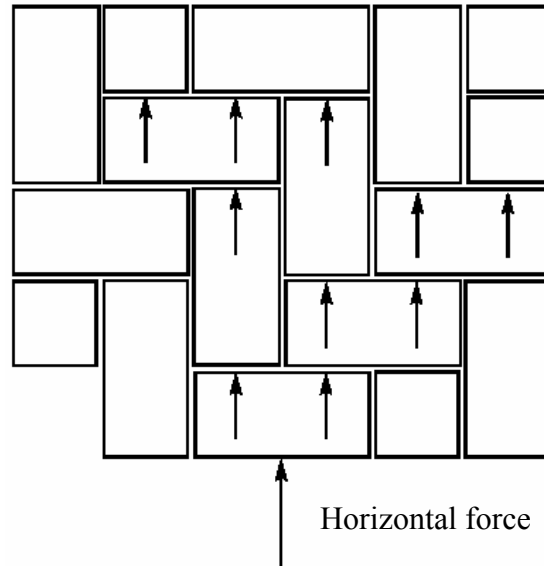
Figure 5.6   Horizontal load interlock

For horizontal force test, 2 m x 2 m steel frame is used in laboratory test for example the specification of CBP sample; rectangular block shape, 60 mm block thickness, stretcher bond laying pattern and 3 mm joint width (Figure 5.8). the test was conducted by pushing CBP sample from edge started from 0 kN until failure (block uplift). It is found the maximum horizontal creep as shown in the equation $y = -0.0307x2 + 0.6623x + 0.05$ in Figure 5.6. For equation of other cases are as shown in Appendix C1 to C4.
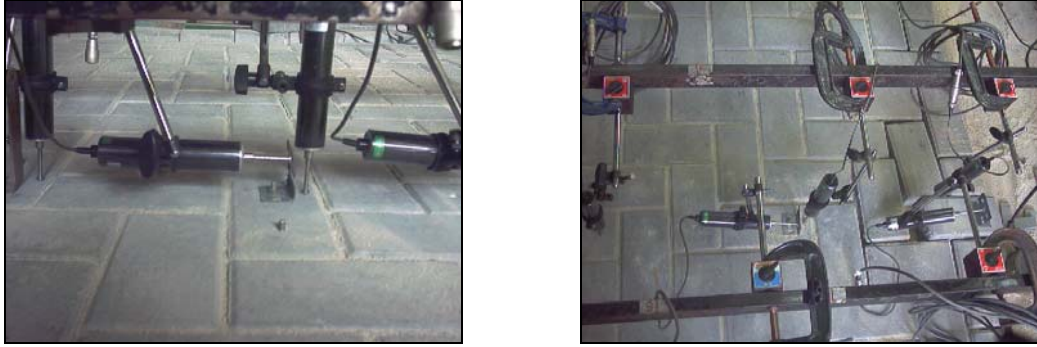
Figure 5.7   The horizontal creep measurement for horizontal force testing
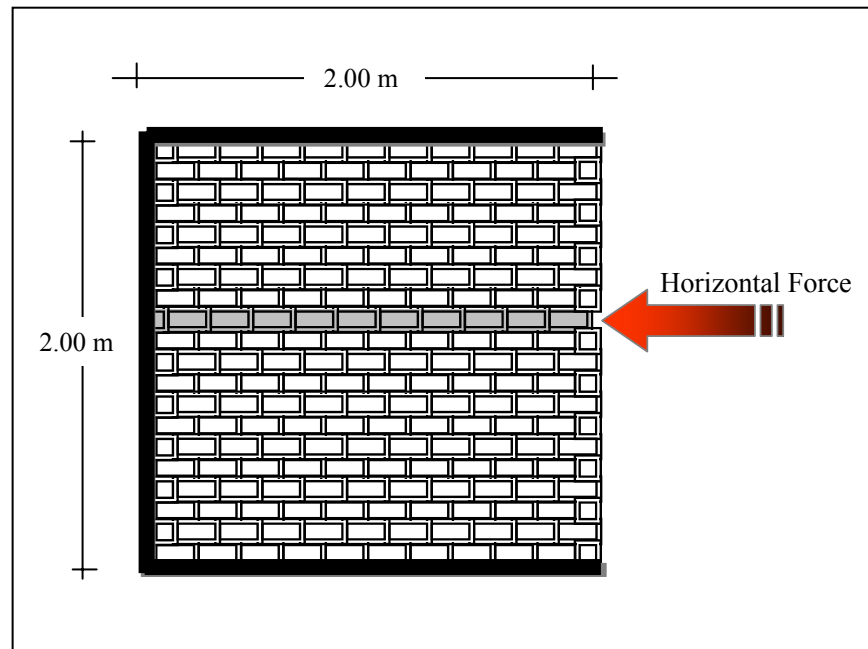
Figure 5.8   Horizontal force test
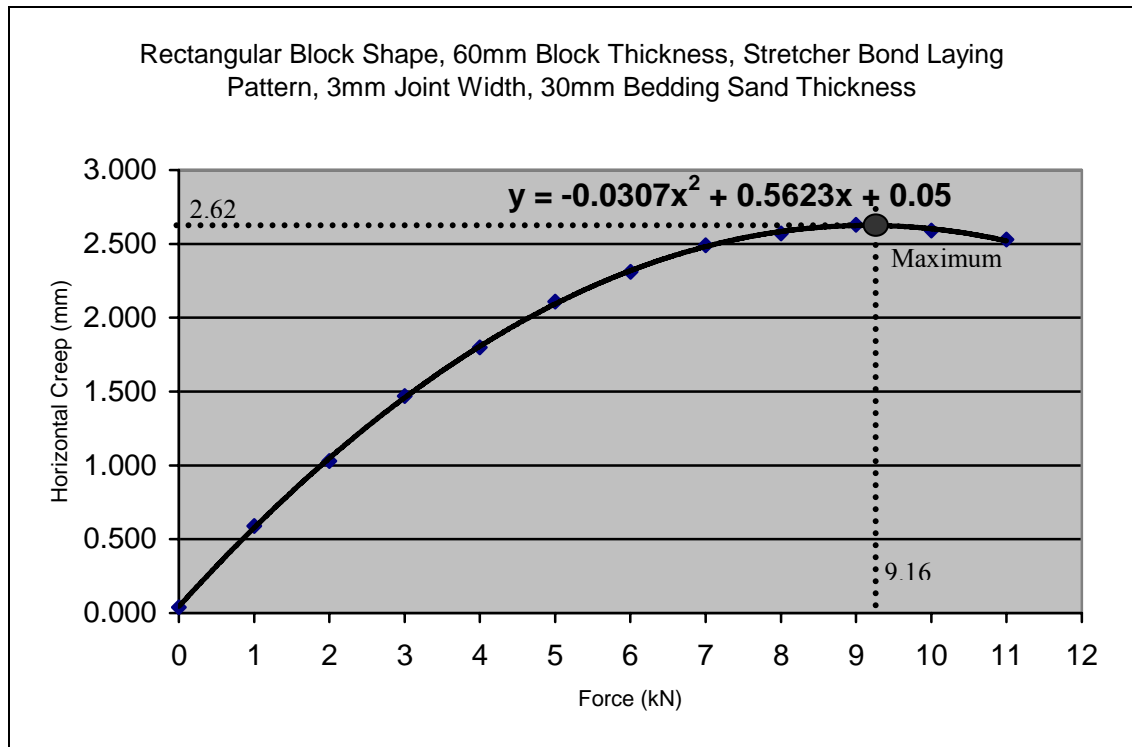
Figure 5.9 Relationship between horizontal forces with horizontal creep   in horizontal force test.

In the Figure 5.9 shown, the horizontal forced was untill 9.16 kN, than the construction of CBP failure (uplift) and maximum horizontal creep is 2.62 mm.

5.3.1.2 Push-in Test

For the example of push-in test, CBP sample laid on 1 m x 1 m steel frame as shown in Figure 5.10. The specification of CBP sample used rectangular block sahape, 60 mm block thickness, stretcher bond laying pattern, 3 mm joint width and 50 mm bedding sand thickness. The CBP sample was loaded by hydraulic jack step by step until 51 kN with 12° degree of slope. The load position was set up on three points; 40 cm, 60 cm and 80 cm from edge restraint as shown in Figure 5.11. The measurement of horizontal creep was used the transducer that connected to the data

logger. The results of experimental found the equation of maximum horizontal creep as shown in Figure 5.12.

Figure 5.10   Measurement horizontal creep on push-in test
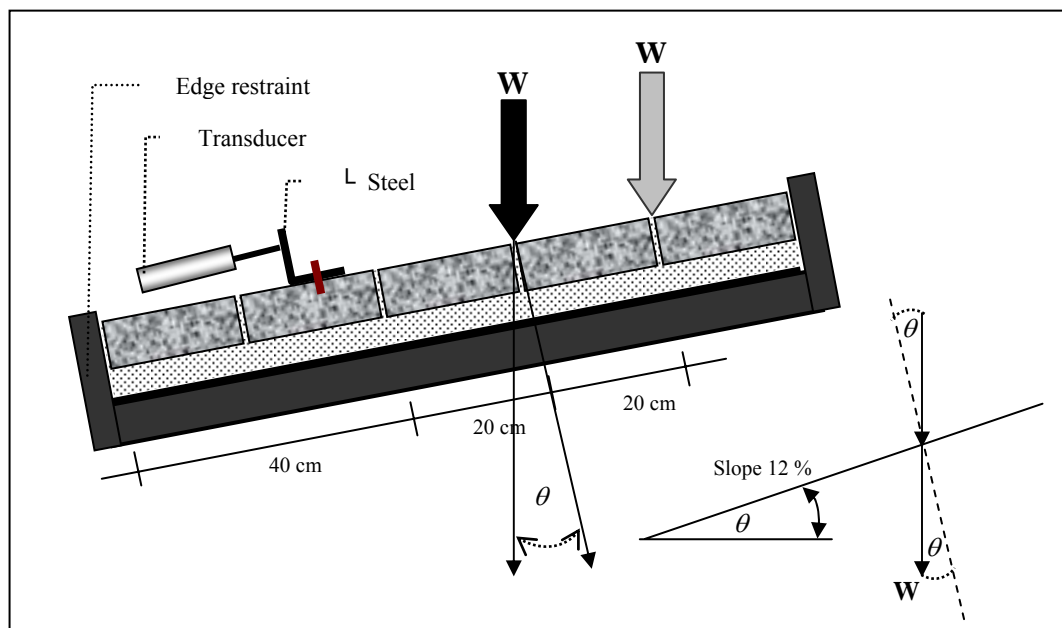
Figure 5.11   Position of load in push-in test

Horizontal force in push-in test (F) = W sin θ

Where: W   = 51 kN

                F   = 51 sin 12°

                      = 10.60 kN ~ 10.79 kN
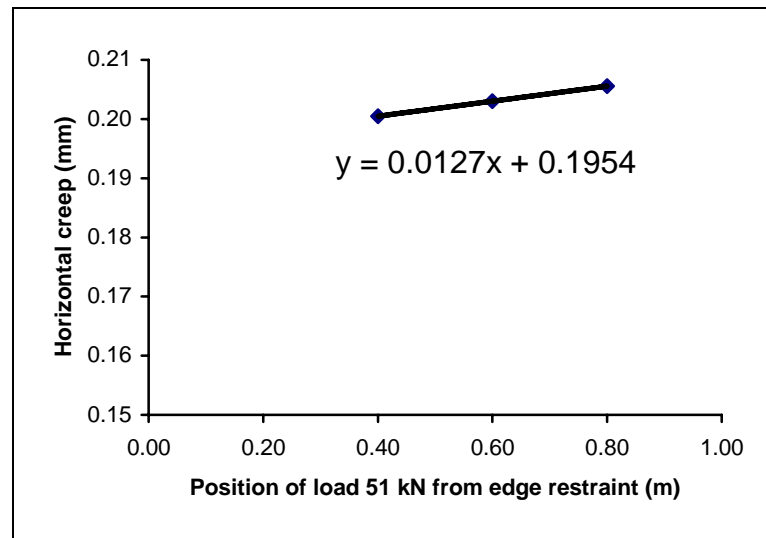
Figure 5.12   Relationship between load positions from edge restraint with horizontal creep on push-in until 51 kN

5.3.2.3 Defining of Anchor Beam Spacing

The definition of spacing of anchor beam in this study using three steps. First, defining x maximum (horizontal force). Second, defining y maximum (horizontal creep). From the equation in Figure 5.6, $y = -0.0307x^2 + 0.5623x + 0.05$, it is found the maximum horizontal force and maximum horizontal creep.

$$y = -0.0307x^2 + 0.5623x + 0.05$$

$$\frac{dy}{dx} = 0$$

$$2(-0.0307)x + 0.5623 = 0$$

$$x = \frac{-0.5623}{2*-0.0307} = 9.16kN$$

Where; x = 9.16 kN is horizontal force until construction of CBP failure (uplift). Substitute x =9.16 kN in equation $y = -0.0307x^2 + 0.5623x + 0.05$, it found y = 2.62. Where y = 2.62 mm is maximum horizontal creep.

The third step is combining x maximum and y maximum to equation $y = 0.0127x + 0.1954$ (Figure 5.8). Substitute y = 2.62 mm, found x = 191.3. The interval distance of the load is 0.20 m as shown in (Figure 5.7), so the spacing of anchor beam is 192.3 x 0.20 m = 38.26 m.
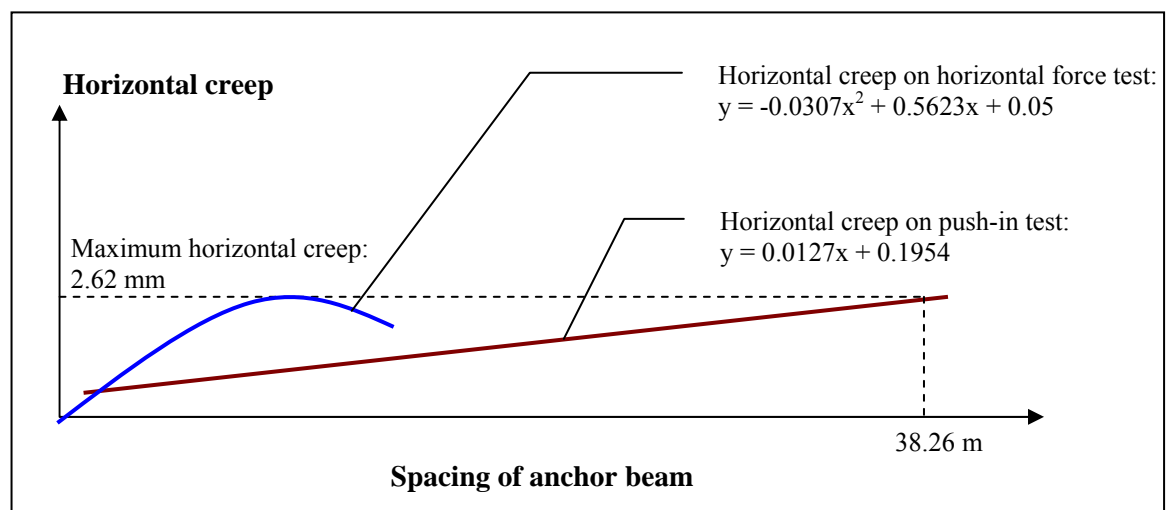
Figure 5.13   The definition of anchor beam spacing

The next section would explain about spacing of anchor beam on various degrees of slopes, that is based on the effects of laying pattern, block thickness, block shape, joint width between blocks and thickness of bedding sand, respectively.

5.4   The Spacing of Anchor Beam Based on the Effect of Laying Pattern

This section explains the estimated spacing of anchor beam based on the effect of laying pattern. There are three laying patterns that been used in this test i.e. stretcher bond, herringbone 90° and herringbone 45°. Each of these laying patterns was tested on four various degree of slope (0 %, 4 %, 8 % and 12 %). In this case, the CBP sample was used 3 mm joint width. The result of relationship between the estimation spacing of anchor beam with degree of slope is shown in Figure 5.9.
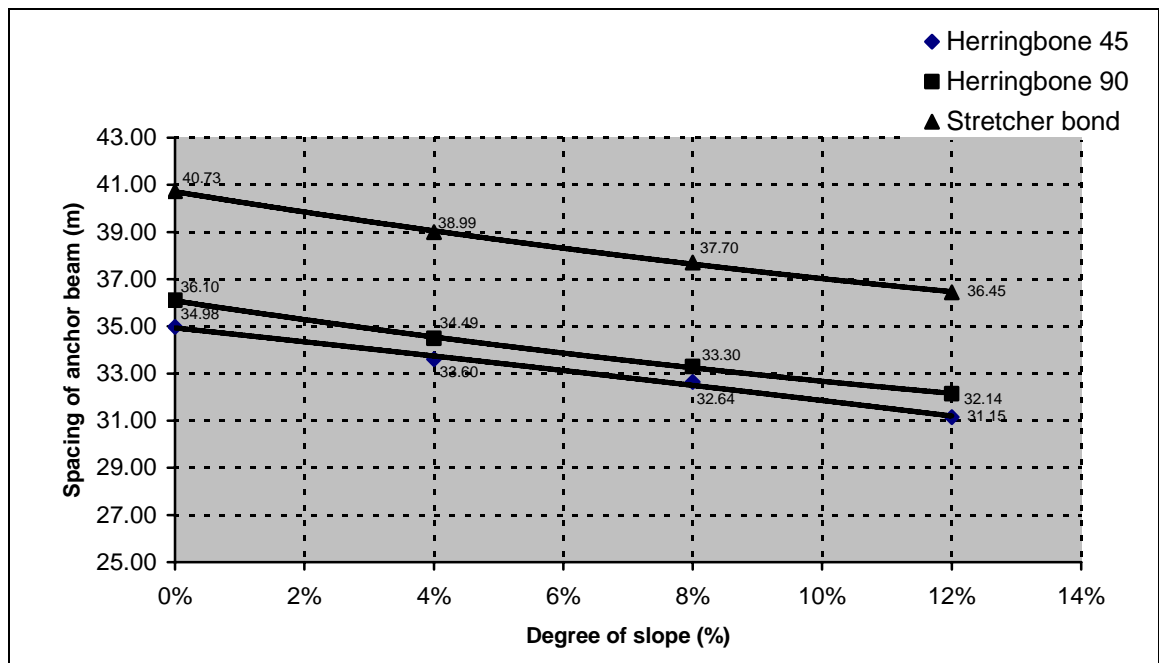
Figure 5.14   Spacing of anchor beam based on laying pattern effect used rectangular block shape, 60 mm block thickness, 50 mm bedding sand thickness and 3 mm joint width
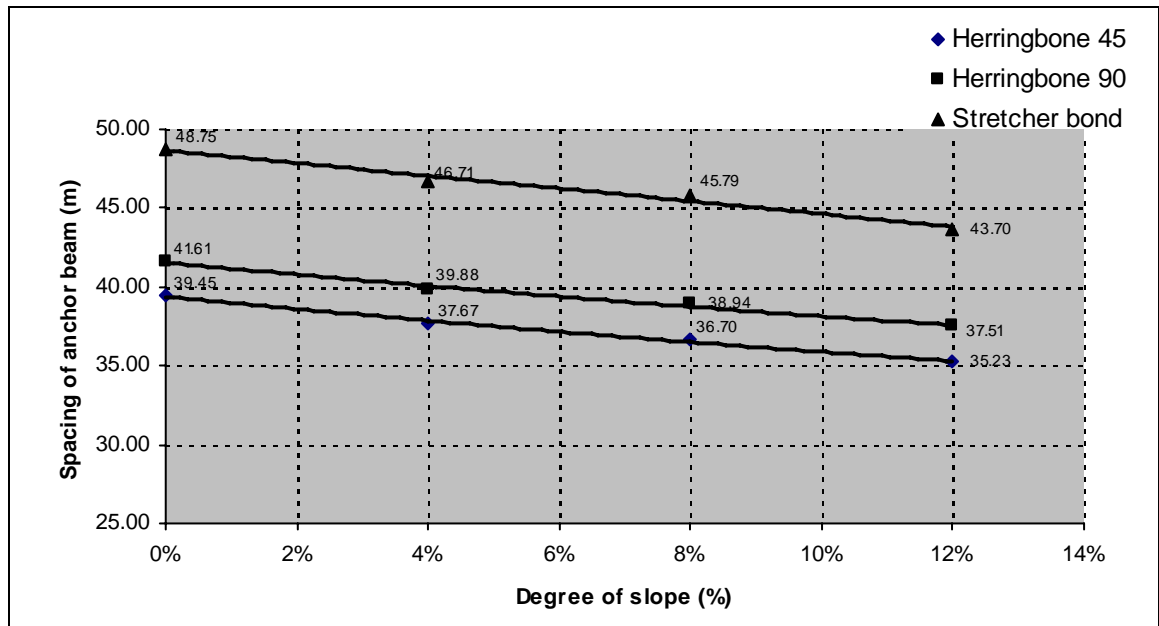
Figure 5.15   Spacing of anchor beam based on laying pattern effect with used rectangular block shape, 100 mm block thickness, 50 mm bedding sand thickness and 3 mm joint width
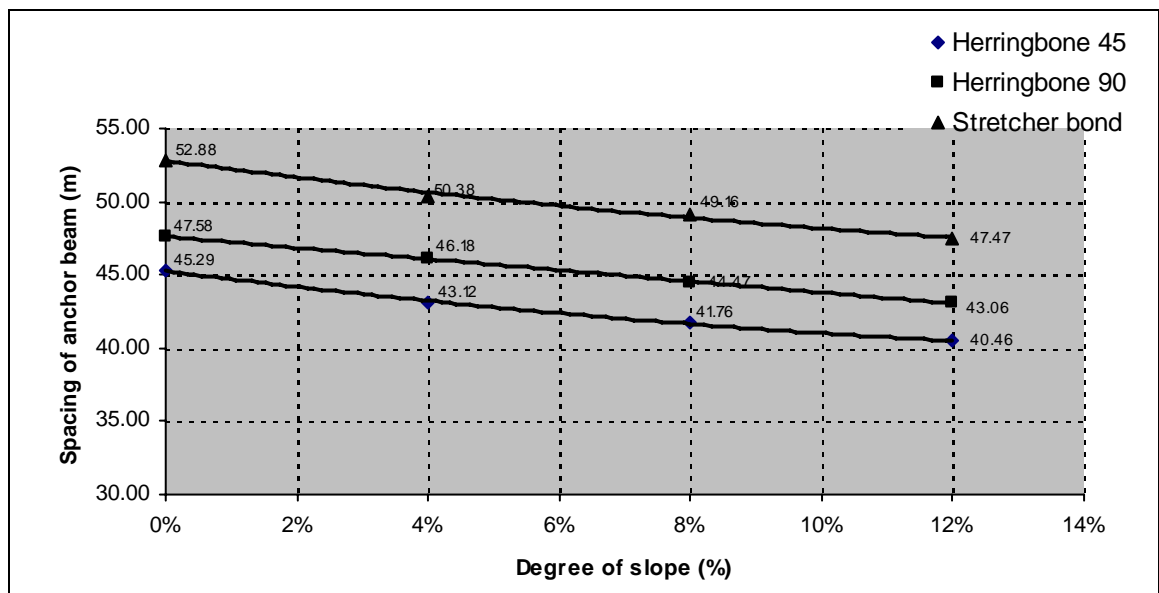
Figure 5.16   Spacing of anchor beam based on laying pattern effect used uni-pave block shape, 60 mm block thickness, 50 mm bedding sand thickness and 3 mm joint width
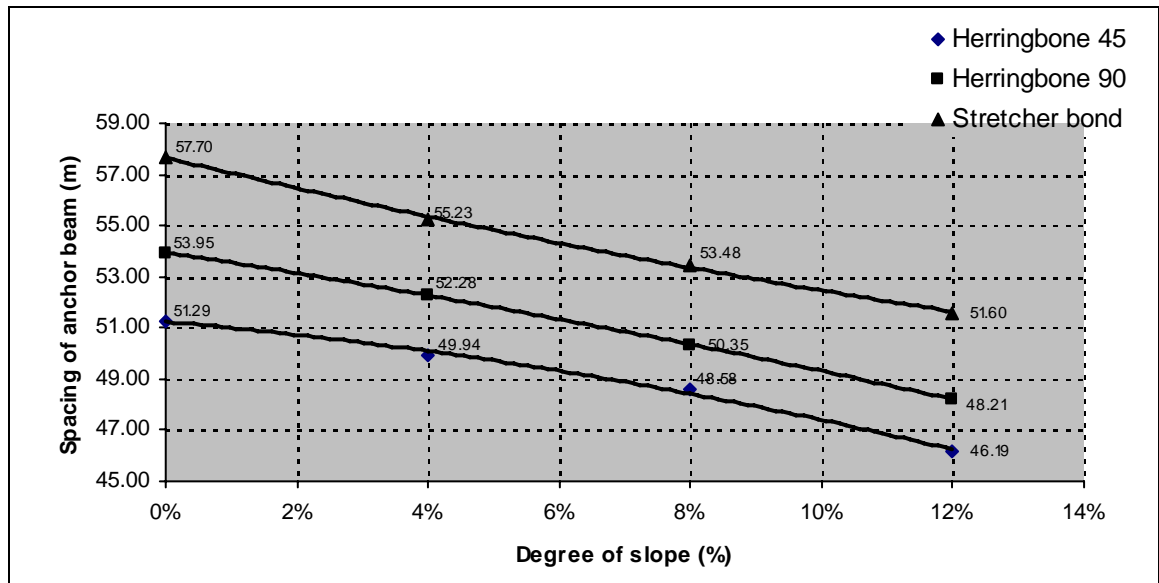
Figure 5.17   Spacing of anchor beam based on laying pattern effect used uni-pave block shape, 100 mm block thickness, 50 mm bedding sand thickness and 3 mm joint width

Figure 5.14 to 5.17 shows the variation of laying pattern affecting the spacing of anchor beams in each variation degree of slope. The herringbone 45° is the best laying pattern compared to herringbone 90° and stretcher bond to restraint the horizontal force. So the spacing of anchor beam in CBP used herringbone 45° laying pattern is longer than herringbone 90° also stretcher bond.

5.5   The Spacing of Anchor Beam Based on the Effect of Joint Width

This section explains the estimated spacing of anchor beam based on the joint width effect. There are three joint width used in this test i.e. 3 mm, 5 mm and 7 mm. Each of these joint widths was tested on four various degree of slope (0 %, 4 %, 8 % and 12%).
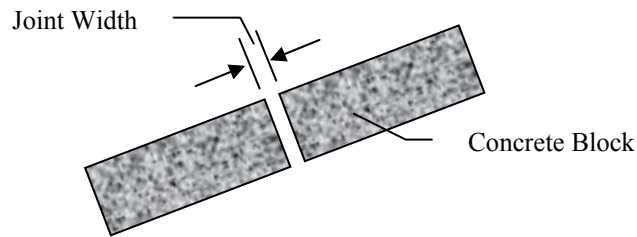
Figure 5.18   The effect of joint width in sloping road section

The relationship between spacing of anchor beam with variation of degrees of slopes is shown in Figure 5.19 to 5.22.
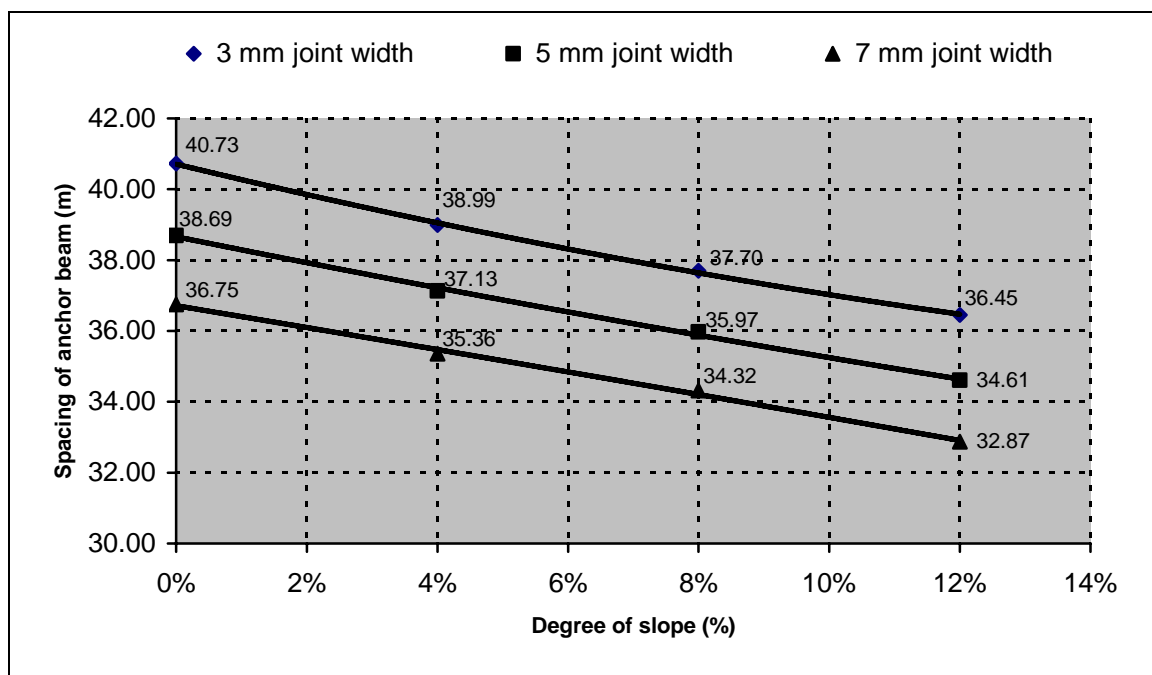
Figure 5.19   Spacing of anchor beam based on joint width effect used rectangular block shape, 60 mm block thickness, 50 mm bedding sand thickness and stretcher bond laying pattern
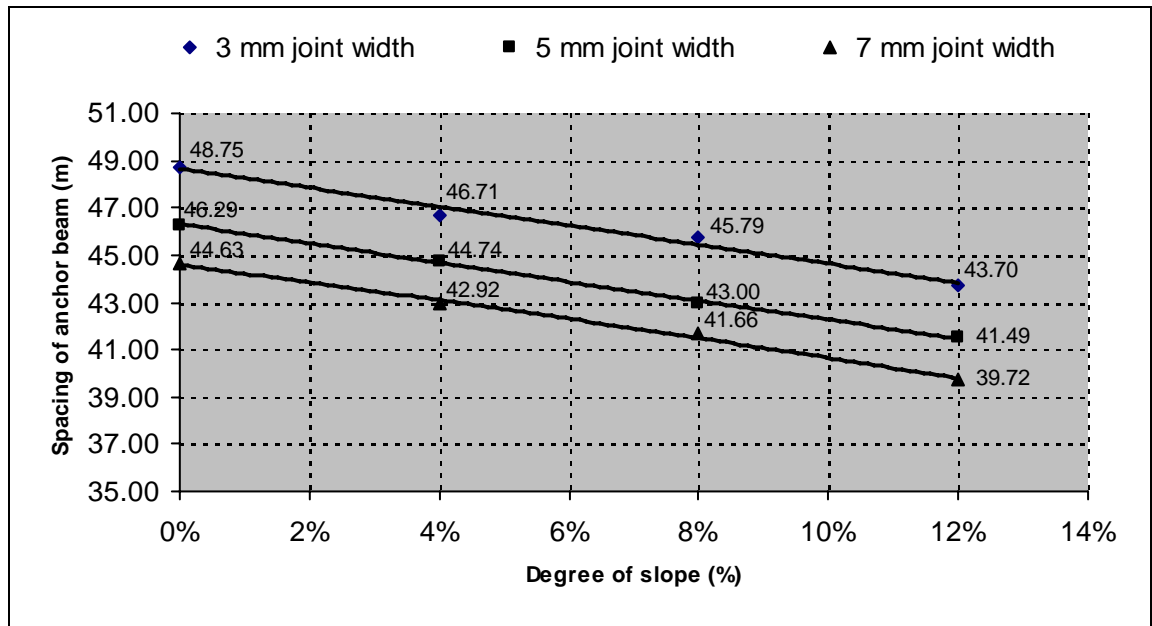
Figure 5.20   Spacing of anchor beam based on joint width effect used rectangular block shape, 100 mm block thickness, 50 mm bedding sand thickness and stretcher bond laying pattern
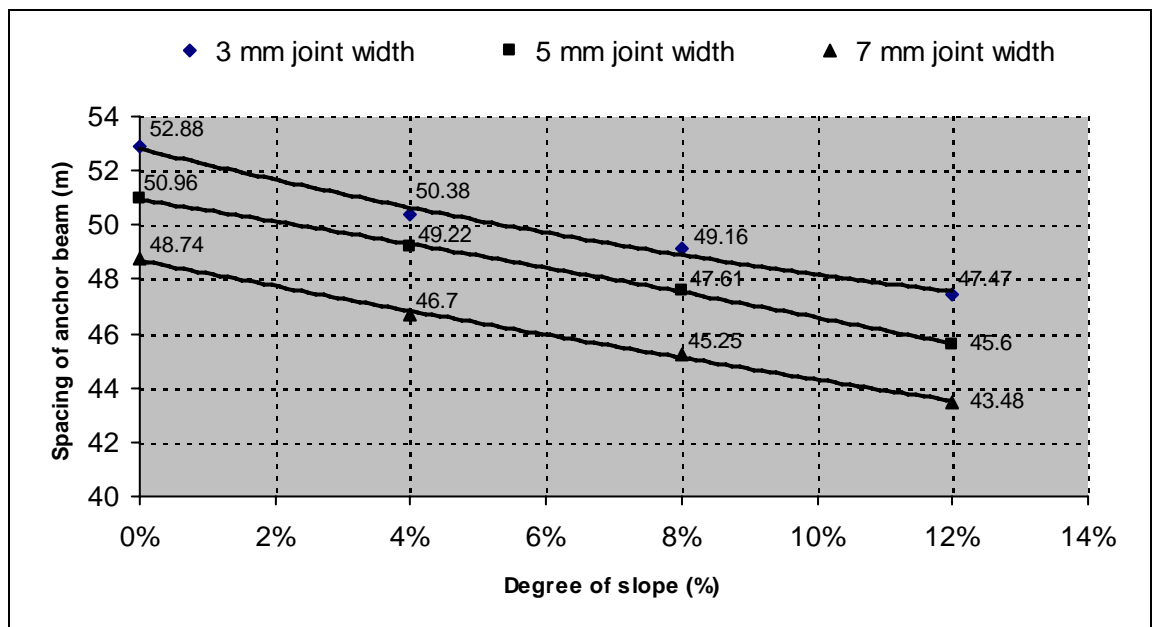
Figure 5.21   Spacing of anchor beam based on joint width effect used uni-pave block shape, 60 mm block thickness, 50 mm bedding sand thickness and stretcher bond laying pattern
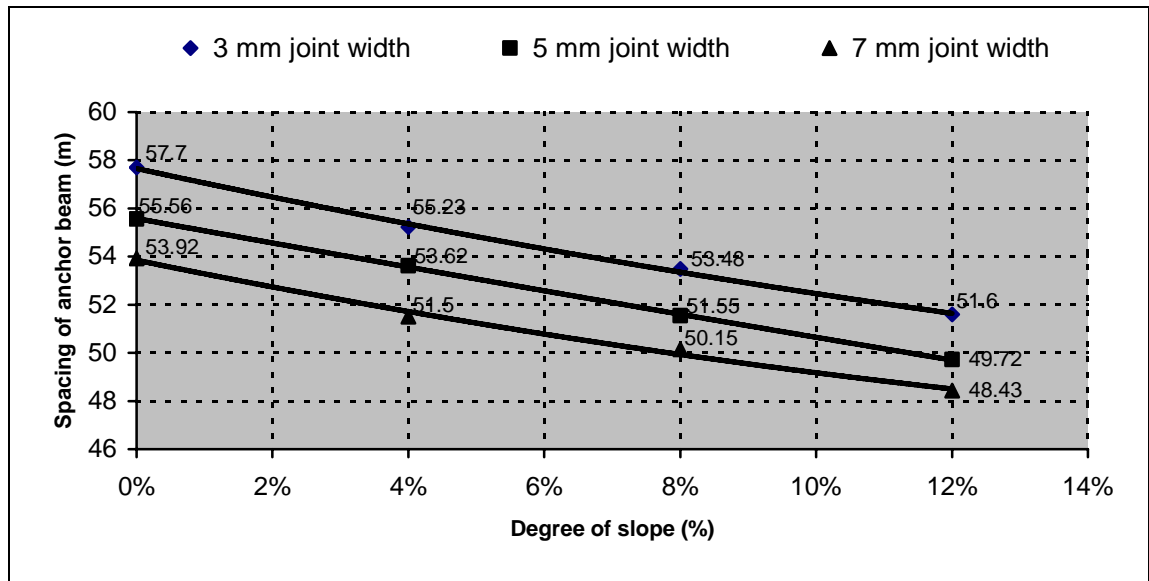
Figure 5.22   Spacing of anchor beam based on joint width effect used uni-pave block shape, 100 mm block thickness, 50 mm bedding sand thickness and stretcher bond laying pattern

Figure 5.19 to 5.22 were shown that the variation of joint width affecting the spacing of anchor beams in each variation degree of slope. The wider the joint width, the spacing of anchor beam is shorter for each variation degree of slope. The higher degree of slope, the shorter the spacing of anchor beams for each variation degree of slope.

5.6   The Spacing of Anchor Beam Based on the Effect of Block Thickness

This section explains the estimated spacing of anchor beam based on the block thickness effect. There are two block thickness used in this test i.e. 60 mm and 100 mm. Each of these block thicknesses was tested on four various degree of slope (0 %, 4 %, 8% and 12 %). The result of relationship between the estimation spacing of anchor beam with thickness of block is shown in Figure 5.25 and Figure 5.26.
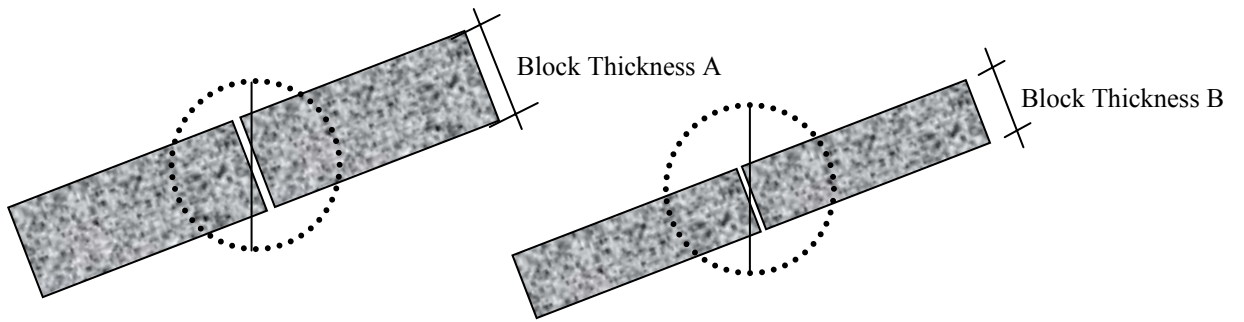
Figure 5.23   The difference of block thickness
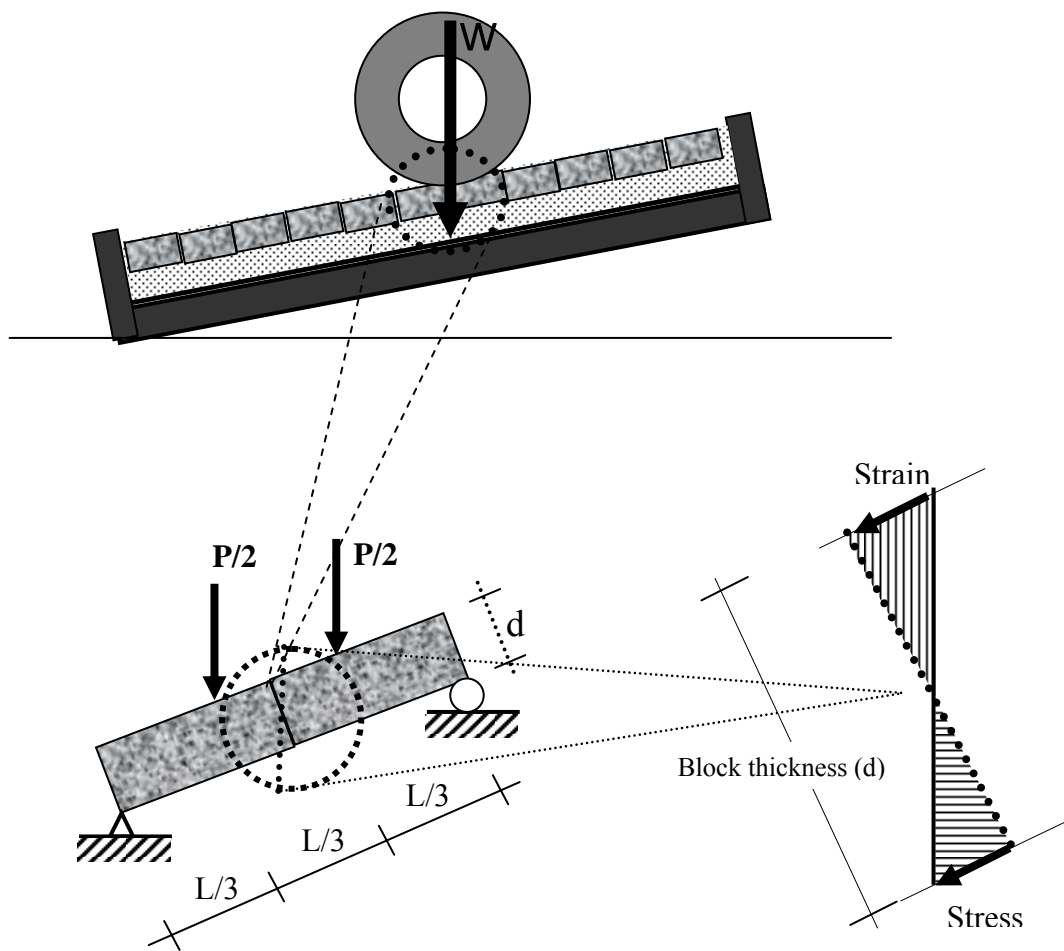
Figure 5.24   The effect of block thickness on sloping road section
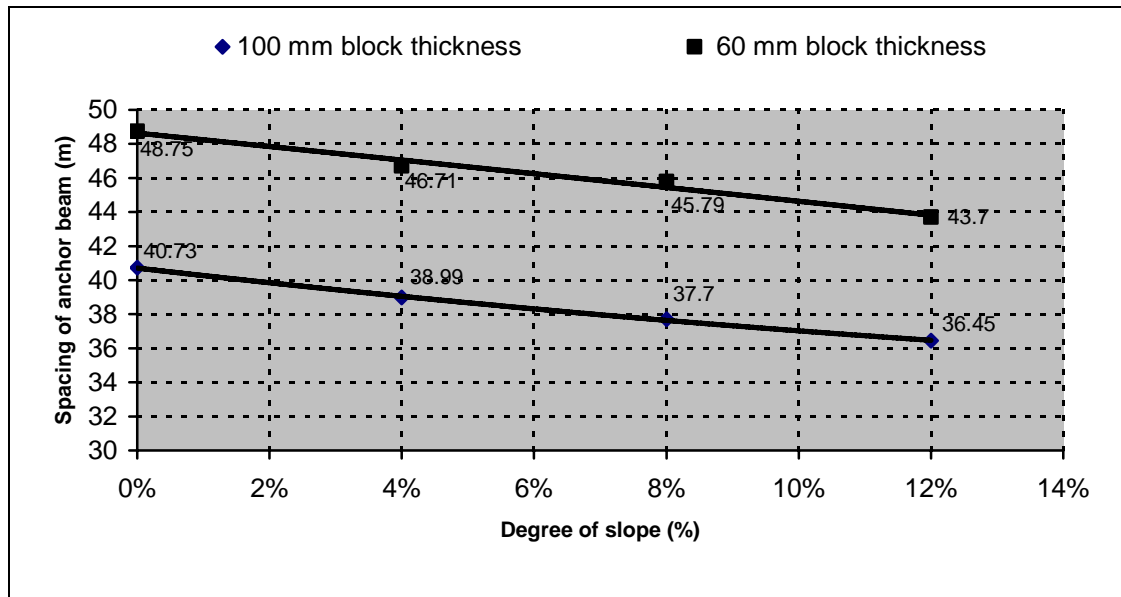
Figure 5.25   Spacing of anchor beam based on block thickness effect used rectangular block shape, 50 mm bedding sand thickness, 3 mm joint width and stretcher bond laying pattern
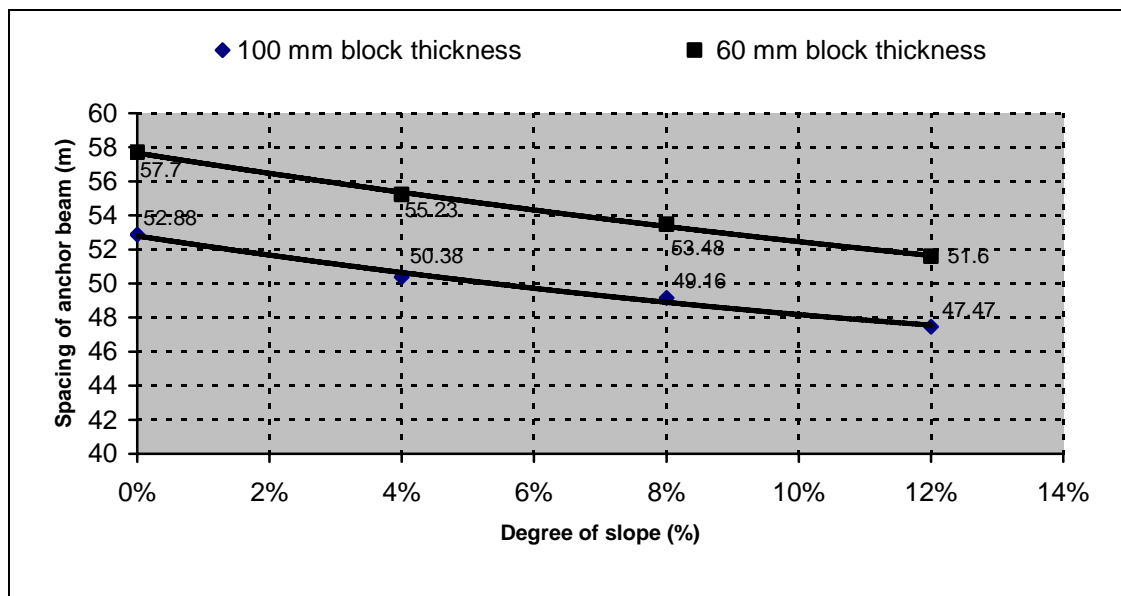
Figure 5.26   Spacing of anchor beam based on joint width effect used uni-pave block shape, 50 mm bedding sand thickness, 3 mm joint width and stretcher bond laying pattern

The variation of block thickness is affecting the spacing of anchor beam. The thicker of block thickness, the longer the spacing of anchor beam for each variation degree of slope. The higher degree of slope, the shorter the spacing of anchor beams for each variation of block thickness. From this test also found that 100 mm block thickness is more stable than 60 mm block thickness.

5.7 The Spacing of Anchor Beam Based on the Effect of Block Shape

This section explains the estimated spacing of anchor beam based on the block shape effect. There are two block shapes that used in this test i.e. rectangular and uni-pave shape. Each of these block shapes was tested on four various degree of slope (0 %, 4 %, 8 % and 12 %). In this case, the CBP sample was used 3 mm joint width. The result of relationship between the estimation spacing of anchor beam with degree of slope is shown in Figure 5.27.
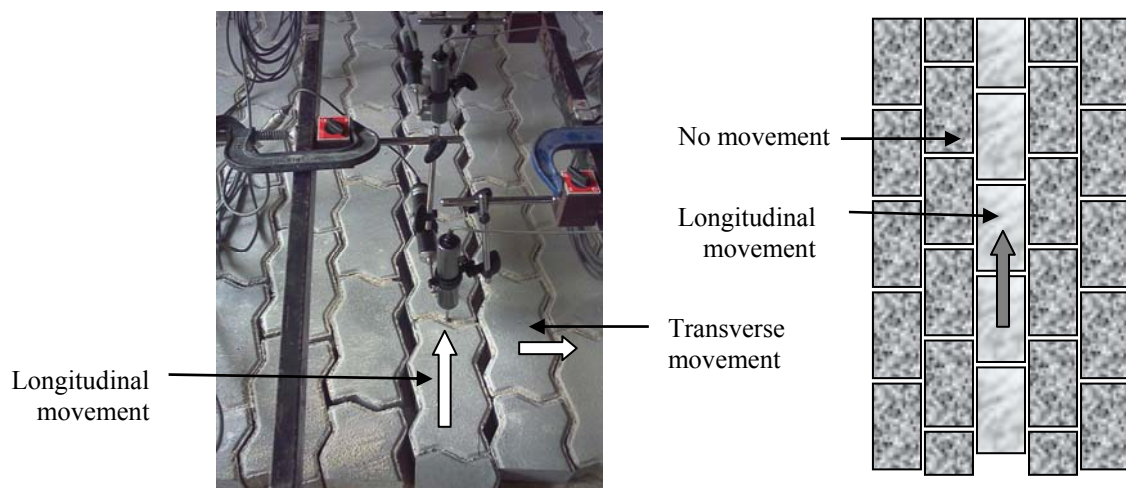
Figure 5.27 The different effect of uni-pave by rectangular blocks loaded horizontally
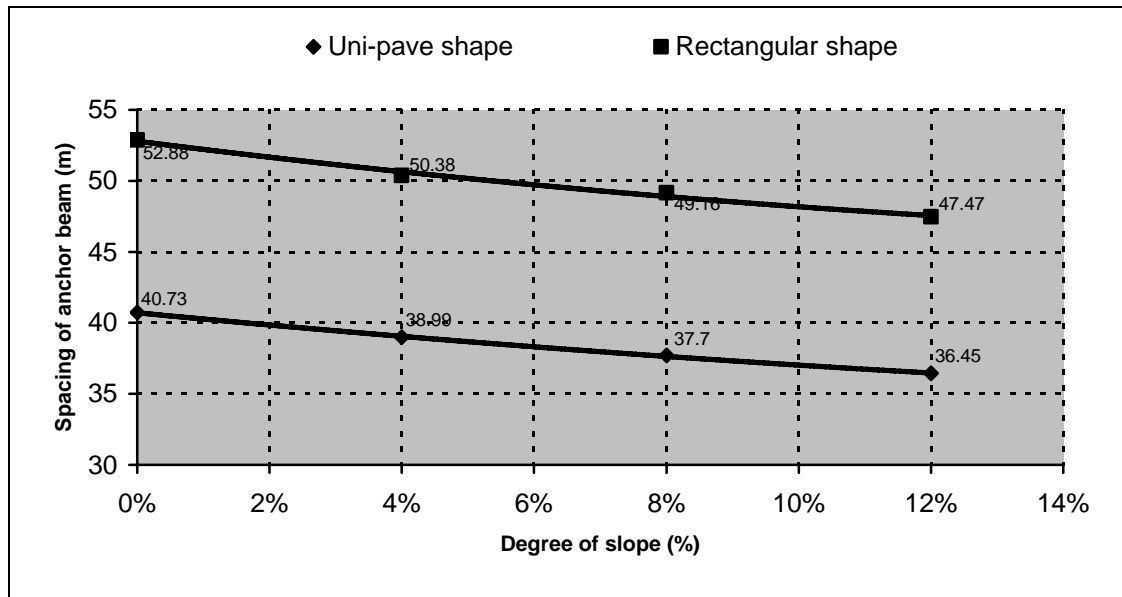
Figure 5.28   Spacing of anchor beam based on joint width effect used 60 mm block thickness, 50 mm bedding sand thickness, 3 mm joint width and stretcher bond laying pattern
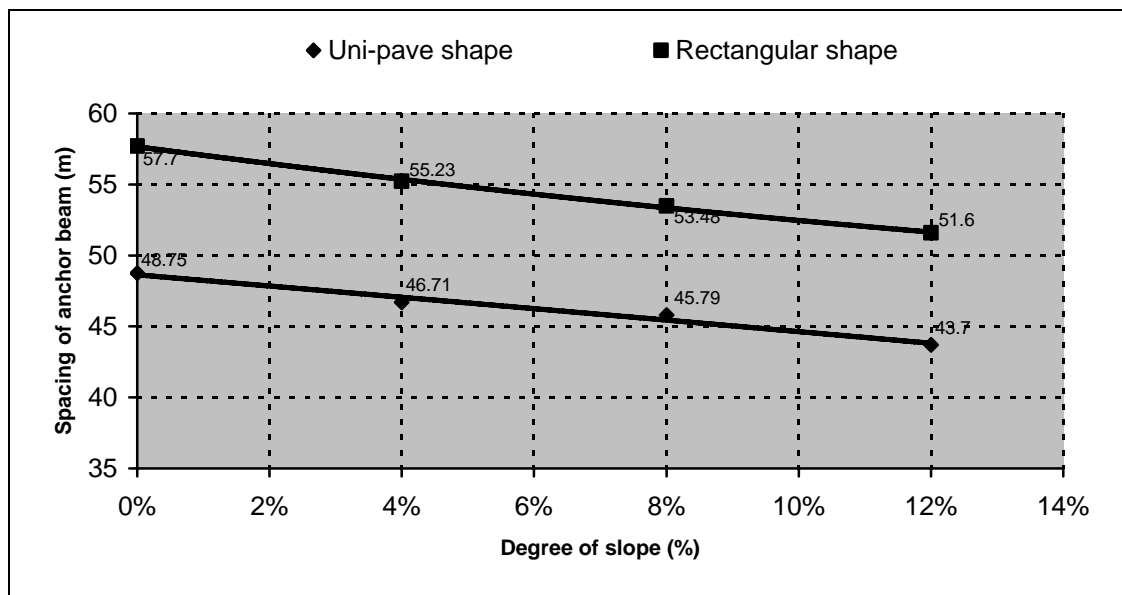
Figure 5.29   Spacing of anchor beam based on joint width effect used 100 mm block thickness, 50 mm bedding sand thickness, 3 mm joint width and stretcher bond laying pattern

Figure 5.28 and Figure 5.29 are shows that the variation shapes of block affecting the spacing of anchor beam for each variation degree of slope. The uni-pave block shape has more restraint of horizontal creep than rectangular block shape, because uni-pave block shape has gear (four-dents), while rectangular block shape no gear (no dents), so the spacing of anchor more than rectangular block shape. The higher degree of slope, the shorter the spacing of anchor beams for each variation shape of block.

5.8 The Spacing of Anchor Beam Based on the Effect of Bedding Sand Thickness

This section explains the estimated spacing of anchor beam based on the bedding sand thickness effect using 3 mm joint width. The bedding sand thickness used in this study are; 30, 50 and 70 mm. Each of these bedding sand thicknesses was tested on 0 %, 4 %, 8 % and 12 % degrees of slope. In Figure 5.31 to 5.34, the bedding sand thickness of 30 mm has almost no difference effect if applied on sloping road section 0 to 8 %, because too small difference thickness. But, the bedding sand thickness of 50 mm and 70 mm, the difference is significant for about 1.5 mm to 8.4 mm additional thickness. The effect of bedding sand thickness on CBP slopes 0 to 12 %, the deflection in the pavement increase. The increase degree of slope will cause shorter spacing of anchor beam for each bedding sand thickness as shown in Figure 5.30 to Figure 5.34.
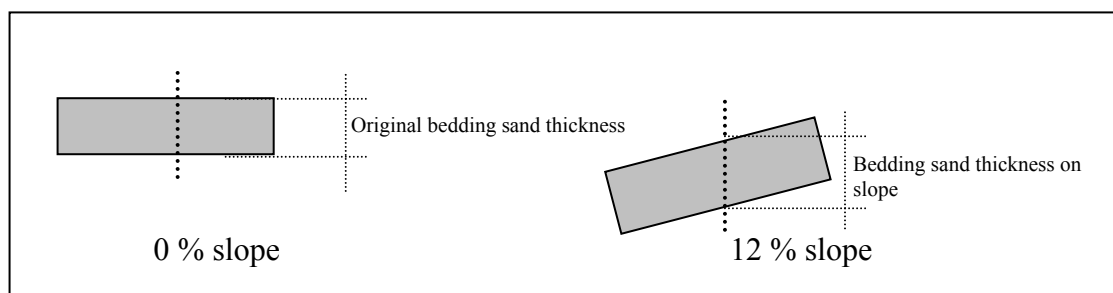
Figure 5.30 The effect of slope in bedding sand thickness
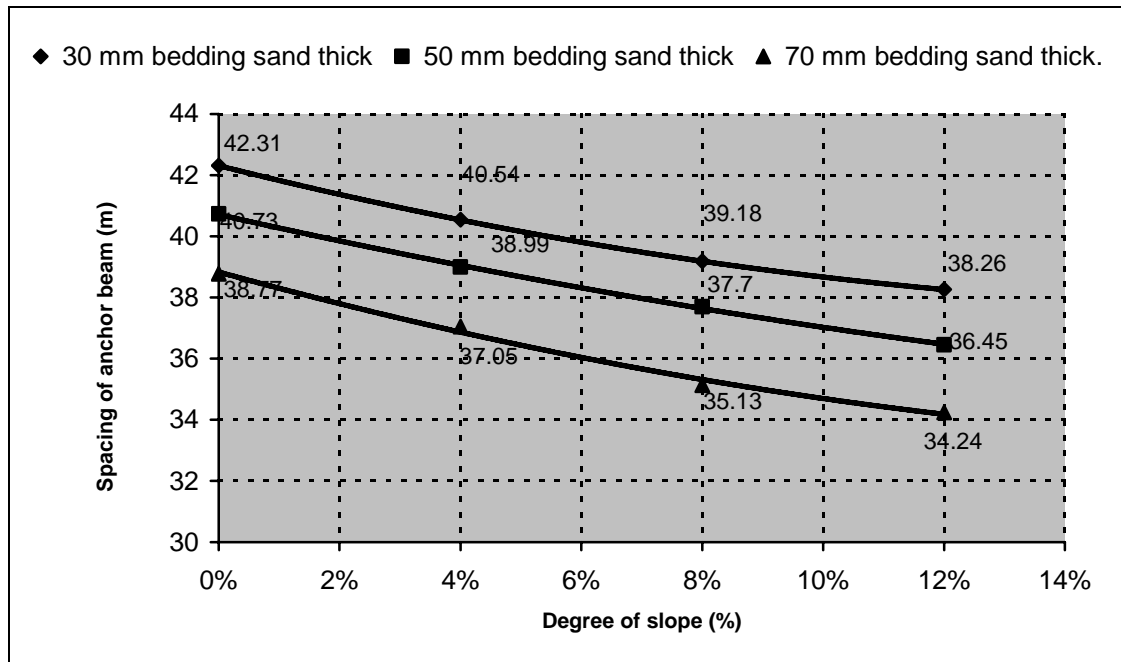
Figure 5.31   Spacing of anchor beam based on bedding sand thickness effect used rectangular block shape, 60 mm block thickness, 3 mm joint width and stretcher bond laying pattern
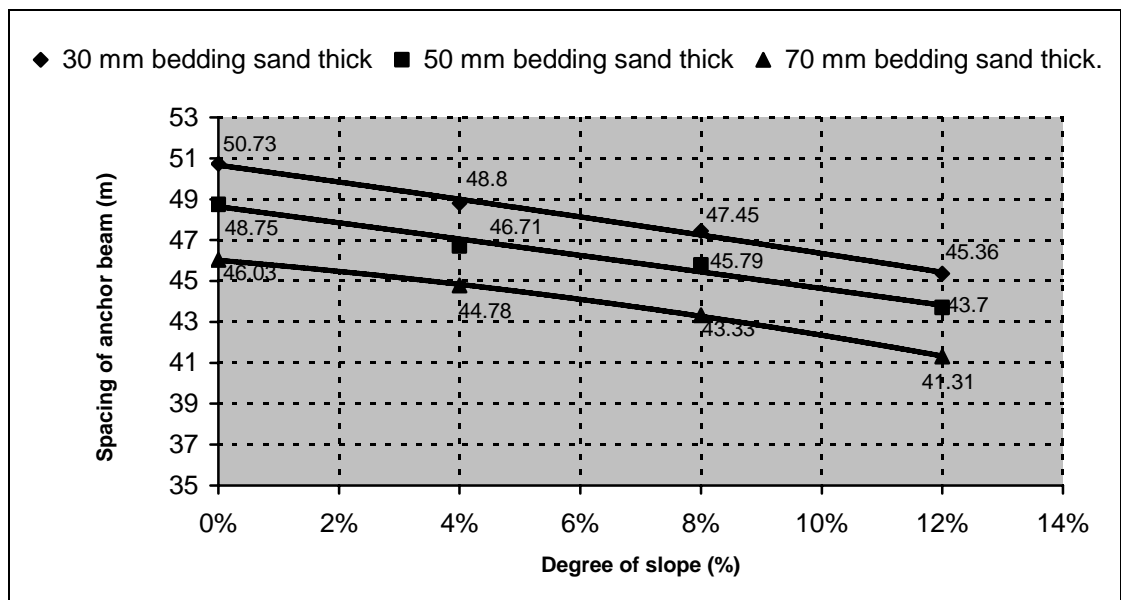
Figure 5.32   Spacing of anchor beam based on bedding sand thickness effect used rectangular block shape, 100 mm block thickness, 3 mm joint width and stretcher bond laying pattern
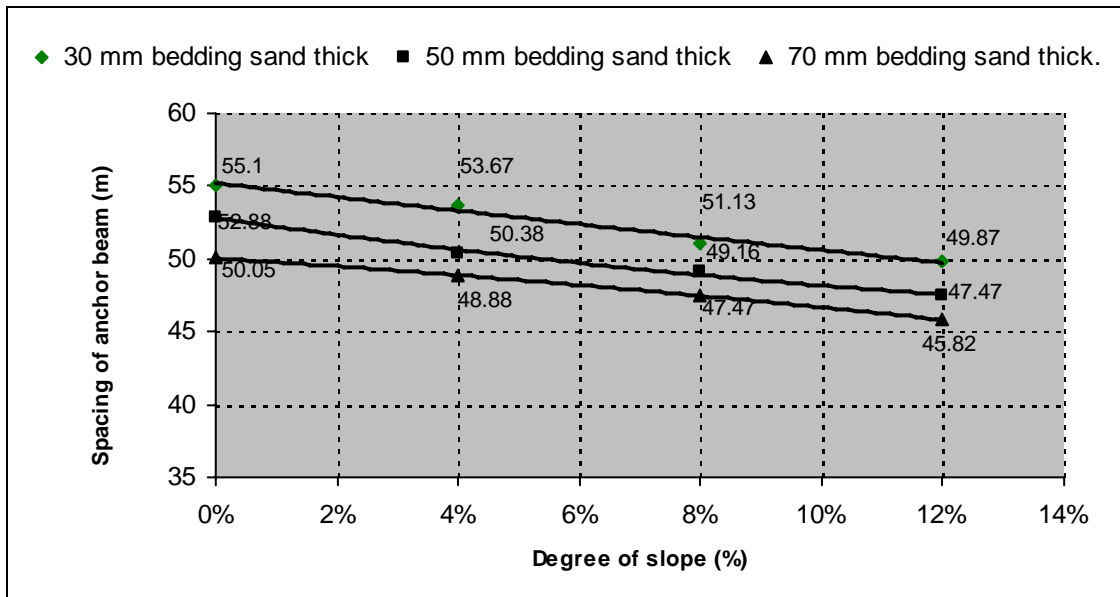
Figure 5.33   Spacing of anchor beam based on bedding sand thickness effect used uni-pave block shape, 60 mm block thickness, 3 mm joint width and stretcher bond laying pattern
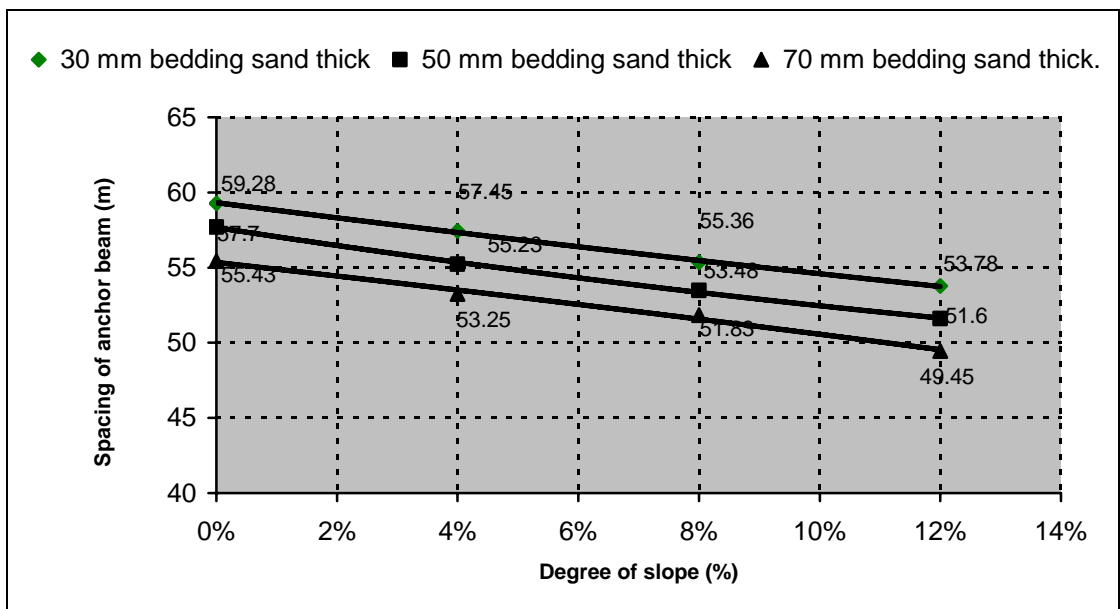
Figure 5.34   Spacing of anchor beam based on bedding sand thickness effect used uni-pave block shape, 100 mm block thickness, 3 mm joint width and stretcher bond laying pattern

5.9   Summary

The spacing of anchor beam on various degrees of slopes, that is based on the effect of laying pattern, block thickness, block shape, joint width between blocks and thickness bedding sand, is summarized below:

➢   The herringbone 45° is the best laying pattern compared to herringbone 90° and stretcher bond to restraint the horizontal force.

➢   For the case horizontal creep, the uni-pave block shape is more restraint than rectangular, because uni-pave block shape has gear (four-dents), while rectangular block shape no gear.

➢   The increase of degree of slope will cause shorter spacing of anchor beam.

➢   The increase of joint width will cause shorter spacing of anchor beam.

➢   The optimum joint width is 3 mm.

➢   The increase of block thickness will cause longer spacing of anchor beam.

➢   The increase of bedding sand thickness will cause shorter spacing of anchor beam.

CHAPTER 6

CBP BEHAVIOUR USING FINITE ELEMENT METHOD

6.1   Introduction

It is difficult to model block pavements by finite elements for structural analysis, because their surface layer consists of a large number of very small blocks with complicated laying patterns. In this study, a programme package of the structural analysis for block pavements, Kuo (1994) used COSMOS Design Star version 4.0, has been developed based on a three dimensional finite element model for pavement structure. The SOLID Works version 2004 programme package can draw meshing of each element structure model pre-processor. They have to input information only on loading and pavement structural conditions including block size, joint width, laying pattern and mechanical characteristics of bedding sand layer. The solver computes displacements, stresses and strains in the blocks. In the model, the blocks are divided into solid elements and the bedding sand course and jointing sand are modelled by a general interface element. The post processor graphically displays deformations and stress contours of the entire or partial region of the pavement structure. The effects of block thickness, stiffness of joint, bedding sand course and laying pattern on deflection, also stress and strain in concrete block pavements are investigated using this tool.

6.2   Three Dimensional Finite Element Model (FEM)

In this study, in order to simulate mechanical behaviour of concrete block pavements, a structural model based on a Three Dimensional Finite Element Model (3DFEM) was developed. In this section, outline of 3DFEM model for pavement structures and its application to concrete block pavements are presented.

6.2.1   Three Dimensional FEM for Pavement

Figure 6.1 shows a pavement structure considered in SOLID WORKS. This pavement consists of elastic layers that represent concrete block, jointing sand, and bedding sand, all of which are divided into solid elements in the steel frame box. The interface between the blocks and jointing sand is modelled using a general interface element.
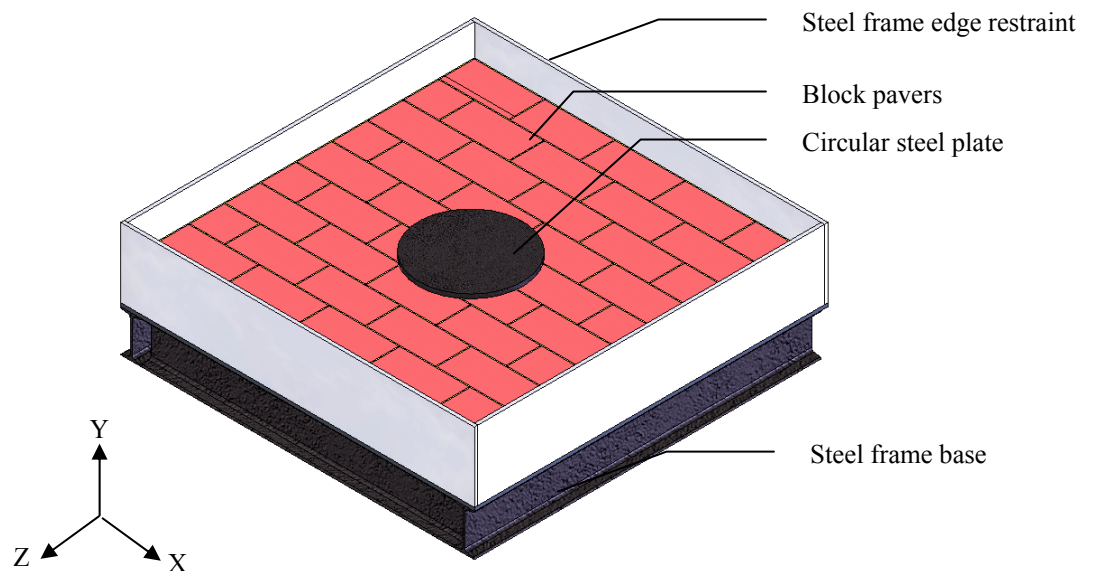
Figure 6.1   Structural model of concrete block pavement

Each layer has a finite horizontal extent and displacement in the normal direction is fixed on all side faces of the layer; other displacements are free. This boundary condition is not applied to the top layer. All displacements are fixed at nodes on the bottommost surface of the structure. Loads up to 51 kN were applied on the surface CBP vertically as uniformly distributed steel circle loads 250 mm diameter and 12 mm thickness (assumed wheel contact area on pavement).

6.2.2   Diagram Condition of Sample Tested

A block pavement consists of small blocks, joints between the blocks, a bedding sand course and steel frame as base course. The pavement structure is modelled as a combination of solid elements and tested on various slope as shown in Figure 6.2.
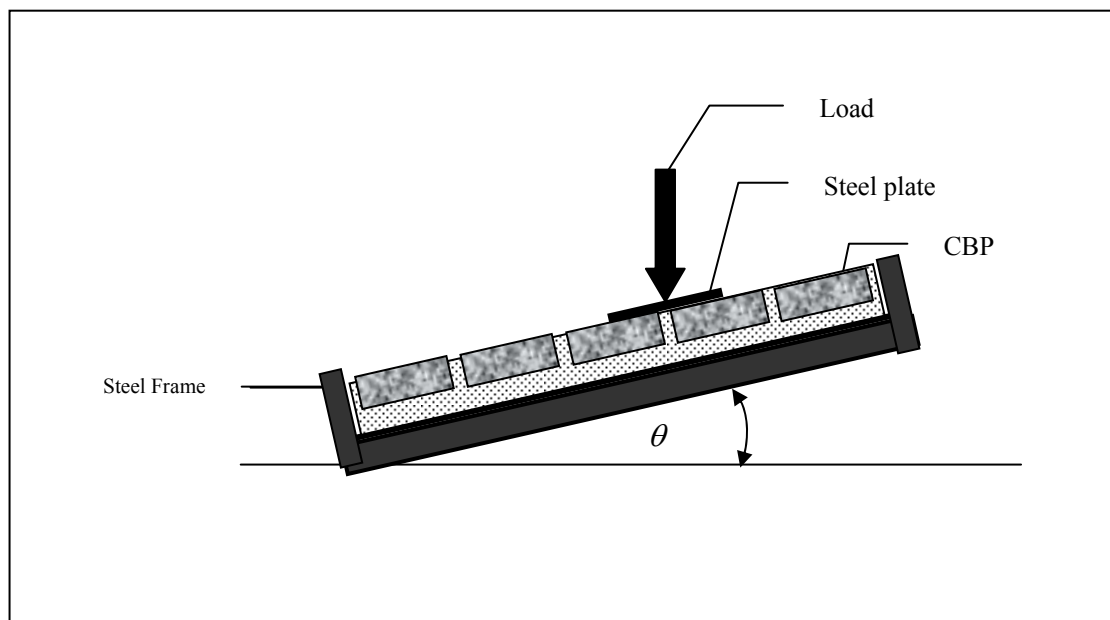
Figure 6.2   CBP tested on various slope
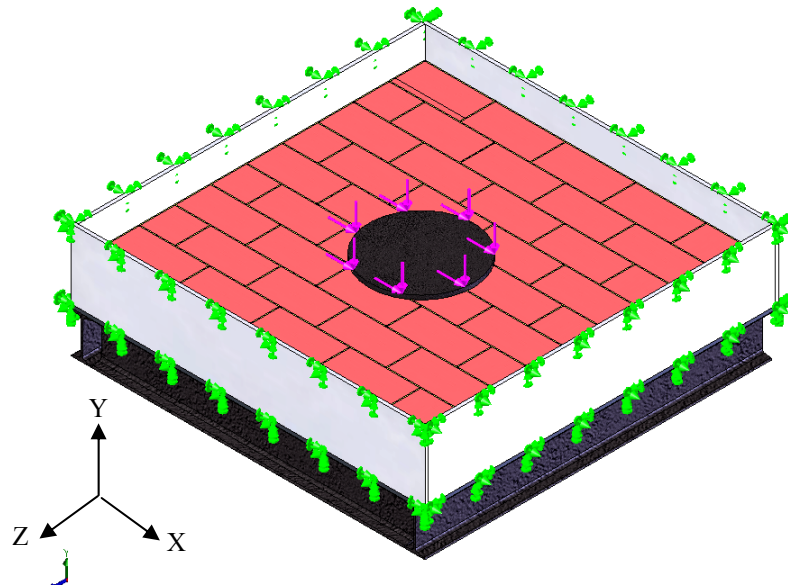
Figure 6.3   Three dimensional finite element model for a block pavement

6.3   Programme Package

6.3.1   Outline

The programme package (COSMOS Design Star) developed in this study for structural analysis of block pavements consists of a pre-processor, a solver and a post-processor. The pre-processor has a user-friendly interface, through which users input data regarding the meshing of concrete block pavement CBP and material properties of each element as well as loading condition. The solver runs the FEM programme using the input data file and stores the results in an output data file report. The post processor graphically displays the computed results and provides response data of specified nodes.

6.3.2   Pre-processor

6.3.2.1 Meshing

Meshing is a very crucial step in design analysis. The automatic mesher in COSMOS Works generates a mesh based on a global element size, tolerance, and local mesh control specifications. Mesh control could specify different sizes of elements for components, faces, edges, and vertices.
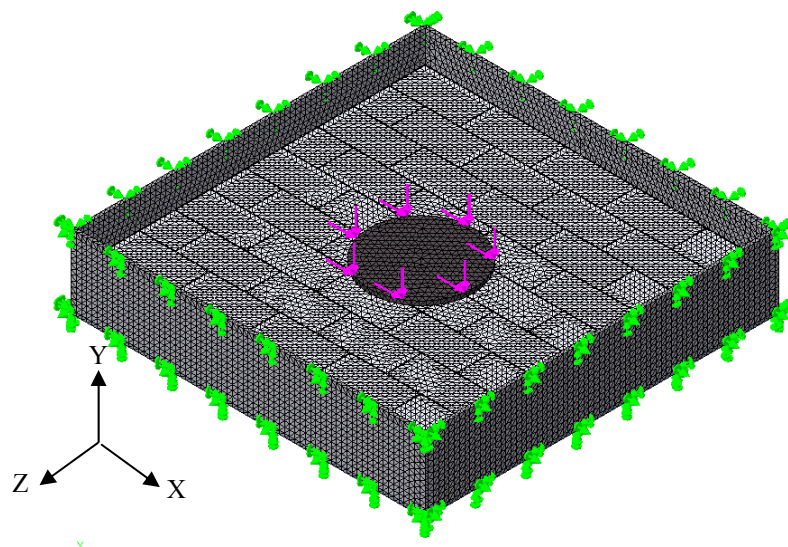
Figure 6.4   User interface of pre-processor of the package

6.3.2.2 Material Properties

In this study each material is characterized by its modulus of elasticity, density, and Poisson's ratio. The material properties used in this study are obtained from an information research and development of block company (SUN-Block Sdn. Bhd). The block thickness and the stiffness of the joint and bedding sand varied as presented in Table 6.1.

Table 6.1   Material properties used in 3DFEM *(Source: Cosmos Material Properties)*

Material	Elastic Modulus (kN/m^2)	Poisson's Ratio	Mass Density (kg/m^3)
Block	3.5E+05	0.25	2,435
Bedding and jointing sand	43E+02	0.35	1,732
Steel	27E+06	0.30	4.817

For the non-linear three-dimensional analyses, concrete blocks are considered to be elastic. Bedding and jointing sand layers were assumed to have elastic perfectly plastic behaviour; it was utilized as their failure criteria. The layers were assumed to have full contact with no relative displacement between.

6.3.3   Solver

The solver, 3D FEM, computes displacements, stresses and strains using the input data file created by PRE3D. The 3D FEM opens a COSMOS Design Star showing an iterative solution process for a nonlinear equation. The computation will take several minutes up to several hours depending on the problem size and the platform.

6.3.4   Post-processor

Clicking [Run]-[Graphics] from the COSMOS Design starts the post-processor and then open file SOLID Works. On the COSMOS, the user is able to load the report file and view displacement, stress and strain results. The Report tool

helps a document user to study quickly and systematically by generating internet-ready reports. The reports are structured to describe all aspects of the study. Plots created in the COSMOS Works Manager tree can be included automatically in the report. User can also insert images, animations (AVI videos), and VRML files in the report. A printer-friendly version of the report can be generated automatically. Reports provide an excellent way to share study results with others online or in printed format. User can modify the various sections of the report by inserting text or graphics. To share a report, send all associated image files along with the html files. The receiver should place all files in the same folder for viewing.

6.4 Simulations

This section examines the effects of block thickness, friction of joint and bedding sand on deflection, stresses in block and strain at the top of each element based on the simulation results.

Pavement structures used in the simulation have a block layer with 98 mm x 198 mm block; 60 mm block thickness, 50 mm thick bedding sand. The type stretcher bond of laying pattern of blocks was employed. 3DFEM models used in the simulation are shown in Figure 6.1. The area of the pavement was 1.00 m by 1.00 m. 98 mm by 198 mm rectangular load of 51 kN was applied at the centre of the area.

6.5   Results

6.5.1   Displacement

Figure 6.5 shows the effects of the block thickness on the deflection (downward deflection is defined as negative) at the centre of the pavement on 0 %, 4 %, 8 % and 12% slopes. If the joint stiffness is high, the deflection decreases as the block thickness increases. On the other hand, if the joint stiffness is low, the thickness hardly affects the deflection. If the stiffness of the cushion layer is low, the deflection is large.
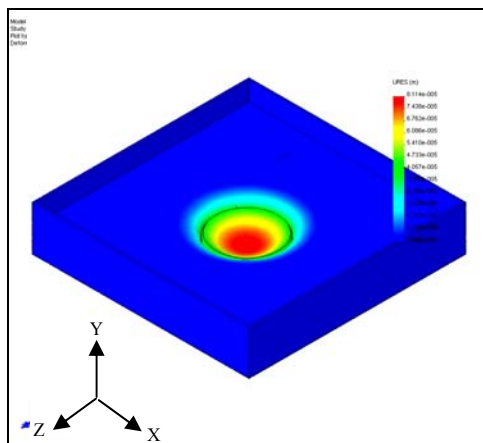
(a) Displacement of CBP on Slope 0 %   (b) Displacement of CBP on Slope 4 %
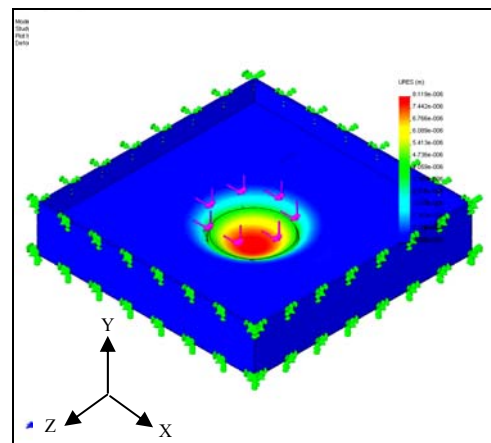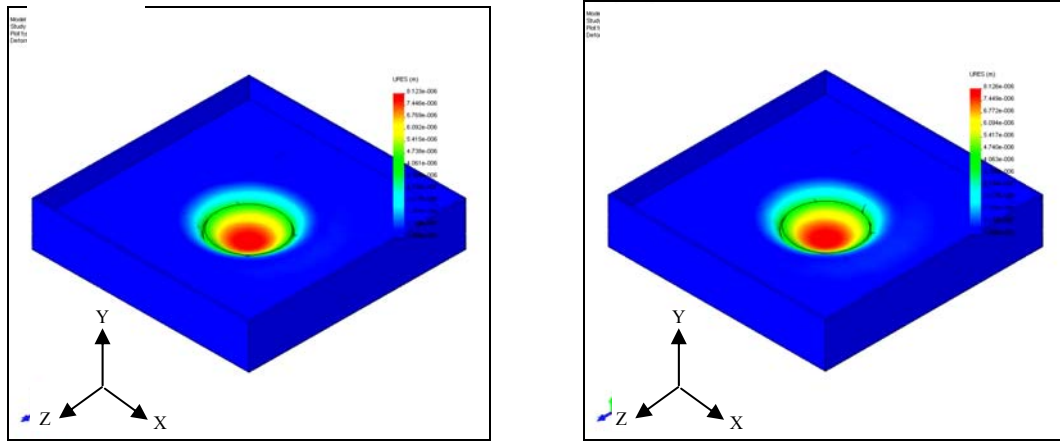
(c) Displacement of CBP on Slope 8 %   (d) Displacement of CBP on Slope 12 %

Figure 6.5   The displacement of CBP in the simulation (455277 nodes).

Table 6.2:   Displacement and horizontal creep results

Slope	Type	Min	Location	Max. Displacement	Max. Horizontal Creep	Location
0 %	URES: Resultant displacement	0 m Node: 74604	(510 mm, 10 mm, 500 mm)	1.811446 mm Node: 120045	0.263242 mm Node: 120045	(-10.838 mm, 125.921 mm, 0.097129 mm)
4 %	URES: Resultant displacement	0 m Node: 74604	(510 mm, 10 mm, 500 mm)	1.811884 mm Node: 120045	0.325741 mm Node: 120045	(-10.838 mm, 125.921 mm, 0.097129 mm)
8 %	URES: Resultant displacement	0 m Node: 74604	(510 mm, 10 mm, 500 mm)	1.812273 mm Node: 120045	0.413583 mm Node: 120045	(-10.838 mm, 125.921 mm, 0.097129 mm)
12 %	URES: Resultant displacement	0 m Node: 74604	(510 mm, 10 mm, 500 mm)	1.812599 mm Node: 120045	0.582025 mm Node: 120045	(-10.838 mm, 125.921 mm, 0.097129 mm)
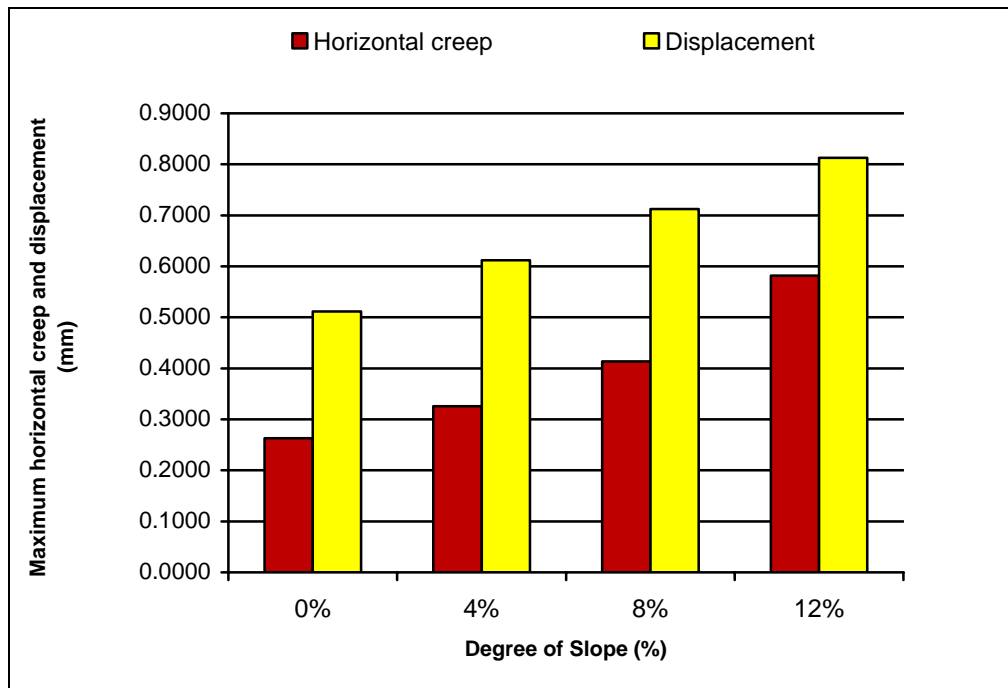
Figure 6.6 The results of displacement and horizontal creep finite element model on various slopes

6.5.2 Strain
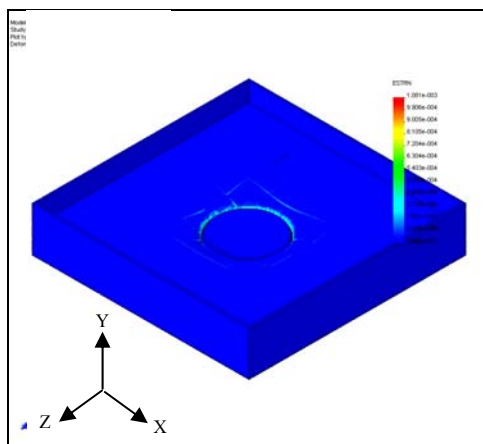
(a) Strain of CBP on Slope 0 %
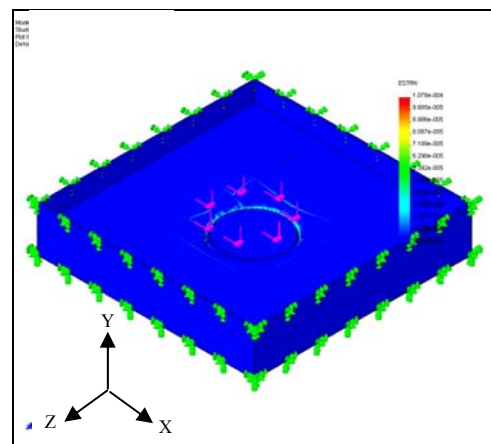
(b) Strain of CBP on Slope 4 %
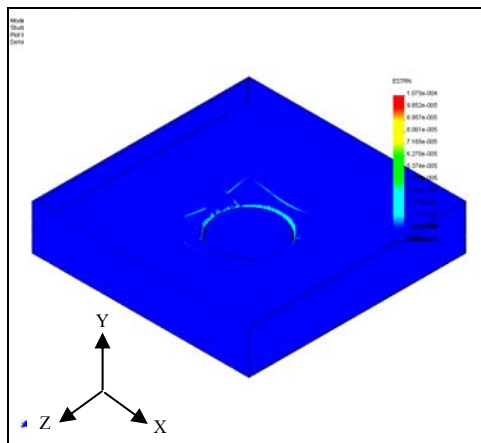
(c) Strain of CBP on Slope 8 %
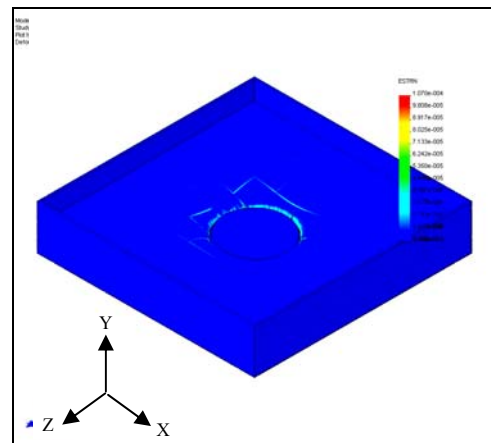
(d) Strain of CBP on Slope 12 %

Figure 6.7   Strain of CBP in the simulation (455277 nodes).

Table 6.3:   Strain results

Slope	Type	Min	Location	Max	Location
0 %	ESTRN : Equivalent strain	2.68256e-012 Element: 170547	(491.287 mm, 206.25 mm, 502.5 mm)	0.000106999 Element: 234094	(19.7308 mm, 58.4109 mm, 18.9279 mm)
4 %	ESTRN : Equivalent strain	2.85803e-012 Element: 170233	(505.515 mm, 206.429 mm, 501.985 mm)	0.00010748 Element: 234094	(19.7308 mm, 58.4109 mm, 18.9279 mm)
8 %	ESTRN : Equivalent strain	2.9816e-012 Element: 171682	(508.015 mm, 206.429 mm, 504.485 mm)	0.000107831 Element: 234094	(19.7308 mm, 58.4109 mm, 18.9279 mm)
12 %	ESTRN : Equivalent strain	4.20765e-012 Element: 170547	(491.287 mm, 206.25 mm, 502.5 mm)	0.00108064 Element: 234094	(19.7308 mm, 58.4109 mm, 18.9279 mm)
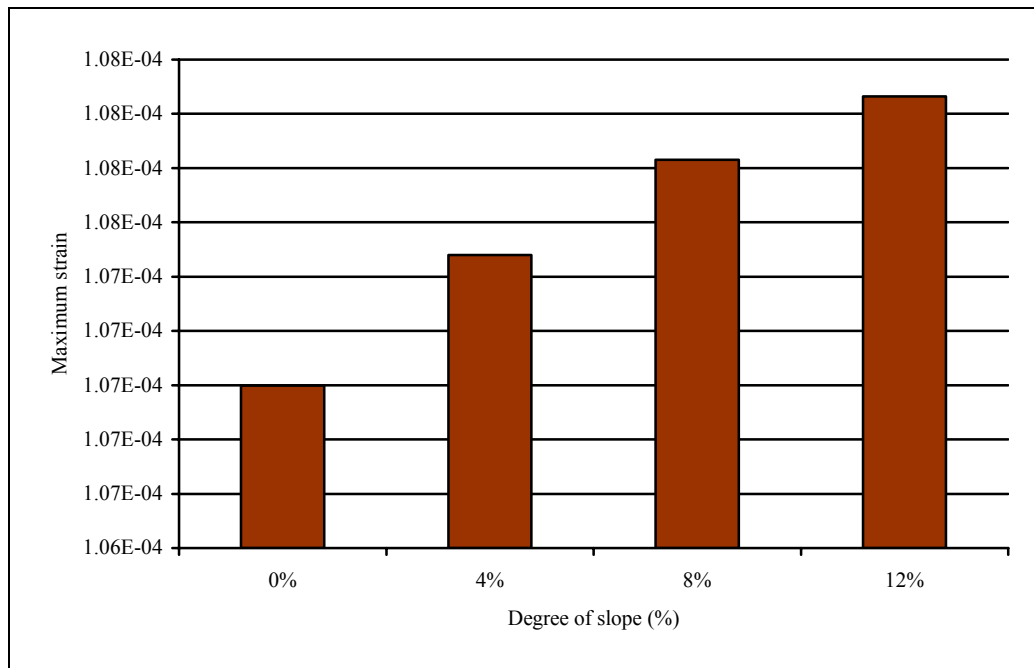
Figure 6.8   The results of strain finite element model on various slopes

6.5.3   Stress
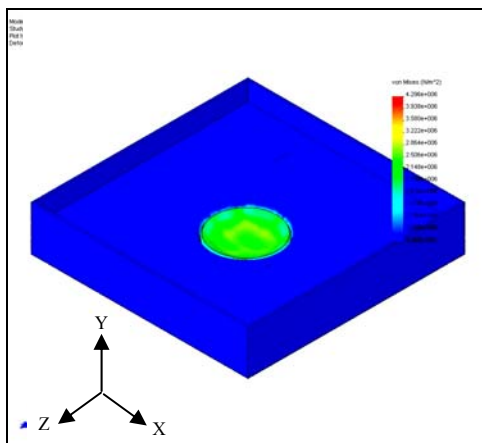
(a)   Stress of CBP on Slope 0 %   (b)   Stress of CBP on Slope 4 %
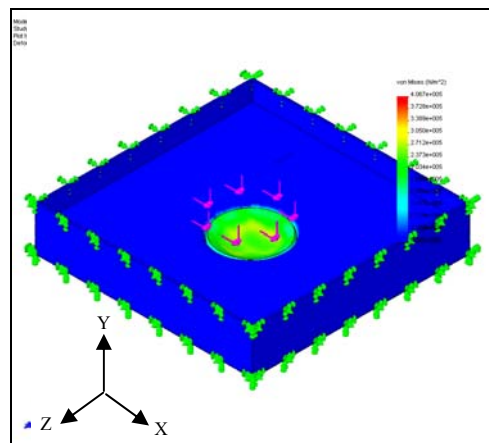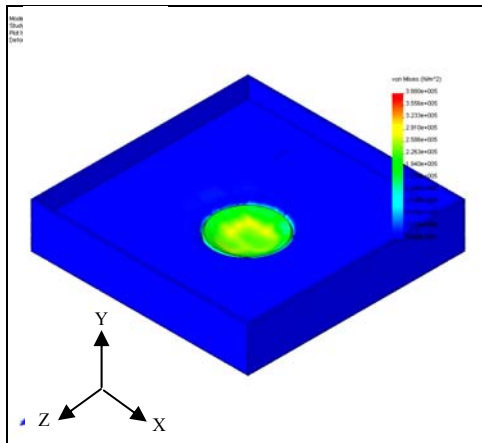
(c) Stress of CBP on Slope 8 %   (d) Stress of CBP on Slope 12 %
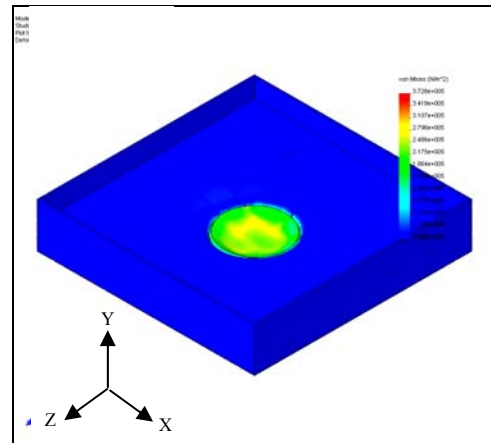
Figure 6.9   Stress of CBP in the simulation (455277 nodes).

Table 6.4:   Stress results

Slope	Type	Min	Location	Max	Location
0 %	VON: von Misses stress	0.00787986 N/m² Node: 73177	(480.545 mm, 66.6963 mm, 483.721 mm)	3.72842e+05 N/m² Node: 121523	(-96.6129 mm, 120 mm, 122.834 mm)
4 %	VON: von Misses stress	0.00680915 N/m² Node: 73177	(480.545 mm, 66.6963 mm, 483.721 mm)	3.87955e+05 N/m² Node: 121523	(-96.6129 mm, 120 mm, 122.834 mm)
8 %	VON: von Misses stress	0.0058612 N/m² Node: 73177	(480.545 mm, 66.6963 mm, 483.721 mm)	4.06725e+05 N/m² Node: 121523	(-96.6129 mm, 120 mm, 122.834 mm)
12 %	VON: von Misses stress	0.0495464 N/m² Node: 73177	(480.545 mm, 66.6963 mm, 483.721 mm)	4.29577e+05 N/m² Node: 121523	(-96.6129 mm, 120 mm, 122.834 mm)
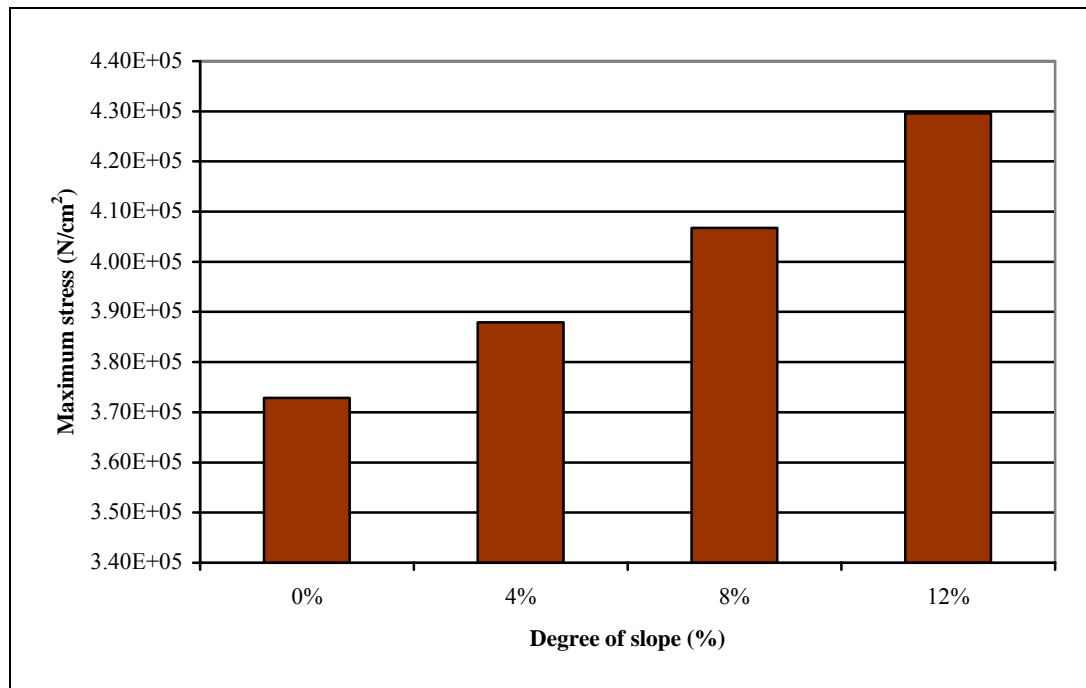
Figure 6.10   The results of strain finite element model on various slopes

6.6   Conclusions

In this study, a 3DFEM model was applied to concrete block pavements to investigate the performance behaviours of the pavements. In order to create complicated meshes in the block layer with various laying patterns, a pre-processor with a user interface was developed, which allows users to specify various features of a block pavement and generates a mesh for the pavement without time consuming data handling relating to meshing of 3DFEM. A 3DFEM solver computes deflections, stresses and strains in CBP. The results are displayed graphically on a window of a post-processor.

Using this tool, the effect of the block thickness, laying pattern, stiffness of joint and bedding sand on deflection, stress and strain in pavements were investigated. As a result, the following conclusions can be made:

a. The bending stresses in the block and base are larger in case of high joint stiffness than those of low joint stiffness. In that case, the block thickness largely affects the stresses.

b. The tensile stress in the base due to bending action is larger in the stretcher laying pattern than in the herringbone laying pattern.

c. There is very little difference in the tensile stress of the bedding sand and the compressive strain of the bedding sand between the herringbone and stretcher bond laying pattern.

CHAPTER 7

DEVELOPMENT AND PERFORMANCE OF HIGHWAY ACCELEREATED LOADING INSTRUMENT

7.1   Introduction

This chapter describes the Highway Accelerated Loading Instrument (HALI) and the test methods to investigate the deformation development of rubberized concrete paving block (RCPB) pavement under the accelerated trafficking test. An overview of the research procedure is illustrated in Figure 7.1.

The concept of HALI development, including design, fabrication, calibration and equipment performance monitoring is presented. The design of HALI mainly referred to the design of RUB-StraP carried out by Koch (1999) and NUROLF designed by Professor John Knapton (1991). Design details and operating manual of HALI is shown in Appendix A. The fabrication of the instrument was conducted by a local supplier. Calibration of loading rate, speed of the mobile carriage and tyre pressure were carried out to ensure accuracy to produce reliable result.

```
┌─────────────────────────────────────────────┐
│ Development of Highway Accelerated           │
│ Loading Instrument                           │
│ 1) Design                                    │
│ 2) Fabrication                               │
│ 3) Calibration                               │
│ 4) Equipment Performance Monitoring          │
└─────────────────────────────────────────────┘
                        │
                        ▼
┌─────────────────────────────────────────────┐
│ Investigation of Structural Performance on RCPB │
│ Pavement based on                            │
│ 1)  Longitudinal and Transverse Rutting Profiles │
│ 2)  Three-Dimensional Surface Deformation    │
│ 3)  Open Joint Width                         │
│ 4)  Skid Resistance                          │
│ 5)  Impact Resistance                        │
│ 6)  Interlocking Resistance between RCPB     │
└─────────────────────────────────────────────┘
```

Figure 7.1: Research flow chart of HALI

Prior to the accelerated trafficking test, a pavement track model was prepared. Hard neoprene with the thickness of 3 mm was fixed in the 1.7 m × 5.5 m test bed of HALI. The bedding sand with thickness of 50 mm, jointing sand and rectangular CPB with the dimension of 210 mm × 105 mm × 60 mm were prepared to form the pavement track model for accelerated testing.

Monitoring of the equipment performance was based on behavior and performance of concrete block pavement under HALI accelerated trafficking test. The constant deformation, accelerating and braking sections of the pavement was observed and determined. The test was conducted under several cycles load repetition to investigate the deformation development for the pavement track. Rut depth was determined by obtaining the relationship between distance and deformation which occurred to the pavement track. In addition, pavement deformation behaviour was investigated to determine the reliable section and the braking area.

Before RCPB products can be greatly introduced for real trafficked pavement use at sites, clearly it must possess sufficient strength to resist handling, construction and traffic stresses. Therefore it is necessary to ensure RCPB have good in-service performance. A RCPB pavement model comprised of 60 mm thick CCPB, 10-RCPB, 20-RCPB and 30-RCPB at surface layer was constructed. A series of accelerated trafficking test on the RCPB pavement was subjected to HALI. Rutting, pavement deformation and effect of joint width were evaluated before the commencement of trafficking and after 50, 100, 250, 500, 1000, 2500, 5000 and 10000 load repetitions. Additional tests, including shear resistance, skid resistance, and impact resistance were also conducted in order to compare their performances with conventional paving blocks.

7.2   Design of HALI

HALI allows a laboratory assessment to be made on the performance and behavior of pavement model during complete life cycle simulation tests. It is Universiti Teknologi Malaysia (UTM)'s first laboratory rolling load facility specifically developed for the assessment of concrete block pavement deformed by low speed traffic. The HALI was successfully setup on August 2006, at Highway laboratory, UTM (see Figure 7.2).
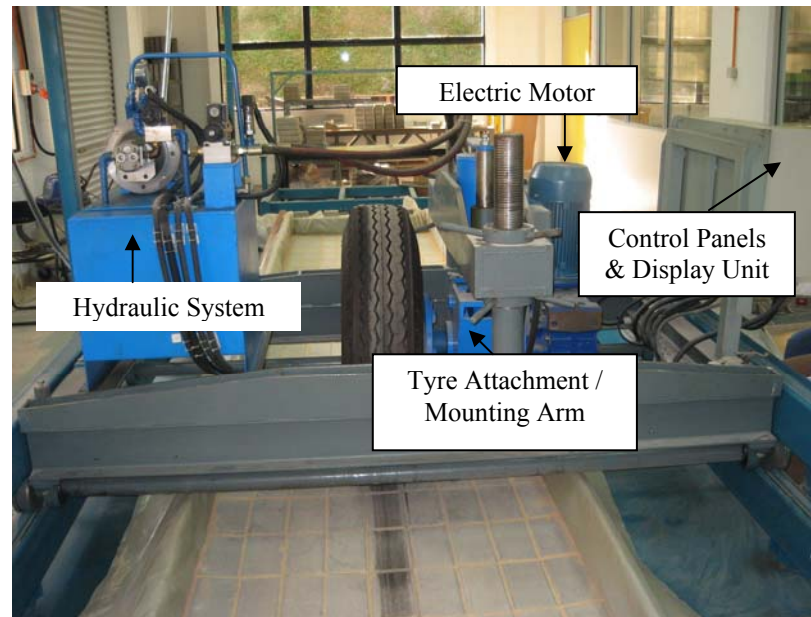
Figure 7.2   Highway Accelerated Loading Instrument

The mild steel test bed with a dimension of 1.7 m x 5.5 m x 0.25 m was designed to ensure that a full-scale life cycle assessment of the paving materials could be achieved. The examination of a pavement's durability is permitted since the design allows the evaluation of different base and surface materials. HALI consist of several components which are attached to the base frame. The loading mechanism is applied to the pavement by a mobile carriage. The mobile carriage which is mounted on two rigid and frictionless guide rails, enables loading to be moved forward and back along the rail. The mobile carriage consists of the following essential components:

(i)   Tyre attachment / mounting arm
        A standard radial inflatable tyre (for 10 ton heavy vehicle) is mounted on the mounting arm. It is equipped with heavy-duty hydraulic jacks to enable the mounting arm to be swung or locked. This design allows for a sufficient clearance during removal of sample tray. Rigid and effective contact between tyre and test pavement materials can be achieved by adopting the locking devices.

(ii)   Electric motor

3-phase power with maximum capacity of 5 HP is used to drive the mobile carriage, enabling it to move back and forth along the guide rail. Motor is a heavy-duty type that enables it to run the instrument continuously for at least 24 hours.

(iii)   Hydraulic system

It is used to generate a constant and continuous load from 0 to 40 kN. This hydraulic system is equipped with valves and sensors to ensure generation of constant pre-selected load level throughout the test duration. A closed-circuit system which consists of hydraulic reservoir, related valves and heavy-duty hydraulic piping and fitting is used to provide the hydraulic pressure for the loading mechanism and tyre attachment arm.

(iv)   Control panels and display unit

The control panel can be programmed to provide different levels of speed (range from 0 to 1.2 m/s) and varying the load that applied to the test bed. The display unit is also included in the control panel to exhibit the applied load and test duration, and a mechanism switch for selecting and setting the required test repetitions (up to 20,000 cycles) and duration.

7.3 Calibration of HALI

Before starting the accelerated trafficking test, the HALI was calibrated to the actual value of operation. Calibration which was made on the loading applied to wheel, speed of the mobile carriage and tyre pressure.

7.3.1 Loading Applied to Wheel

The actual loading applied to the wheel was checked with the design wheel load that is programmed in the control panel. Load cell was used to measure the impose load applied from the wheel. The load cell was positioned centrally at the bottom of the wheel and was connected to a data logger. When the wheel load applied to the load cell, it received the loading and then transformed the data into a data logger in order to save and display the value.

Several set points were made to calibrate the loading on the wheel. Data received by the load cell was compared to the value of set point. The calibration works was carried out and the actual loading from the wheel was identified. Figure 7.3 shows the equipment used to calibrate the loading instrument.

Figure 7.3   Load cell and data logger

7.3.2   Speed of Mobile Carriage

The actual speed of mobile carriage was determined by obtaining the time of a complete cycle and dividing with the length of pavement track.

7.3.3   Tyre Pressure

The tyre pressure used in the experiment was 600 kPa. The tyre pressure was checked before the commencement for an accelerated trafficking test.

7.3.4   Results and Discussions of HALI Performance Monitoring

7.3.4.1 Transverse Rutting Profiles

Figure 7.4 shows the results of transverse rutting profiles of the wheel track loaded with the standard wide single tyre. The results are the mean values of 18 adjacent transverse profiles. As expected, rutting mainly occurred under the wheel path. It is clearly seen that not only the rut depth increased with the increasing number of load repetitions, but also the heaves at both sides of the wheel track. The total mean rut depth in the wheel path after 2500 load repetitions of 1000 kg load magnitude is approximately 9.09 mm. An interesting observation obtained is that the right side heave level of the wheel path is higher than the left side heave level. There is a difference of 5.92 mm between the right heave level and the left heave level after 2500 cycles of load repetitions.

This difference of heaves level at both sides is believed to be due to the single side of load application from the instrument. The load applied to the tyre is generated from the hydraulic jack, located at the right hand side of the tyre. Therefore, during loading, the load distribution of the tyre concentrates more on the right hand side of the wheel path. As a result, the heave level at the right side is higher.

Figure 7.4 The development of the transverse deformation profiles for different load repetitions

7.3.4.2 Mean Rut Depth in the Wheel Path

Figure 7.5 shows the graph of mean rut depth in the wheel path of the test pavement at different load repetitions. It is seen that the pavement deflection increases in a nonlinear manner when the load repetition cycles keeps increasing. It

is also noticed that the rate of deflection decreases when the load repetitions keep increasing.

During loading, additional compaction of sand under CPB occurs, and some part of the energy is lost in that way. After a certain number of repetitions, the compaction of the underlying layers reaches its full extent and no energy is lost during additional loadings. As a result, the deflection and recovery become the same. Thus, it is established that concrete block pavements stiffen progressively with an increase in the number of load repetitions.
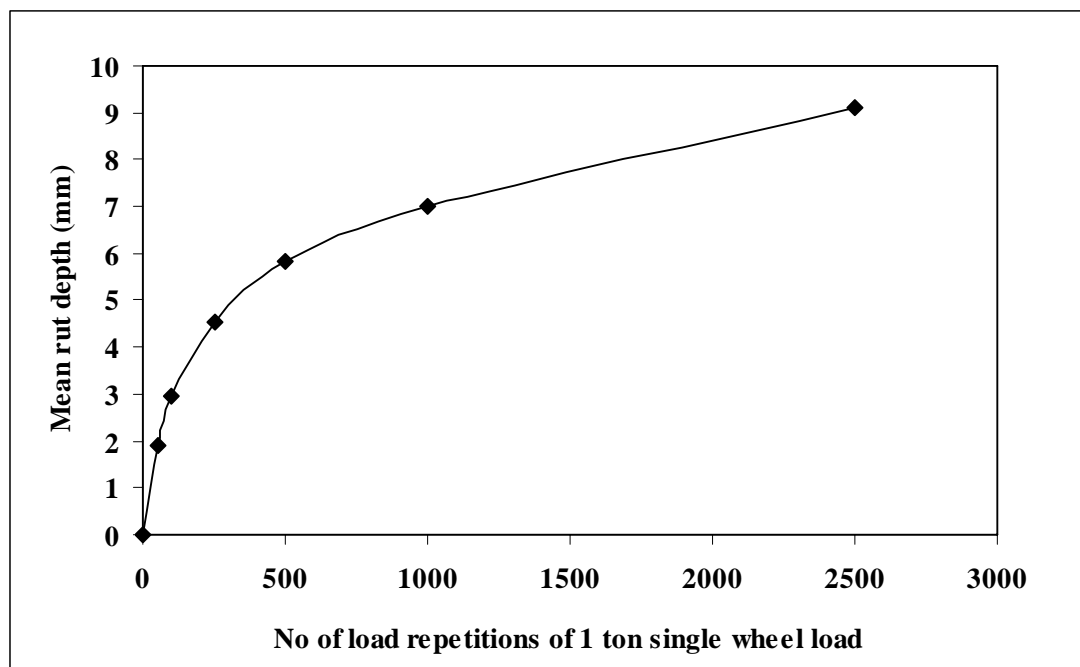
Figure 7.5   Mean rut depth of test pavement up to 2500 load repetitions

7.3.4.3 Longitudinal Rut Depth for Various Load Repetitions

Figure 7.6 shows the typical longitudinal view of rut depth for different load repetitions. The rut depths are taken from the central wheel path along the test pavement. It is seen that the front part and the end part of the pavement track have a greater deflection than the middle section. For the front part section, rutting is subjected to increase significantly until the 3rd cross section of the test pavement track with a distance of 440 mm. After that, the rutting remains constant at the middle section of the pavement track. The constant rutting distance of the test pavement section is approximately 2420 mm, starting from the 3rd cross section to the 14th cross section of the test pavement.
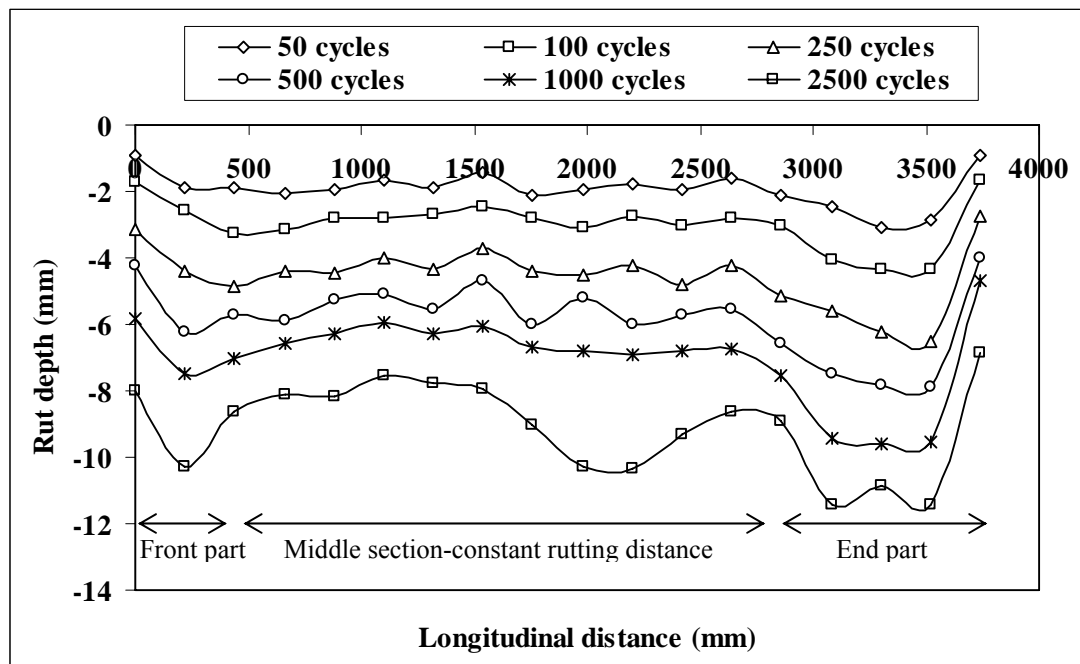
Figure 7.6   Typical longitudinal view of rut depth for various load repetitions

Then, the rutting begins to increase until the 17th cross section before it decreases at the last cross section. It is noticed that this section of rutting magnitude is greater than the rutting magnitude occurred at the front part of the pavement track. This significant increase in rut depth resulted from the loading application from the

instrument when it started to move forward along the pavement track. The front part and end part of the pavement section is considered as the accelerating and decelerating part. The length of the front part is about 440 mm, while for the end part of the pavement it has a length of 880 mm.

7.3.4.4 Three-Dimensional View of Deformed Pavement

A three-dimensional view of the deformed surface is obtained from using the SURFER computer program. These three-dimensional view graphs are plotted in order to investigate the development of deformation on pavement after having undertaken various load repetitions. Figures 7.7 and 7.8 are the three-dimensional view of deformed pavement for 50 and 2500 load repetitions, respectively. A comparison was made between these two three-dimensional views of deformed pavement.

From the Figures 7.7 and 7.8, it is clearly observed that shoving occurs at the right hand side of the wheel path. The shoving begins to increase after 200 cm from the origin of measurement point. Compared to deformation after 50 load repetitions, deformation that occurs on the pavement after 2500 load repetitions is more critical. The deformations became excessive and substantial rotations and heaving of the individual CPB occurred.
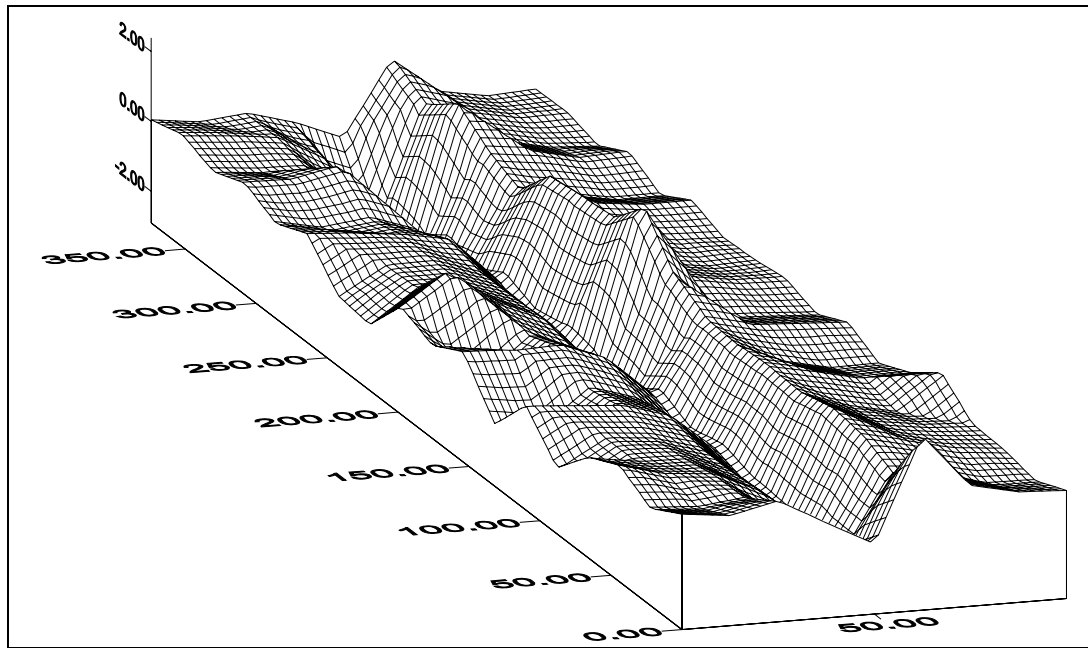
Figure 7.7   Three-dimensional view of deformed pavement after 50 load repetitions
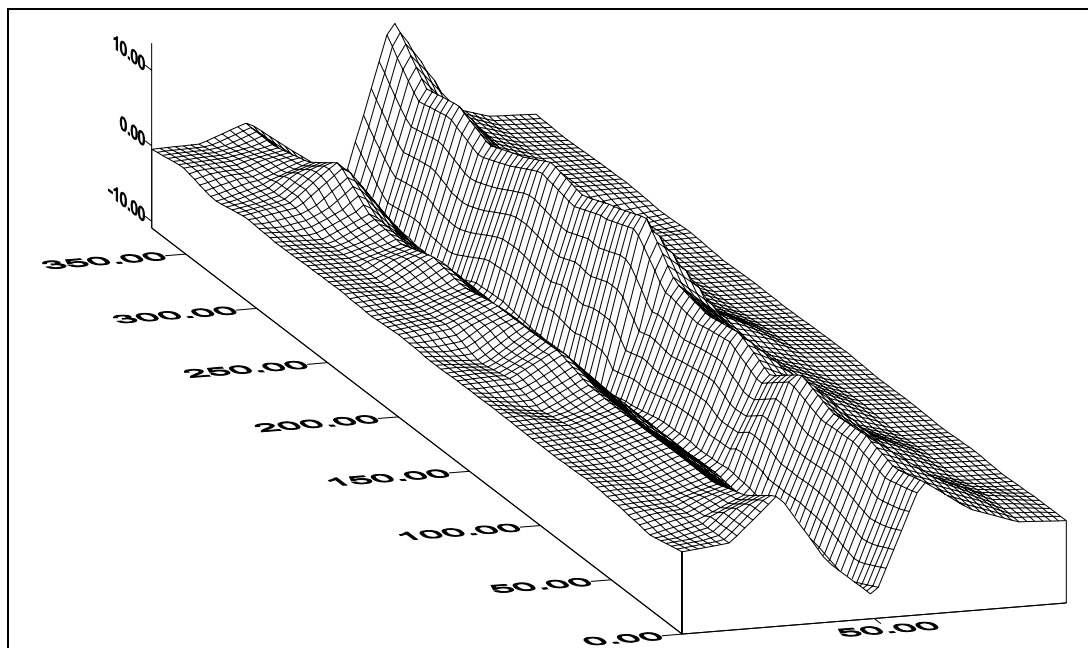
Figure 7.8   Three-dimensional view of deformed pavement after 2500 load repetitions

7.3.4.5 Joint Width

Table 7.1 shows the mean joint width at both sides of the wheel path for various load repetitions. From the data, it is clearly seen that the mean joint width for panel A and panel D increases with the increments of the load repetitions. Meanwhile, the mean joint width for panels B and C decreases significantly when the load repetitions keep increasing. These two sections finally decrease to 0 mm when two CPB nearby are stuck together adjacently and no joint width is exposed. Figure 7.9 shows the location of the joint width panel of A, B, C and D.

Table 7.1: Mean joint width for various load repetitions

No of load cycles	Mean joint width (mm)			
	Panel A	Panel B	Panel C	Panel D
0	5.00	5.00	5.00	5.00
50	5.72	4.44	3.38	6.60
100	5.99	4.07	0.78	8.16
250	6.47	3.41	0.07	9.37
500	6.55	2.53	0.12	9.60
1000	7.04	1.29	0.00	10.94
2500	7.52	0.00	0.00	12.54
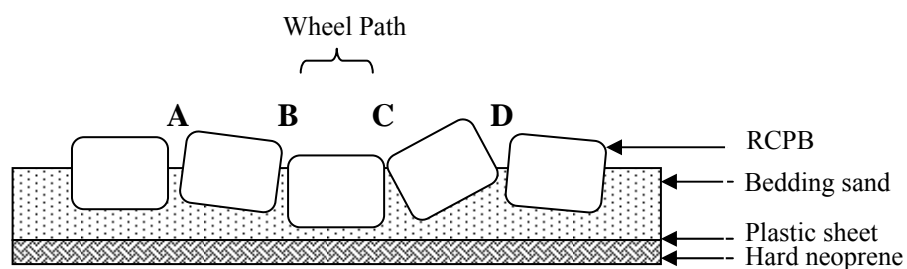
Figure 7.9   Joint width at panel A, B, C and D of the transverse deformation profile

7.3.5   Summary

The principal summary that can be drawn based on the test results provided in this study is as follows:

➢ The concrete block pavement exhibited progressive stiffening with the increase in the number of load repetitions.

➢ The magnitude of the heave at the right hand side is higher if compared to the heave at the left hand side of the wheel path.

➢ The constant deformation length of concrete block pavement has been determined at about 2.42 m of length at the middle section of the test pavement.

➢ The accelerating and braking area of the pavement has been determined at about 0.44 m at the front part and 0.88 m at the end part sections of the test pavement.

7.4   Structural Performance of RCPB Pavement

The RCPB used in this section are manufactured to dry compressive strength ranging between 23 MPa and 64 MPa (measured at the time of testing). The RCPB pavement was subjected to 10000 cycles of load repetition under a full size single truck wheel via a tyre inflated to 600 kPa. Nine measuring times of pavement deformation development and joint width were made at various stages of the trafficking. Skid resistances of the entire RCPB surface are monitored prior to and after trafficking by a British pendulum tester. Additional tests, including, pull-out test is then carried out in order to compare their shear resistance characteristic by extracting the RCPB from the pavement. The falling weight is used to assess the impact resistance.

7.4.1 Results and Discussions of RCPB Pavement

7.4.1.1 Transverse Rutting Profiles

Figure 7.10 shows the results of transverse rutting/cross section profiles of the wheel track loaded with the standard wide single tyre. This figure was obtained from the results of test pavement of 50 and 10000 load repetitions. Each of the results shown is the mean of 3 cross section transverse profiles. As expected, most of the rutting occurred under the wheel path. It is clearly seen that not only the rut depth increases with the increasing number of load repetitions, but also the heaves at each sides of the wheel track. The total mean rut depth in the wheel path after 50 and 10000 load repetitions of 1000 kg load magnitude is approximately 2.0 mm and 14.5 mm, respectively. An interesting observation obtained is that the right side heave level of the wheel path is higher than the left side heave level. There is a difference of 9.53 mm between the right heave level and the left heave level after 10000 cycles of load repetitions.
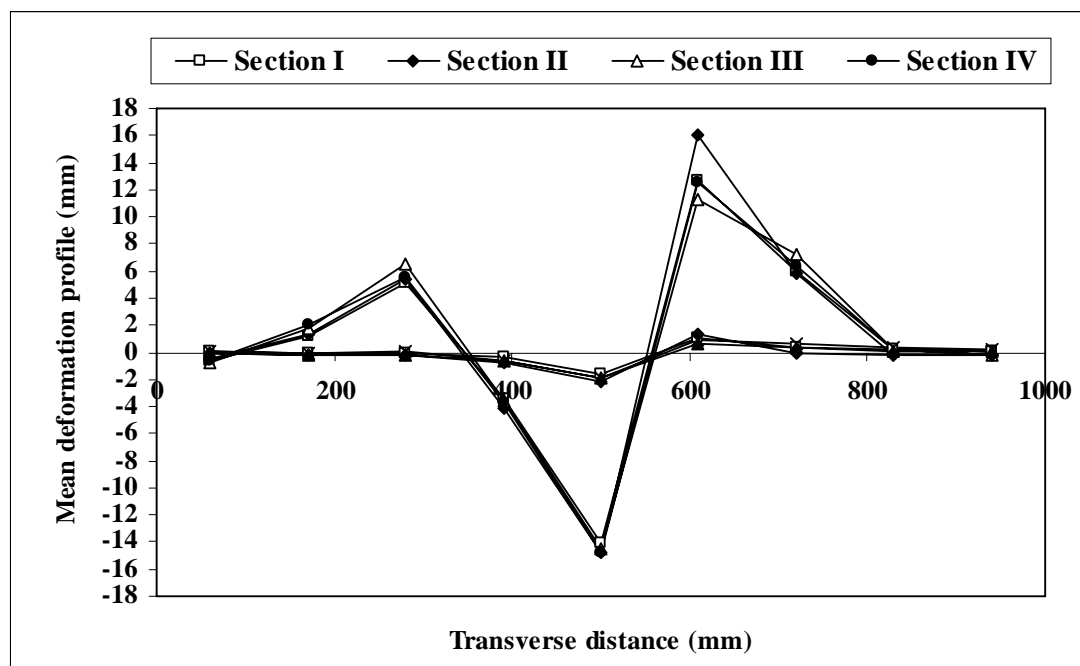
Figure 7.10   Transverse rutting profiles after 50 and 10000 load repetitions

This difference of heaves level at both sides is believed to be caused by the off-centered load distribution from the wheel. Therefore during trafficking test; the load distribution of the wheel concentrates more on the right hand side of the wheel path. As a result, the heave level at the right side is higher.
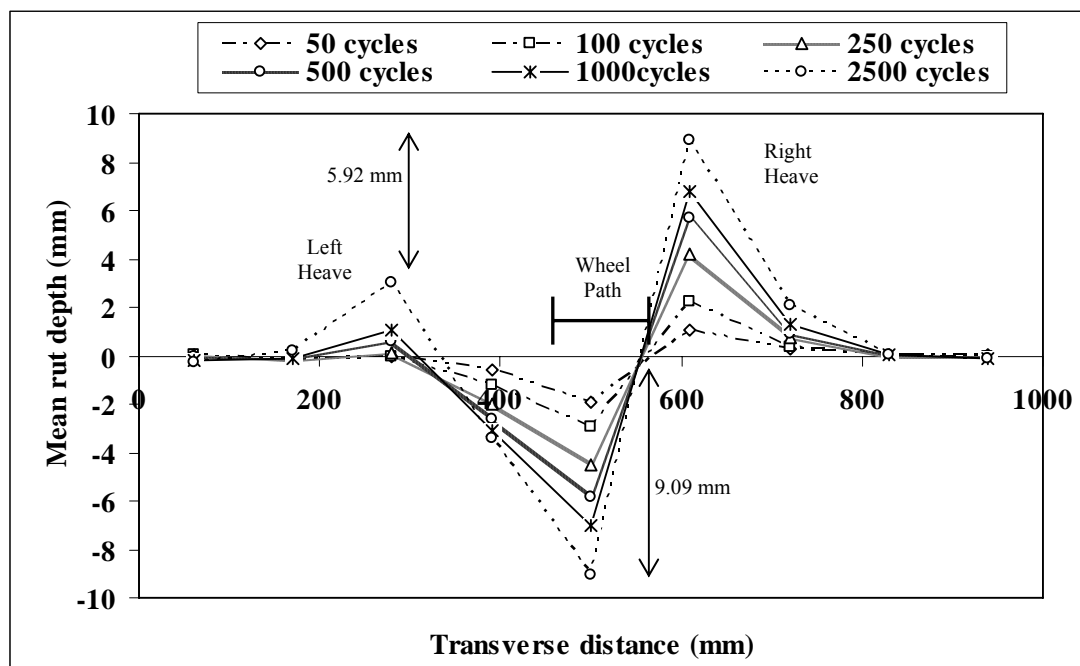
7.4.1.2 Mean Rut Depth in the Wheel Path

Figure 7.11 shows a composite graph of mean rut depth in the wheel path of the four test sections from the initial reading to the final reading at 10000 load repetitions. The trend shows that the pavement deflection increases in a nonlinear manner when the load repetition cycles keep increasing. It is also noticed that the rate of deflection decreases when the load repetitions keep increasing.
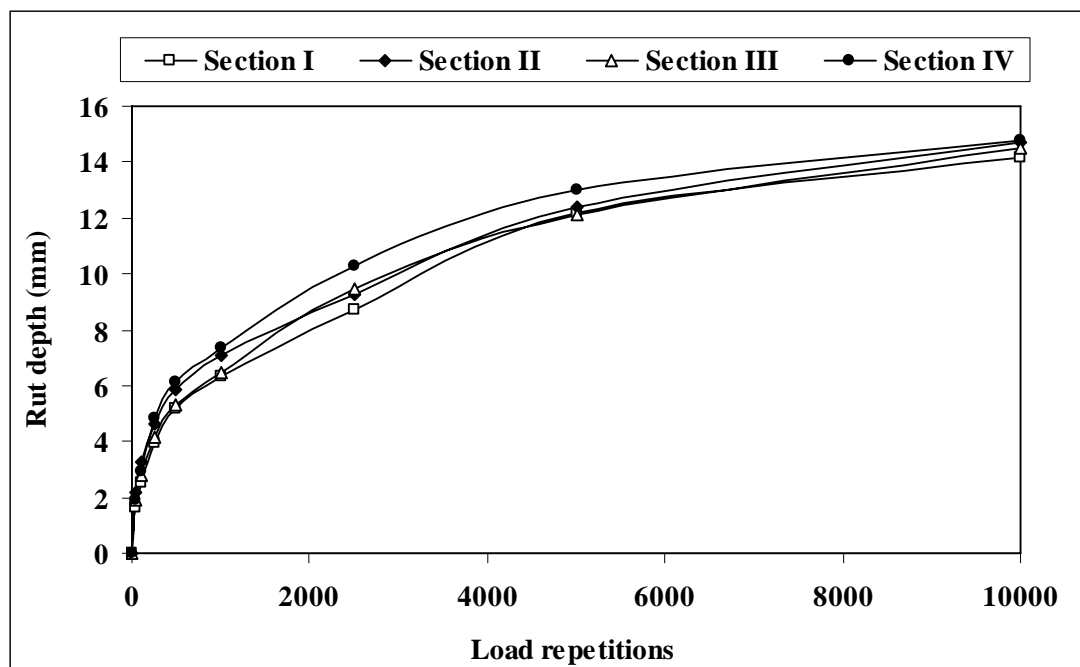
Figure 7.11   Mean rut depth of four test sections up to 10000 load repetitions

From the figure, it is observed that the test bed had "settled-in" after 10000 load repetitions during which the rate of rut depth formation was relatively rapid. The rate of increase of rut depth with load repetitions was substantially reduced. Differences in settling-in deflections are shown in the results given in the figure. Practically, the pavement would be trafficked over a greater width, and settlement would not generally be limited to a narrow section.

The deflections from all the test sections are almost the same; despite Section I which is slightly better in rut resistance than other test sections RCPB pavement. Comparing Section II, III and IV, results are similar, irrespective of the percentage of crumb rubber content mixed in RCPB.

7.4.1.3 Longitudinal Rut Depth

Figure 7.12 shows the typical longitudinal view of rut depth at different load repetitions. The longitudinal rut depths are taken from the central wheel path along the RCPB pavement. It is seen that the test Section IV of the pavement track has a greater deflection than the other test sections. At Section IV, rutting is subjected to increase significantly at the last three cross sections of the pavement track with a distance of 660 mm. Other than that, the rutting remains constant at Section I, II and III of the pavement track. The constant rutting distance of the pavement section is approximately 1980 mm, which started from the 1st cross section to the 9th cross section of the RCPB pavement.

The principal conclusion that can be drawn based on the results show in transverse rutting profiles is that there is an insignificant difference of rut depth for four test sections within the limit of the test (10000 load repetitions under single wheel load of 1000 kg).
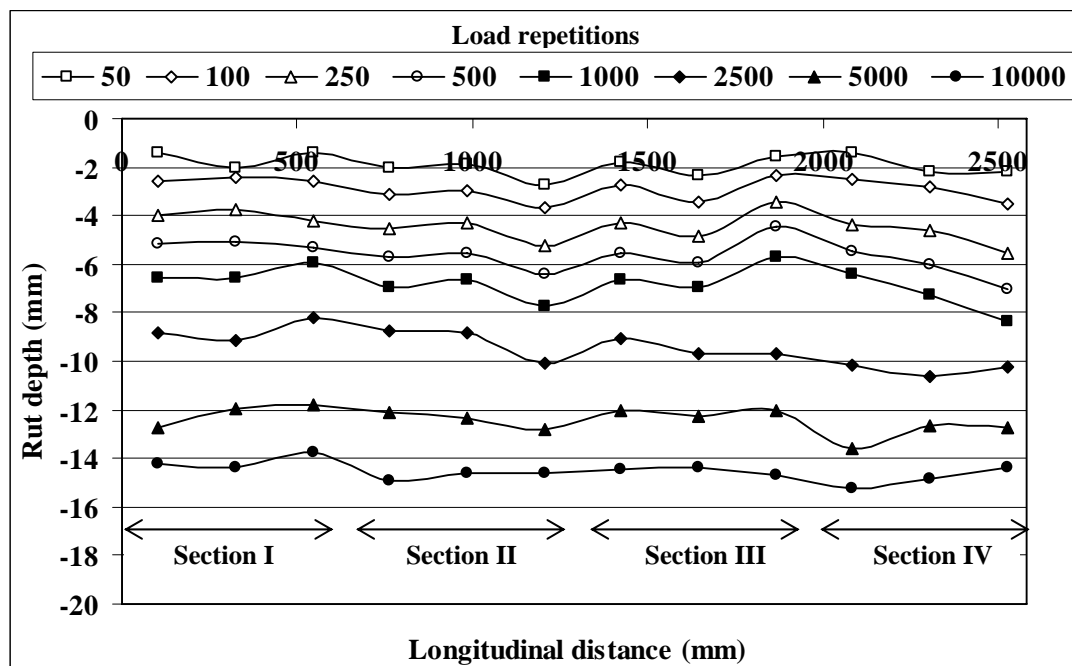
Figure 7.12   Typical longitudinal view of rut depth after various load repetitions

These findings are in agreement with the earlier researches (Shackel 1979, Shackel 1980, Rollongs 1982, Panda and Ghosh 2002) which have concluded that the compressive strength of the paving units has little influence on the response of RCPB pavements subjected to traffic due to their small size subjected to compressive stress with negligible bending stress. It is also noticed that, the elastic modulus of the entire RCPB layer (surface layer) is much higher than that of underlying materials. The RCPB behave as rigid bodies in the pavement and transfer the external load by virtue of its geometrical characteristics, rather than its strength, to the adjacent RCPB and underlying layers. It is established that load-associated performance of RCPB pavements is independent of the compressive strengths of the RCPB considered in this study (compressive strengths range from 23 MPa to 64 MPa).

However, these findings should not be interpreted to mean that compressive strength is unimportant because high concrete strength is often needed to ensure adequate ability to sustain traffic loading.

7.4.1.4 Three-Dimensional View of Deformed RCPB Pavement

A three-dimensional view of the deformed surface is obtained from using the SURFER computer program. These three-dimensional view graphs were plotted to investigate the development of deformation after having undertaken various load repetitions.

From Figures 7.13 and 7.14, compared to deformation after 50 load repetitions, deformation and shoving that occurs on the pavement after 10000 load repetitions is more critical.
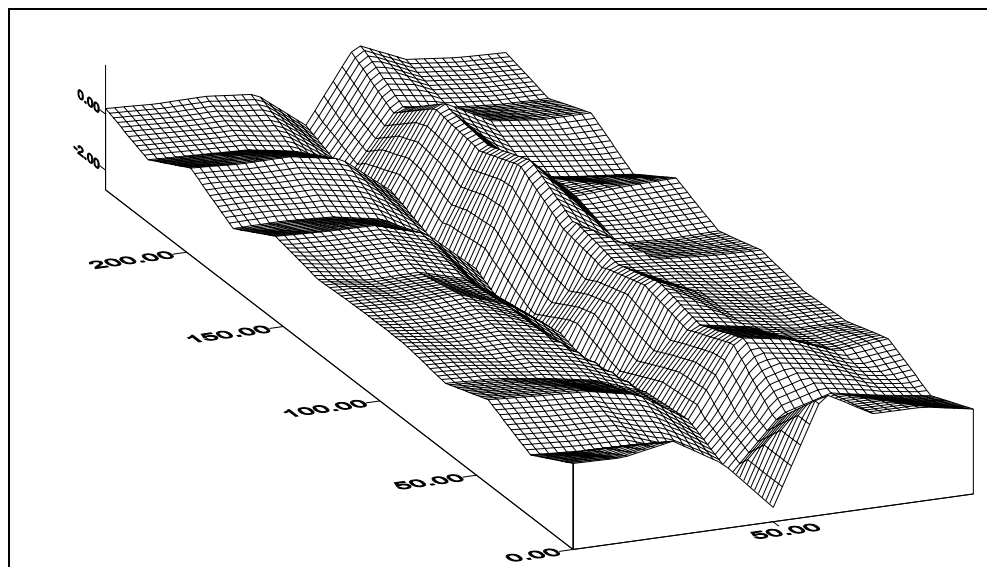
Figure 7.13   Three-dimensional view of four sections deformed RCPB pavement after 50 load repetitions
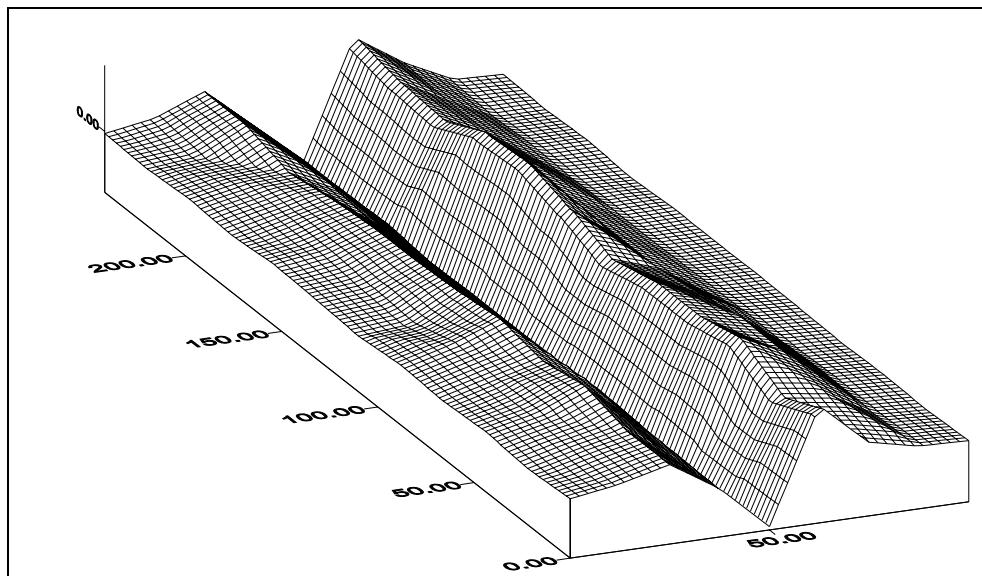
Figure 7.14   Three-dimensional view of four sections deformed RCPB pavement after 10000 load repetitions

It was observed that heaving occurred in the whole cross sections homogenously instead of the individual RCPB. This point was to the similarity of four test sections of RCPB in transferring the external load to the adjacent RCPB. Figure 7.13 reveals a ridge running along the length of the RCPB pavement surfaces, which is due to deformation after 50 load repetitions. The ridge becomes more pronounced after load repetitions achieved 10000 (see Figure 7.14). However, Figure 7.13 shows a rougher pavement surface compared with Figure 7.14 due to bigger scale in Z axis.

A comparison was made on the three-dimensional profile and contour views of deformed pavement between these four test sections in Figures 7.15a, 7.15b, 7.15c and 7.15d. Maximum and minimum permanent deformation achieved under the test wheel of 10000 load repetitions for Section I, II, III and IV were (14.11, -13.50), (16.87, -14.08), (12.09,-13.67) and (14.54, -14.39), respectively.
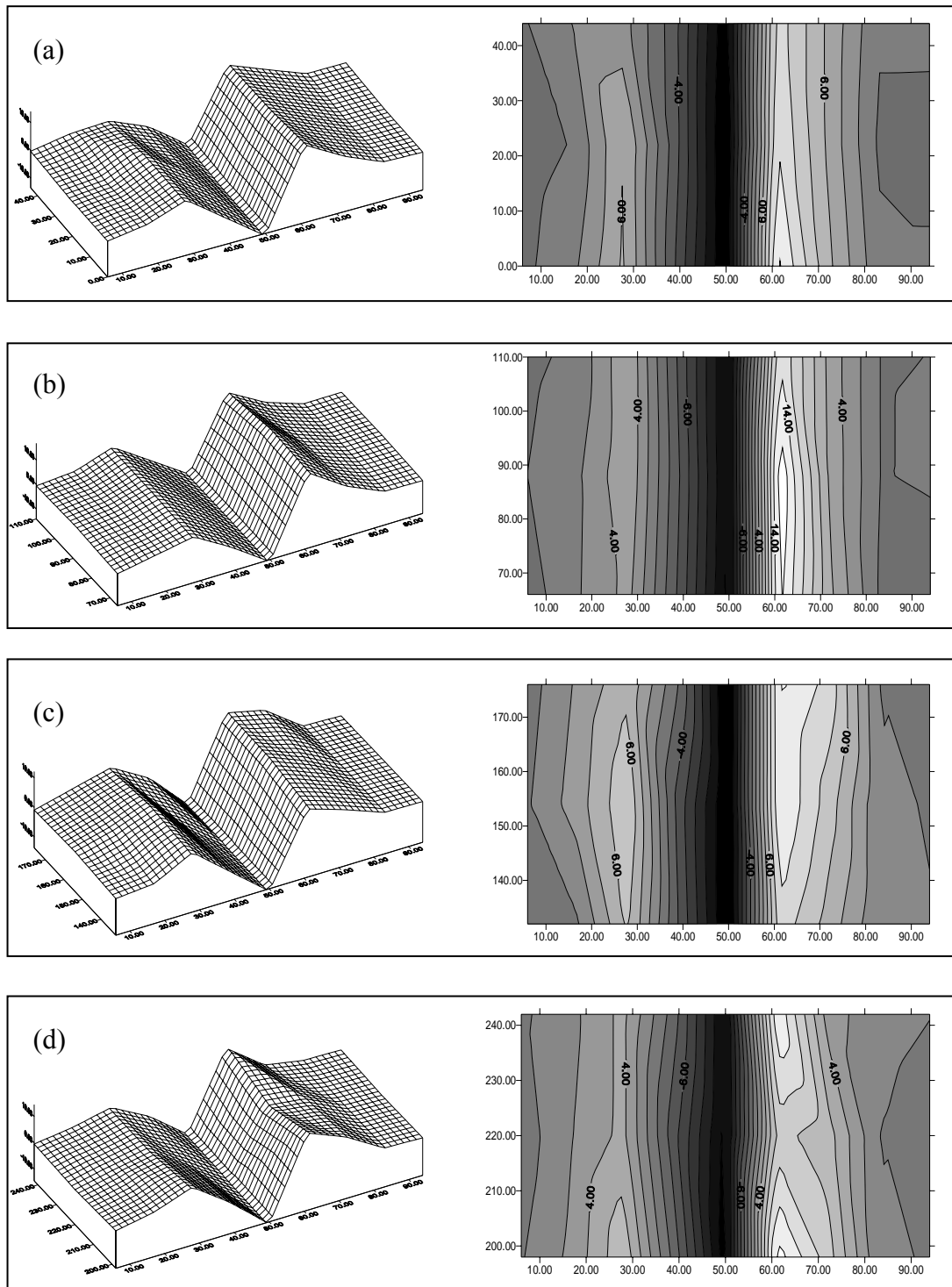
Figure 7.15   Three-dimensional profile and contour view of single section
deformed pavement after 10000 load repetitions (a) Section I (b)
Section II (c) Section III (d) Section IV

The results show that all the test sections have slightly different levels of developed deformation with Section I having performed best and the others having developed greater deformations. The "non-trafficked RCPB" on both sides of the wheel track were significantly influenced by the excessive deformation in the wheel paths when load repetition achieved 10000 at all four sections.

7.4.1.5 Joint Width

Figure 7.16 shows the mean joint width at both sides of the wheel path for various load repetitions. From the data, it is clearly seen that similar results were obtained for all test sections. The mean joint width for panel A and panel D increases with the increments of the load repetitions. Meanwhile, the mean joint width for panel B and C decreases significantly when the load repetitions keep increasing. The panel B and C finally decrease to 0 mm when two RCPB nearby were stuck together adjacently and no joint width was exposed when the load repetitions reached 2500 and 500, respectively. Joint widths that were too narrow at these panels can be precursors to edge chipping or interlock damage.

It was also observed that joint width was too wide at panel D due to the loss of jointing sand in the joint spacing. Thus, the degree of shear resistance (or shear transfer) between RCPB was significantly reduced.
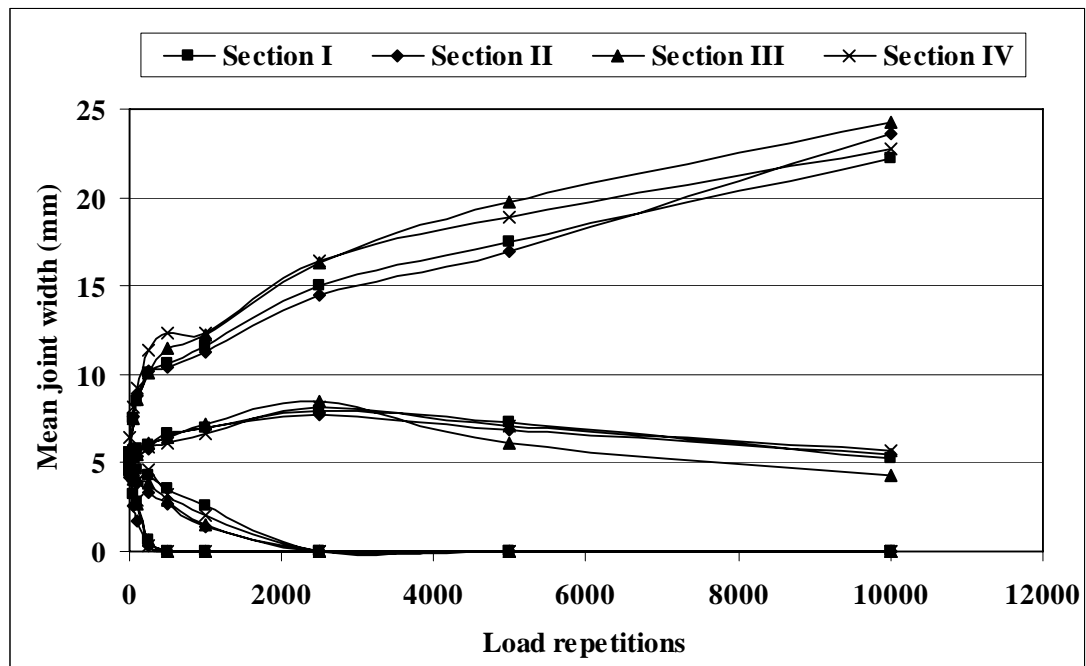
Figure 7.16   Mean joint width at various load repetitions

7.4.1.6 Shear Resistance

Two unit of RCPB at each test sections were selected (refer to Figure 5.12) for pull-out test. Two 12 mm diameter holes spaced at 125 mm and along its centerline were drilled to a depth of 40 mm and installed during the construction of RCPB pavement. Once the trafficking test was completed, 12 mm diameter masonry anchors were installed into the drilled holes for pull-out test.

Figure 7.17 shows the relationship between pull-out force and displacement over CCPB, 10-RCPB, 20-RCPB and 30-RCPB. Typically, when extracted, CCPB display a linear load/displacement relationship until the load attains approximately 1.07 kN at a displacement of 3.2 mm. While, for 10-RCPB, 20-RCPB and 30-RCPB, sudden reduction in force occurred before the 2.0 mm displacement. At that force, it is noticed that a slip occurred as interlock is lost. The RCPB rotate and then

grip its adjacent RCPB so that they continue to sustain pull-out force until eventually the RCPB are fully extracted out. In the case of the 10-RCPB, initial slip occurred at loads of 0.59 kN. The 20-RCPB lost interlock at 0.81 kN and the 30-RCPB lost interlock at 0.68 kN. Therefore, only CCPB met the minimum acceptable extraction force proposed by Clifford (1984) of 1 kN.
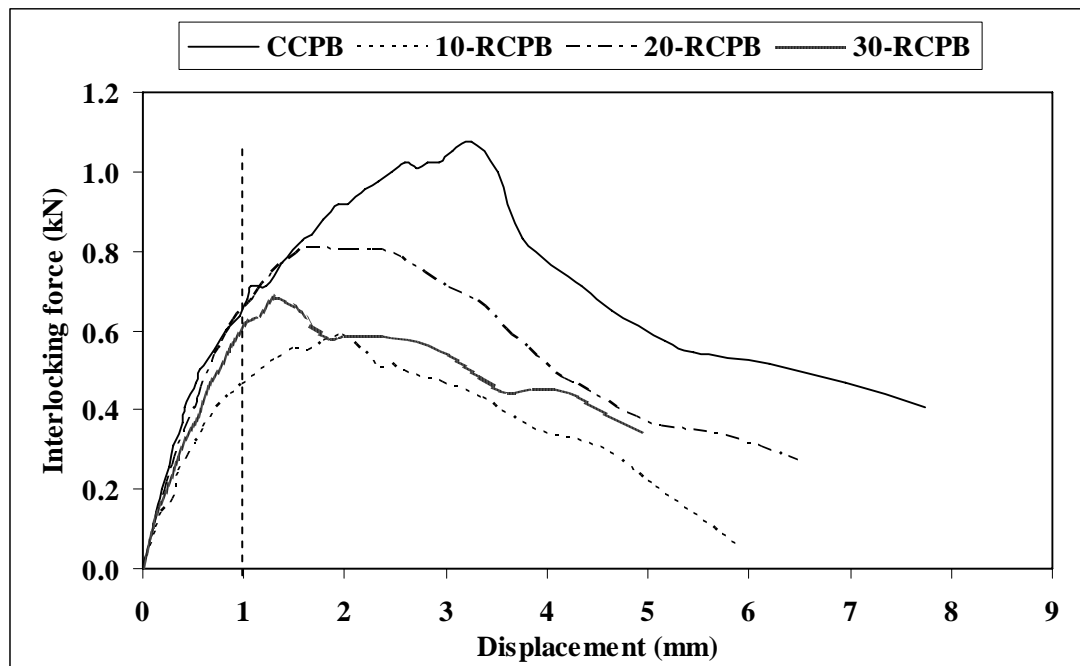
Figure 7.17   Relationship between pull-out force and displacement

The maximum pull-out force is often referred to by others but it is not the critical value. It is of less interest than the relationship between pull-out force and displacement at low levels of displacement that occurs at working displacement. This is considered to be a more relevant figure since it is the displacement at which initial loss of interlock occurred and is closer to the surface elastic displacements in a highway or heavy duty pavement.

Thus, comparison was made for the pull-out force in kN at a displacement of 1.0 mm. As shown in the figure, sustained force of the CCPB, 10-RCPB, 20-RCPB and 30-RCPB at a displacement of 1.0 mm were 0.68, 0.47, 0.65 and 0.61 kN,

respectively.   10-RCPB showed the lower shear resistance, reflecting weaker interlocking among the others. One of the reasons may be caused by the higher rut depth and shoving occurred in that particular sections which may influence the function of joint to provide a good shear resistance.

In general, the low pull-out force gained in this study may be due to wide (5 mm) joint width installed in this study. It can be clarified that shear strength of the joint depends largely upon width and the average particle size of jointing sand rather than strength of the RCPB.

7.4.1.7 Skid Resistance

The results presented in Figure 7.18 shows a systematic reduction in skid resistance with the increase in rubber content from 0% (CCPB) to 30% (30-RCPB). Overall, all types of RCPB showed similar reduction in the BPN after 10000 cycles of load repetitions.
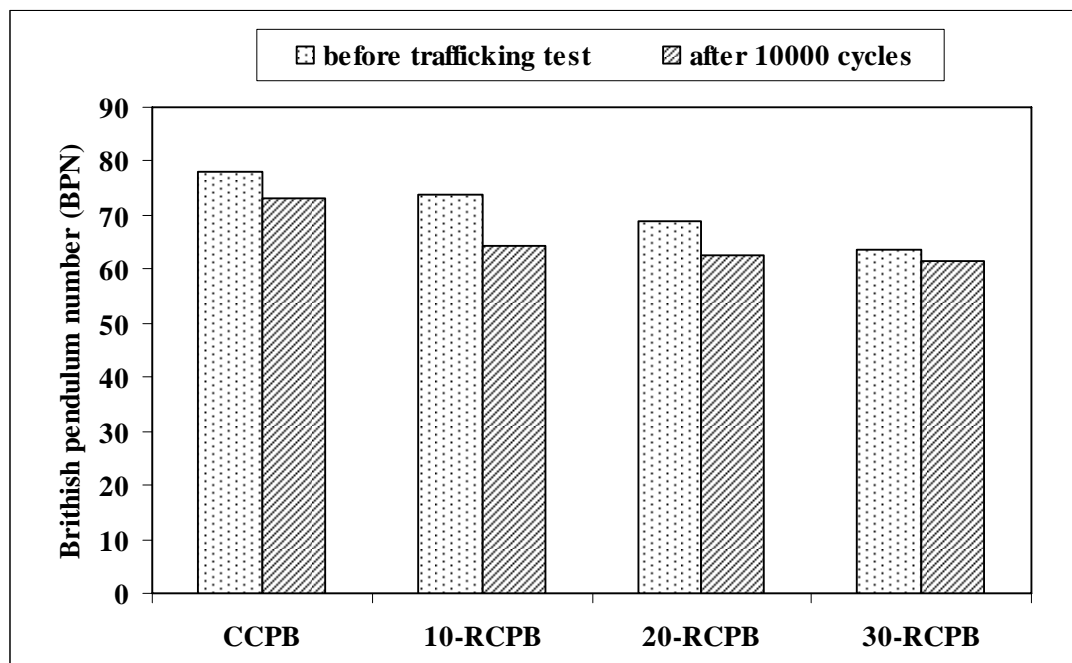
Figure 7.18   Skid resistance before trafficking test and after 10000 load repetitions
of trafficking test

From the figure it is clearly shown that all the values met the minimum requirement in accordance to ASTM requirement. The BPN of CCPB approached 73, whilst the other types did not exceed 65 after 10000 cycles of load repetitions. The high values on the RCPB at the end of the testing were encouraging from the point of view that no deterioration but only a little polishing of the RCPB surface had occurred for 20-RCPB and 30-RCPB. However, there was no damage caused to any of the RCPB units even at the end of the trafficking test.

It is found that skid resistance is slightly higher for low percentages of crumb rubber in RCPB. It might be contributed by the rough surface texture of the RCPB that creates more friction as the pendulum passed across it.

7.4.1.8 Impact Resistance

Table 7.2 shows the number of drops for causing damage by means of falling weight test on a set of RCPB. The initial height of drop for the loading was set at 50 cm for this test. However, after the 5th drop, 30-RCPB suffered hairline crack only. The height was then increased to 100 cm, and the loading was dropped. Examination of the 20-RCPB and 30-RCPB showed that both only suffered small cracking at the 7th and 9th drop, respectively. After the 13th and 15th drop, a number of cracks occurred at all directions. However, CCPB and 10-RCPB had the first cracking at the 1st and 2nd drop, respectively. After the 3rd and 8th drop, the CCPB and 10-RCPB were broken completely. This means that the rubber-filled concrete paving blocks have a significant capability in absorbing dynamic load and in resisting crack propagation.

Table 7.2   Number of drops for causing damage on a set of RCPB

Degree of damage	Small crack		Transverse crack		All directions crack		Completely broken	
Sample	S1	S2	S1	S2	S1	S2	S1	S2
CCPB	1	2	2	3	-	-	3	4
10-RCPB	3	3	6	5	-	-	10	8
20-RCPB	7	7	-	-	13	12	13	12
30-RCPB	9	10	-	-	15	16	15	16

The failure patterns of the CCPB, 10-RCPB, 20-RCPB and 30-RCPB under the impact test are shown in Figure 7.19. A comparison of the failure patterns of CCPB and 10-RCPB showed transverse crack and failed breaking into two pieces after a few number of shocks. As the volume of rubber was increased to 20% and 30% for 20-RCPB and 30-RCPB, the number of cracks happened in all directions instead of transverse and the size of the failure zone was found to increase on RCPB surface, but, maintained the integrity of the broken pieces. From the figure, it is observed that the energy absorption by rubber-filled concrete paving blocks (exhibit a higher displacement at failure mode as rubber content increases) is much larger than that by the conventional concrete paving blocks.
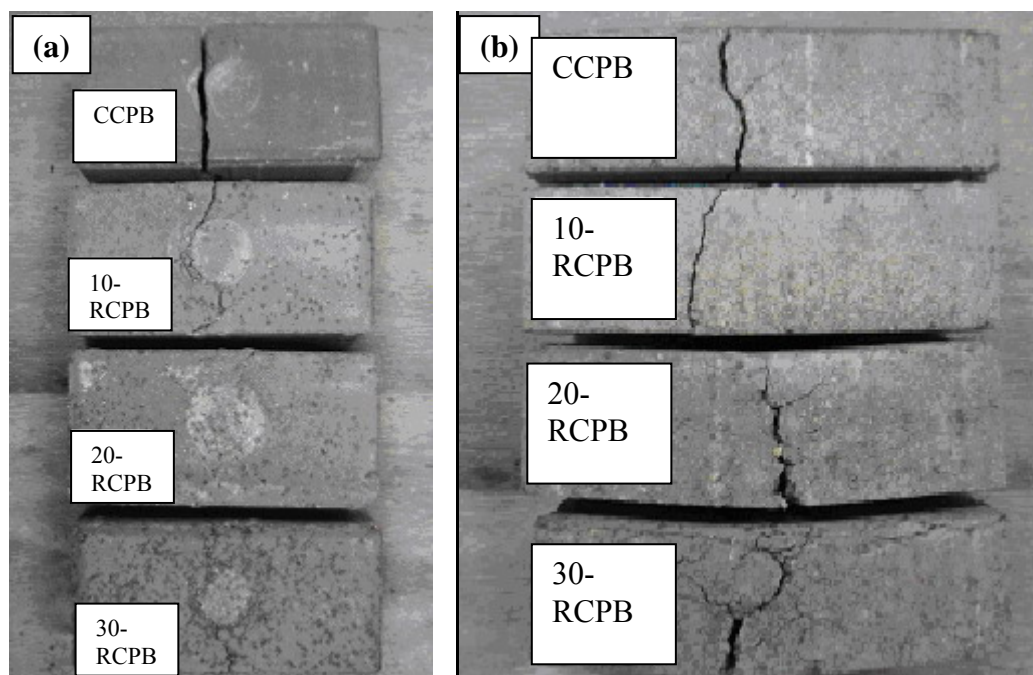
Figure 7.19   Failure patterns of CCPB and RCPB (a) plan view (b) side view

7.4.2   Summary

In order to investigate the performance of RCPB pavements, four types of test sections RCPB pavement have been subjected to accelerated trafficking test and other additional tests.   The conclusions that can be drawn based on the results presented in this project are as follows:

➢   In general, Section I tends to yield better level of performance in rut resistance, regardless of transverse rut depth profile, mean rut depth and longitudinal rut depth than other test sections.   The RCPB perform as rigid bodies in the pavement which show that load-associated performance of the RCPB pavements is independent due to its geometrical characteristics.

➤ It must be noted that the deformation is a result of sub-layer consolidation and densification since the RCPB themselves are not affected significantly by the loading in terms of compressibility. Distress in bedding sand was caused by lateral movement, loss into voids in lower layer due to compaction and densification, thus it caused the deformations to become excessive and substantial rotations. Visual observations indicated heaving occurred in the whole cross sections instead of the individual RCPB. This points at the similarity of the four test sections in transferring the external load to adjacent RCPB.

➤ Joints have opened out as a result of substantial movement of the RCPB after 10000 of loading repetitions. The open joint width results from the entire panel A, B, C, and D were similar, irrespective of whole cross sections. However, the mean joint width for panel A and panel D increases whilst panel B and C decreases significantly with the increments of the load repetitions.

➤ Comparison was made for the pull-out force in kN at a displacement of 1.0 mm of CCPB, 10-RCPB, 20-RCPB and 30-RCPB. 10-RCPB showed the lower shear resistance, reflecting weaker interlocking among the others. One of the reasons may be it is caused by the higher rut depth and shoving occurred in that particular cross section and influence the function of joint to provide a good shear resistance.

➤ Skid resistance results obtained showed a systematic reduction in BPN with the increase in rubber content. At the end of the trafficking test, all types of RCPB showed similar reduction in BPN. However, the values met the minimum requirement in accordance to ASTM requirement. The only observation after trafficking was that no deterioration but only a little polishing of the rubber particles happened in 20-RCPB and 30-RCPB surface.

➤ The falling weight test results have shown that the rubber-filled concrete paving blocks have a significant improvement in toughness, energy absorption and more flexibility than control concrete paving blocks. Comparing the types of the RCPB, 20-RCPB and 30-RCPB perform better than CCPB and 10-RCPB. It was observed that extra forces was needed to fully open the high rubber-filled RCPB because they maintained the integrity of the broken pieces even after numbers of falling weight drops.

➢ Based on the unique characteristics of four types of RCPB, the RCPB can be categorized as high strength and low toughness (CCPB); high strength and moderate toughness (10-RCPB); low strength and high toughness (20-RCPB and 30-RCPB). Therefore, all types of RCPB tested in this study can be introduced to various types of pavement according to their pavement traffic volume and application.

Overall, the rut and deformation tests results represented in three-dimensional models showed CCPB tend to yield slightly better than other types of RCPB. Despite better skid resistance and interlocking force of CCPB, the other types of RCPB containing crumb rubber showed a great improvement in toughness. Thus, all the developed RCPB studied in this project has great potential to be used according to traffic volume and type of applications.

CHAPTER 8

DISUCUSSIONS OF RESULTS

8.1   Introduction

Concrete block pavement (CBP) differs from other forms of pavement in that the wearing surface is made from small paving units bedded and jointed in sand rather than continuous paving. The principal components of a typical block pavement have been illustrated in the Chapter 2, as concrete block, jointing sand, bedding sand, road base, sub-base and sub-grade. In concrete block pavement (CBP), the blocks are a major load-spreading component. The blocks are available in a variety of shapes (as rectangular shape, uni-pave shape, etc). CBP is installed in a number of patterns, such as stretcher bond, herringbone 90°, herringbone 45°, etc. This research presented three dimensional finite element models (3DFEM) to compare the results from one of tests conducted in the laboratory as mentioned in Chapter 6.

8.2   The Behaviour of CBP under Horizontal Force

A block pavement may present various types of mechanical behaviour when submitted to a horizontal force, depending on the blocks shape, as well as on joint width between blocks, the laying pattern and on the direction of the horizontal force relatively to the laying pattern.

The experiments described that the horizontal force test with rectangular block shape and stretcher laying pattern, which is parallel to the continuing lines of the joints, shows that the cohesion of such a plate is near to zero whatever the restraining of the edges. Indeed, for a relatively low value of the applied force, the line of loaded blocks moves monolithically, the friction forces which are the only ones capable of reacting on the continuous lines being too weak to perform this role.

As described, the horizontal force test in herringbone 90° or 45° laying pattern shows that the blocks contribute as a whole to the cohesion of the pavement, the blocks being successively locked by their rotation following their horizontal creep. The herringbone 45° laying pattern provides better interlock than herringbone 90° and stretcher bond. The results obtained are similar to that established by (Shackel 1993, Knapton 1976; Clark 1978; Miura *et al.* 1984).

| Herringbone 90° bond | Herringbone 45° bond |
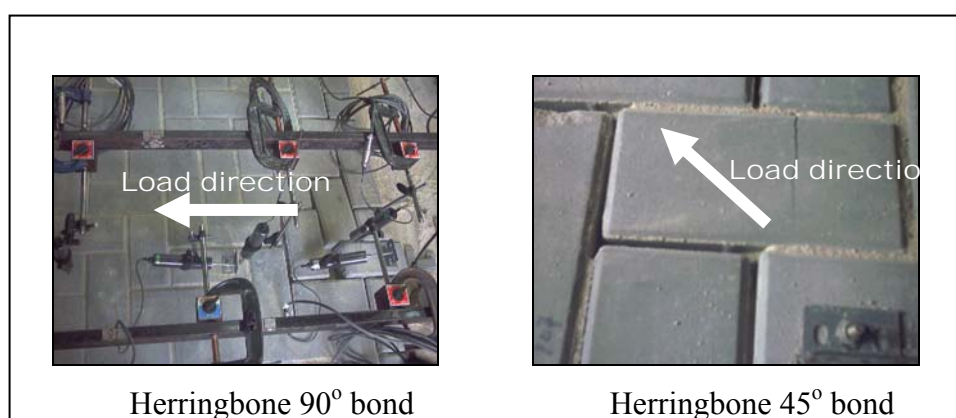
Figure 8.1   The herringbone laying pattern being successively interlock on horizontal creep.

For concrete block pavement with interlocking blocks, in which the horizontal force is parallel to the continuous joint lines, we observe that the joint lines contiguous to the loaded line contribute progressively to the load transfer through an interlocking effect. However this effect induces a lateral movement of the blocks, so that their action stops as soon as the clearance of the joints became too large. If the lateral movement is not possible because of an edge restraint, all the blocks at the plate contribute to the transfer of the horizontal force and the pavement cohesion is then assured.

.

8.3   Load Deflection Behaviour

An interesting observation is that the rate of deflection decreases with increasing load (within the range of magnitude of load considered in this study) rather than increases, which is the case with flexible and rigid pavements. Increase in the load, the rotation of individual blocks increases. This will lead to an increase in the translation of blocks and in turn an increase in the thrusting action between adjacent blocks at hinging points. As a result, the rate of deflection of the pavement decreases. It is established that the load-distributing ability of a concrete block surface course increases with increasing load. The results obtained are similar to that established in earlier plate load tests by Knapton (1996).

All the design procedures to be discussed depend upon interlock being achieved within the blocks. Interlock can be defined as the inability of a block to move in isolation from its neighbours. Three types of interlock must be achieved by adequate design and construction.

8.3.1   Vertical Interlock

If a vertical load were applied to a block without vertical interlock, that block would slide down vertically between its neighbours, placing high vertical stress into the underlying course. Vertical interlock is achieved by vibrating the blocks into a well graded sharp sand during construction. This induces the sand particles to rise 25 mm into the gaps between the blocks. These gaps are from zero to 7 mm. The well graded sand has particles from almost zero to 2.36 mm. Therefore, in any position around the perimeter of a block, particles of sand wedge between neighbouring blocks so allowing a vertically loaded block to transfer its load to its neighbour through shear. These findings are similar to those observed by Knapton and O'Grady (1983) and contradictory to those reported by Shackel (1980). Knapton and O'Grady (1983) have found coarse sand to be suitable for use in joints. Shackel (1980) had observed an improvement in pavement performance using finer sand in joints.

8.3.2   Rotational Interlock

A vertical load applied asymmetrically to a block tries to rotate that block. In order for an individual block to rotate, it must displace its neighbours laterally. Therefore, if the neighbouring blocks are prevented from moving laterally by edge restraint, an individual block is prevented from rotating and rotational interlock is achieved. Evidence also exists to support the theory that fine round sand brushed into the surface also helps to induce rotational interlock.

For the test pavement without edge restraint, block rotation and translation occurred under loading. Deflections were measured on the top face (at two of its opposite edges) of one block to assess the rotations of block. The block was situated adjacent to the edge restraint in the middle row.

For the test pavement with edge restraint, rotation and translation of blocks are limited to the point that was impractical to measure. Block rotations are generally associated with following mechanisms of shear stress in the joints between loaded block and adjacent blocks causes rotation of adjacent blocks. The vertical load covering partially on a block tries to rotate that block. The blocks are rotated themselves to acquire the deflected shape of underlying layers.

8.3.3   Horizontal Interlock

The phenomenon of creep was observed in preview research, particularly when rectangular blocks were laid in stretcher bond laying pattern with their longer axis transverse to the principal direction of traffic. Horizontal braking and accelerating force move blocks along the line of the road and eventually the blocks impart high local tensile stress into the next row. This phenomenon can be eliminated by using a shaped block or by using a rectangular block laid in a herringbone laying pattern. Although creep can not be totally eliminated at severe braking location, its effect can be reduced to a level whereby breakage is eliminated and there is no visual consequence.

The horizontal expansion is prevented by edge restraint. As a result, the block translation will lead to compression of the jointing sand and thus to buildup of the joint stresses. These joint stresses prevent the blocks from undergoing excessive relative rotations and translations and transmit part of the load to adjacent blocks. The block layer assumes a final form as shown in Figure 8.2 above. A number of blocks participate through hinging points to share the external load. Thus, the deflection of pavement is less for the pavement with edge restraint.
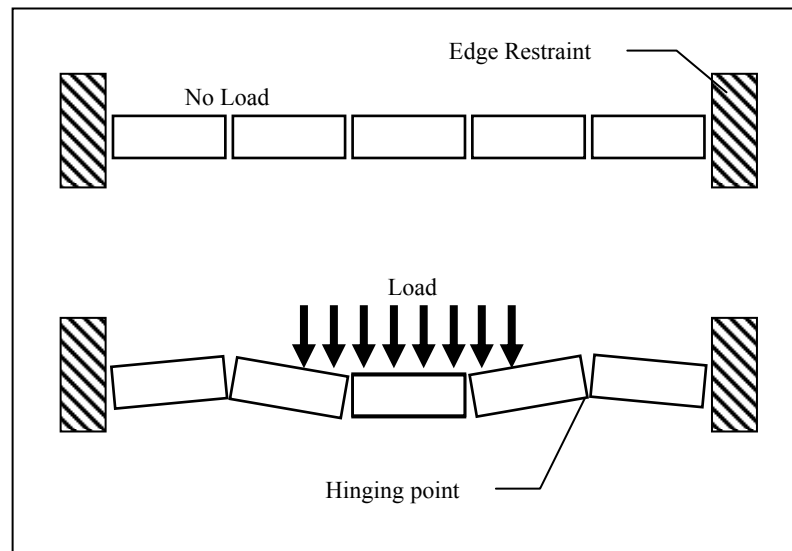
Figure 8. 2   Deflected shape of pavement with edge restraint

8.4   The Behaviour of CBP on Sloping Road Section

The construction of roads on steep slopes poses particularly interesting challenges for road engineers. The horizontal (inclined) forces exerted on the road surface are severely increased due to traffic accelerating (uphill), braking (downhill) or turning. These horizontal forces cause distress in most conventional pavements, resulting in rutting and poor riding quality. Experience has shown that concrete block pavement (CBP) performs well under such severe conditions. Although CBP performs well on steep slopes, there are certain considerations that must be taken into account during the design and construction of the pavement: The construction of concrete block pavement (CBP) on sloping road section that influences of degree of slope, laying pattern, blocks shape, blocks thickness, joint width between blocks, bedding sand thickness to define the spacing of anchor beam.

8.4.1   The Effect of Bedding Sand Thickness

The most commonly specified thickness for the bedding sand thickness has been 50 mm after compaction. A result, the bedding sand thickness was a major contributor to restraint the rutting. Thus, after compaction, the layer thickness will be 30 to 40 mm. The tolerance on the sub-base surface level is 15 ± mm. where better tolerances are achieved the thickness may be reduced to 20 mm but in no circumstances is to be less than 15 mm thick.

Knapton (1996) have reported that, in a block pavement subjected to truck traffic, a significant proportion of the initial deformation occurred in the bedding sand layer which had a compacted thickness of 40 mm. similar results have been reported by Shackel (1990). These investigations tend to confirm the findings of the earlier Australian study which demonstrated that a reduction in the loose thickness of the bedding sand from 50 mm to 30 mm was beneficial to the deformation (rutting) behaviour of block pavements. Here an almost fourfold reduction in deformation was observed. Experience gained in more than twenty five heavy vehicle simulator (HVS) traffic tests of prototype block pavements in South Africa has confirmed that there is no necessity to employ bedding sand thickness greater than 30 mm in the loose (initial) condition which yields a compacted typically close to 20 mm.

The role of the laying course or bedding sand has been discussed, a number of main functions are: to fill the lower part of the joint spaces between adjacent blocks in order to develop interlock, to provide uniform support for the blocks and to avoid stress concentrations which could cause damage to the blocks, to provide an even surface on which to lay the blocks, to accommodate the manufacturing tolerances in block thickness and to accommodate accepted tolerances in sub-base surface level. The effect of bedding sand thickness on sloping road section is very important, as shown in Figure 8.3.
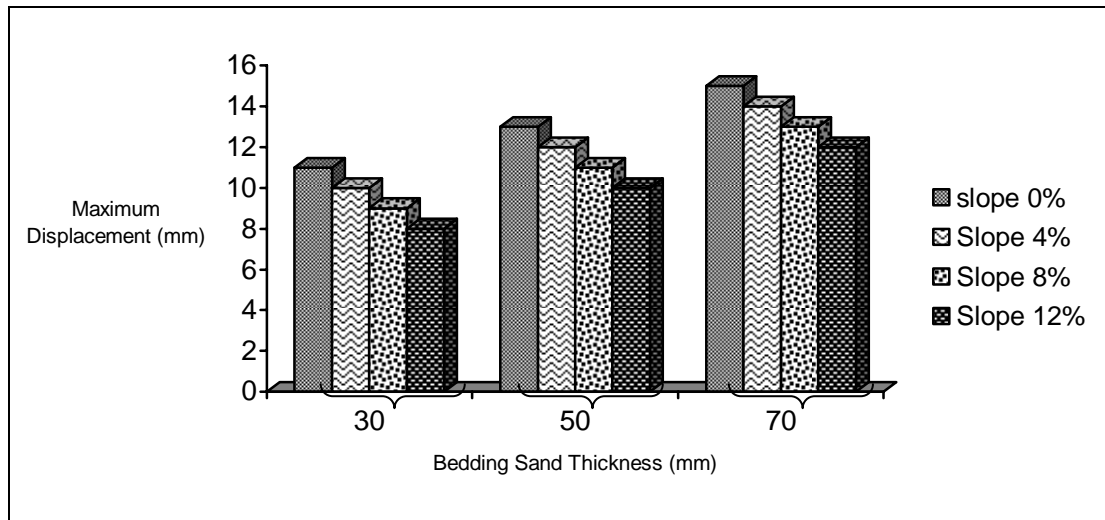
Figure 8.3   Relationship between bedding sand thickness with maximum displacement

8.4.2   The Effect of Block Thickness

Rectangular blocks of the same plan dimension with 60 mm and 100 mm different thickness were selected for testing. Blocks were laid in a stretcher bond laying pattern for each test. The shapes of the load deflection paths are similar for all block thicknesses. A change in thickness from 60 to 100 mm significantly reduces the elastic deflection of pavement. Thicker blocks provide a higher frictional area. Thus, load transfer will be high for thicker blocks. For thicker blocks, the individual block translation is more with the same amount of block rotation. As a result, the back thrust from edge restraint will be more. The thrusting action between adjacent blocks at hinging points is more effective with thicker blocks. Thus, deflections are much less for thicker blocks. The combined effect of higher friction area and higher thrusting action for thicker blocks provides more efficient load transfer. Thus, there is a significant change in deflection values from increasing the thickness of blocks. It is concluded that the response of the pavement is highly influenced by block thickness. The results obtained are similar to that found in earlier plate load tests by Shackel *et al.*(1993).

8.4.3   The Effect of Joint Width

The width of joints in block paving is more important than that perhaps been realized in the past. A serious disadvantage of pavements laid in this way is that joints of less than 2 mm in width often contain little of no jointing sand. This would obviously reduce the contribution of individual blocks to the structural properties of the pavement. Width use the individual blocks move is relation to one another which results in spelling of the edges. Although this is not structurally damaging, the overall appearance of the pavement is less desirable and the small piece of broken corners could cause problems if not swept away.

Blocks laid to a poor standard were seen where joint widths of more than 5 mm were common. The amount of sand required to fill the joints was too great to allow intimacy between blocks forming the joint to develop. The shear strength of the jointing sand would be the limiting factor in the structure of the pavement. The increase of joint width between blocks and degree of slope, decrease the friction resistant between blocks. Thus, the result is an increase of the displacement.

The optimum joint width between blocks is 3 mm. For joint widths less than the optimum, the jointing sand was unable to enter inside between blocks. A large amount of sand remained outside the joint showing sand heaps on the block surface.

8.4.4   The Effect of Block Shape

Two shapes of blocks were selected for study. These were rectangular shape and uni-pave shape. These block types have the same thickness and nearly same plan area. Blocks were laid in stretcher bond for push-in test and laid in stretcher bond,

herringbone 90° and herringbone 45° for horizontal force test. The smallest deflections are observed for rectangular shape and uni-pave shape, whereas the highest deflections are associated with uni-pave block shape. In general, uni-pave shaped (dents) blocks exhibited smaller deformations as compared with rectangular and square blocks. Complex shape blocks have larger vertical surface areas than rectangular or square blocks of the same plan area. Consequently, shaped blocks have larger frictional areas for load transfer to adjacent blocks. The friction area for uni-pave block shape is more than rectangular shape. It is concluded that the shape of the block influences the performance of the block pavement under load. It is postulated that the effectiveness of load transfer depends on the vertical surface area of the blocks. These results obtained are consistent with those found in earlier plate load tests by Shackel *et al.* (1993).

8.4.5   The Effect of Laying Pattern

Rectangular and uni-pave blocks shapes were tested in the horizontal force test. Each CBP sample tested in three laying patterns i.e. stretcher bond, herringbone 90° bond and herringbone 45° bond (Figure 2.5). The results show that horizontal creep is highest in stretcher laying pattern, almost 40 % more than laid in herringbone 90° and 45 – 50 % more than laid in herringbone 45°. (See Figure 8.4)
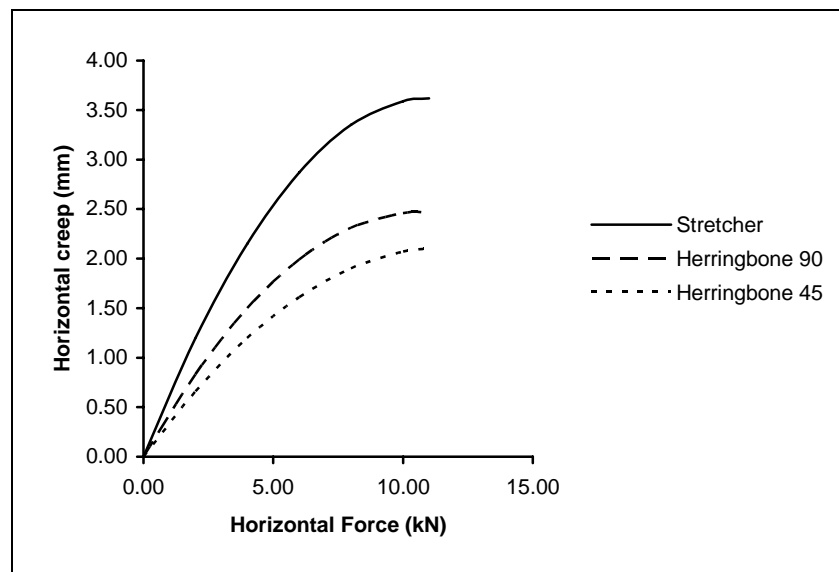
Figure 8.4   The effect of laying pattern in horizontal force test

It is established that horizontal creep of concrete block pavements is dependent on the laying pattern in the pavement. The finding is contradictive with that reported by Panda and Ghosh (2002), but similar to Shackel (1993).

8.5   Comparison of Experimental Results and Finite Element Modelling

In the experimental tests reported in Chapter 4, the value of displacement and horizontal creep of CBP was measured. The measurement was conducted used transducers by connected to the data logger. While in the next work using finite element analysis, it is possible to measure the displacement and horizontal creep due to the capabilities of the software to tabulate a result on the model depending on the nodes generated. In this research, the vertical displacement and horizontal creep on several degree of slope was measured as a comparison between the COSMOS Star DESIGN and experimental result.

There are some differences between the experimental result and the COSMOS Star DESIGN result. The biggest percentage different between the experimental data with COSMOS Star DESIGN analysis was 25.4 % for the vertical displacement reading and 14.1 % for the horizontal creep reading. The results as shown in the Table 8.1

Table 8.1   The comparison result of experimental in laboratory with FEM analysis

Slope	Experimental Max. Displacement	Experimental Max. Horizontal Creep	FEM Max. Displacement	FEM Max. Horizontal Creep	Different of Displacement Experimental with FEM	Different of Hz Creep Experimental with FEM
0 %	2.27 mm	0.28 mm	1.81 mm	0.26 mm	20.2 %	5.9 %
4 %	2.33 mm	0.36 mm	1.81 mm	0.32 mm	22.2 %	9.2 %
8 %	2.40 mm	0.47 mm	1.81 mm	0.41 mm	24.4 %	12.2 %
12 %	2.43 mm	0.68 mm	1.81 mm	0.58 mm	25.4 %	14.1 %

The difference might be due to the fact that in this research, the vertical displacement and horizontal creep in finite element model obtained using the material properties packages in software whereas the experimental results were obtained with presence material. The experimental CBP in laboratory used parameters of jointing sand, width of joint, block thickness there were some deviations of standard. Otherwise, the finite element modelling obtained using the SOLID Works and COSMOS Star DESIGN software, so the optimum meshing may generate more accurate than experimental in laboratory reality.

8.6   Development and Performance of HALI

(i)   Design of HALI

The entire operation of HALI was controlled by a microprocessor. HALI consist several components which were attached to the base frame. The loading mechanism was applied to the pavement by a mobile carriage. The mobile carriage, mounted on two rigid and frictionless guide rails, enable the loading to be moved forward and back along the rail. The mobile carriage consists of single wheel loading attachment, 3-phase electric motor, hydraulic system and control display unit. The HALI was also equipped with dial gauges for data acquisition purpose and three dimensional pavement views can be generated by using SURFER program. However, the machine also had limitation on temperature control for the pavement under accelerated trafficking test.

(ii)   Calibration of HALI

Calibration was made on the loading applied to wheel, speed of the mobile carriage and tyre pressure. The actual loading applied to the wheel was checked with the design wheel load that was programmed in the control panel by load cell. The actual speed of mobile carriage was determined by obtaining the time of a complete cycle and dividing with the length of pavement track. The tyre pressure of 600 kPa was checked at the workshop before it commenced for an accelerated trafficking test.

(iii)   Monitoring of HALI performance

The magnitude of the heave at the right hand side was higher if compared to the heave at the left hand side of the wheel path. The difference of heaves level at both sides was believed to be caused by the off-centered load distribution from the wheel. The constant deformation length of tested pavement was determined at about 2.42 m of length at the middle section. The accelerating and braking area of the pavement were identified at about 0.44 m at the front part and 0.88 m at the end part sections of the tested pavement.

(iv)   Monitoring of structural performance of RCPB pavement

In general, Section I (consist of CCPB at surface layer) tends to yield better level of performance in rut resistance, regardless of transverse rut depth profile, mean rut depth and longitudinal rut depth than other test sections. The RCPB perform as rigid bodies at the surface layer of the pavement which show that load-associated performance of the RCPB pavements was independent due to its geometrical characteristics.

Joints have opened out as a result of substantial movement of the RCPB after 10000 of loading repetitions. The open joint width results from the entire panel A, B, C, and D were similar, irrespective of whole cross sections. However, the mean joint width for panel A and panel D increased whilst panel B and C decreased significantly with the increments of the load repetitions.

10-RCPB showed a lower shear resistance than CCPB and other RCPB, reflecting weaker interlocking among the others. One of the reasons may be it is caused by the higher rut depth and shoving occurred in that particular cross section and influenced the function of joint to provide a good shear resistance.

Skid resistance results obtained showed a systematic reduction with an increase in rubber content and similar reduction at the end of the trafficking test. The only observation after trafficking was that was no deterioration but only a little polishing of the rubber particles which happened in 20-RCPB and 30-RCPB surface.

CHAPTER 9

CONCLUSIONS AND RECOMMENDATIONS

9.1   Introduction

This chapter discusses the conclusions on the concrete block pavement (CBP) for sloping road section in relation to performance of CBP deformation (horizontal creep and vertical displacement) that is affected by bedding sand thickness, laying pattern, block thickness, block shape and joint width between blocks. Structural performance of rubberized concrete block pavement by means of a newly developed Highway Accelerated Loading Instrument (HALI) was also compressively discussed and concluded.

9.2   Conclusions

The experimental work performed in this study leads to the following applicable conclusions:

➢ The joints in between blocks should be properly filled with sand. The optimum joint width between blocks is 3 mm. For joint widths less than the optimum, the jointing sand was unable to enter between blocks. A large amount of sand remained outside the joint showing sand heaps on the block surface.

➢ A block pavement may present various types of mechanical behaviour when submitted to a horizontal force, depending on the blocks shape, as well as on joint width between blocks, the laying pattern and on the direction of the horizontal force relative to the laying pattern.

➢ The horizontal force test with rectangular block shape and stretcher laying pattern, which is parallel to the continuing lines of the joints, shows that the cohesion of such a plate is near to zero whatever the restraining of the edges. Indeed, for a relatively low value of the applied force, the line of loaded blocks moves monolithically, the friction forces which are the only ones capable of reacting on the continuous lines being too weak to perform this role.

➢ To define the spacing of anchor beam of CBP on sloping road section, factors as degree of slope, joint width between blocks, laying pattern, blocks shape, blocks thickness, bedding sand thickness should be included.
   – The increase of degree of slope will cause shorter spacing of anchor beam.
   – The increase of joint width between blocks will cause shorter spacing of the anchor beam.
   – The herringbone 45° is the best laying pattern compared with herringbone 90° and stretcher bond to restraint the horizontal force. It was indicated that the spacing of anchor beam would be longer.
   – The uni-pave block shape has more restraint of horizontal creep than rectangular block shape, because uni-pave block shape has gear (four-dents), while rectangular block shape no gear (no dents), so the spacing of anchor beam has a difference of about 10 m.

- A change in thickness from 60 to 100 mm significantly reduces the elastic deflection of pavement. Thicker blocks provide a higher frictional area. Thus, load transfer will be high for thicker blocks. For thicker blocks, the individual block translation is more with the same amount of block rotation. The increase of block thickness will cause longer spacing of anchor beam.

- The role of the bedding sand is very important, a number of main functions are: to fill the lower part of the joint spaces between adjacent blocks in order to develop interlock, to provide uniform support for the blocks and to avoid stress concentrations which could cause damage to the blocks, to provide an even surface on which to lay the blocks, to accommodate the manufacturing tolerances in block thickness and to accommodate accepted tolerances in sub-base surface level. The increase of bedding sand thickness will cause shorter spacing of anchor beam.

➢ The biggest percentage differences between experimental data reading with finite element model analysis was 25.4 % for vertical displacement and 14.1 % for horizontal creep.

➢ HALI is found to provide a low cost, operational guideline and simple accelerated loading facility for road authorities and highway research institutions. Structural performance of concrete block pavement can be easily investigated by carrying out a simple developed HALI subjected to typical load repetitions and several tests for shear, skid and impact resistance.

8.3 Recommendations for Future Studies

➢ Stretcher bond is suited to pedestrian areas and very lightly trafficked areas not subjected to regular turning movements or frequent braking or acceleration. Block rows should be laid at right angles to traffic flow.

➢   Herringbone laying patterns are suitable for all applications. Either 90° or 45° Herringbone pattern oriented to the longest straight edge should be used with vehicular areas. This reduces the incidence of creep and distributes wheel loads more evenly to the underlying pavement construction.

➢   The shape of the load deflection path is similar for two block types. The deflections are essentially the same for rectangular shape and uni-pave shape. The small deflections observed for uni-pave shape are less compared to the rectangular shape. In general, shaped (dented) blocks exhibited smaller deformations as compared to rectangular and square blocks. Complex shape (uni-pave) blocks have larger vertical surface areas than rectangular or square blocks of the same plan area.

➢   There is a limitation of laboratory accelerated trafficking test by HALI. More accurate structural performance of concrete block pavement can be achieved if concrete block pavement is constructed and investigated under actual traffic (field test). This will take into account more parameters of pavement structure during the trafficked test.

REFERENCES

Armitage R. J. (1998). *Concrete Block Pavement with the Falling Weight Deflectometer.* Proceeding of Third International Conference on Concrete Block Paving: Roma-Italy, 203-2-8.

Akpinar, M V. (2001). Defining Roller Compactor Position and Slope of Tappered Surface in a Longitudinal Joint Construction Using 2-D Finite Element Model. PhD Thesis, Kanas State University, Manhattan.

Barber, S. D. and Knapton, J. (1980). An Experimental Investigation of the Behaviour of a Concrete Block Pavement with a Sand Sub-base. *Proc. Inst. Civil Engrs.* 69: 139-155.

Barber, S. D. and Knapton, J. (1980). Structural Desgn of block Pavements for Ports. Proceeding of Frist International Conference on Concrete Block Paving: Newcastle.

Bathe and Nishazaw (1982). Analysis Interlocking Block Pavements by Finite Element Method, Paper Submitted to Annual Meeting of Transportation Research Board.

Beaty, A. (1993). Personal Communication. Royal Military College, Kingston.

Beaty, A. (1994). Bedding Sand for Concrete Block Pavements Subject to Heavy Chanelised Loading. *Proc. 2nd International Workshop on Block Paving, Oslo, Norway..*

Beaty, A. and Raymond G. P. (1995). Concrete Block Road Paving. Journal of Concrete International, March: 16-20.

British Standards. (1973). Specification for aggregates from natural sources for concrete. *BS 882, 1201: Part 2*, London.

British Standards. (1989). Precast Concrete Paving Block: code of Practice for Laying Pattern. *BS 6717: Part 3*, London.

Candy, C. C. E. and Shackel, B. (1998). The Fuction and Safety of Interlocking Concrete Road Surface. Proc. 14th ARRB Conference, Part 8: 65-75.

Chatti, K. (1992). Dynamic analysis of jointed concrete pavements subjected to moving transient load. PhD Thesis, Institute of Transportation Studies, University of California at Barkeley.

Clifford, J.M. (1984). Segmental block pavement- optimizing the joint width and joint materials. Proc. Second Int. Conf on Concrete Block Paving, Delft.

Clifford, J.M. (1984). *Some Aspects of the Structural Design of Segmental Block Pavements in Southern Africa.* University of Petoria: PhD Thesis.

Concrete Manufactures Association (2000). Concrete block paving for steep slopes technical note, CMA.

Concrete Segmental Pavements (T54) (1997). *Design Guide for Residential Accessways and Roads.* Australia: Cement and Concrete Association of Australia/Concrete Masonry Association of Australia.

David, W. G. (1998). Modeling of rigid pavements: joint shear transfer mechanisms and finite element solution strategies. PhD Thesis, University of Washington.

Dossetor, J. E. and Leedham, A. G. (1976). Concrete Block Pavements. *III C T Seminar.* South Australian Institute Technology.

Drejir, P. A. (1980). Laboratory abd fieldwork on block paving. Proceeding of Frist International Conference on Concrete Block Paving: Newcastle.

Dutruel, F. and Dardare, J. (1984). Contribution to the study of structural behaviour of a concrete block pavement. Proceeding of 2nd International Conference on Concrete Block Paving: Delft.

Eisenmann, J. and leykauf, G. (1998). Design of concrete block pavement in FRG. Proceeding of 3rd International Conference on Concrete Block Paving: Rome.

Emery, J. A. (1993). Stabilization of jointing sand in block paving. Journal of Transportation Engineering, Vol. 119, No. 1: 143-147.

Fahmy, M. R. (2000). Finite element modeling of dowel jointed plain concrete pavement response to thermal and moving traffic loads. PhD Thesis, Morgantown, West Virginia.

Ghafoori, N. and Mathis, R. (1997). Sulfate resistance of concrete pavers. Journal Materials Civil Engineering, ASCE, 9(1): 35-40.

Glickman, M. (1984). The G-block system of vertically interlocking paving. Proceeding of 2nd International Conference on Concrete Block Paving: Delft.

Hasanan Bin Md Nor (1996). Toward better concrete block pavements in Malaysia. The 2nd Malaysia Road Conference, Kuala Lumpur.

Hasanan Bin Md Nor (1999). Good practice for concrete block pavement. Seminar Kejuruteraan Awam. Universiti Teknologi Malaysia.

Hasanan Bin Md Nor (2005). The developement and application of concrete block pavement. International Seminar and Exhibition on Road Construction (ISERC), Semarang, Indonesia.

Houben, L. J. M. and Jacobs, M M. J. (1998). Wheel track testing and finite element analysis of concrete block pavements. Proceeding of 3rd International Conference on Concrete Block Paving: Rome.

Hua, J. (2000). Finite element modeling and analysis of accelerated pavement testing device and rutting phenomenon. PhD Thesis, Purdue University.

Huanf, Y. H. and Wand, s. T. (1973). Finite element analysis of concrete slabs and its implications for rigid pavement design, highway Research Record, 466: 55-69.

Hudson, K. C. and SIdaharja, E. P. (1992). Bedding course material. Proceeding of 4th International Conference on Concrete Block Paving: Auckland, New Zealand.

Hugo, F. and Martin, A. L. E. (2004). *Significant Findings from Full-Scale Accelerated Pavement Testing.* NCHRP Synthesis Report 325. Transportation Research Board.

Huurman, M. (1997). Permanent deformation in concrete block pavements. PhD Thesis, Delft University of Technology.

Interlocking Concrete Pavement Institute (2000). Glossary of terms used in the production design, Construction and Testing of Interlocking Concrete Pavement. Tech. Spec. 1.

Interlocking Concrete Pavement Institute (2000). Construction of Interlocking Concrete Pavement. Tech. Spec. 2.

Interlocking Concrete Pavement Institute (2000). Structural design of interlocking concrete pavement for roads and parking lots. Tech. Spec. 4.

Interlocking Concrete Pavement Institute (2000). Reinstatement of interlocking concrete pavements. Tech. Spec. 6.

Interlocking Concrete Pavement Institute (2000). Slip and skid resistance of interlocking concrete pavements. Tech. Spec. 13.

Interpave (2004). Construction of concrete block pavements. Publication, The Precast Concrete Paving and Kerb Association, The British Precast Concrete Federation.

Interpave (2004). Design and detailing of concrete block pavements. Publication, The Precast Concrete Paving and Kerb Association, The British Precast Concrete Federation.

Ioannides, A. M. (1988). Interlayer and sub-grade friction: a brief review of the State-of-the art, Field Evaluation of Newly Developed Rigid Pavement Design Features, Phase I-Modification No. 3.

Ioannides, A. M. (1988). Thee-dimensional analysis of slab on stress dependent foundation, Transportation Research Record 1996, TRB, 72-84.

Jacobs, M. M. J. and Houben, L. J. M. (1988). Wheel track testing and finite element analysis of concrete block pavements. Proceeding of 3rd International Conference on Concrete Block Paving: Rome.

Kagata, M. and Utumi, G. (1996). Review of function of jointing sand, bedding course sand and base structure in concrete block pavement. Proceeding of 5th International Conference on Concrete Block Paving: Tel-Aviv: Israel.

Karahara, A. (1988). Estimation if apparent elastic modulus of concrete block layer. Proceeding of 3rd International Conference on Concrete Block Paving: Rome.

Knapton, J. (1976). The design of concrete block roads. Cement and Concrete Association, Technical Report 42.515, Wexham, Springs: UK.

Knapton, J. and Barber, S. D. (1979). The Behaviour of a Concrete Block Pavement. *Proc. Inst. Civ. Engrs, Part 1.* 66: 227-292.

Knapton, J., and O'Grady, M. (1983). *Structural Behavior of Concrete Block Paving*. Journal Concrete Society: 17–18.

Knapton, J. (1996). The mathematical solution to interlock in concrete block paving. Proceeding of 5th International Conference on Concrete Block Paving: Tel-Aviv: Israel.

Koch, C. (1999). *Bearing of Paving Surfaces. Institute for Highways and Railways Constructions*. Bochum: PhD Dissertation.

Kuo, C. M. (1994). Three-dimensional finite element analysis of concrete pavement. PhD Thesis, University of Illinois at Urbana-Champaign.

Lee, K. L., and Seed, B. H. (1967). Drained strength characteristics of sands. *J. Soil Mech. and Found. Div.*, ASCE, 93(6), 117–141.

Lilley, A. A. (1980). A review of concrete block paving in the UK over the last five years. Proceeding of 1st International Conference on Concrete Block Paving: Newcastle-Upon-Tyne. .

Lilley, A. A and Dowson, A. J. (1988). Laying course sand for concrete block paving. Proceeding of 3rd International Conference on Concrete Block Paving: Rome.

Lilley, A. A. (1994). Size and block shape: do the matter? Concrete Pant and Production, Edition Sept-Oct.

Livneh, M. Ishai, I. and Nesichi, S. (1988). Development of a pavement design methodology for concrete block pavements in Israel. Proceeding of 3rd International Conference on Concrete Block Paving: Rome.

Maya, A. (1996). Improved joint sand. Proceeding of 5th International Conference on Concrete Block Paving: Tel-Aviv: Israel.

Mavin, K. C. (1980). Interlocking block paving in Australian residential streets. Proceeding of 1st International Conference on Concrete Block Paving: Newcastle-Upon-Tyne. .

Metcalf, J. B. (2004). Full Scale Accelerated Pavement Testing: A Northern Hemisphere Perspective. Proceedings of 2nd International Conference on Accelerated Pavement Testing. September. Minneapolis.

Mills, J.P., Newton, I. and Pierson, G.C. (2001). Pavement Deformation Monitoring in a Rolling Load Facility. *Photogrammetric Record*. 17(97): 7 – 24.

Miura, Y., Takura, M. and Tsuda, T. (1984). Structural design of concrete block pavements by CBR method and its evaluation. Proceeding of 2nd International Conference on Concrete Block Paving: Delft, The Netherlands.

Molenaar, A. A. A., Moll, H. O. and Houben, L. J. M. (1984). Structural model for concrete block pavement. Paper submitted to Annual Meeting of Transportation Research Board.

Morrish, C. F. (1980). Interlocking concrete paving- The State of the Art in Australia. Proceeding of 1st International Conference on Concrete Block Paving: Newcastle-Upon-Tyne.

Muraleedharan, M. P. and Nanda, P. K. (1988). Concrete block paving- full scale fiels experiments in India. Proceeding of 3rd International Conference on Concrete Block Paving: Rome.

Nasim, M. A. (1992). Effect of heavy vehicle dynamic loading on rigid pavements. PhD Thesis, University of Michigan.

Nishazaw, T., Matsuno, S. and Komura, M. (1984). Analysis interlocking block pavements by finite element method. Proceeding of 2nd International Conference on Concrete Block Paving: Delft

Rollings, R. S. (1982). *Concrete Block Pavement.* Technical Report GL82. US Army Engineer Waterways Experiment Station.

Panda, B. C. and Ghosh, A. K. (2002a). Structural Behavior of Concrete Block Paving. I: Concrete Blocks. *Journal of Transportation Engineering.* 128 (2): 130-135.

Panda, B. C. and Ghosh, A. K. (2002b). Structural Behavior of Concrete Block Paving. I: Sand in Bed and Joints. *Journal of Transportation Engineering.* 128 (2): 123-129.

Panda, B. C. and Ghosh, A. K. (2002). Source of jointing sand for concrete block paving. *Journal of Materials in Civil Engineering.* 13 (3): 235-237.

Pearson, A. R. and Hodgkinson, J. R. (1992). Some factor affecting success and distress in segmental concrete block pavement in Australia. Proceeding of 4th International Conference on Concrete Block Paving: Auckland: New Zealand

Pittman, D. W. (1993). Development of a design procedure for roller-compacted concrete (RCC) pavements. PhD Thesis, The University of Texas at Austin.

Rada, G. R., Smith, D. R., Miller, J. S. and Witzak, M. W. (1990). Structural design of concrete block pavements. *Journal of Transportation Engineering.* 116 (5): 615-635.

Rohleder, M. (2002). Horizontal shifting of paving surface and their visualization. PhD Thesis, Institute for Highways Constructions Bochum.

Saro, I., Shibuya, K. and Yasui, S. (1988). Common use of interlocking blocks in cold districts. Proceeding of 3rd International Conference on Concrete Block Paving: Rome.

Seddon, P. A. (1980). The behaviour of interlocking concrete block paving at the Canterbury test track. Proceeding ARRB, Volume 10 Part 2.

Shackel, B. and Arora, M. G. (1978a). The Evaluation of Interlocking Block Pavements- An Interim Report. *Proc. Conf. Concrete Masonry Assn of Australian*, Sydney.

Shackel, B. (1979a). A Pilot Study of the Performance of Block Paving Under Traffic Using Heavy Vehicle Simulator. *Proc.Symp. on Precast Concrete Paving Block*, Johannesburg.

Shackel, B. (1979b). *An Experimental Investigation of the Response of Interlocking Block Pavements to Simulated Traffic Loading.* Australia Road Research Board Research Report ARR No. 90. Australia, 11-44.

Shackel, B. (1979c). *The Design of Interlocking Concrete Block Pavements.* Australian Road Research Board Research Report ARRB No. 90, 53-70.

Shackel, B. (1980a). An Experimental Investigation of the Roles of the Bedding and Jointing Sands in the Performance of Interlocking Concrete Block Pavements. *Concrete/Beton.* 19: 5-15.

Shackel, B. (1980b). *Loading and Accelerated Trafficking Tests in Three Prototype Heavy Duty Industrial Block Pavements.* Technical Report 12. National Institute for Transport and Road Research, CSIR, Pretoria.

Shackel, B. (1980c). The Performance of Interlocking Block Pavements under Accelerated Trafficking. *Proc. of 1st Int. Conf. on Concrete Block Paving.* September 2-5. Newcastle-upon-Tyne, U.K., 113–120.

Shackel, B. (1980d). A Study of the Performance of Block Paving under Traffic using a Heavy Vehicle Simulator. *Prerecording of 10th Australian Road Research Board Conference.* 10(2): 19 – 30.

Shackel, B. (1980). The performance of interlocking block pavements under accelerated trafficking. *Proc., 1st Int. Conf. on Concrete Block Paving*, Newcastle-upon-Tyne, U.K., 113–120.

Shackel, B. (1985). Evaluation, design and application of concrete block pavements. *Proc., 3rd Int. Conf. on Concrete Pavement Design and Rehabilitation*, Purdue University, West Lafayette, Ind., 113–125.

Shackel, B. (1990). Design and construction of interlocking concrete block pavements. Elsevier Applied Science: London, 229.

Shackel, B., O'Keeffe, W. and O'Keeffe, L. (1993). Concrete block paving tested as articulated slabs. Proc. of 5th Int. Conf. on Concrete Pavement Design and Rehabilittation, Purdue Univ.

Shackel, B., Litzka, J. and Zieger, M. (2000). Loading tests of conventional and ecological concrete block paving. *Proc., 6th Int. Conf. on Concrete Block Paving*, Tokyo.

Shackel, B. (2003). The challenges of concrete block paving as a mature technology. *Proc., 7ᵗʰ Int. Conf. on Concrete Block Paving*, South Africa.

Shackel, B., and Lim, D. O. O. (2003). *Mechanisms of Paver Interlock*. Proceeding 7ᵗʰ International Conference on Concrete Block Paving, South Africa.

Sharp, K. G. and Simmons, N. J. (1980). Interlocking concrete blocks: State-Of-The-Art-Review. ARRB Proceeding Volume 10: Part 2.

Sharp, K. G. and Armstrong, P. J. (1985). Interlocking concrete block pavements. Australia Road Research Board.

Shoukry, S. N., Martinelli, D. R. and Selezneva, O. I. (1996). Dynamic considerations in pavements layers moduli evaluation using falling weight deflectometer. Proceeding of the International Society for Optical Engineering, Nondestructive Evaluation of Bridges and Highways, 2496: 109-120.

Simmons, M. J. (1979). Construction of interlocking concrete block pavements. Australia Road Research Board, Report ARRB No. 90: 71-80.

Steyn, W. J. vdM., De Beer, M. and Du Preez, W. (1999). Simulation of Dynamic Traffic Loading For Use in Accelerated Pavement Testing (APT). *Proc. of International Conference on Accelerated Pavement Testing*. Reno: GS01 – 04.

Tabatabaie, A. M. and Barenberg, E. J. (1978). Finite element analysis of jointed or cracked concrete pavements. Transportation Research Record 671: 11-19.

Van der Vlist, A. A. (1980). The development of concrete blocks in the Netherlands. *Proc. of 1ˢᵗ Int. Conf. on Concrete Block Paving*. September 2-5. Newcastle-upon-Tyne, U.K.

Teiborlang, L. R., Mazumdar, M. and Pandey, B. B. (2005). Structural Behaviour of Cast in Situ Concrete Block Pavement. *Journal of Transportation Engineering*. 131(9): 662 – 668.

UNILOCK (1997). *Design Considerations for Interlocking Concrete Pavement*. United States of American: UNI Group.

Vanderlaan, F. J. M. (1994). *The Performance of Bedding Sands in Concrete Block Pavements*. The University of New Brunswick: M. Sc. in Engineering Thesis.

Zaghloul, S. M., White, T. D. and Kuczek, T. (1994). Evaluation of heavy load damage effect on concrete pavements using three-dimensional nonlinear dynamic analysis. Transportation Research Record 1449: 123-133.

APPENDIX A:Highway Accelerated Loading Instrument
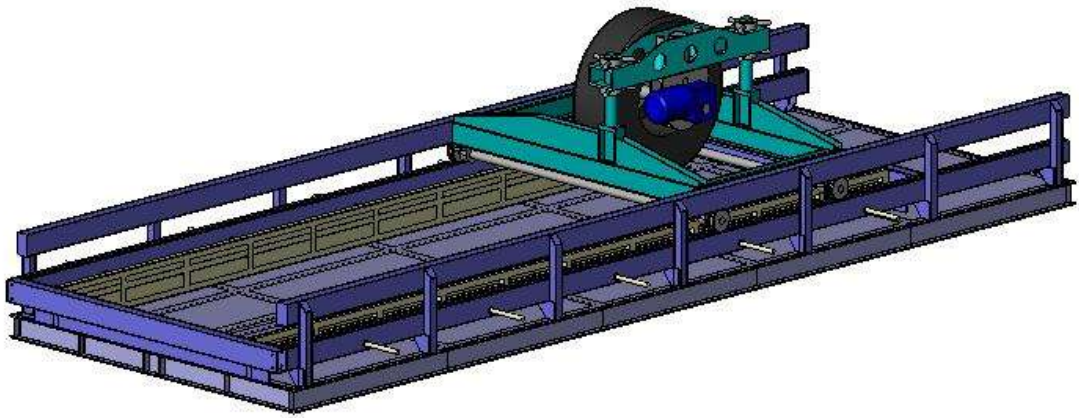
Operating Manual

CONTENT :-

(1).   <u>Powered up the System</u>

   Descriptions :

   *   Switch the Incoming Supply Isolator 20amps to 'ON' position (refer to dwg : Panel Layout)
           (Ensure all the power control element (mcb) in control panel is in 'ON' position. Inverter
           will 'ON').

   *   Switch the 'Main Power' Selector to 'ON' position (refer to dwg : Panel Layout)
           (This will powered up Power supply unit, PLC units and the Hydraulic pump).

   *   Also ensure the emergency pushbutton and 'START/STOP Selector switch are released
           and in the correct position.

   *   Green Indicator lamp will light up to indicate the power is 'ON'.

(2)   <u>Shut Down the System</u>

   Descriptions :

   *   Arranged the **Machine Sequence** back to 'Home' position.

   *   Switched **'OFF'** the Main Power selector switch (this will cut off P/S unit and PLC supply).

   *   Switched the Incoming Supply Isolator 20amps to **'OFF'** position.

   *   To cut off the Inverter supply individually ,switch off the control MCB to Inverter (refer to dwg :
           Main Circuit Diagram).

   *   Green Indicator lamp is off right after the power **cut off**.

(3)   <u>Manual Mode Setting</u>

   Descriptions :

   *   Switched **'Auto/Man'** selector to **'Man'** position.

   *   **Press 'Forward'** pushbutton for forward direction, release pushbutton to stop the functions.

   *   **Press 'Reverse'** pushbutton for reverse direction, release pushbutton to stop the functions.

   *   **Press 'Up'** pushbutton for upper position, release pushbutton to stop the functions.

   *   **Press 'Down'** pushbutton for lower position, release pushbutton to stop functions.

(4)   Automatic Mode Setting

   *   Switched **'Auto/Man'** selector to **'Auto'** position.

   *   Sets traverse speed (Inverter).

   *   Sets the 'total cycles' (Counter) .

   *   Sets the 'Load Test Pressure'(Data memory).

   *   Ensure all the **controlled** elements is in **'home'** position.

   *   **Press 'OK'** button attached for 2 second on FX1N-14MR display panel to start the process.

   *   To cancel the process immediately swtch to **Manual** mode.

(5)   Inverter speed

   The speed of motor in frequency (Hz) is displayed on the inverter digital display during
   run operations. It's can be changes according to the speed required by the operator.

   *   Press **'Increment'** button and **'Decrement'** button to change the value of speed in
           Freq (hz) on the Inverter control panel.

   *   **Press 'Edit / Enter'** after changing the value of the speed to confirm the new setting
           is accepted.

   *   **To convert the Freq (hz) reading to Speed (m/s)**
           Calculate Circumference of Wheel (D) in metre (Circumference = 3.142 * Wheel Diameter)
           Calculate No. of Revolution per second (R) = (Freq/50)*(1420/60)/60
           Speed = D * R (m/s)

(6)   Counter (Setting the **'total cycle'** of the machine)

   The micro display module FX1N-5DM is mounted on the top face of the FX1N series PLC basic
   unit and can monitor/update internal PLC data. The **'Total Cycles'** of the machine is sets in Data
memory
   in FX1N-5DM and to acces the 5DM module screen for counter:-

   *   Press '+' and '-' button to change the display between D0 to D3
   *   Press and hold 'OK' for 2 second to enable data edit
   *   Set D0 (Total Cycle) data with '+' and '-'
   *   Press and hold 'OK' for 2 second to save new data.
   *   Press and hold 'ESC' for skip save function
   *   D1 is "Cycle Elapsed", you need to reset D1 to 0 to restart the cycle.

(7)   <u>Load test pressure setting</u> (Data Memory)

In this micro display module FX1N-5DM contents up to 8000 data memory can be used to storage a data. In this case only monitored data memory are displayed to let the users to make any changes .(D3) for 'Forward Loading' setting and (D4) for 'Reverse Loading' setting.
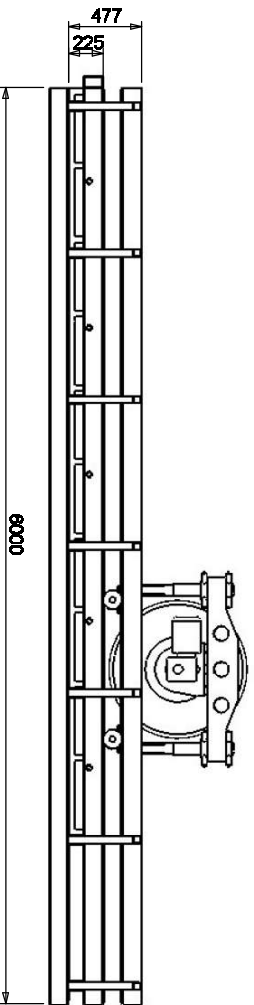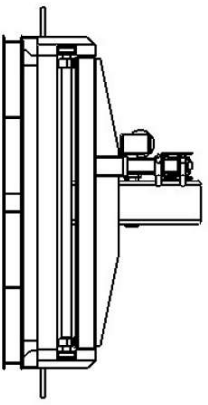The setting has been calibrated into kN unit.
 To set a Load Test Pressure the operator has to :-

*   **Press '+' and '-'** button together to access data memory D3 or D4 screen.
*   Press and hold 'OK' for 2 second to enable data edit
*   Set D3 or D4 data with '+' and '-'
*   Press and hold 'OK' for 2 second to save new data.
*   Press and hold 'ESC' for skip save function

(8)   <u>Trouble shooting</u>

Problems	**Action Taken**	**Remarks**
- No incoming supply	- Check Incoming Isolator - Check ELCB	
- Voltage drop	- Measure Incoming supply - Check cable connections	
- MCB trip	- Check controlled elements condition	
- M/C operation failure	- Check PLC I/O signal - Check controlled elements - Check 24v supply - Check 415v/240v supply - Check setting - Check Hydraulic system	- Rearrange M/C sequence (Manually) - Do calibration
- Input/Output Failure	- Check 24v supply - Check cable connections/signal - Check controlled elements	- Testing device (programs)
- Hydraulic pressure drop	- Check hydraulic piping - Check hydraulic controlled element - Check amplifier card output - Check hydraulic oil - Check motor pump condition	- Ensure no leakage occurred
- Over pressure	- Check Hydraulic controlled element - Check Transmitter output - Check power amps card output	

2180

44

420

1108.80

2070

1920

95

980

6000

477

225

Front Guide Frame

Side Guide Frame

Wheel Hollow
Guide with Flat bar

Adjustable length
/lock with nut

Base Frame
Structure

Dynamic
Compressive
Test Unit

Rear Guide Frame

25

3kw gearbox

Stroke = 50mm

70

Flange mount
Gearbox
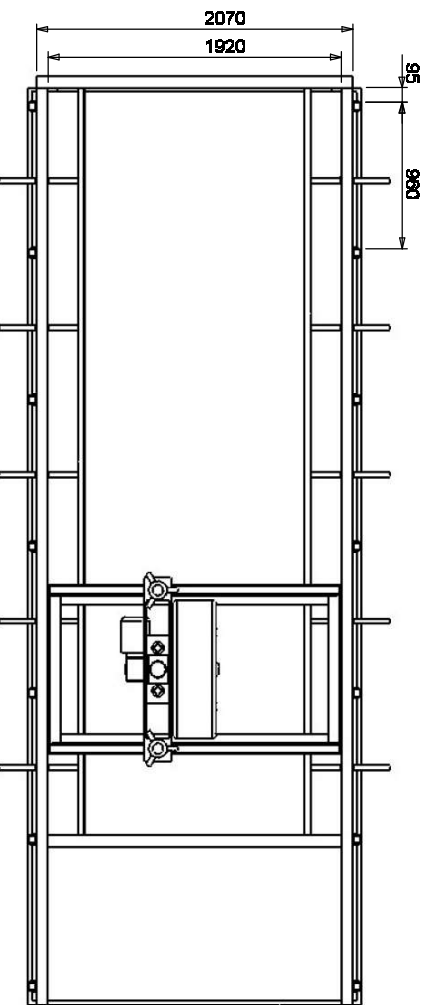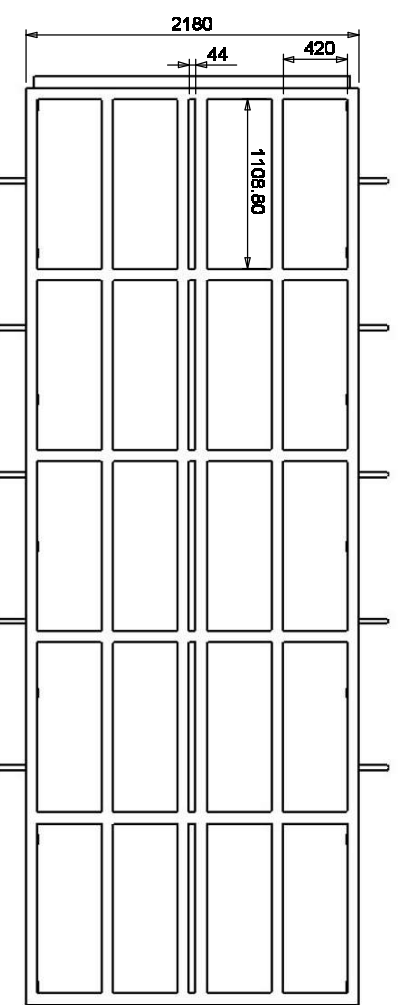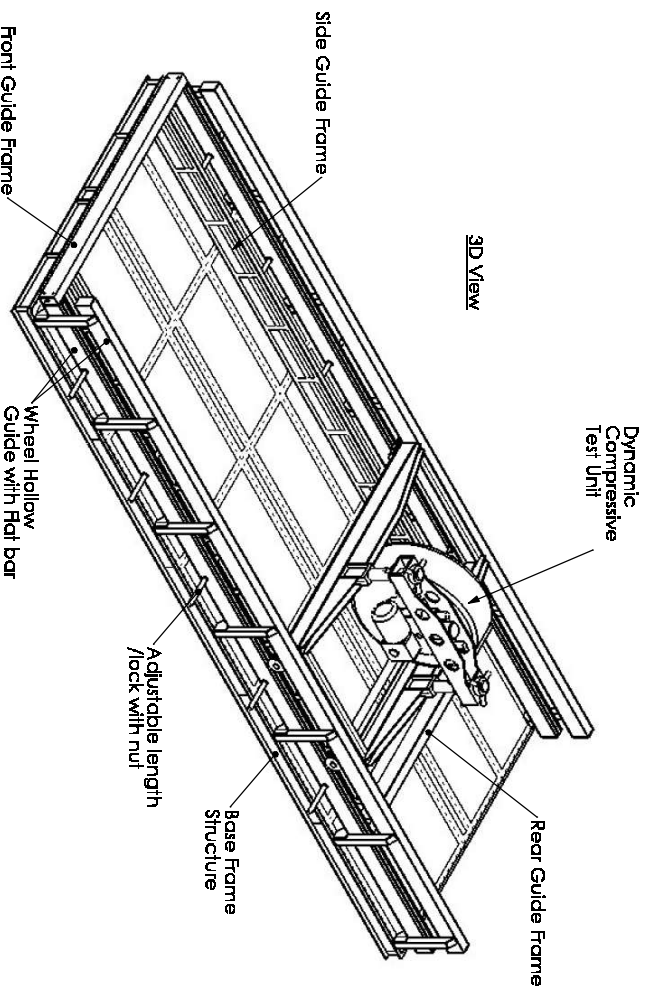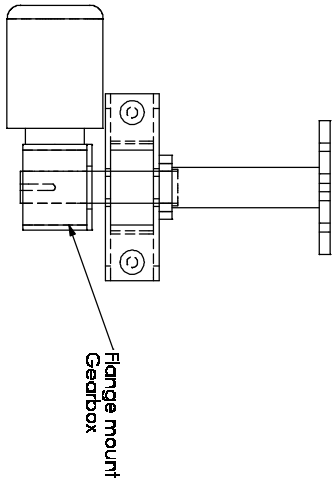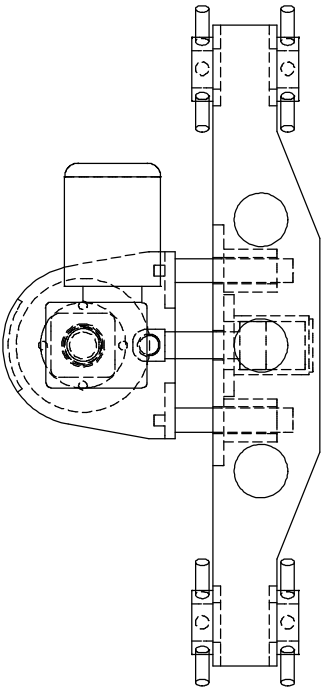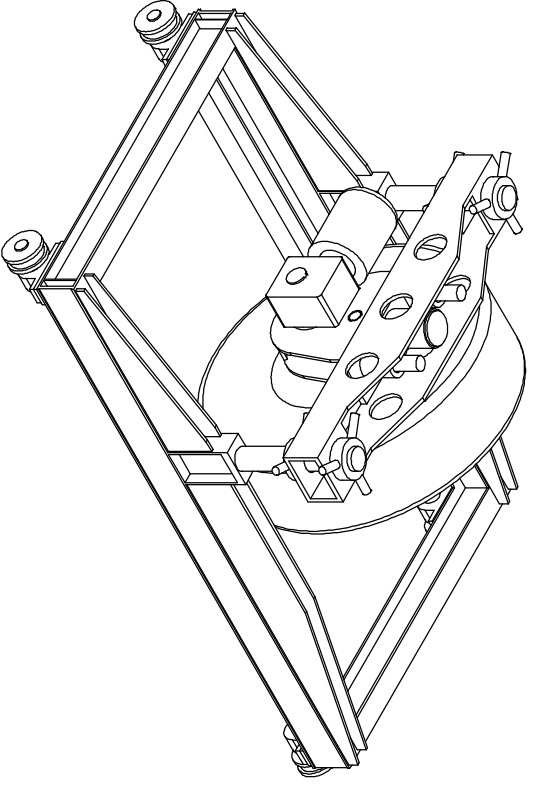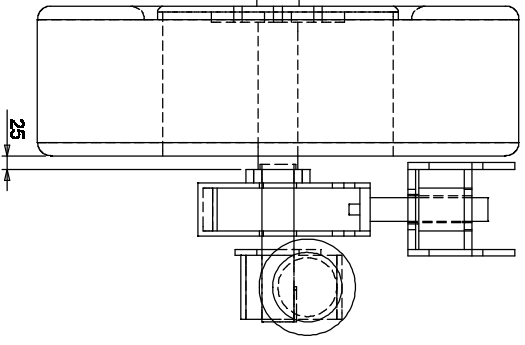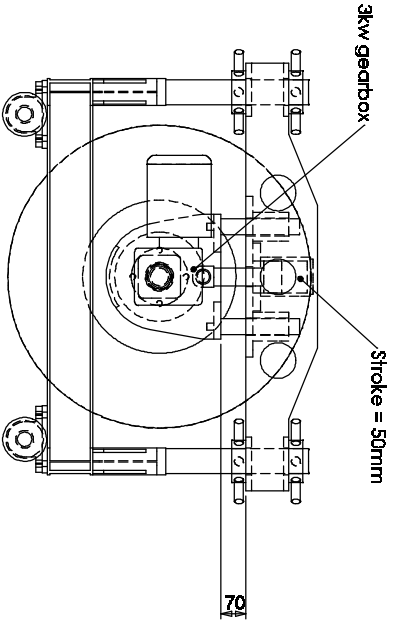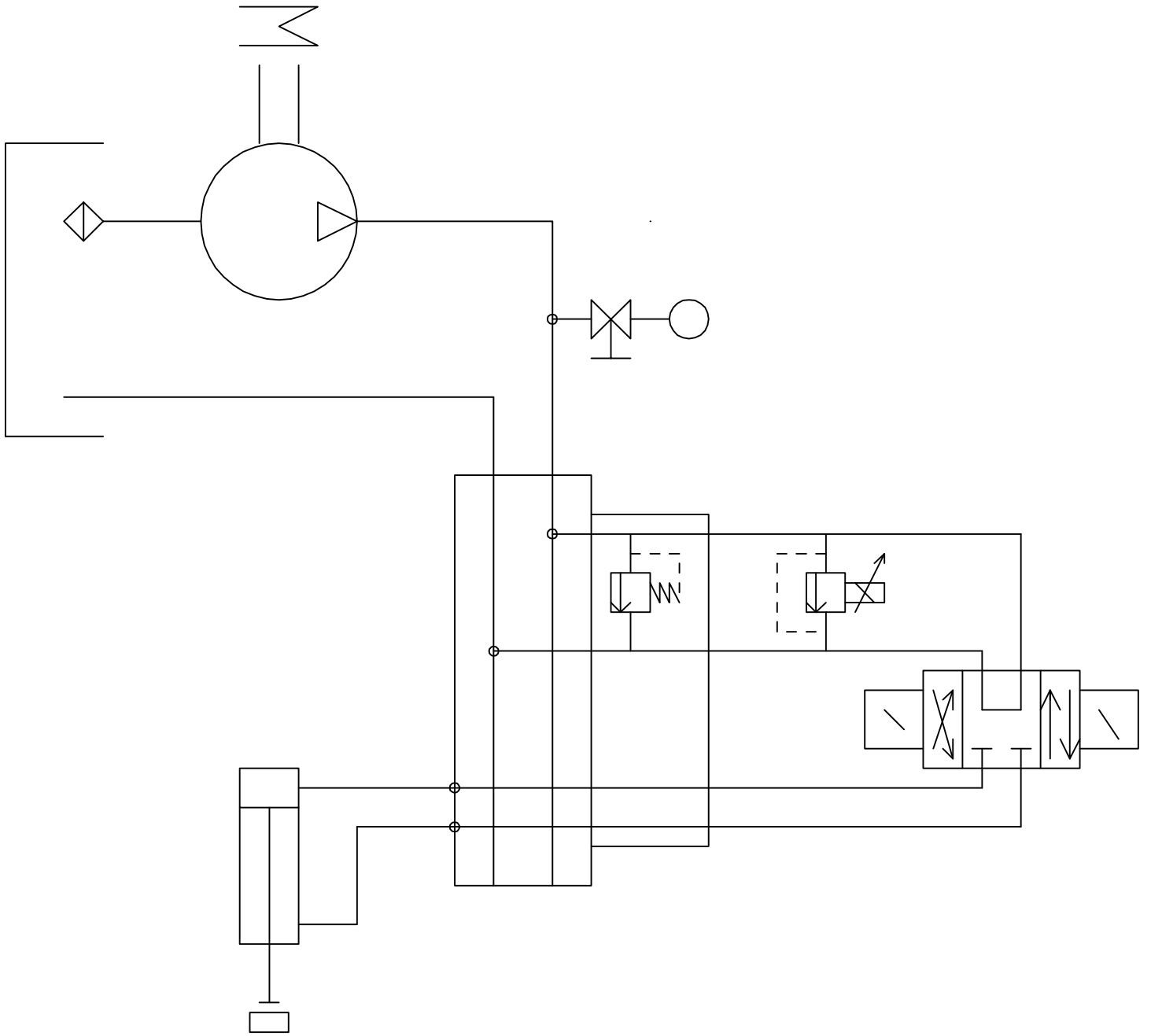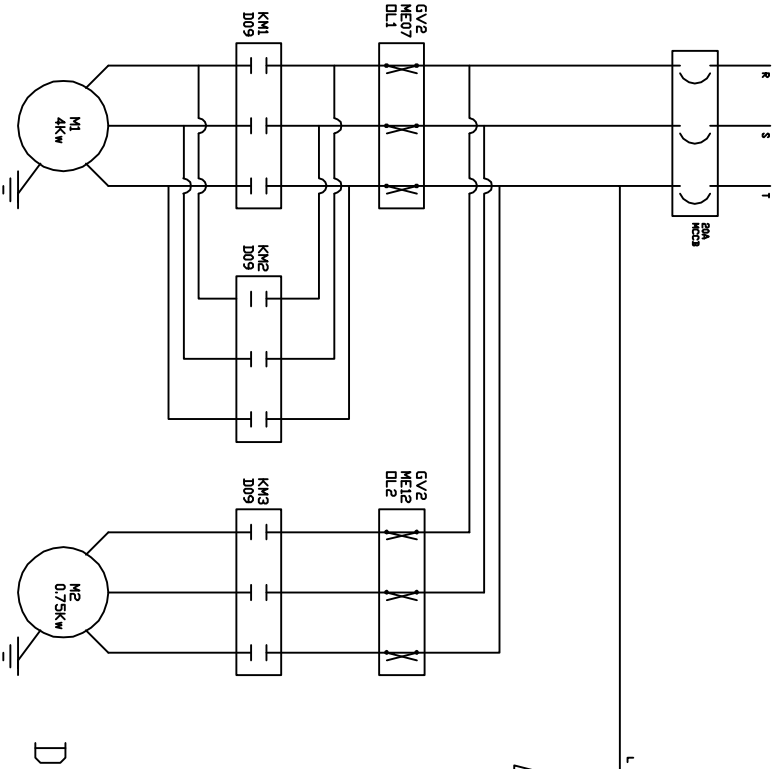
Dynamic Compressive Load Tester Electrical Drawing

APPENDIX B

List of Journal Articles and Proceeding Papers Has Been Published Based On the Work Presented in this Report

<u>**International Journal Articles**</u>

Status: Accept to be published in the first issue in 2008.

1) Ling, T. C., Nor, H. M., Hainin, M. R. and Chow, M. F. (2008). "Highway Accelerated Loading Instrument (HALI) Testing of Permanent Deformation in Concrete Block Pavement." *Road and Transport Research Journal (Invited paper by Kieran Sharp and submitted on 22nd July 2007)*

Status: Under review

2) Ling, T. C., Nor, H. M. and Hainin, M. R. (2008). "Laboratory Performance of Crumb Rubber Concrete Block Pavement." *International Journal of Pavement Engineering (Submitted on 10th October 2007)*

<u>**National, Regional and International Conference Papers**</u>

1) Ling, T. C., Nor, H. M. and Chow, M. F. (2007). "Highway Accelerated Loading Instrument (HALI) Testing of Permanent Deformation in Concrete Block Pavement." *7th Malaysia Road Conference 2007.* 17th – 19th July 2007. Kuala Lumpur, Malaysia. **(Best Paper Award)**

2) Ling, T. C. Nor, H. M., Hainin, M. R. and Chow, M. F. (2006). "Highway Accelerated Loading Instrument (HALI) for Concrete Block Pavement." *SEPKA*. 19th – 20th December 2006. Universiti Teknologi Malayisa, Skudai, Malaysia.

3) Rachmat Mudiyono, Hasanan Md Nor and Ling Tung Chai (2006). "The Effect of Joint Width on Concrete Block Pavement" *1st Proceeding of the Regional Postgraduate Conference on Engineering and Science* July 2006, School of Graduate Studies UTM and Indonesian Students Association.

3) Rachmat Mudiyono and Hasanan Md Nor (2005). "Improving CBP on Performance on sloping Road Section" *Proceeding of the International Seminar and Exihibition on Road Constructions.* May 26th, 2005, Semarang – Indonesia pg: 29 – 42

4) Rachmat Mudiyono and Hasanan Md Nor (2005).. "The Development and Application of Concrete Blocks Pavement. "*Proceeding of the International Seminar and Exihibition on Road Constructions.* May 26th, 2005, Semarang – Indonesia, pg: 1 – 12

5) Hasanan Md Nor and Rachmat Mudiyono (2005). "The Construction of Concrete Block Pavement on Sloping Road Section Using Anchor Beam." *Proceedings Seminar Kejuruteraan Awam (SPKA) 200*4, Sofitel Palm Resort Hotel, Senai – Johor Bahru.

6) Rachmat Mudiyono and Hasanan Md Nor (2004). "The Effect of Changing Parameters of Bedding and Jointing Sand on Concrete Block Pavement." *Proceedings Seminar Kejuruteraan Awam (SPKA) 200*4, FKA-UTM, Skudai – Johor Bahru.

7) Hasanan Md Nor and Rachmat Mudiyono (2002). "Construction of Concrete Block Pavement for Uphill Area in Campus" *Proceedings Seminar Kejuruteraan Awam (SPKA) 200*2, FAB-UTM, Skudai – Johor Bahru.